Processing of TOP2-DNA covalent complexes by the ubiquitin-proteasome system

Rebecca Louise Swan

Thesis submitted for the degree of
Doctor of Philosophy

Institute for Cell and Molecular Biosciences
Faculty of Medical Sciences
Newcastle University

July 2018

Abstract

DNA topoisomerase II (TOP2) poisons are widely used anticancer drugs which induce cytotoxic protein-DNA crosslinks termed TOP2-DNA covalent complexes. The TOP2-DNA covalent complex is a normally transient intermediate of the TOP2 reaction mechanism, whereby an intact DNA duplex is passed through an enzyme-mediated double strand break (DSB) in another DNA molecule. A covalent linkage between the TOP2 active site tyrosine and each DNA end conceals the break and prevents its recognition by DNA damage response proteins. However, in the presence of a TOP2 poison the TOP2-DNA complex is stabilised, leading to the accumulation of enzyme-linked DSBs which ultimately lead to cell death. Repair of the TOP2-DNA covalent complex first requires the removal of TOP2 from DNA ends, leading to the liberation of a protein-free DSB. While a number of pathways are available for the removal of the TOP2 adduct, one mechanism involves the proteasomal degradation of TOP2. The proteasomal degradation of proteins is largely regulated through the conjugation of ubiquitin to target proteins (ubiquitination). However, the requirement for ubiquitination in the processing of TOP2-DNA covalent complexes is unclear, with conflicting studies reporting both ubiquitin-dependent and -independent mechanisms. In the current study, inhibition of ubiquitination slowed the removal of TOP2 adducts from DNA and reduced the appearance of protein-free DSBs following etoposide treatment. Inhibition of the ubiquitin-dependent AAA ATPase VCP/p97 also prevented the processing of TOP2-DNA complexes to protein-free DSBs, indicating a previously unreported role for VCP/p97 in the repair of TOP2 poison-induced DNA damage. Inhibition of the ubiquitin-proteasome system increased the growth-inhibitory effects of four clinically relevant TOP2 poisons, and may be a viable strategy for the improvement of therapy with TOP2 poisons. This work confirms a ubiquitin-dependent mechanism of TOP2-DNA complex processing by the proteasome, which may be facilitated by the unfolding and extraction of TOP2-DNA complexes by VCP/p97.

Acknowledgements

I would first and foremost like to thank my supervisors, Professor Caroline Austin and Dr Ian Cowell, for their constant guidance and support both in the completion of this project and my personal development as a scientist. This work would not have been possible without their patience and expertise. I am also grateful to Bloodwise for providing this opportunity and funding the project (Gordon Piller Studentship, 13063). In addition, I would like to thank all members of the Austin laboratory, past and present, for their kindness and moral support over the last four years.

I am indebted to my family and friends, and especially my parents, who have encouraged and supported me in every way. I would like to thank my husband Scott for sustaining me with his love and amazing cooking skills. I am also thankful to our golden retriever Jack, for bringing me joy every day.

The experiments included in this thesis were performed solely by me, with the exception of the western blots shown in Figure 3.11 (Chapter 3, section 3.5.1) and γH2AX experiments shown in the Appendices (Figures 2-5). These experiments were performed by undergraduate students Elliot Trofimowicz and Charlotte Sanders respectively, under my supervision. Some of the research displayed in this thesis led to the publication of the following paper:

Lee, K. C., R. L. Swan, Z. Sondka, K. Padget, I. G. Cowell and C. A. Austin (2018). "Effect of TDP2 on the Level of TOP2-DNA Complexes and SUMOylated TOP2-DNA Complexes." Int J Mol Sci **19**(7).

Table of contents

Abbreviations

53BP1	p53-binding protein 1
5’-EU	5’-ethynyl uridine
AML	Acute myeloid leukaemia
ANOVA	Analysis of Variance
ATCC	American type culture collection
ATM	Ataxia-Telangiectasia Mutated
ATP	Adenosine triphosphate
BMI1	B cell-specific Moloney murine leukemia virus integration site 1
BRCA1	Breast cancer susceptibility gene 1
BSA	Bovine serum albumin
CAD	Chromatin-associated degradation
CML	Chronic myeloid leukaemia
CO_2	Carbon dioxide
CtIP	CtBP-interacting protein
DAPI	4',6-Diamidino-2-phenylindole
DMSO	Dimethyl sulfoxide
DNA	Deoxyribonucleic acid
DNA-PK	DNA-dependent protein kinase
DNA-PKcs	DNA-PK catalytic subunit
Dox	Doxorubicin

DRB	5,6-dichloro-1-β-D-ribofuranosylbenzimidazole
DSB	Double strand break
DTT	Dithiothreitol
ECL	Enhanced chemiluminescence
EDTA	Ethylenediaminetetraacetice acid
ERAD	Endoplasmic reticulum-associated degradation
FBS	Fetal bovine serum
FDA	Food and Drug Administration
FITC	Fluorescein isothiocyanate
H2AX	Histone H2AX
HDM2	Human double minute 2
HECT	Homologous to the E6-AP Carboxyl Terminus
HEPES	4-(2-hydroxyethyl)-1-piperazineethanesulfonic acid
HR	Homologous recombination
hrs	Hours
IC_{50}	50% maximum inhibitory concentration
IP	Immunoprecipitation
IR	Irradiation
KCl	Potassium chloride
kDa	kilo Daltons
m-AMSA	amsacrine

MLL	Mixed lineage leukaemia
MMS	Methyl methanesulfonate
MRE11	Meiotic recombination 11
MTX	Mitoxantrone
NaCl	Sodium chloride
NHEJ	Non-homologous end-joining
OECD	Organisation for Economic Co-operation and Development
PBS	Phosphate buffered saline
PRC1	Polycomb repressive complex 1
Rb	Retinoblastoma protein
RING	Really interesting new gene
RICC	Relative increase of cell count
RNA	Ribonucleic acid
RNAPII	RNA polymerase II
RNF8	Ring finger 8
RNF168	Ring finger 168
RPM	Revolutions per minute
RPMI	Roswell Park Memorial Institute
SDS	Sodium dodecyl sulfate
SDS-PAGE	SDS polyacrylamide gel electrophoresis
SEM	Standard error mean

siRNA	Small interfering RNA
SUMO	Small ubiquitin-like modifier
TARDIS	Trapped in agarose DNA immunostaining
TBS	Tris buffered saline
TBS-T	TBS + 0.1% Tween 20
TDP2	tyrosyl DNA phosphodiesterase 2
TOP1	DNA topoisomerase I
TOP2A	DNA topoisomerase II α
TOP2B	DNA topoisomerase II β
UIM	Ubiquitin interacting motif
UPS	Ubiquitin proteasome system
VCP	Valosin-containing protein
VM-26	Teniposide
VP-16	Etoposide
v/v	volume/volume
w/v	weight/volume
XTT	(2,3-bis-(2-methoxy-4-nitro-5-sulfophenyl)-2H-tetrazolium-5-carboxanilide)

List of Figures

List of Tables

Chapter 1 Introduction

Topoisomerase II (TOP2) poisons are widely used and effective anticancer drugs which disrupt the normal TOP2 reaction mechanism. In the absence of TOP2 poison, TOP2 induces an enzyme-bridged double strand DNA break (DSB) in one DNA molecule so that another DNA duplex can be passed through, thereby alleviating topological constraints in DNA such as knots and supercoils. However, TOP2 poisons inhibit religation of the TOP2-mediated DSB, leading to the persistence of TOP2-DNA covalent complexes in which TOP2 remains covalently attached to each 5' end of the DSB. Misrepair of the TOP2-DNA covalent complex is associated with the development of therapy-related leukaemias, and therefore a better understanding of how this damage is repaired may inform improvements in therapy with TOP2 poisons. A key step in TOP2-DNA complex repair is the removal of TOP2 from the break, which is required for recognition of the DSB by DNA damage response proteins. Among other pathways, this is largely achieved through the proteasomal degradation of the TOP2 protein adduct, yet little is known about how the proteasomal processing pathway is regulated. In particular, the ubiquitin-dependence of TOP2-DNA complex degradation by the proteasome is both suggested and disputed in the literature. This work clarifies a ubiquitin-dependent mechanism of TOP2-DNA complex repair which is required for the processing of TOP2-DNA complexes to protein-free DSBs, and also reveals a potential and previously unreported role of the ubiquitin-dependent protein segregase VCP/p97. With the ongoing development of proteasome and ubiquitination inhibitors, this suggests that targeting the ubiquitin-proteasome system would be a viable strategy to improve TOP2 poison therapy. The purpose of the current chapter is to first outline the cellular roles of TOP2 enzymes, the TOP2 reaction mechanism and how it is targeted by anticancer drugs. Known mechanisms of TOP2-DNA complex repair are then discussed, including existing evidence for the role of the ubiquitin-proteasome system.

1.1 DNA topoisomerases and DNA topology

The double-helical structure of DNA ensures the high fidelity transmission of genetic information, but is also prone to various topological problems. For example, separation of DNA strands during replication or transcription leads to compensatory over-winding (positive supercoiling) which restricts access to affected genes (Gilbert and Allan, 2014). Consequently, DNA-dependent processes such as replication and transcription are inhibited in regions of supercoiled DNA. As a large biological polymer, DNA can also form knots in which a single DNA molecule becomes self-entangled, while entanglement of more than one DNA molecule leads to the formation of catenanes (Lim and Jackson, 2015). Supercoils, knots and catenanes are resolved by an important group of enzymes called DNA topoisomerases.

Type I and type II topoisomerases induce single- and double- stranded DNA breaks (SSBs and DSBs), respectively (Pommier *et al.*, 2010). Topoisomerase I (TOP1 and TOP1mt) and Topoisomerase III (TOP3α and TOP3β) are type I topoisomerases which relieve positive supercoiling by introducing a nick in one strand and rotating the opposite intact strand around the SSB, or by passage of the intact strand through the break, respectively. This strand passage mechanism is also common to Topoisomerase II (TOP2), a type II topoisomerase which instead passes an intact double-stranded DNA duplex through a DSB in another DNA molecule (Figure 1.1). While type I topoisomerases alleviate positive supercoils during replication and transcription, TOP2 can also unknot and untangle complex DNA structures such as the catenanes formed between sister chromatids following DNA replication (DiNardo *et al.*, 1984; Uemura *et al.*, 1987; Clarke *et al.*, 1993; Sumner, 1995; Bower *et al.*, 2010). While both TOP1 and TOP2 are important anticancer drug targets, TOP2-targeting agents are also associated with the development of therapy-related leukaemias, and are the focus of this study.

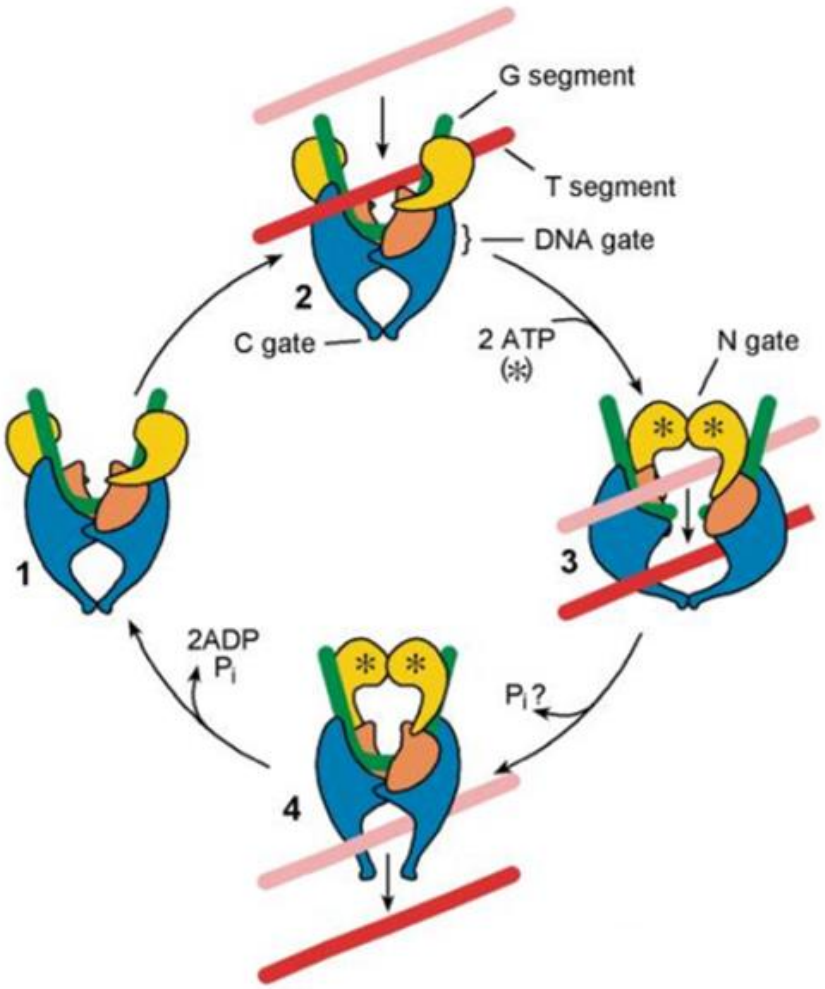

Figure 1.1. Strand passage by TOP2 enzymes. TOP2 unwinds and decatenates DNA by inducing a double strand break (DSB) in one DNA molecule, so that another DNA duplex can be passed through. 1) TOP2 binds G segment DNA (green). 2) T segment DNA (red) is captured within the N gate upon ATP binding. 3) Nucleophilic attack of the G segment leads to the induction of an enzyme-bridged DSB termed the TOP2-DNA covalent complex. T segment DNA is passed through the break. 4) G segment DNA is religated and T segment is released. TOP2 dissociates from DNA, ready for another round of catalysis. Figure reproduced from (Bates *et al.*, 2011), licenced under a CC BY NC licence (https://creativecommons.org/licenses/by-nc/4.0/legalcode).

1.1.1 The TOP2-DNA covalent complex

DSBs are potentially lethal events, leading to cell death or mutagenesis. To avoid unnecessary DNA damage responses or illegitimate recombination events during strand passage, each monomer of the dimeric TOP2 enzyme remains covalently linked to each DNA end during induction of the TOP2-mediated DSB. This enzyme-linked DSB is a transient intermediate of the normal TOP2 reaction mechanism, termed the TOP2-DNA covalent complex. The TOP2-DNA complex is formed following a transesterification reaction between the TOP2 active site tyrosine and the

phosphate backbone of DNA. Specifically, the nucleophilic tyrosine residue donates an electron pair to the electrophilic 5' phosphate of DNA, forming a 5'-phosphotyrosyl bond with a 4 base overhang (Deweese and Osheroff, 2009). Meanwhile, the 3'OH end of each broken DNA strand interacts non-covalently with TOP2. Subsequently, an intact DNA duplex is passed through the TOP2-concealed DSB, and the DSB is religated following nucleophilic attack of the 5'-phosphotyrosyl bond by the free 3'OH end of DNA. TOP2 poisons inhibit this final religation step, leading to the stabilisation of TOP2-DNA complexes and the persistence of TOP2-mediated DSBs.

1.1.2 Structure of TOP2 isoforms

There are two TOP2 isoforms in human cells sharing 68% overall amino acid sequence identity and the same reaction mechanism (Austin *et al.*, 1995). TOP2A and TOP2B are encoded by separate genes on chromosome 17 and chromosome 3 respectively, thought to have arisen through a gene duplication event (Lang *et al.*, 1998). Both contain three structural domains, including an N-terminal domain, a catalytic centre (known as the breakage-reunion core or DNA binding and cleavage core) and a C terminal domain (Austin *et al.*, 1995). The N-terminal domain contains one ATPase domain per protomer of the dimeric enzyme, which together form the N gate upon ATP binding and dimerization (Wu *et al.*, 2011) (Figure 1.2). The DNA binding and cleavage core includes the TOPRIM domain and WHD domain, which contain Mg^{2+} chelating residues and an active site tyrosine, respectively. Together with the Tower domain, this forms the DNA gate, which is primarily responsible for DNA binding (Wendorff *et al.*, 2012). The catalytic centre also contains the C gate, which mediates DNA exit after strand passage. Finally, the C terminal domain (CTD) displays the least sequence identity (34%) between TOP2 isoforms (Austin *et al.*, 1993), and has been used to generate isoform-specific antibodies. While not directly involved in catalysis, the CTD is implicated in the regulation of catalytic activity and nuclear localisation (Cowell *et al.*, 1998; Meczes *et al.*, 2008; Gilroy and Austin, 2011; Clarke and Azuma, 2017). The C terminus is subject to various post-translational modifications such as phosphorylation and SUMOylation (Cardenas *et al.*, 1992; Wells *et al.*, 1994; Ishida *et al.*, 1996). In particular, SUMOylation of the TOP2A CTD leads to recruitment of Claspin to the centromere during mitosis, and is essential for successful chromosome segregation (Ryu *et al.*, 2015; Clarke and Azuma, 2017). Modifications can also occur elsewhere in the TOP2 protein which

modulate TOP2 activity (Chikamori *et al.*, 2003; Grozav *et al.*, 2009; Ryu *et al.*, 2010). For example, SUMOylation of Lys662 in the DNA gate leads to inhibition of decatenation activity (Ryu *et al.*, 2010; Higgins, 2012; Wendorff *et al.*, 2012), and this is thought to be important for the regulation of centromeric decatenation during mitosis.

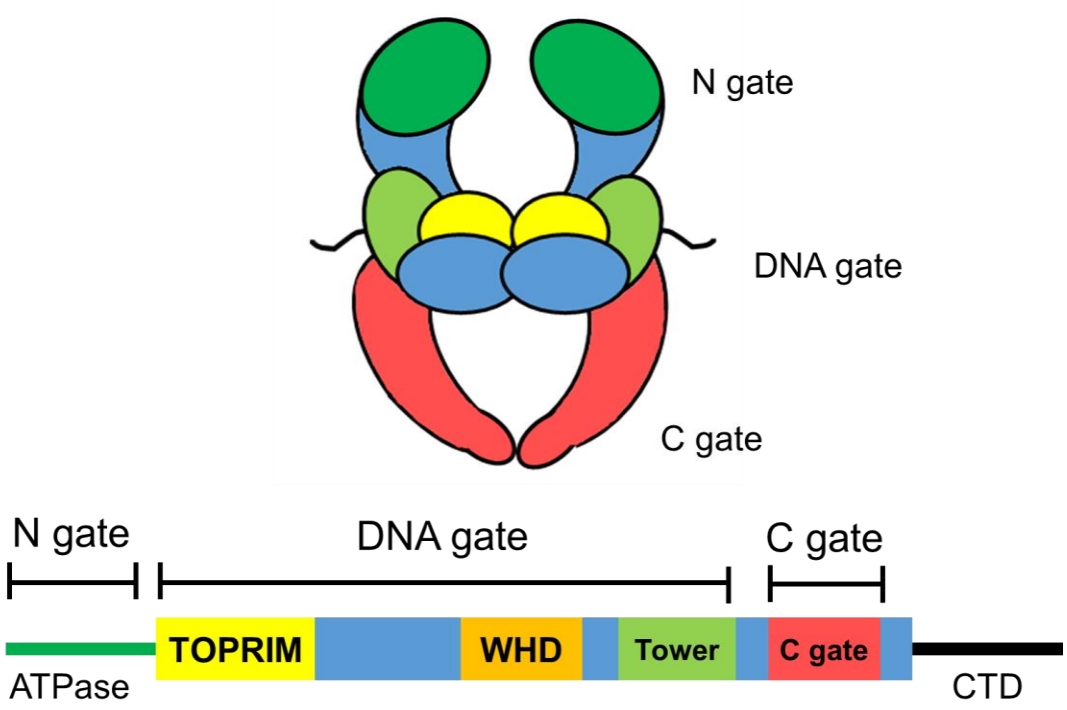

Figure 1.2. TOP2 domain structure. Upon dimerization, TOP2 forms three interfaces (the N gate, DNA gate and C gate) which control strand passage. The N gate is formed by the ATPase domain, while the DNA gate is formed between the TOPRIM, WHD and Tower domains. Figure adapted from (Wendorff *et al.*, 2012) and (Schoeffler and Berger, 2008).

1.1.3 The TOP2 catalytic cycle

Dimerisation of TOP2 protomers leads to the formation of three inter-protomer interfaces termed “gates” through which an intact or “transport” DNA segment (T segment) is passed during strand passage. This includes the N gate (formed by adjacent ATPase domains), the DNA gate (formed by TOPRIM and WHD domains together with DNA) and the C gate. Firstly, the “gate” DNA segment (G segment) is passed through the N gate and positioned near the catalytic tyrosine and Mg^{2+} ions for cleavage. ATP binding facilitates capture of the T segment within the N gate, followed by cleavage of the G segment (Wendorff *et al.*, 2012). Nucleophilic attack of the DNA backbone by the active site tyrosine leads to formation of the TOP2-DNA covalent complex, characterised by the 5’-phosphotyrosyl bond between TOP2 and

DNA. The T segment is then passed through the enzyme-linked DSB, and the G segment is religated. ATP hydrolysis of a second ATP molecule then leads to dissociation of the TOP2 protein from DNA, ready for another round of catalysis.

1.1.4 Cellular roles of TOP2 isoforms

Despite their structural similarity, TOP2A and TOP2B are differentially expressed and are responsible for different roles in the cell. For example, levels of TOP2A peak during G2/M phase (Heck *et al.*, 1988; Woessner *et al.*, 1991), where it mediates the recruitment of Claspin to mitotic centromeres (Ryu *et al.*, 2015; Clarke and Azuma, 2017) and the decatenation of sister chromatids (DiNardo *et al.*, 1984; Uemura *et al.*, 1987; Clarke *et al.*, 1993; Sumner, 1995; Bower *et al.*, 2010). Consequently, TOP2A is essential for successful segregation of chromosomes during anaphase, and is almost absent in non-proliferating cells (Woessner *et al.*, 1991). In contrast, levels of TOP2B remain relatively constant throughout the cell cycle, and is present in non-cycling quiescent cells (Woessner *et al.*, 1991; Austin and Marsh, 1998).

TOP2B-specific functions are mostly associated with transcription, and the expression of specific genes are up or downregulated in TOP2B knockout cells (Lyu *et al.*, 2006; Tiwari *et al.*, 2012; Madabhushi *et al.*, 2015). This includes many genes which are involved in neuronal functions, such as neurotrophin factor p75, and early response genes *Fos* and *Npl4* (Tiwari *et al.*, 2012; Madabhushi *et al.*, 2015). Consistently, TOP2B is directly implicated in the differentiation of neural cells, as knockout mice are non-viable due to defective neural development (Yang *et al.*, 2000), and cultured neurons lacking TOP2B display reduced neurite outgrowth (Nur *et al.*, 2007). TOP2B is also recruited to promoters in response to hormones including oestrogen, androgens and retinoic acid (Ju *et al.*, 2006; McNamara *et al.*, 2008; Perillo *et al.*, 2008; Haffner *et al.*, 2010; Manville *et al.*, 2015), thereby further implicating TOP2B in the regulation of transcription. Other studies have since shown that TOP2B binding is not restricted to promoters but is detected throughout the genome at sites of open chromatin (Manville *et al.*, 2015; Uuskula-Reimand *et al.*, 2016; Canela *et al.*, 2017). Specifically, TOP2B directly binds CTCF and loop anchor sites, where it is thought that DNA unwinding facilitates the formation of loop extrusions (Manville *et al.*, 2015; Uuskula-Reimand *et al.*, 2016; Canela *et al.*, 2017). Loop extrusions are formed by cohesin and CTCF, mediating long range interactions

between enhancer and promoter elements which facilitates transcription initiation. Therefore, TOP2B is involved in the initiation of transcription both through binding of promoters and through regulation of higher order chromatin structure. Interestingly, TOP2A has also been detected at specific promoters (Thakurela *et al.*, 2013) and is shown to interact with both RNA polymerase I and RNA polymerase II (Mondal and Parvin, 2001; Ray *et al.*, 2013). In a recent study, TOP2A cleavage sites were not detected within promoters but were detected in genes associated with high levels of transcription elongation (Yu *et al.*, 2017). Therefore, both TOP2 isoforms have specific and distinct roles in transcription.

1.1.5 TOP2 poisons

The ability of TOP2 enzymes to induce DSBs is exploited in cytotoxic anticancer therapy through the use of TOP2 poisons, which prevent religation of TOP2-induced DSBs (Nitiss, 2009; Pommier *et al.*, 2010; Pommier, 2013). This leads to the accumulation of DNA damage in the form of DSBs and stabilised TOP2-DNA complexes. In contrast, catalytic TOP2 inhibitors like dexrazoxane inhibit TOP2 activity without stabilising TOP2-DNA covalent complexes and DSBs. TOP2 poisons are widely used and effective drugs in the treatment of both solid and haematological tumours, often prescribed in combination with other cytotoxic drugs such as alkylating agents and microtubule inhibitors. Therefore, TOP2 poisons remain highly clinically relevant in the landscape of increasingly targeted anticancer therapies.

Clinically used TOP2 poisons include the non-intercalating epipodophyllotoxins (etoposide and teniposide), and intercalating poisons like mitoxantrone (an anthracenedione), doxorubicin and epirubicin (anthracyclines) and mAMSA (an acridine) (Figure 1.3). While TOP2 is the only known target of etoposide and teniposide, the intercalation of other poisons into DNA produces other DNA damaging effects which may also contribute to their cytotoxicity. For example, high concentrations of doxorubicin lead to alterations in DNA structure which prevents TOP2 binding (Pommier *et al.*, 2010). Cardiotoxicity is an important dose-limiting effect of doxorubicin therapy, which is thought to involve redox cycling of doxorubicin and the production of reactive oxygen species (Tsang *et al.*, 2003; Kim *et al.*, 2006; Pommier *et al.*, 2010). Although TOP2 is undoubtedly an important target for mitoxantrone cytotoxicity (Errington *et al.*, 1999; Toyoda *et al.*, 2008; Lee *et al.*,

2016), DNA binding by mitoxantrone also induces the compaction of chromatin and the inhibition of transcription and replication (Kapuscinski and Darzynkiewicz, 1986; Chiang *et al.*, 1998). In addition, mitoxantrone inhibits the polymerisation of microtubules (Ho *et al.*, 1991). Because of the potential TOP2-independent effects of intercalating poisons, etoposide and teniposide were used in the current project to study the repair of TOP2-mediated DNA damage.

Etoposide, teniposide, mitoxantrone, mAMSA and the anthracyclines are all interfacial poisons which prevent religation of the TOP2-mediated DSB. Interfacial inhibitors are those which bind and inhibit transient reaction intermediates of macromolecular complexes (Pommier *et al.*, 2015). This is in contrast to covalent poisons, which bind TOP2 away from the active site and form covalent adducts with TOP2 (Lindsey *et al.*, 2014). Specifically, interfacial TOP2 poisons bind within the DNA binding and cleavage core, increasing the distance between the active site tyrosine residue and the Mg^{2+}-chelating residues of the TOPRIM domain (Wu *et al.*, 2011; Wu *et al.*, 2013). Furthermore, drug binding physically blocks nucleophilic attack of the 5'-phosphotyrosyl bond by the 3'OH of DNA, which is required for religation.

The chemical biology of TOP2 poisons has been partly elucidated through studies of drug-resistant or hypersensitive TOP2A and TOP2B mutants. Many of these mutations are located within the core catalytic domain, where resistance may occur due to alterations in drug binding or steps in catalysis. For example, the E522K TOP2B mutant was identified in a number of independent studies following selection with mAMSA and other acridines (Leontiou *et al.*, 2004; Leontiou *et al.*, 2007). While the E522K mutation confers increased resistance to mAMSA, resistance to etoposide is decreased, as previously shown following mutation of the homologous residue in the bacteriophage T4 TOP2 enzyme (Leontiou *et al.*, 2004). Other mutations in this region of human TOP2A (R486K and E571K) have also been shown to increase resistance to TOP2 poisons including both mAMSA and etoposide (Patel *et al.*, 2000), and are proposed to disrupt a drug binding pocket. Q778 of human TOP2B was recently identified as an important residue for etoposide binding, while the equivalent methionine residue in TOP2A (M762) did not affect etoposide binding (Zdraljevic *et al.*, 2017). This indicates the existence of isoform-specific

differences in drug binding, which may influence the differential targeting of TOP2 isoforms by different TOP2 poisons (discussed below in section 1.1.7).

Other mutations have been identified which specifically interfere with enzyme catalysis. For example, the TOP2B P732L mutation inhibits DNA cleavage in the presence of calcium ions, and increases resistance to mAMSA, etoposide and doxorubicin (Leontiou *et al.*, 2006; Leontiou *et al.*, 2007). A mutation in the ATPase domain has also been described which reduces the affinity of TOP2 for ATP and ATP hydrolysis activity (Gilroy *et al.*, 2006).

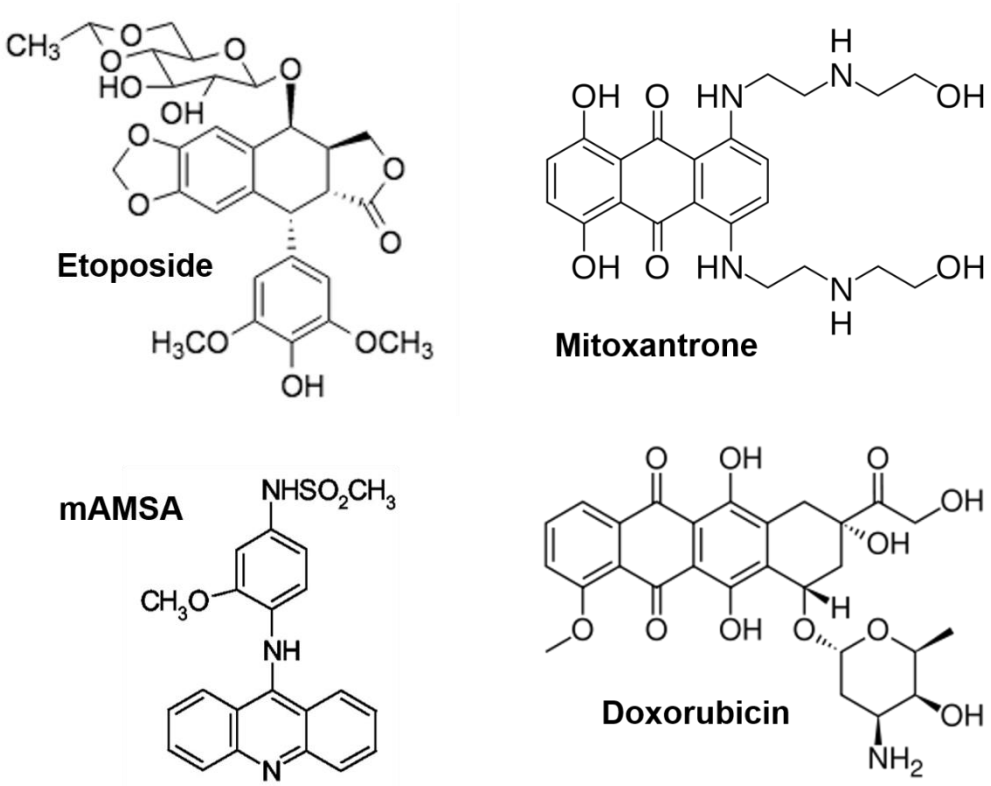

Figure 1.3. Chemical structures of clinically used TOP2 poisons.

1.1.6 Etoposide

Etoposide (VP-16) is used in combination with other chemotherapeutic drugs in the treatment of a range of cancers including testicular cancer, small cell lung cancer, non-Hodgkin's lymphoma, Hodgkin's lymphoma, acute myeloid leukaemia and ovarian cancer. A two-drug model was proposed for TOP2 poisoning by etoposide whereby two etoposide molecules are required to poison both monomers of the dimeric TOP2 protein (Bromberg *et al.*, 2003). As such, poisoning of a single TOP2 monomer (for example at lower doses of etoposide) prevents the religation of one

DNA break but not the other, leading to the induction of SSBs. TOP2 poison-induced SSBs themselves are cytotoxic (Rogojina and Nitiss, 2008) and can be converted to DSBs upon collision with the replication machinery (Avemann *et al.*, 1988; D'Arpa *et al.*, 1990; Lin *et al.*, 2009). It was initially estimated that for each etoposide-induced DSB there are 7-20 SSBs (Pommier *et al.*, 2010), while more recent studies suggest that only 2-3% of etoposide-induced breaks are DSBs (Muslimovic *et al.*, 2009; Yu *et al.*, 2017).

1.1.7 Targeting of TOP2 isoforms by TOP2 poisons

TOP2 poisons target both TOP2A and TOP2B (Willmore *et al.*, 1998; Errington *et al.*, 1999; Willmore *et al.*, 2002; Errington *et al.*, 2004). This has been demonstrated using the TARDIS assay to visualise and quantify levels of TOP2A- and TOP2B-DNA complexes following treatment with etoposide, mitoxantrone, mAMSA and idarubicin (Willmore *et al.*, 1998; Errington *et al.*, 1999; Willmore *et al.*, 2002; Errington *et al.*, 2004). TOP2-DNA complexes are reversed upon drug removal from cells, and TOP2-DNA complex reversal has also been studied using the TARDIS assay. These studies have shown that TOP2-DNA complexes induced by intercalating TOP2 poisons like mitoxantrone and idarubicin are significantly more stable than those induced by non-intercalating TOP2 poisons such as etoposide (Willmore *et al.*, 2002; Errington *et al.*, 2004; Lee *et al.*, 2016). Strikingly, while 50% of etoposide-induced TOP2A-DNA complexes are reversed within 40 minutes of drug removal, the half-life of mitoxantrone-induced TOP2A-DNA complexes is significantly greater, with 50% TOP2A-DNA complexes remaining after 10 hours (Errington *et al.*, 2004; Lee *et al.*, 2016). This suggests that the stability of TOP2-DNA complexes may be increased through additional contacts between intercalating TOP2 poisons and DNA.

Various studies have demonstrated the importance of TOP2A in TOP2 poison cytotoxicity. For example, Nalm-6 cells heterozygous for TOP2A (Nalm-6$^{TOP2A+/-}$) are significantly more resistant to etoposide than wild type cells or Nalm-6 TOP2B knockout cells (Toyoda *et al.*, 2008; Lee *et al.*, 2016). This may be related to the stability of etoposide-induced TOP2A-DNA complexes compared to etoposide-induced TOP2B-DNA complexes, which have half-lives of 40 minutes and 20 minutes, respectively (Errington *et al.*, 2004). Similarly, doxorubicin resistance is also

highest in Nalm-6$^{TOP2A+/-}$ cells compared to wild type or TOP2B knockout cells (Toyoda *et al.*, 2008; Lee *et al.*, 2016). However, TOP2B knockout cells are also significantly more resistant to etoposide than wild-type cells, albeit to a lesser extent than Nalm-6$^{TOP2A+/-}$ cells (Errington *et al.*, 1999; Toyoda *et al.*, 2008; Lee *et al.*, 2016). TOP2B knockout cells are also less sensitive to mAMSA and mitoxantrone (Errington *et al.*, 1999; Toyoda *et al.*, 2008; Lee *et al.*, 2016) and therefore, TOP2B is also an important mediator of TOP2 poison cytotoxicity.

1.1.8 TOP2 poison genotoxicity and the development of therapy-related leukaemia

While both isoforms are involved in TOP2 poison cytotoxicity, TOP2B is most associated with TOP2 poison genotoxicity (Azarova *et al.*, 2007; Azarova *et al.*, 2010; Cowell *et al.*, 2012; Smith *et al.*, 2013). For example, skin-specific knockout of TOP2B in a mouse carcinogenesis model showed that etoposide-induced melanoma is largely TOP2B-dependent (Azarova *et al.*, 2007), although the role of TOP2A was not investigated in the same study. Evidence for TOP2B-dependent genotoxicity is also extended to lymphoblastic cell lines whereby TOP2B knockout in Nalm-6 cells significantly reduces the appearance of etoposide-induced micronuclei, and specifically reduces the appearance of etoposide-induced chromosomal breaks in translocation-prone loci such as *MLL* and *RUNXI* (Cowell *et al.*, 2012; Smith *et al.*, 2013). TOP2 poison genotoxicity is associated with the development of therapy-related acute myeloid leukaemia (t-AML), which accounts for approximately 5-10% of all AML cases, and is associated with a poor prognosis (Cowell and Austin, 2012; Pendleton *et al.*, 2014). Therefore, the development of t-AML after TOP2 poison therapy is an important clinical problem.

Although t-AML is also associated with alkylating agents, TOP2 poison-associated t-AML is specifically characterised by a short latency period (<2 years) and balanced chromosome translocations, frequently involving the *MLL* (KMT2A) gene (11q23) (Allan and Travis, 2005; Cowell and Austin, 2012). Other common gene translocations following TOP2 poison therapy include the *RUNXI:RUNXITI* t(8;21) translocation and the *PML:RARA* t(15;17) translocation (Allan and Travis, 2005; Chen *et al.*, 2010; Cowell *et al.*, 2012; Smith *et al.*, 2013). Intriguingly, etoposide-induced translocation sites in the *MLL* locus are concentrated in a 1 Kb region at the

telomeric end of the 8 Kb breakpoint cluster region (BCR), the latter of which is associated with *de novo* AML (Cowell and Austin, 2012; Pendleton *et al.*, 2014).

Leukaemogenic chromosomal translocations occur upon the aberrant repair of DSBs at translocation-prone loci. Like radiation-induced damage, TOP2 poison-induced DNA damage can be repaired by non-homologous end joining (NHEJ) or by homologous recombination (HR) repair, depending on the cell cycle phase. However, most TOP2 poison-induced damage is repaired by NHEJ which operates throughout the cell cycle (Jin *et al.*, 1998; Adachi *et al.*, 2003; Willmore *et al.*, 2004; Ayene *et al.*, 2005; Malik *et al.*, 2006; de Campos-Nebel *et al.*, 2010; Maede *et al.*, 2014). While HR repair utilises a homologous sister chromatid as a template for high fidelity repair, NHEJ involves the potentially error-prone ligation of DNA ends (Hoeijmakers, 2001). Misrepair by NHEJ or a parallel alternative end joining (alt-EJ) pathway is thought to be associated with chromosome translocations (Ghezraoui *et al.*, 2014), and binding of NHEJ proteins such as Ku80 and DNA-PKcs occurs within a known AML breakpoint cluster region following etoposide treatment (Kantidze *et al.*, 2006). It is therefore thought that TOP2 poison-induced chromosome translocations occur at susceptible TOP2 cleavage sites due to aberrant end joining repair. It is unclear why TOP2 poison genotoxicity appears to show isoform preference, but is thought to involve the role of TOP2B in transcription (Cowell *et al.*, 2012). It is proposed that transcription factories provide the close proximity required for interaction between translocation partners at susceptible TOP2B cleavage sites (Cowell *et al.*, 2012). In contrast, Canela et al. suggest that TOP2B-mediated DSBs within breakpoint cluster regions are not transcription-dependent but are instead related to the role of TOP2B at loop anchor sites, which are vulnerable to DNA breaks (Uuskula-Reimand *et al.*, 2016; Canela *et al.*, 2017). Importantly, recent evidence also implicates TOP2A in the induction of etoposide-induced translocations, as TOP2A cleavage cluster regions were also detected within known cancer fusion genes including *MLL*, *PML*, *RARA* and *RUNXI* (Yu *et al.*, 2017). Therefore, targeting of TOP2A may also contribute to the genotoxicity of TOP2 poisons.

1.2 Repair of TOP2 poison-induced DNA damage

TOP2 poison-induced DSBs are concealed by the covalently bound TOP2 protein, and cannot be repaired until TOP2 is removed from the trapped TOP2-DNA complex. As mentioned in section 1.1.1, the 5'-phosphotyrosyl linkage between TOP2 and the TOP2-mediated DSB conceals DNA ends from DNA damage detection systems during the normal TOP2 reaction mechanism. Consistently, processing of drug-stabilised TOP2-DNA complexes to protein-free DSBs is required for the activation of DNA damage-dependent kinase DNA-PK (Martensson *et al.*, 2003). It was therefore hypothesised that preventing the processing of TOP2-DNA complexes to DSBs could reduce the likelihood of aberrant NHEJ, and hence the occurrence of leukaemogenic chromosomal translocations. Inhibition of TOP2-DNA complex processing with small molecule inhibitors is proposed in the current study as a viable approach to reduce the overall genotoxicity of TOP2 poisons. To achieve this, more must be understood about the various mechanisms of TOP2 removal from TOP2-DNA complexes. There are at least two types of processing pathways to convert TOP2-DNA complexes to ligatable DNA ends, including a nucleolytic and a proteolytic mechanism. These pathways are described in more detail below.

1.2.1 Nucleolytic processing

In the nucleolytic processing pathway, TOP2 adducts are removed by targeting the DNA. Nucleases such as Mre11 (of the MRN complex) can cleave the DNA end bearing the TOP2 protein (Neale *et al.*, 2005; Hartsuiker *et al.*, 2009; Lee *et al.*, 2012). Mre11 is a nuclease with both endonuclease and exonuclease activities which are utilised during HR repair for the processing of DNA ends to 3' single stranded DNA (DNA end resection) (Cannavo and Cejka, 2014; Liu and Huang, 2016). Importantly, Mre11 nuclease activity is also specifically involved in the resection and removal of 5'-adducts from DNA ends (Moreau *et al.*, 1999; Stohr and Kreuzer, 2001; Connelly *et al.*, 2003; Neale *et al.*, 2005), including TOP2-DNA complexes (Hartsuiker *et al.*, 2009; Hamilton and Maizels, 2010; Aparicio *et al.*, 2016; Hoa *et al.*, 2016; Wang *et al.*, 2017). Interestingly, basal levels of TOP2-DNA complexes (in the absence of TOP2 poison) are increased upon Mre11 inhibition, or in cells lacking full length Mre11 (Nakamura *et al.*, 2010; Lee *et al.*, 2012; Hoa *et al.*, 2016). This suggests that Mre11 is involved in the repair of endogenously trapped

TOP2-DNA complexes, which are thought to arise in the presence of abasic sites or other DNA-distorting lesions (Wilstermann and Osheroff, 2001; Stingele and Jentsch, 2015). The Mre11-dependent removal of TOP2 adducts also involves the nuclease CtIP (Sae2 in yeast). Like Mre11, depletion of CtIP significantly increases etoposide sensitivity and increases levels of etoposide-induced TOP2-DNA complexes in yeast and vertebrate cells (Hartsuiker *et al.*, 2009; Rothenberg *et al.*, 2009; Nakamura *et al.*, 2010; Quennet *et al.*, 2011; Aparicio *et al.*, 2016; Liao *et al.*, 2016). This may involve the nuclease activity of CtIP itself, or the CtIP-dependent stimulation of Mre11 nuclease activity (Anand *et al.*, 2016; Liao *et al.*, 2016). Furthermore, the interaction of CtIP with BRCA1 is required for the removal of TOP2 adducts from DNA, and depletion of BRCA1 also increases levels of etoposide-induced TOP2-DNA complexes (Nakamura *et al.*, 2010; Aparicio *et al.*, 2016). Alternatively, etoposide-induced DSBs can be resected by the exonuclease DNA2, although this occurs after the removal of TOP2 from the TOP2-DNA complex (Tammaro *et al.*, 2016).

1.2.2 Proteasomal processing

TOP2-DNA complexes can also be removed by targeting the TOP2 protein to the proteasome. In the proteasomal processing pathway, the bulk of the TOP2 protein is degraded by the proteasome, leaving behind short peptides linked to DNA via a phosphotyrosyl linkage which can be removed by TDP2 (Figure 1.4). TDP2 is a 5'-phosphodiesterase which specifically cleaves the 5'-phosphotyrosyl bond between degraded or denatured TOP2 and DNA (Cortes Ledesma *et al.*, 2009; Gao *et al.*, 2014). Alternatively, intact TOP2-DNA complexes can be removed directly by TDP2 in co-operation with the ZATT SUMO ligase in a proteasome-independent manner (Schellenberg *et al.*, 2017). However, this TDP2-dependent processing pathway appears to contribute significantly only upon proteasome inhibition, suggesting that the proteasomal pathway is a major mechanism of TOP2 complex removal.

The proteasomal degradation of TOP2-DNA complexes has been demonstrated in a number of cell lines, including mouse embryonic fibroblasts (MEFs) (Mao *et al.*, 2001; Zhang *et al.*, 2006; Ban *et al.*, 2013), HeLa cells (Alchanati *et al.*, 2009), K562 cells (Lee *et al.*, 2016), U2OS cells (Tammaro *et al.*, 2013) and a panel of colorectal cancer cell lines (Fan *et al.*, 2008). Specifically, proteasomal inhibition prevents the TOP2 poison-induced degradation of TOP2A and TOP2B (Mao *et al.*, 2001; Zhang *et al.*, 2006; Alchanati *et al.*, 2009; Ban *et al.*, 2013) and prolongs the half-life of etoposide- and mitoxantrone- induced TOP2-DNA complexes (Fan *et al.*, 2008; Lee *et al.*, 2016). Subsequently, proteasome inhibition also suppresses the etoposide-induced phosphorylation and activation of various DNA damage response proteins, including histone H2AX, RPA, and p53 (Zhang *et al.*, 2006; Fan *et al.*, 2008). Interestingly, the retinoblastoma tumour suppressor protein pRb has been implicated in the proteasomal degradation of TOP2B-DNA complexes, as the etoposide-induced degradation of TOP2B and phosphorylation of histone H2AX is also impaired in pRb null MEFs (Xiao and Goodrich, 2005). pRb also mediates the interaction between TOP2B and BRCA1, which may contribute to the repair of etoposide-mediated damage through its role in DNA repair, or as a function of its E3 ubiquitin ligase activity.

The proteasomal degradation of TOP2B in response to TOP2 poisons is reported to be transcription-dependent (Mao *et al.*, 2001; Fan *et al.*, 2008; Tammaro *et al.*,

2013). Proteasomal degradation also occurs in the absence of DNA damage with the TOP2 catalytic inhibitor, ICRF-193 (Isik *et al.*, 2003; Xiao *et al.*, 2003). Consequently, it has been proposed that TOP2B degradation is induced upon the collision of the transcription machinery with the trapped TOP2 cleavable complex, rather than by DNA damage per se (Mao *et al.*, 2001; Xiao *et al.*, 2003). In contrast, the proteasomal degradation of TOP2 is not replication-dependent (Mao *et al.*, 2001; Fan *et al.*, 2008), although replication may be involved in the activation of a distinct etoposide-induced DNA damage response which is important for etoposide cytotoxicity (Fan *et al.*, 2008). Fan et al. show that both transcription-dependent and replication-dependent mechanisms were required for NHEJ repair, demonstrating the importance of TOP2 processing in the repair of TOP2-mediated DNA damage (Fan *et al.*, 2008).

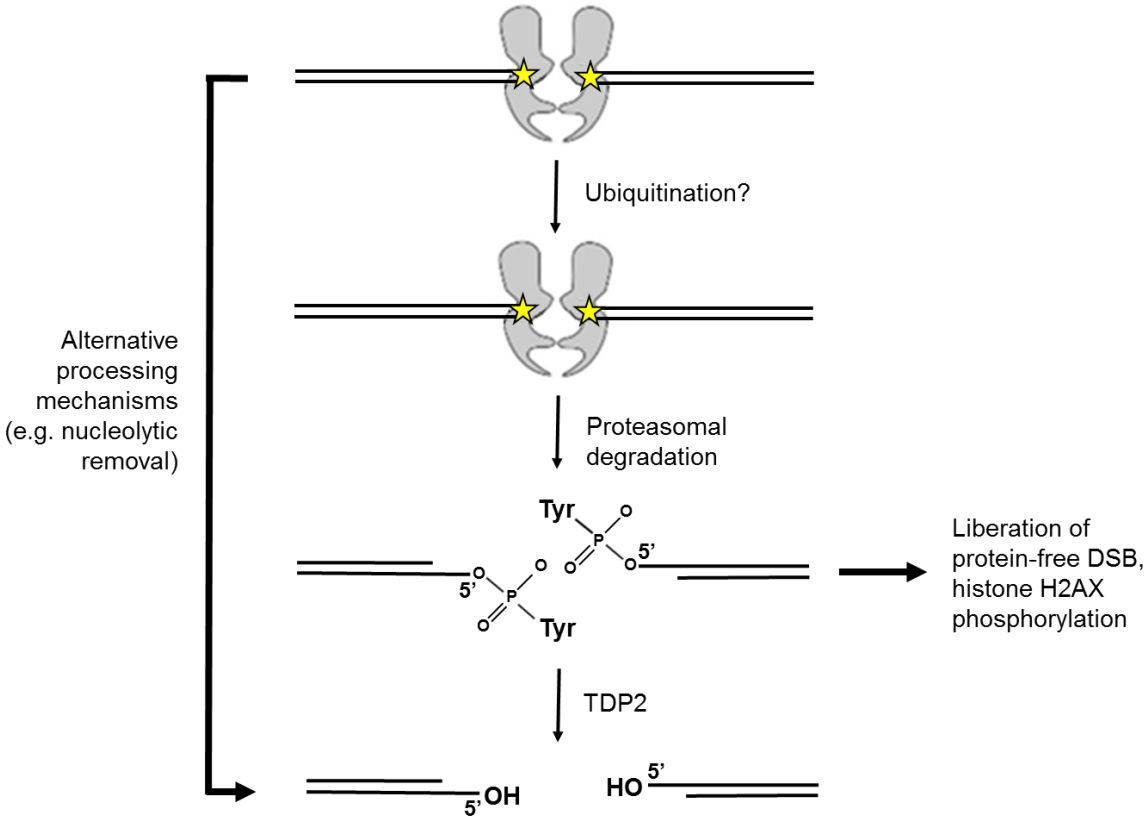

Figure 1.4. Processing of TOP2-DNA complexes to protein-free DSBs. For DSB repair to occur, TOP2 protein adducts must first be removed from the drug-stabilised TOP2-DNA complex. This is partly achieved through the proteasomal degradation of TOP2, leaving behind small tyrosyl peptides which are directly removed by TDP2. TDP2 generates ligatable ends for non-homologous end joining (NHEJ), which is predominantly required for the repair of TOP2 poison-induced DSBs. Alternatively, TOP2-DNA complexes can be removed by proteasome-independent mechanisms such as direct removal by TDP2 in co-operation with ZATT, or by cleavage of DNA ends by nucleases such as Mre11/CtIP.

1.2.3 Other mechanisms of TOP2-DNA complex removal

The nucleolytic and proteolytic pathways of TOP2-DNA complex processing are considered the two major pathways of TOP2 removal from DNA. However, in addition to the TDP2/ZATT-dependent pathway mentioned above, other mechanisms have also been described. For example, the half-life of mitoxantrone-induced TOP2-DNA complexes is increased in cells deficient for CSB (Rocha *et al.*, 2016). CSB is an essential component of transcription coupled nucleotide excision repair (TCR-NER), which is initiated upon transcription stalling. This suggests that collision of drug-stabilised TOP2-DNA complexes with elongating RNA polymerase II may lead to the removal of TOP2 by NER, which would presumably depend on the NER nucleases XPF and XPG. Roche et al. also show that mitoxantrone (and etoposide) sensitivity is increased in CSB-deficient and other NER-deficient cell lines. Interestingly, siRNA knockdown of Ku70 increases sensitivity to etoposide in a manner that is independent of its role in NHEJ repair (Ayene *et al.*, 2005), indicating a potential Ku-dependent mechanism of repair which may involve the AP lyase activity of Ku (Roberts *et al.*, 2010). It is therefore plausible that multiple pathways exist for the removal of TOP2-DNA complexes and the subsequent repair of TOP2 poison-induced DNA damage.

While many pathways contribute to the repair of TOP2 poison-induced DNA damage, the proteasomal degradation of TOP2-DNA complexes appears to be a major removal mechanism. Although it was initially thought that only TOP2B-DNA complexes are proteasomally degraded (Mao *et al.*, 2001; Isik *et al.*, 2003), subsequent studies showed that TOP2A-DNA complexes are also degraded via proteasomal activity, but at a slower rate (Zhang *et al.*, 2006; Fan *et al.*, 2008; Alchanati *et al.*, 2009; Lee *et al.*, 2016). Timely proteasomal degradation is largely regulated through ubiquitination, yet little attention has been given to the potential role of ubiquitin in the processing of TOP2-DNA complexes. The proteasomal degradation of TOP2A-DNA complexes appears to be ubiquitin-dependent (Alchanati *et al.*, 2009), but conflicting studies report both ubiquitin dependent and independent mechanisms of TOP2B degradation after etoposide or teniposide treatment (Mao *et al.*, 2001; Ban *et al.*, 2013). Clarification of the ubiquitin-dependent pathway would provide valuable mechanistic insights into the repair of TOP2 poison-induced DNA damage, which could be used to improve therapy with TOP2 poisons.

Indeed, this was a primary aim of the current project. The remainder of this chapter will therefore outline what is known about the ubiquitin-proteasome system, and the ubiquitin-dependent degradation of TOP2.

1.3 The ubiquitin-proteasome system

1.3.1 Cellular roles of the proteasome

The principal function of the proteasome is to degrade intracellular proteins. Protein degradation must be a tightly regulated process, and this is largely achieved through the conjugation of ubiquitin to target proteins (ubiquitination). While initially considered a route for the destruction of damaged or potentially toxic misfolded proteins, the cellular roles of the proteasome are much more widespread than originally anticipated (Adams, 2003). The proteasome regulates the turnover of many proteins, thereby maintaining appropriate concentrations of proteins in cells. This affects many cellular processes, including DNA damage repair, cell survival and proliferation (Jacquemont and Taniguchi, 2007; Murakawa *et al.*, 2007). For example, proteasomal degradation of the inhibitor protein IκB is required for the translocation of NFκB into the nucleus, where it mediates the transcription of genes encoding anti-apoptosis proteins and pro-inflammatory cytokines (Adams, 2003). The proteasome also regulates cell cycle progression, and is overexpressed in various cancers (Rastogi and Mishra, 2012). Due to its apparent role in tumorigenesis, the ubiquitin-proteasome system became a viable drug target for cancer therapy, which was achieved following FDA and EMA approval of the proteasome inhibitor bortezomib. Bortezomib (as well as the approved second generation proteasome inhibitor carfilzomib) is now used in the treatment of multiple myeloma alone or in combination with other chemotherapeutic drugs (Merin and Kelly, 2014).

1.3.2 Structure of the 26S proteasome

The 26S proteasome is a multi-subunit complex comprising the 20S core particle and the 19S regulatory particle (Figure 1.5). The 20S core adopts a barrel-like conformation, formed by four stacked heptameric rings ($\alpha_7\beta_7\beta_7\alpha_7$). The two outer α-rings (α1-7) form a narrow pore which restricts access to the proteolytic active sites situated within the internal chamber of the inner β-rings (β1-7) (Navon and

Ciechanover, 2009; da Fonseca *et al.*, 2012; Budenholzer *et al.*, 2017). In each β-ring there are three active sites containing a catalytic threonine residue at the N terminus of the β1, β2 and β5 subunits. These sites differ in their precise proteolytic activity, cleaving after preferred amino acid residues (where B1 is caspase-like, B2 is trypsin-like and B5 is chymotrypsin like) (Navon and Ciechanover, 2009; Tomko and Hochstrasser, 2013).

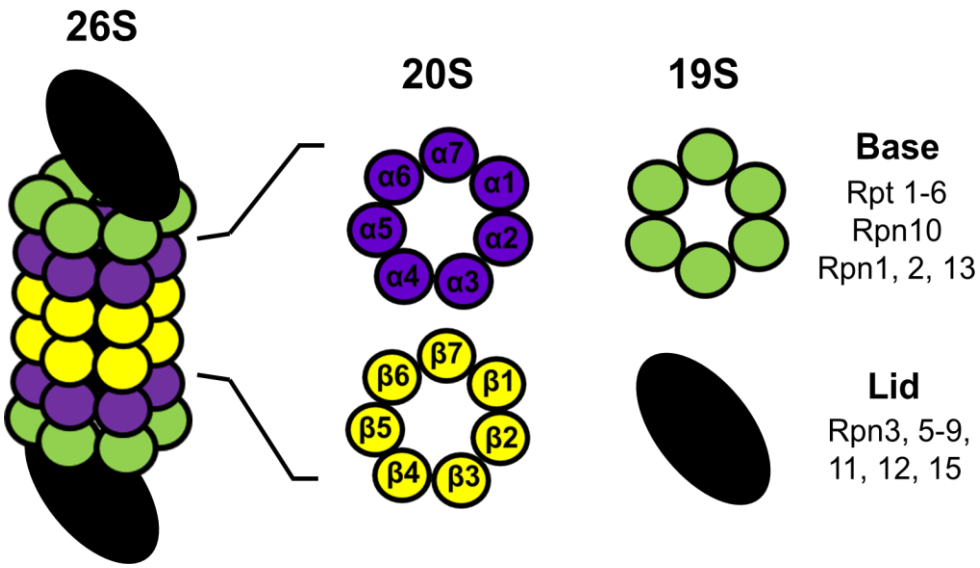

Figure 1.5. Structure of the 26S proteasome. The 26S proteasome consists of the 20S core particle and the 19S regulatory particle. The 20S is made up of four heptameric rings (two α rings and two β rings), while the 19S contains a hexameric ATPase ring (Rpt 1-6) which mediates protein unfolding. The 19S is also associated with ubiquitin receptors and deubiquitinase enzymes, which facilitate the proteasomal degradation of ubiquitinated proteins. Figure adapted from (Murata *et al.*, 2009).

Substrate entry into the 20S core is controlled in part by the opening and closing of the 20S narrow pore. Opening of the pore requires additional proteasome activators, which bind each end of the 20S core. For example, the proteasome activators PA28 and PA200 facilitate pore opening and degradation in an ATP- and ubiquitin-independent manner, although this is restricted to a small subset of unstructured proteins (Inobe and Matouschek, 2014). Most proteasomal degradation requires the 19S regulatory particle which, as well as pore opening, mediates the degradation of ubiquitinated proteins by unfolding and deubiquitinating substrates prior to their translocation into the 20S proteasome.

The 19S consists of two structural elements termed the lid and the base. However, the lid does not cap the base but interacts with both the base and the 20S core, seemingly holding the two together (Tomko and Hochstrasser, 2013). The interaction between the lid and the base is stabilised through binding to Rpn10, which also functions as a ubiquitin receptor (Budenholzer *et al.*, 2017). The base contains six AAA ATPases (Rpt1-6), which are arranged in pairs to form a ring structure. Like PA28 and PA200, Rpt2, Rpt 3 and Rpt5 contain HbYX motifs which are inserted into the outer α-ring of the 20S core. This induces a conformational change in the outer α-ring which facilitates pore opening, and subsequent translocation of proteins into the 20S core for proteolysis. In addition to pore opening, the 19S AAA ATPases regulate the translocation of ubiquitinated substrates through the 20S core by protein unfolding. The proteasome-associated deubiquitinases (DUBs) Rpn11, Usp14 and Uch37 remove ubiquitin chains from proteins prior to degradation, which are recycled into free ubiquitin.

1.3.3 Ubiquitin and ubiquitin-dependent proteasomal degradation

Ubiquitin is a small protein (8.5 kDa, 76 amino acids) which is coupled to target lysine residues through the successive action of three enzymes; an E1 activating enzyme, E2 conjugating enzyme and E3 ubiquitin ligase (Figure 1.6). Firstly, ubiquitin is processed by DUBs to reveal a C terminal double glycine motif. Ubiquitin is then activated by one of two E1 activating enzymes which involves the formation of a high-energy thioester bond between ubiquitin and the E1 active site cysteine in an ATP-dependent manner (Komander, 2009). The activated ubiquitin moiety is then transferred to the catalytic cysteine residue of an E2 conjugating enzyme through the formation of another thioester bond. Subsequently, ubiquitin is transferred to the target protein by an E3 ligase enzyme, which binds the substrate together with the E2 conjugating enzyme. The precise mechanism by which ubiquitin is transferred to the target differs according to the type of E3 ligase enzyme (Komander and Rape, 2012). For example, while RING ubiquitin ligases simply facilitate the transfer of ubiquitin from the E2 to the substrate lysine, ubiquitin is first transferred to the catalytic cysteine residue of HECT ubiquitin ligases before conjugation to the target protein. The human genome encodes two E1 enzymes, 37 E2s and >600 E3s. Therefore, ubiquitin enzymes represent a large group of potential drug targets for the modulation of ubiquitin-dependent proteasomal degradation.

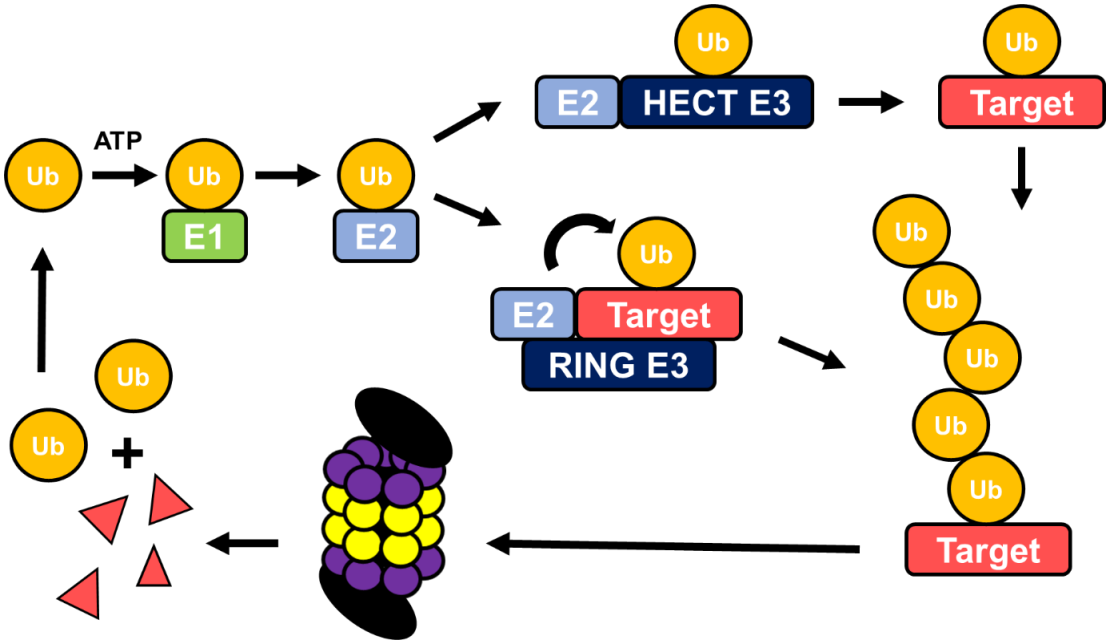

Figure 1.6. Ubiquitin conjugation by E1, E2 and E3 enzymes. Ubiquitin is first activated upon the formation of a high energy thioester bond with the E1 ubiquitin activating enzyme. Ubiquitin is then transferred to an E2 conjugating enzyme, which is bound by an E3 ubiquitin ligase. Ubiquitin may then be transferred to the target protein directly (RING E3 ligases) or indirectly following transfer to the E3 ligase (HECT E3 ligases). The formation of polyubiquitin chains may or may not lead to proteasomal degradation, where the target is destroyed and ubiquitin chains are recycled.

Ubiquitin can be conjugated singly to target proteins (monoubiquitination) or to multiple sites on the target protein (multimonoubiquitination). However, ubiquitin also contains 7 lysine residues (K6, K11, K27, K29, K33, K48, K63) which themselves can be ubiquitinated leading to the formation of polyubiquitin chains (polyubiquitination). The consequence of polyubiquitination is related to the distinct topology of alternative polyubiquitin chains. While K48-, K11- or K29- linked ubiquitin chains are most commonly associated with ubiquitin-dependent proteolysis, all chain types (with the exception of K63-linked chains) have been implicated in proteasomal degradation (Xu *et al.*, 2009; Bedford *et al.*, 2011). It is important to note that ubiquitination serves many functions which are unrelated to proteasomal degradation. For example, K63-linked chains are associated with the regulation of protein-protein interactions and signalling (including during the DNA damage response) (Komander, 2009).

1.3.4 TOP2 ubiquitination

Multiple ubiquitination sites have been detected in TOP2A and TOP2B, including many which reside in the DNA binding and cleavage core (Kim *et al.*, 2011) (Figure 1.7). However, little is known about their function. Ubiquitination of TOP2A is associated with proteasomal degradation in response to various stimuli, including glucose starvation, HDAC inhibition, and teniposide treatment (Alchanati *et al.*, 2009; Yun *et al.*, 2009; Chen *et al.*, 2011). Specifically, ubiquitination of TOP2A is implicated in the proteasomal processing of drug-stabilised TOP2A-DNA complexes, as inhibition of the BMI1/RING1A ubiquitin ligase prevents the proteasomal degradation of TOP2A after teniposide exposure (Alchanati *et al.*, 2009). Similarly, Mao et al. demonstrated a requirement for ubiquitination in the proteasomal degradation of TOP2B following teniposide treatment. Mao et al. showed that inactivation of a temperature-sensitive ubiquitin E1 enzyme in ts85 murine cells prevented the teniposide-induced degradation of TOP2B (Mao *et al.*, 2001). However, an equivalent study showed that etoposide-induced TOP2B degradation was unaffected in ts85 cells at the non-permissive temperature, implicating a ubiquitin-independent mechanism of proteasomal degradation (Ban *et al.*, 2013). Therefore, the requirement for ubiquitin in the proteasomal processing of TOP2B-DNA complexes remains unclear. A major aim of the current project is thus to determine the requirement for ubiquitin in the proteasomal processing of TOP2A- and TOP2B- DNA complexes.

Given that there are over 600 human E3 ubiquitin ligases, identification of the E3 ubiquitin ligases involved in the ubiquitination of TOP2-DNA complexes may enable more specific inhibition of TOP2-DNA complex processing by the proteasome. Importantly, the E3 ubiquitin ligases involved in TOP2 degradation varies by type of stress. For example, the ECV ubiquitin ligase complex is involved in TOP2A degradation in response to glucose starvation (Yun *et al.*, 2009), while Fbw7 is a Csn5-associated ubiquitin ligase involved in HDAC inhibitor-induced TOP2A downregulation (Chen *et al.*, 2011). Interestingly, HDAC inhibitor induced TOP2A degradation involves the upregulation of casein kinase II, which phosphorylates TOP2A and primes it for a second phosphorylation by GSK3β. In this instance, TOP2A phosphorylation was required for the recruitment of Fbw7 and its subsequent proteasomal degradation. Furthermore, BRCA1-mediated TOP2A ubiquitination first

requires the phosphorylation of TOP2A (Lou *et al.*, 2005). This emphasises the importance of other post-translational modifications in the regulation of TOP2 ubiquitination.

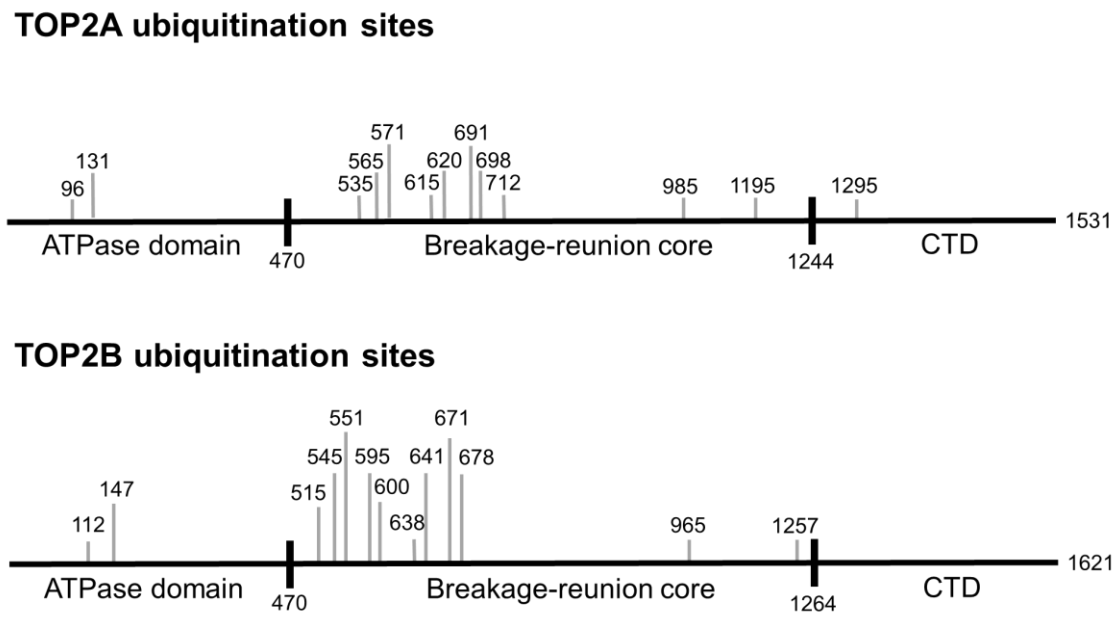

Figure 1.7. TOP2 ubiquitination sites. Schematic of known ubiquitination sites in TOP2A and TOP2B as identified and reported by (Kim *et al.*, 2011). Metabolically labelled HCT116 cells were treated with 1 µM bortezomib (proteasome inhibitor) for 8 hours and lysed. Digestion of ubiquitinated peptides with trypsin produces a K-ε-GG (diglycine or "DiGly") motif which were isolated by immunoprecipitation with a DiGly-specific antibody. Eluted peptides were then identified and analysed by LC-MS/MS. Data is accessible online at https://ggbase.hms.harvard.edu.

1.3.5 TOP2 SUMOylation

SUMOylation can also lead to the ubiquitin-dependent proteasomal degradation of proteins. SUMO is a ubiquitin-like (UBL) protein (of which there are four isoforms; SUMO-1, SUMO-2, SUMO-3 and SUMO-4) which can be conjugated to target lysines following activation, conjugation and ligation by a SUMO E1, E2 and E3 enzyme, respectively. SUMO-targeted ubiquitin ligases (StUBLs) are E3 ubiquitin ligases containing a SUMO-interacting motif (SIM), which binds non-covalently to SUMOylated proteins (Geoffroy and Hay, 2009). Recruitment of a StUBL to a SUMOylated protein can lead to the formation of hybrid SUMO-ubiquitin chains following the conjugation of ubiquitin to the existing SUMO chain. RNF4 is a StUBL known to generate hybrid SUMO-ubiquitin chains at DSBs, which are bound by SIM- and UIM- (ubiquitin-interacting motif) containing proteins such as VCP/p97 and

Rap80 (Guzzo *et al.*, 2012; Nie and Boddy, 2016). Binding of hybrid SUMO-ubiquitin chains by Rap80 mediates the recruitment of BRCA1, and is thus involved in the regulation of DSB repair (Guzzo *et al.*, 2012).

RNF4 mediates the ubiquitination of mitotic chromosomes in response to etoposide in a SUMO-dependent manner, although the SUMOylated target was not identified in the same study (Saito *et al.*, 2014). This may be important as TOP2A and TOP2B are SUMOylated in response to etoposide and teniposide (Mao *et al.*, 2000; Agostinho *et al.*, 2008; Schellenberg *et al.*, 2017), and previous studies using the TARDIS assay have demonstrated the presence of SUMO-1 and SUMO-2/3 chains on etoposide-induced TOP2-DNA complexes (Jobson, 2004). Indeed, a SUMO-dependent pathway of TOP2-DNA complex processing was recently proposed whereby SUMOylation of TOP2-DNA complexes by the ZATT SUMO ligase facilitates the direct removal of TOP2 adducts by TDP2 (Schellenberg *et al.*, 2017; Zagnoli-Vieira and Caldecott, 2017). TDP2 does not contain a canonical SIM, but contains five SUMO binding elements which are required for the interaction between TDP2 and TOP2. Intriguingly, TDP2 also contains a ubiquitin binding domain which is also required for the repair of TOP2-DNA complexes, although the precise function of this domain is unknown (Rao *et al.*, 2016). While the SUMO- and TDP2-dependent pathway was independent of proteasomal degradation, other studies suggest a role for SUMO in the degradation of TOP2. For example, studies in yeast have shown that Rrp2 (a DNA translocase) competes with Slx8 (the yeast homolog of RNF4) for binding to SUMOylated TOP2 and thus prevents its ubiquitin-dependent proteasomal degradation (Wei *et al.*, 2017). Furthermore, depletion of the SUMO E2 enzyme (Ubc9) in a mutant chicken DT40 cell line prevented the ICRF-193 induced proteasomal degradation of TOP2B (Isik *et al.*, 2003). This suggests that crosstalk between SUMO and ubiquitin is involved in the regulation of TOP2 degradation.

1.4 VCP/p97

VCP/p97 is an evolutionarily conserved and highly abundant protein which is also involved in the regulation of the ubiquitin-proteasome system. As a AAA ATPase, VCP/p97 uses the energy from ATP hydrolysis to unfold ubiquitinated proteins. This facilitates the extraction of proteins from protein complexes or cellular components, often (but not always (Ramadan *et al.*, 2007)) for proteasomal degradation. For example, VCP/p97 is well known for its role in endoplasmic reticulum associated degradation (ERAD), whereby the segregase activity of VCP/p97 enables the extraction of ubiquitinated p90 from the SPT23 transcription factor for nuclear targeting (Rape *et al.*, 2001). This function is not limited to the ER, but has also been described for the removal of proteins from chromatin. This is discussed in detail in section 1.4.3.

1.4.1 VCP/p97 is an important mediator of the ubiquitin-proteasome system

Importantly, the function of VCP/p97 in the ubiquitin-proteasome system is much more extensive than initially thought. VCP/p97 is required for the proteasomal degradation of many ubiquitinated proteins (Dai and Li, 2001), which accumulate in response to VCP/p97 inhibition similarly to proteasomal inhibition (Heidelberger *et al.*, 2018). Notably, VCP/p97 is not required for the degradation of all proteins targeted to the proteasome, as the abundance of accumulated ubiquitinated proteins upon complete VCP/p97 inhibition is less than that induced by proteasomal inhibition (Heidelberger *et al.*, 2018). Beskow et al. used a series of Drosophila VCP/p97 ATPase mutants to test the role of VCP/p97 enzymatic activity in the ubiquitin-proteasome system. These studies revealed a widespread role for VCP/p97 in the pre-processing of many substrates, which was required for their proteasomal degradation (Beskow *et al.*, 2009). In addition to the extraction of proteins from the ER and chromatin, Barthelme and Sauer propose that, like the 19S regulatory particle, VCP/p97 functions as an alternative proteasome activator (Barthelme and Sauer, 2013; Inobe and Matouschek, 2014). Therefore, VCP/p97 may act to facilitate the unfolding of proteins required for translocation into the 20S proteasome. In support of this, various studies have demonstrated an interaction between VCP/p97 and the proteasome. Besche et al. were the first to detect VCP/p97 on purified proteasomes, occurring in very small quantities which suggests that the interaction is

transient under normal conditions (Besche *et al.*, 2009). This interaction is stabilised in conditions of proteotoxic stress following treatment with arsenite or proteasome inhibitor, and leads to a 4-fold increase in proteasome activity (Isakov and Stanhill, 2011). This suggests that VCP/p97 increases the efficiency of proteasomal degradation when the proteasome is compromised, likely by providing additional unfoldase activity.

1.4.2 VCP/p97 structure

AAA ATPases utilise energy from ATP hydrolysis to induce large conformational changes which are transduced to bound substrates for protein unfolding and remodelling. AAA ATPases are characterised by the presence of a 250 amino acid AAA domain, which is highly conserved in all domains of life from archaea to eukaryotes (Snider *et al.*, 2008). The AAA domain binds and hydrolyses ATP, which is mediated by a Walker A and Walker B motif, respectively (Pye *et al.*, 2006). AAA ATPases may contain one (type I) or two (type II) hexameric AAA domains.

VCP/p97 is a hexameric type II AAA ATPase, with each protomer containing two ATPase domains, D1 and D2. The twelve resulting ATP binding sites form stacked rings arranged around a central pore (Figure 1.8). Hexamerisation and assembly of VCP/p97 requires the D1 domain, while a large proportion of ATPase activity is attributed to D2. It is thought that ATP induces large conformational changes in VCP/p97 which are transduced to the substrate protein, although these changes have been difficult to elucidate in structural studies due to limited resolution and the tight binding of ADP to the D1 domain (Pye *et al.*, 2006). Nonetheless, studies describe a rotation of D1 and D2, and in particular the opening and closing of the D2 central pore for the threading through of the unfolded protein substrate (van den Boom and Meyer, 2018).

The VCP/p97 hexameric assembly also contains six N terminal domains which protrude from each protomer repeat of the D1 domain, where they mediate interactions with cofactors and adaptor proteins. Cofactors include a number of ubiquitin ligases and deubiquitinase enzymes, further implicating VCP/p97 as an important component of the ubiquitin-proteasome system. In addition, ubiquitin adaptor proteins such as p47 and Ufd1-Npl4 direct VCP/p97 to a multitude of cellular functions, interacting with VCP/p97 via UBX or UBXL domains (Meyer *et al.*, 2000).

The interaction of all VCP/p97-interacting domains (including UBX, UBX-L, VIM/VBM, SHP and PUB/PUL domains) with VCP/p97 have now been resolved by X-ray crystallography (Stach and Freemont, 2017). UBX-containing proteins such as p47 and UBXD1 contain a C terminal UBX (ubiquitin regulatory X) domain, which binds the N terminal region of VCP/p97 (Dreveny *et al.*, 2004). UBX-containing proteins typically interact with ubiquitin via an N terminal UBA domain. While p47 is most associated with membrane fusion events and UBXD1 is involved in lysosomal autophagy (Papadopoulos *et al.*, 2017), other UBX-containing proteins such as FAF1 have been implicated in chromatin-associated degradation. Specifically, FAF1 is required for the VCP/p97-dependent degradation of the replication licensing factor CDT1, which facilitates replication fork progression (Franz *et al.*, 2016; Stach and Freemont, 2017).

Similarly, UBX-L (UBX-like domain)-containing proteins (such as the VCP/p97-associated DUB YOD1) also bind the VCP/p97 N terminus. Npl4 is a UBX-L-containing protein which, together with Ufd1, is involved in various VCP/p97-dependent functions including ERAD, ribosome-associated degradation (RAD) and chromatin-associated degradation (CAD) (Vaz *et al.*, 2013; Stach and Freemont, 2017) (Figure 1.8). The interaction between the Npl4 UBX-L domain and VCP/p97 is stabilised by Ufd1, which makes additional contacts with the VCP/p97 N terminus via a SHP motif (another VCP/p97-interacting sequence) (Le *et al.*, 2016). Both Npl4 and Ufd1 also bind ubiquitin via a zinc finger domain and UT3 domain respectively, with a preference for K48-linked ubiquitin chains (Ye *et al.*, 2003).

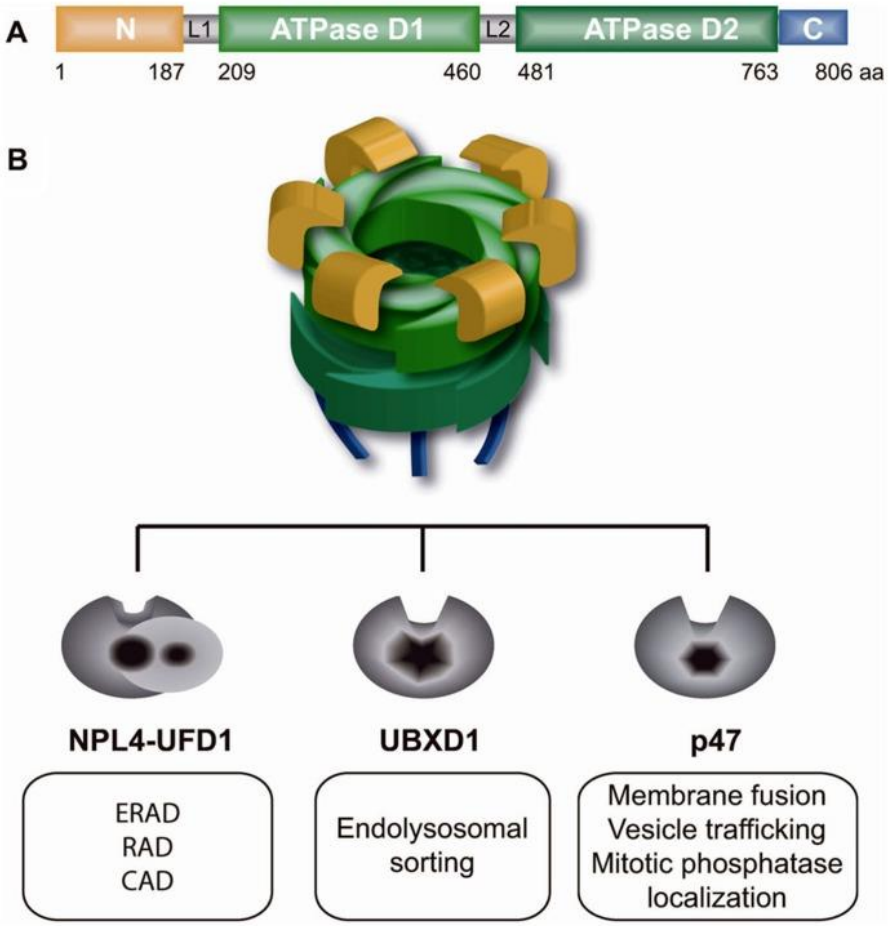

Figure 1.8. Structure and functions of VCP/p97. A) Domain structure of a VCP/p97 monomer, containing an N terminal domain, two ATPase domains (D1 and D2) and a C terminal domain. B) Structure of the VCP/p97 hexameric assembly and associated functions, mediated by specific ubiquitin adaptor proteins Npl4-Ufd1, UBXD1 and p47. Figure reproduced from (Vaz *et al.*, 2013), licenced under a CC BY licence (https://creativecommons.org/licenses/by/4.0/legalcode).

1.4.3 Role of VCP/p97 in the DNA damage response

The role of VCP/p97 in the extraction and removal of chromatin-associated proteins is particularly evident during the DNA damage response. After the initial wave of DNA damage-induced phosphorylation by ATM, ATR and DNA-PK kinases, ubiquitination regulates both the recruitment and removal of repair proteins from the damage site. The ubiquitin-dependent recruitment of DNA repair proteins such as BRCA1 and 53BP1 to DSBs is mediated by the E3 ubiquitin ligases RNF8 and RNF168 (Huen *et al.*, 2007; Mailand *et al.*, 2007; Doil *et al.*, 2009; Panier and Durocher, 2009; Bekker-Jensen and Mailand, 2011; Mattiroli *et al.*, 2012). VCP/p97 itself is recruited to DSBs in a ubiquitin- and Ufd1-Npl4- dependent manner, which seems to be mediated mostly through the binding of K48-linked ubiquitin chains

(Meerang *et al.*, 2011). The ubiquitin-dependent removal of DNA repair proteins is then largely mediated by VCP/p97. For example, VCP/p97 is required for the removal of polycomb protein L3MBTL1 from the H4K20me2 histone mark, which otherwise antagonises the binding of 53BP1 (Acs *et al.*, 2011). Thus, VCP/p97 enables the recruitment of 53BP1 to DSBs. VCP/p97-dependent chromatin extraction is observed for a number of other repair proteins, including DNA-PKcs and Rad51-Rad52 (Bergink *et al.*, 2013; Jiang *et al.*, 2013). The removal of chromatin-associated proteins by VCP/p97 is therefore important for the co-ordination of DNA repair.

VCP/p97 is also required to restore DNA to its undamaged state by removing repair proteins once DSB repair has occurred. Ku70/80 adopts a ring structure, which loops onto DNA ends and mediates the recruitment of NHEJ proteins such as DNA-PKcs, XRCC4, DNA ligase IV, and Artemis (Postow, 2011). Once the break is repaired, Ku70/80 becomes sterically trapped on DNA, and is removed in a ubiquitin-dependent manner (Brown *et al.*, 2015). VCP/p97 was recently identified as an ATPase activity required for the unfolding and extraction of ubiquitinated Ku70/80 from DNA following DNA repair (van den Boom *et al.*, 2016).

1.4.4 Role of VCP/p97 in the repair of UV-induced DNA damage

UV irradiation induces bulky DNA adducts and interstrand crosslinks which are repaired by nucleotide excision repair (NER). As the name suggests, NER involves the excision of the damaged DNA strand, recognised by DDB2 and XRC. Importantly, siRNA knockdown of VCP/p97 leads to the accumulation of ubiquitinated DDB2 at UV damage sites (Puumalainen *et al.*, 2014), suggesting the removal of DDB2 is VCP/p97-dependent.

Another consequence of UV-induced DNA damage is the stalling of RNA polymerase II (RNAPII) on DNA. Transcription stalling can also occur due to topological constraints, dNTP depletion, and bulky DNA adducts (including TOP2-DNA complexes). There are a number of available mechanisms to overcome these obstacles. However, irreversible transcription stalling leads to the induction of the “last resort” pathway of RNAPII proteasomal degradation on chromatin (Wilson *et al.*, 2013). Specifically, it is the large subunit of RNAPII (Rpb1) which is degraded, while other subunits of the elongation complex remain to be reused.

Being such a crucial enzyme, the proteolysis of RNAPII is highly regulated, and this is achieved by ubiquitination of Rpb1 (Harreman *et al.*, 2009; Wilson *et al.*, 2013). Firstly, Rpb1 is polyubiquitinated by Rsp5, which forms K63-linked ubiquitin chains. Secondly, these ubiquitin chains are trimmed back to monoubiquitin by the DUB, Usp2. Subsequently, Rpb1 is polyubiquitinated with K48-linked ubiquitin chains. At this point, RNAPII can be rescued by another DUB which removes K48-linked ubiquitin chains (Usp3). Otherwise, the proteasome is recruited to chromatin leading to degradation of Rpb1. Verma et al. showed that the interaction between Rpb1 and the proteasome is VCP/p97-dependent in yeast, and indeed the proteasomal degradation of Rpb1 requires the ATPase activity of VCP/p97 (Verma *et al.*, 2011; Lafon *et al.*, 2015). This was later demonstrated in human cells (He *et al.*, 2017a). Therefore, VCP/p97 extracts protein complexes from chromatin which are otherwise trapped or tightly associated.

Interestingly, it has been suggested that the proteasomal processing of TOP2-DNA complexes requires additional unfoldase activity, such as that of RNAPII-associated 19S AAA ATPases (Ban *et al.*, 2013). Given the ability of VCP/p97 to extract and unfold trapped protein complexes from DNA, it was hypothesised that VCP/p97 could facilitate the proteasomal processing of TOP2-DNA complexes. Notably, inactivation of a temperature-sensitive Cdc48 (the yeast homolog of VCP/p97) leads to the accumulation of ubiquitinated TOP2 (Wei *et al.*, 2017). In addition, Cdc48 is required for the degradation of TOP1-DNA complexes by the non-specific protease, Wss1 (Stingele *et al.*, 2014; Balakirev *et al.*, 2015).

1.5 Aims

The major aims of the current project are as follows:

- To determine the requirement for ubiquitin in the processing of etoposide-induced TOP2A- and TOP2B- DNA complexes (Chapter 3).
- To investigate the ubiquitination of TOP2 in the presence and absence of etoposide (Chapter 4).
- To investigate the potential role of VCP/p97 in the processing of etoposide-induced TOP2-DNA complexes (Chapter 5).
- To test the effect of inhibitors of the ubiquitin-proteasome system on TOP2 poison-induced growth inhibition and genotoxicity (Chapter 6).

Chapter 2 Materials and Methods

2.1 Drugs and Chemicals

All drugs and chemicals were purchased from Sigma-Aldrich (Dorset, UK) except for PYR-41, PRT4165 and HLI373 (purchased from Merck Millipore, Massachusetts, USA), MLN7243 (Active Biochem Ltd, Hong Kong), MLN4924 (R&D systems, Minneapolis, USA) and PR-619 (Tocris Bioscience, Bristol, UK). All drugs were dissolved in DMSO, unless otherwise stated. Sea-prep agarose (with ultra-low gelling temperature) used for TARDIS experiments was purchased from Fisher Scientific (New Hampshire, US).

2.2 Cell culture

Cells were grown in RPMI medium containing 10% FBS and 5% v/v penicillin-streptomycin, and incubated at 37°C, 5% CO_2 in a humidified atmosphere. Cell culture was performed under aseptic conditions. Cells were passaged every 2 or 3 days and maintained between 1 x 10^5 – 1 x 10^6 cells/mL for K562, and between 2 x 10^5 – 2 x 10^6 cells/mL for Nalm-6 cells.

2.2.1 Cell lines

The K562 leukemic cell line is derived from the bone marrow of a 53 year old female CML patient, characterised by the presence of the Philadelphia chromosome, t(9;22).

Nalm-6 is a human pre-B ALL cell line derived from the peripheral blood of a 19 year old male patient. Nalm-6$^{TOP2A+/-}$ and Nalm-6$^{TOP2B-/-}$ cells were generated as previously described by Adachi et al. (Adachi *et al.*, 2006).

2.3 Trapped in Agarose DNA Immunostaining (TARDIS) assay

2.3.1 Drug treatment

K562 cells were seeded at a density of 2 x 10^5 cells/mL and incubated overnight. Exponentially growing cells were treated with etoposide alone or in combination with small molecule inhibitors as indicated in the text, and an additional 100 µM etoposide positive control was used for data normalisation. After drug treatment, etoposide-containing media was removed by centrifugation (1000 rpm for 5 minutes) and cells were washed in ice cold Phosphate Buffered Saline (PBS). Alternatively, cells were

incubated for a further 2 hours in fresh media containing DMSO or relevant small molecule inhibitor, and cells were collected and washed at half-hour intervals (0, 0.5, 1 and 2 hours). After removal of the supernatant, cells were stored on ice for no longer than 30 minutes to minimise the reversal and repair of TOP2-DNA complexes.

2.3.2 Slide preparation and cell spreading

Microscope slides were coated with 0.5% Sea-prep low melting point agarose (Fisher Scientific, US) prior to cell spreading. Cells were resuspended in 50 µL ice cold PBS and briefly heated in a 37°C water bath for approximately 20 seconds. An equivalent volume of 2% molten agarose was added to the cells and mixed thoroughly. 50 µL of cell suspension was added to duplicate slides (one for staining for TOP2A and one for TOP2B) and spread evenly using a clean microscope slide. Slides were subsequently placed on an ice-cooled glass plate in order to rapidly set the agarose and to minimise TOP2 complex reversal.

2.3.3 Cell lysis

Cells were lysed in buffer containing 1% w/v SDS, 20 mM $NaPO_4$ (pH 6.5), 10 mM EDTA and 0.25% v/v protease inhibitor cocktail (AEBSF, Aprotinin, Bestatin, E-64, Leupeptin and Pepstatin A purchased from Sigma-Aldrich, Dorset, UK) for 30 minutes. Cells were incubated for a further 30 minutes in 1 M NaCl prior to three successive washes in PBS.

2.3.4 Antibody incubations

All antibody incubations were carried out for 1.5 hours at room temperature. Primary antibodies specific for TOP2A or TOP2B (see Table 1 for antibody details) were diluted in PBS containing 1% w/v BSA and 0.1% v/v Tween 20. For the study of TOP2-DNA complex ubiquitination or SUMOylation by TARDIS, slides were incubated with anti-ubiquitin antibodies (APU2, APU3 or FK2) or an anti-SUMO-2/3 antibody. Slides were then washed three times in PBS-T (1x 30 seconds, 2x 5 minutes) and stored at 4°C overnight in PBS-T containing protease inhibitors. Secondary antibody was diluted in blocking buffer and added to slides in subdued light. Finally, slides were washed in PBS (2x 5 minutes, 1x 20 minutes) prior to staining with 2 µg/mL Hoechst 33258 DNA stain (Life Technologies, USA). Slides

were mounted using Vectashield mounting medium (Vector Laboratories, CA) and stored at 4°C until further analysis.

2.3.5 Fluorescence microscopy

Microscopy was performed using an Olympus IX-81 confocal microscope fitted with a Hamamatsu Orca-AG camera. Analysis was performed using Volocity software (Perkin-Elmer) and GraphPad Prism version 4 as previously described by Cowell et al. (Cowell *et al.*, 2011). Optimal exposure time was determined by autoexposure of the brightest sample, which was set at the beginning of each experiment.

2.4 Immunofluorescence

Cells were washed and resuspended in ice-cold PBS then added to wells of poly-L-lysine coated multi-well reaction slides. After 10 minutes, surplus cells were washed away in PBS and the remaining cells were fixed in 4% paraformaldehyde for 10 minutes. Slides were washed twice in PBS then transferred to a coplin jar containing KCM-T [120 mM KCl, 20 mM NaCl, 10 mM Tris-HCl pH 8.0, 1 mM EDTA, 0.1% Triton X-100] for 15 minutes to permeabilise the cells. Cells were then incubated in blocking buffer [KCM-T + 10% dried milk powder + 2% BSA] for 1 hour at room temperature, or overnight at 4°C. Antibodies were used as described in Table 1. Primary antibodies (TOP2A, TOP2B, histone, RNAPII, Ku80, ɣH2AX), were diluted in blocking buffer and added to slides for 1 hour at room temperature. Slides were then washed three times in KCM-T (3x 10 minutes) before the addition of secondary antibody. Secondary antibodies (anti-mouse or anti-rabbit, Alexa Fluor 488 or 594) were also diluted in blocking buffer and added to slides for 1 hour at room temperature in the dark. Slides were washed as above, prior to mounting of cover slips using Vectashield mounting medium with DAPI. Slides were stored at 4°C until further analysis.

2.5 siRNA knockdown

K562 cells were suspended in culture medium to a density of 2 x 10^7 cells/mL. For each siRNA, 300 µL of cell suspension was transferred to an electroporation cuvette and the indicated siRNA was added to a final concentration of 500 nM. Electroporation was executed using the Fischer EPI2500 electroporator at 330 V and 10 mS pulse length. Cells were allowed to recover for 15 minutes at room

temperature, then transferred to fresh media in a T25 or T75 cell culture flask. All siRNA was used at a concentration of 500 nM, and handled under DNase- and RNase- free conditions.

2.6 SDS-PAGE

2.6.1 Preparation of whole cell extracts

Cells were first lysed in ice-cold extraction buffer [10 mM $MgCl_2$, 50 mM Tris-HCl, pH 7.4, 4 µM DTT and 50 µL/mL protease inhibitor cocktail (Sigma-Aldrich, UK)], then SDS was added to 0.25 % v/v to lyse the nuclear membrane. Chromatin-bound proteins were released by digestion of the DNA with 50 µg/mL DNase I, and incubated on ice for at least 10 minutes (until the viscosity of the lysate was reduced). The lysate was mixed 1:1 with solubilisation buffer [2% SDS, 20% glycerol, 5% β-mercaptoethanol, 0.6 M Tris-HCl, pH 7.2], and heated at 68°C for 10 minutes. Whole cell extracts were stored at -80°C until required.

2.6.2 Estimation of protein concentration

The total protein concentration of whole cell extracts was determined by Bradford assay using a standard BSA curve of known concentration. Whole cell lysates contain SDS, which can interfere with the Bradford dye reagent. To account for this, a 2 mg/mL BSA stock was initially diluted 1:1 with solubilisation buffer to give a final SDS concentration of 1% as in whole cell lysates. The 1 mg/mL BSA standard and whole cell lysates were then serial diluted 1:2 across a 96 well plate in dH_2O, together with a blank dH_2O control for background subtraction. Quickstart Bradford dye reagent (BioRad, UK) was added to each well and incubated at room temperature for 10 minutes. The absorbance of each well was measured using a BioRad microplate reader 550 at 595nm, and the average absorbance of the blank control wells was subtracted from each reading. The linear region of the blank-corrected BSA standard curve was used to generate a line equation to deduce x (protein concentration, mg/mL) from y (A_{595nm}). The estimated protein concentration from at least 3 dilutions of each sample was multiplied by the dilution factor, then combined to produce an average.

2.6.3 Polyacrylamide gel electrophoresis

Samples were mixed 1:1 with 2x SDS sample buffer and heated at 68°C for 10 minutes. Unless otherwise stated, samples were run on 4-20% gradient gels (Generon, or BioRad, UK) at 120 V, 500 mA for up to 2 hours using Tris-HEPES running buffer [60% HEPES, 35% TRIS, 5% SDS] or Tris-Glycine running buffer [Tris, Glycine, 5% SDS].

2.7 Western blotting

After gel electrophoresis, proteins were transferred to nitrocellulose membrane (Hybond ECL, GE Healthcare, UK) by wet transfer [25 mM Tris, 192 mM glycine, 20% v/v methanol, pH 8.3] at 100 V for 1 hour. The membrane was transferred to blocking buffer [5% milk in TBS-T; 20 mM Tris-HCl, pH 7.4, 150 mM NaCl and 0.1% Tween 20] for at least 1 hour, then incubated in primary antibody (diluted in blocking buffer as indicated in Table 1) for 1 hour at room temperature or 4°C overnight. The membrane was rinsed in TBS-T, followed by consecutive washes in TBS-T for 1x 15 minutes, and 2x 5 minutes. An HRP-linked secondary antibody (diluted 1:10,000 in blocking buffer) was added to the blot for 1 hour, followed by washes in TBS-T as above. The blot was incubated for 5 minutes with ECL detection reagent (BioRad, UK), and developed on film or using the LiCor c-DiGit scanner, as indicated.

2.7.1 Western blot quantification

Blots processed on film were scanned and quantified using Image Lab version 5.2.1 (BioRad), and blots processed using the LiCor c-Digit western blot scanner were quantified using Image Studio 5.0 (LiCor). The band density of each lane was normalised to the corresponding actin control, and protein levels were expressed as a percentage of the relevant control.

2.8 5-ethynyl uridine (EU) assay

EU is incorporated into newly synthesised mRNA transcripts and detected by a simple click chemistry reaction between an azide and an alkyne, followed by fluorescence microscopy. Cells were treated with the indicated concentration of α-Amanitin or DRB, followed by 1 hour incubation with 1 mM EU. Cells were adhered onto poly-L-lysine slides and fixed in 4% PFA for 10 minutes, prior to permeabilisation with KCM-T buffer for 15 minutes [120 mM KCl, 20 mM NaCl, 10

mM Tris-HCl pH 8.0, 1 mM EDTA, 0.1% Triton X-100]. The Click-iT reaction cocktail was prepared as specified in the manufacturer's instructions, and added to fixed cells for 30 minutes at room temperature, protected from light. Hoechst 33258 was used to stain DNA, and slides were mounted with coverslips and analysed by fluorescence microscopy.

2.9 Ubiquitin pulldown assays

The isolation of ubiquitinated proteins with TUBEs or MultiDsk2 was performed as described by Anindya et al. (Anindya *et al.*, 2007). 8 x 10^5 cells were lysed in 200 µL TENT buffer [20 mM Tris-HCl (pH 8.0), 2 mM EDTA, 150 mM NaCl, and 1% Triton X-100] containing 10 mM NEM and protease inhibitors. Where indicated, lysates were sonicated using the Bandelin Sonopuls HD 2070 for 5x 15 seconds (5 cycles at 20% power). Other lysis conditions tested during optimisation are outlined in Appendix Table 2. After centrifugation for 10 minutes at 14,000 g (15,300 rpm) and 4°C, the supernatant was collected and incubated in the presence of 1.8 µM GST-TUBE 1 or 2, or 0.2 µM MultiDsk2 for at least 20 minutes on ice (longer incubations were also performed from 1 hour to overnight, see Appendix Table 2). Lysates were then incubated with 35 µL GST-beads for 90 minutes at 4°C on rotation. Beads were collected by brief centrifugation, and the unbound supernatant collected as flow-through (FT). Beads were washed 1x in TENT buffer and 2x in PBS, then stored at -20°C overnight. Ubiquitinated proteins were eluted from the beads by boiling in 2x sample buffer at 95°C for 10 minutes.

2.10 Immunoprecipitation

2 x 10^6 cells were lysed in 200 µL RIPA buffer [50 mM Tris-HCl pH 7.4, 600 mM NaCl, 1% NP40, 0.4% sodium deoxycholate, 0.1% SDS, 1 mM $MgCl_2$, 1 mM EGTA] containing 10 mM N-ethylmaleimide (NEM, Sigma-Aldrich) and protease inhibitor cocktail (20 µL/mL, Sigma-Aldrich). Lysates were treated with DNase I (at a final concentration of at least 50 µg/mL) for 30 minutes on ice. Where indicated, lysates were also sonicated using three 5 second bursts and 35% power, with 3 second pauses, or treated with 250 units of benzonase for 15 minutes. The concentration of NaCl was reduced from 600 mM to 150 mM by diluting the lysate 1:4 in ice-cold dilution buffer (RIPA buffer without NaCl). The lysate was cleared by centrifugation at

15,300 g at 4°C for 10 minutes, and the supernatant was transferred to a clean tube. Lysate was stored at -80°C in 100 µL aliquots for subsequent IPs.

The indicated IP antibody was added to 100 µL cleared lysate and incubated at 4°C on rotation for 2 hours. 30 µL of protein A- or protein G- sepharose beads were washed 3x in dilution buffer and added to each lysate. Lysates were incubated with beads for 90 minutes at 4°C on rotation, and a small volume of supernatant was collected as flow-through (i.e. whole cell lysate after IP). The beads were washed 2x in dilution buffer and 1x in PBS, then used immediately or stored overnight at -20°C. Proteins were eluted from the beads by boiling at 95°C for 10 minutes in 40 µL 2x sample buffer, then analysed by SDS-PAGE and western blotting. Western blotting of IP samples was performed using the HRP-conjugated Veriblot detection reagent for IP (abcam, ab131366, used at 1:2000 in 5% milk-TBS-T) which detects non-reduced IgG, but not denatured IgG which is present as a result of the IP procedure. Therefore, the Veriblot reagent circumvents the detection of antibody heavy and light chains which can interfere with IP interpretation.

2.11 XTT potentiation assay

The XTT growth inhibition assay was performed using the XTT Cell Proliferation kit (Roche, Switzerland). Cells were seeded in 96 well plates at a density of 1×10^4 cells per well (Nalm-6) or 2×10^3 cells per well (K562) and incubated for 24 hours prior to drug treatment. Cells were treated with increasing concentrations of TOP2 poison alone or in combination with a fixed dose of various ubiquitination inhibitors (MLN7243, PYR-41, PRT4165 or HLI373) and incubated for 120 hours (>4 technical replicates). XTT reagent was mixed 50:1 with electron coupling reagent and added to each well, followed by a further 4 hours incubation at 37°C. Absorbance values (OD_{450nm}) were obtained using the BioRad 550 Microplate Reader and analysed using GraphPad Prism version 4.

A sub-lethal concentration (corresponding to 20% growth inhibition, IC_{20}) of each inhibitor was determined by XTT assay for use in combination experiments. To account for this, all data were normalised to the inhibitor-only control (no TOP2 poison) as 100% growth and a media-only control was used as 0% growth. Potentiation factors (Pf_{50}) were calculated as a ratio of the IC_{50} (concentration at 50% growth inhibition with respect to untreated controls) of TOP2 poison alone and the

IC_{50} of TOP2 poison in combination with ubiquitination inhibitor. Pf_{50} values were calculated for each separate experiment, and are therefore presented as the mean Pf_{50} factors of at least 3 biological replicates.

2.12 Micronucleus assay

Cells were treated with the indicated concentration of etoposide alone or in combination with MLN7243 for 48 hours (or MMS as a clastogenic positive control). Cell growth and viability was determined by cell counting and trypan blue exclusion. Cells were washed in PBS then incubated with 2 µg/mL ethidium monoazide bromide (EMA) for the labelling of apoptotic or necrotic cells. Cells were adhered to poly-L-lysine coated slides and fixed in 4% PFA for 10 minutes. After DNA staining with Hoechst 33258, micronuclei were visualised and counted manually by fluorescence microscopy.

2.13 Statistical analyses

Where multiple comparisons were required for two independent variables (drug treatment and time), two-way ANOVA followed by Bonferroni post-test was used to determine statistical significance. For comparison of two sample means, a one-tailed, unpaired t-test was used. All data are presented as the mean ± SEM, and p values >0.05 were considered statistically significant.

Chapter 3 Investigating the role of the ubiquitin-proteasome system in the processing of etoposide-induced TOP2-DNA complexes

3.1 Introduction

The repair of drug-stabilised TOP2-DNA complexes is particularly challenging due to the covalent 5'-phosphotyrosyl linkage between the TOP2 active site tyrosine and DNA. The TOP2-mediated double strand break (DSB) is concealed by the TOP2 protein, preventing its recognition by the DNA damage response machinery (Martensson *et al.*, 2003). Consequently, TOP2 must be removed from the TOP2-DNA complex before DSB repair can occur. Mechanisms of TOP2 removal include the nucleolytic cleavage of DNA ends by Mre11/CtIP (Hartsuiker *et al.*, 2009; Lee *et al.*, 2012; Aparicio *et al.*, 2016), or the degradation of TOP2 by the proteasome (Mao *et al.*, 2001; Zhang *et al.*, 2006; Fan *et al.*, 2008; Sunter *et al.*, 2010; Lee *et al.*, 2016). In the proteasomal pathway, TOP2 is degraded and the remaining TOP2 peptides can be removed from the 5' end by the 5'-phosphodiesterase, TDP2 (Cortes Ledesma *et al.*, 2009; Zeng *et al.*, 2011; Schellenberg *et al.*, 2012; Gao *et al.*, 2014). Alternatively, a proteasome-independent mechanism was recently described whereby TDP2 removes TOP2 adducts in co-operation with the ZATT SUMO ligase in a SUMO-dependent manner (Schellenberg *et al.*, 2017). However, this pathway did not contribute significantly to the clearance of TOP2-DNA complexes in the presence of functional proteasomes, and therefore the proteolytic removal of TOP2 is a major repair pathway.

Many studies have demonstrated a role for the proteasome in the degradation of TOP2 following exposure to TOP2 poisons. While earlier publications suggest that only TOP2B-DNA complexes are processed by the proteasome (Mao *et al.*, 2001; Isik *et al.*, 2003; Azarova *et al.*, 2007), it has since been shown that TOP2A is also degraded in response to TOP2 poisons, including etoposide, teniposide and mitoxantrone (Fan *et al.*, 2008; Alchanati *et al.*, 2009; Sunter *et al.*, 2010; Lee *et al.*, 2016). Inhibition of the proteasome also reduces the activation of etoposide-induced DNA damage signals including phosphorylation of histone H2AX, ATM, Chk1, Chk2 and the induction of RPA foci (Zhang *et al.*, 2006; Fan *et al.*, 2008; Tammaro *et al.*, 2013), consistent with the notion that TOP2 must be removed from DNA before the

DSB can be repaired. Interestingly, the proteasomal pathway of TOP2-DNA complex removal seems to involve transcription, as inhibition of transcription also prevents the proteasome-dependent degradation of TOP2 and the liberation of TOP2 poison-induced DSBs (Mao *et al.*, 2001; Fan *et al.*, 2008; Ban *et al.*, 2013; Tammaro *et al.*, 2013). It has therefore been hypothesised that TOP2 degradation is initiated upon collision of TOP2-DNA complexes with elongating RNA polymerase II.

Proteasomal degradation is often (but not always) preceded by the ubiquitination of the target protein. This is accomplished in a three-step cascade involving an E1 ubiquitin activating enzyme (UAE), E2 conjugating enzyme and E3 ligating enzyme (see Chapter 1, Figure 1.6). Indeed, the ubiquitin-dependent proteasomal degradation of TOP2A has been demonstrated in response to various stimuli, including HDAC inhibition (Chen *et al.*, 2011) and overexpression of the ECV ubiquitin ligase (Yun *et al.*, 2009). Importantly, the BMI1/RING1A ubiquitin ligase was recently implicated in the teniposide-induced proteasomal degradation of TOP2A-DNA complexes, which was inhibited upon siRNA knockdown or chemical inhibition of BMI1/RING1A (Alchanati *et al.*, 2009). The ubiquitin-dependence of TOP2B-DNA complex processing has also been suggested in studies employing a temperature sensitive murine cell line (ts85), whereby inactivation of the major ubiquitin activating enzyme (UAE1) disrupted the teniposide-induced degradation of TOP2B (Mao *et al.*, 2001). While the ubiquitin-dependent degradation of teniposide-induced TOP2A- and TOP2B-DNA complexes has been demonstrated by two independent research groups (Mao *et al.*, 2001; Alchanati *et al.*, 2009), another study showed that the etoposide-induced degradation of TOP2B-DNA complexes did not require UAE1 activity using the UAE1 temperature sensitive cell line previously used by Mao et al. (Ban *et al.*, 2013). The degradation of etoposide-induced TOP2B-DNA complexes was also unaffected by expression of mutated ubiquitin, whereby one or all lysine residues in ubiquitin are mutated to arginine and are therefore unable to form ubiquitin chains (Ban *et al.*, 2013), suggesting that ubiquitin is not required for the processing of etoposide-induced TOP2B-DNA complexes. While the only conceivable difference between the experiments performed by Mao et al. and Ban et al. was the use of teniposide or etoposide respectively, there are a number of caveats with these approaches which may lead to opposing results. Firstly, 15% of ubiquitin activating enzyme activity remains in ts85 cells at the non-permissive

temperature, which could be due to incomplete inactivation of UAE1 or due to the presence of a second ubiquitin activating enzyme, UBA6 (Finley *et al.*, 1984; Groettrup *et al.*, 2008). Therefore, some ubiquitination activity remains in ts85 cells which may account for the conflicting results between two separate studies (Mao *et al.*, 2001; Ban *et al.*, 2013). Secondly, cells overexpressing mutated ubiquitin also contain endogenous wild type ubiquitin, which may form polyubiquitin chains thereby leading to the degradation of TOP2B-DNA complexes. Thus, the requirement for ubiquitin in the proteasomal processing of TOP2-DNA complexes remains elusive.

3.2 Aims

The role of ubiquitin in the proteasomal processing of TOP2-DNA complexes was investigated in the current study by chemical inhibition and siRNA knockdown of the ubiquitin activating enzymes, UAE1 and UBA6. MLN7243 is a highly specific UAE inhibitor which inhibits UAE1 and UBA6 by forming a MLN7243-ubiquitin adduct (Misra *et al.*, 2017; Hyer *et al.*, 2018). The effect of UAE inhibition (as well as specific E3 ubiquitin ligase inhibition) on the processing of TOP2-DNA complexes was first investigated using the TARDIS assay to measure the removal of etoposide-induced TOP2 complexes from DNA. The γH2AX assay was then used to measure the appearance of etoposide-induced protein-free DSBs following UAE inhibition or siRNA knockdown. This approach was also used to investigate the role of transcription and the contribution of other known processing pathways, including the nucleolytic pathway and the proteasome-independent TDP2-mediated pathway.

3.3 Principles of the TARDIS assay

The TARDIS assay is an immunofluorescence-based technique used for the visualisation and quantification TOP2-DNA covalent complexes (Willmore *et al.*, 1998; Cowell *et al.*, 2011; Cowell and Austin, 2018). Unlike standard immunofluorescence where cells are fixed on microscope slides, drug-treated cells are first mixed with 1% low melting point agarose (Figure 3.1A). The agarose-suspended cells are then spread onto microscope slides and allowed to set on an ice-cooled glass plate. The cells, now embedded in agarose, are subjected to stringent lysis: first in buffer containing 1% SDS, then in 1 M NaCl. These steps remove most cellular constituents including proteins which are not covalently bound to the genomic DNA, which itself is too large to escape the agarose and so remains on the slide as a number of “nuclear ghosts”. The remaining DNA can then be probed for TOP2A and TOP2B covalent complexes using isoform-specific antibodies, followed by staining with corresponding fluorescent secondary antibodies and Hoechst DNA stain. TOP2-DNA complexes are detected by fluorescence microscopy through the co-localisation of TOP2 with DNA, and quantified by integrated fluorescence per nucleus. Therefore, the TARDIS assay is a statistically powerful technique which gives a cell-by-cell measurement of TOP2-DNA complex levels. Individual values are presented by scatter diagram, or median values are displayed on histograms (Figure 3.1B). Where data from replicate experiments has been combined, error bars represent the mean of medians ± SEM.

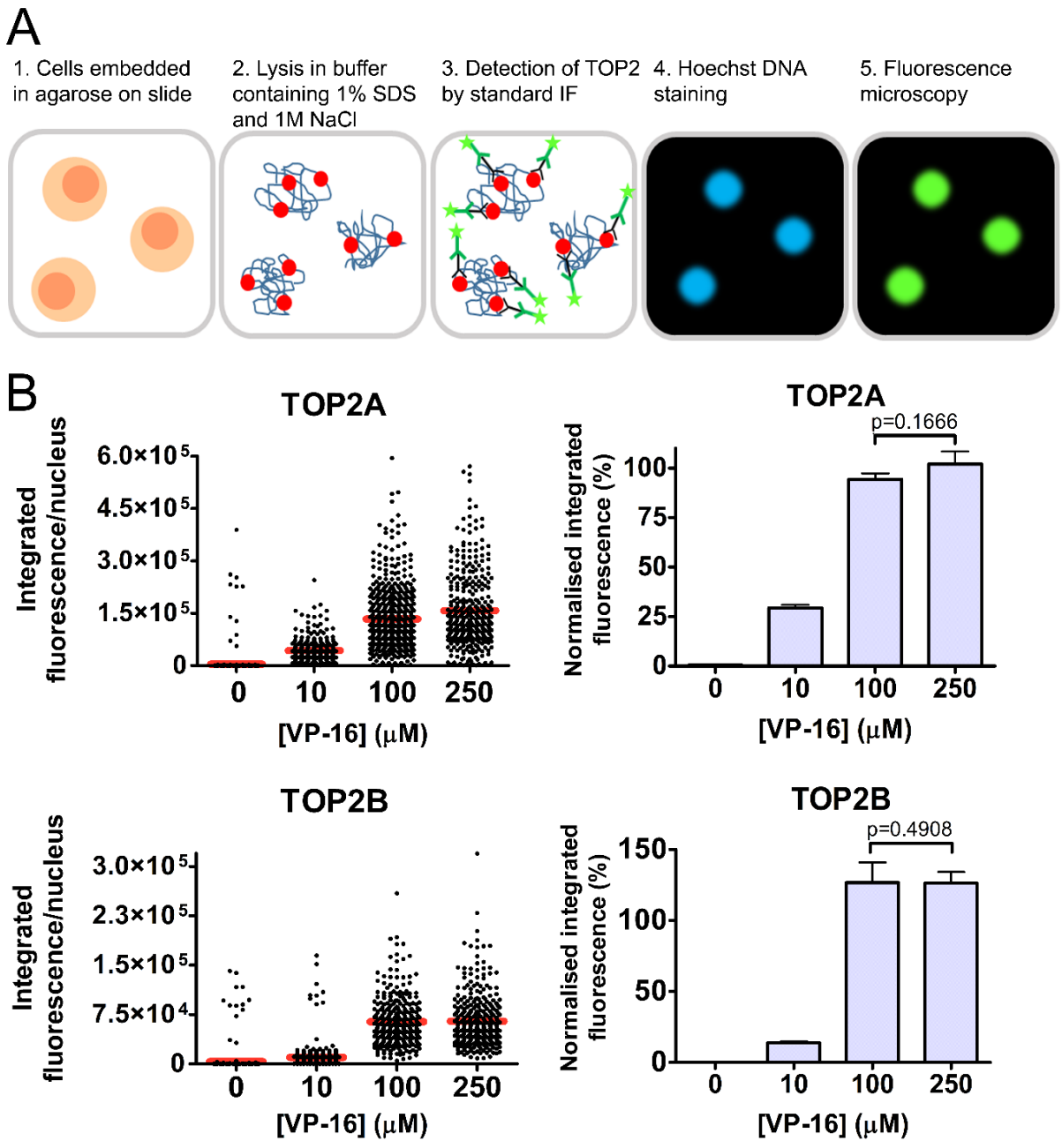

Figure 3.1. Visualisation and quantification of TOP2-DNA complexes using the TARDIS assay. A) Schematic representation of the TARDIS assay. B) Etoposide (VP-16) dose-response in K562 cells. Cells were incubated with 0.5% DMSO or the indicated concentration of etoposide for 2 hours (each containing equivalent volumes of DMSO), and levels of TOP2A- and TOP2B- DNA complexes were measured using the TARDIS assay. Scatter diagrams show the raw integrated fluorescence of individual nuclei from a single experiment, with a red line to denote median values. The data are then normalised to an additional 100 µM etoposide control (set as 100%), and statistical significance is determined using an unpaired t-test to compare normalised median values of triplicate experiments. Histograms represent the mean of median values ± SEM (n=3).

3.3.1 *Etoposide and teniposide dose-response*

Figure 3.1B shows the dose-dependent increase in levels of TOP2A- and TOP2B-DNA complexes in K562 cells following 2 hours treatment with etoposide, quantified using the TARDIS assay. In the absence of etoposide, non-covalently bound TOP2 is washed away during lysis and is therefore not detected in a DMSO-treated negative control. However, TOP2A- and TOP2B- DNA complexes are readily detectable upon treatment with 10 µM etoposide, with signals increasing in a dose-dependent manner up to 100 µM etoposide (Figure 3.1B). Levels of TOP2A- and TOP2B- DNA complexes become saturated at 100 µM, as no significant increase was detected between 100 µM and 250 µM etoposide ($p=0.1666$ and $p=0.4908$, respectively). 100 µM etoposide was therefore used in the TARDIS assay throughout this study, unless otherwise stated.

Existing studies investigating the role of the ubiquitin-proteasome system in the proteasomal processing of TOP2-DNA complexes generally involve the treatment of cells with high doses of etoposide (VP-16) at 250 µM, or the closely related TOP2 poison teniposide (VM-26) at 100 µM (Mao *et al.*, 2001; Zhang *et al.*, 2006; Fan *et al.*, 2008; Alchanati *et al.*, 2009; Ban *et al.*, 2013). Like etoposide, teniposide is an epipodophyllotoxin which differs only by the presence of an aromatic thiophene group at the C4 glycosidic ring (Figure 3.2A). To directly compare the efficacy of etoposide and teniposide, K562 cells were treated with increasing concentrations of etoposide or teniposide for 2 hours, and levels of TOP2-DNA complexes were determined by TARDIS assay. Levels of TOP2A- and TOP2B- DNA complexes became saturated at 10 µM teniposide, reflecting a ten-fold higher potency compared to etoposide (Figure 3.2B). Indeed, there were no significant differences between levels of TOP2A- and TOP2B- DNA complexes induced by 100 µM etoposide and 10 µM teniposide ($p=0.4591$ and $p=0.3298$, respectively). Consistent with this, the IC_{50} (concentration at 50% growth inhibition) of etoposide is approximately 7-fold higher than that of teniposide in K562 cells, as determined by XTT assay (Lee, 2016).

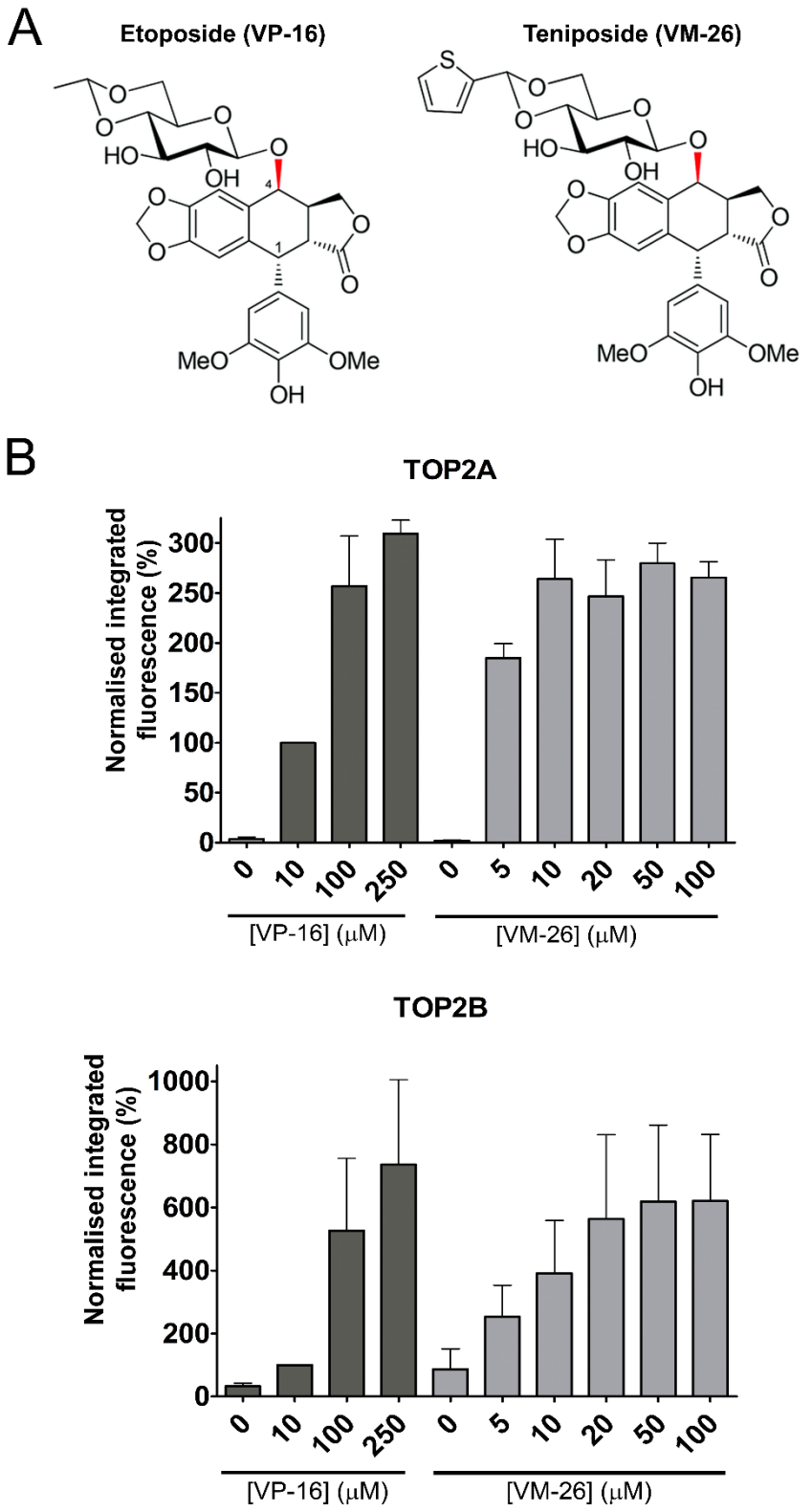

Figure 3.2. Induction of TOP2-DNA complexes by etoposide and teniposide, measured by TARDIS assay. A) Chemical structure of the epipodophyllotoxins etoposide and teniposide. B) K562 cells were treated with increasing concentrations of etoposide (VP-16) or teniposide (VM-26) for 2 hours, and levels of TOP2A- and TOP2B- DNA complexes were measured by TARDIS assay. All data are normalised to 10 µM etoposide as 100%, and error bars represent the mean of medians ± SEM of three replicate experiments (n=3).

3.3.2 *TARDIS removes non-covalently bound proteins from DNA*

It is expected that the rigorous lysis conditions used during the TARDIS procedure will remove all non-covalently bound proteins from DNA, including those that are tightly-associated with chromatin such as RNA polymerase II and Ku70/80. While the tight association of RNA polymerase II with DNA is essential for genome stability during gene transcription (Wilson *et al.*, 2013), Ku70/80 becomes sterically trapped on DNA following DNA damage and repair (Postow, 2011; van den Boom *et al.*, 2016).

To test whether all non-covalently bound chromatin proteins are removed during TARDIS lysis, slides were probed for all histones, Rpb1 (the RNA polymerase II large subunit) and Ku80. K562 cells were treated with 100 µM etoposide (VP-16) or 0.2 % v/v DMSO for 2 hours prior to the quantification of the indicated proteins by standard immunofluorescence (Figure 3.3, left panel) or TARDIS (Figure 3.3, right panel). As anticipated, TOP2A was detected on TARDIS slides following exposure to etoposide. Histones, Rpb1 and Ku80 were readily detectable by standard immunofluorescence, but were not detectable on TARDIS slides. Therefore, lysis in buffer containing SDS followed by incubation in buffer containing high salt is sufficient to remove non-covalently bound chromatin proteins from DNA, but does not disrupt the covalent 5'-phosphotyrosyl linkage between drug-stabilised TOP2 and DNA.

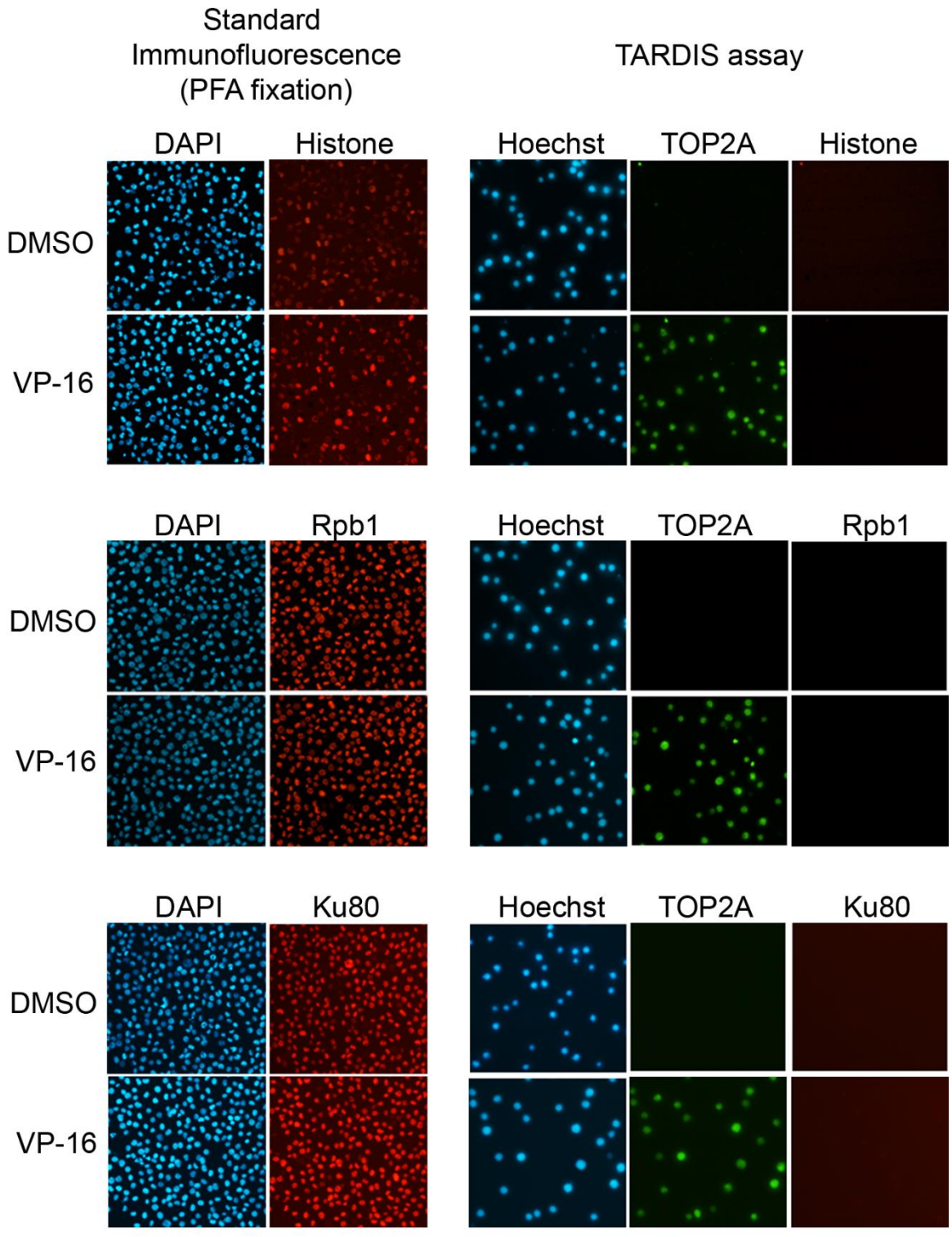

Figure 3.3. Removal of non-covalently bound chromatin-associated proteins (histones, RNA polymerase II and Ku80) from TARDIS slides. K562 cells were treated with 100 µM etoposide (VP-16) for 2 hours, prior to fixation in paraformaldehyde and standard immunofluorescence (left panel) or processing via the TARDIS assay (right panel). Slides were probed for TOP2A and other chromatin-associated proteins including all histones, RNA polymerase II large subunit (Rpb1), and Ku80.

3.4 Using the TARDIS assay to investigate the role of the ubiquitin-proteasome system in TOP2-DNA complex removal

The TARDIS assay can be used to measure the repair of drug-stabilised TOP2-DNA complexes by quantifying levels of TOP2-DNA complexes remaining following drug removal. With the exception of irreversible TOP2 poisons like clerocidin (Binaschi *et al.*, 1997) (see also Appendix Figure 1), drug-stabilised TOP2-DNA complexes are reversible upon drug washout. In this way, TARDIS has been used to measure the half-lives of TOP2A- and TOP2B- DNA complexes following treatment with various TOP2 poisons. For example, the half-lives of etoposide-induced TOP2A- and TOP2B- DNA complexes after etoposide washout are 40 minutes and 20 minutes, respectively (Willmore *et al.*, 2002; Errington *et al.*, 2004; Lee *et al.*, 2016). This approach can also be used to study the contribution of the proteasome to the active removal of TOP2 complexes from DNA, as treatment of cells with a proteasome inhibitor significantly slowed, though did not completely prevent, the reversal of TOP2A- and TOP2B- DNA complexes after etoposide removal (Lee *et al.*, 2016).

In the current study, the TARDIS assay was used to address the potential role of ubiquitination in the removal of TOP2 complexes from DNA. The role of the proteasome was confirmed using the proteasome inhibitor MG132, while the role of ubiquitination was examined using the ubiquitin activating enzyme (UAE) inhibitor MLN7243 (Figure 3.4A). Inhibition of the proteasome can be assessed through the accumulation of ubiquitinated proteins which would otherwise be degraded. In contrast, targeting of ubiquitin activating enzymes inhibits the very first step in the ubiquitination cascade, leading to the absence of ubiquitin conjugates. To test the efficacy of MG132 and MLN7243 in K562 cells, cells were treated with the indicated concentration of MG132 or MLN7243 for 2 hours, and levels of ubiquitin conjugates were measured by western blot. Treatment of cells with 1, 5, 10 and 20 μM MG132 induced the accumulation of ubiquitinated proteins compared to untreated control, while treatment with MLN7243 completely abolished levels of ubiquitin conjugates at all doses tested (Figure 3.4B).

To examine the effect of MG132 and MLN7243 on the removal of etoposide-induced TOP2 complexes from DNA, K562 cells were treated with 100 μM etoposide alone or in combination with 10 μM MG132 or 10 μM MLN7243 for 2 hours. Etoposide was

removed from the culture medium and cells were incubated for a further 2 hours in etoposide-free medium containing MG132 or MLN7243 (or DMSO) to maintain inhibition of the proteasome or ubiquitination, respectively. Levels of TOP2-DNA complexes were measured at 0, 0.5, 1 and 2 hours after etoposide removal using the TARDIS assay (Figure 3.4C).

As previously shown, co-treatment of cells with MG132 did not affect levels of TOP2A- or TOP2B- DNA complexes immediately following 2 hours continuous exposure to etoposide (0 hours after VP-16 removal) (Lee *et al.*, 2016). Similarly, inhibition of ubiquitination with the UAE inhibitor MLN7243 did not affect the induction of TOP2A- or TOP2B- DNA complexes by etoposide, suggesting that ubiquitination does not influence the formation of TOP2-DNA complexes. Neither MG132 nor MLN7243 treatment alone affected basal levels of TOP2-DNA complexes at any of the time points tested.

The effect of proteasome or UAE inhibition on the processing of TOP2-DNA complexes was determined by comparing levels of TOP2-DNA complexes at individual time points after etoposide removal, rather than by rate. Given that levels of TOP2-DNA complexes were not significantly different at the time of etoposide removal (0 hours), it was assumed that any differences in the level of TOP2-DNA complexes at subsequent time points was due to changes in the processing of TOP2-DNA complexes. While rate of TOP2 complex removal could theoretically be measured by comparing the gradient of each curve, more data points (within 2 hours of etoposide removal) are required to accurately determine the rate of TOP2-DNA complex removal. Instead, a two-way ANOVA was used to statistically compare each curve, which accounts for both variables affecting TOP2-DNA complex levels (i.e. drug treatment and time).

As expected, levels of TOP2-DNA complexes reduced with time following the removal of etoposide from the culture medium (Errington *et al.*, 2004; Lee *et al.*, 2016), likely reflecting the combined effect of the spontaneous reversal of complexes (i.e. completion of the TOP2 reaction mechanism upon dissociation of etoposide) and the active removal of TOP2 from DNA by various processing mechanisms including proteasomal degradation. Consistently, levels of remaining TOP2A-DNA complexes were significantly increased in the presence of MG132 at 0.5, 1 and 2

hours following etoposide removal ($p<0.05$), while remaining TOP2B-DNA complexes were significantly increased after 0.5 hours ($p<0.001$). Notably, the reversal of TOP2B-DNA complexes is faster than that of TOP2A-DNA complexes both in the presence and absence of MG132, consistent with the half-lives of etoposide-induced TOP2A- and TOP2B-DNA complexes reported by others (Errington *et al.*, 2004; Lee *et al.*, 2016). Although slowed, the removal of etoposide-induced TOP2 complexes from DNA still occurred in the presence of MG132. Indeed, levels of TOP2B-DNA complexes return to background levels within 1 to 2 hours of etoposide removal even in the presence of MG132, representing proteasome-independent mechanisms of TOP2-DNA complex removal or spontaneous complex reversal following completion of the TOP2 reaction cycle.

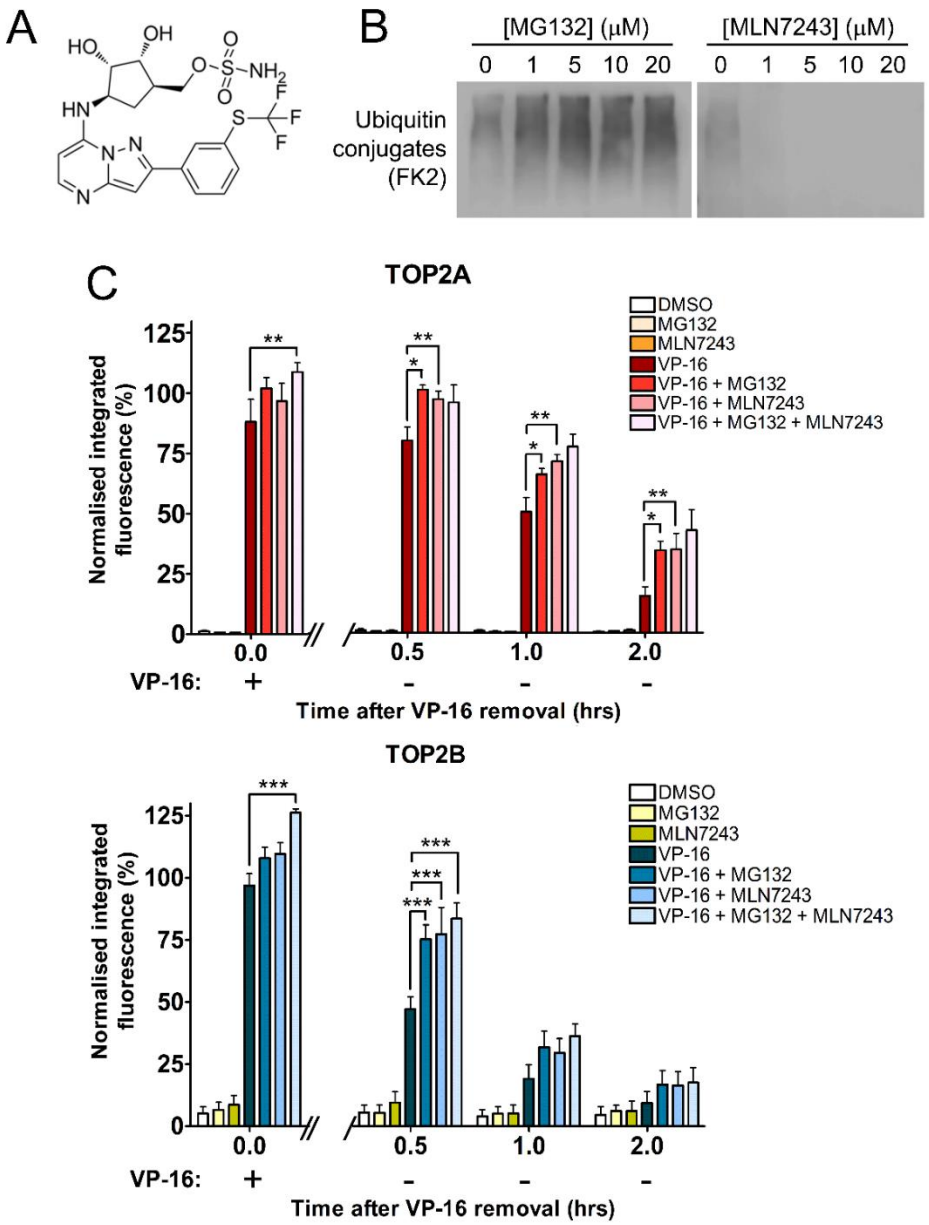

Figure 3.4. Inhibition of the ubiquitin-proteasome system and the effect on etoposide-induced TOP2-DNA complex levels. A) Chemical structure of MLN7243, an inhibitor of ubiquitin activating enzymes (UAE). B) Dose-response of the proteasome inhibitor MG132 and UAE inhibitor MLN7243. K562 cells were treated with the indicated concentration of MG132 or MLN7243 for 2 hours. Whole cell extracts were electrophoresed and total levels of ubiquitination were detected by western blot. Blots were probed with the anti-ubiquitin antibody clone FK2, which recognises all conjugated ubiquitin (mono- and poly-ubiquitinated proteins). C) The effect of MG132 and MLN7243 on levels of TOP2-DNA complexes was measured by TARDIS assay. K562 cells were treated for 2 hours with 100 μM etoposide (VP-16) alone or in combination with 10 μM MG132 and/or 10 μM MLN7243. Etoposide was removed from the culture medium, and cells were incubated for up to 2 hours in etoposide-free medium but in the continued presence of 0.1% v/v DMSO, 10 μM MG132 and/or 10 μM MLN7243. Levels of TOP2A- and TOP2B- DNA complexes were measured following 2 hours continuous drug exposure (0 hours after VP-16 removal) or 0.5, 1 or 2 hours incubation in etoposide-free medium. Statistical significance was determined by two-way ANOVA with Bonferroni post-test to compare replicate means (n=3 for TOP2A, n=6 for TOP2B). Averages represent mean of medians ± SEM.

Interestingly, levels of remaining etoposide-induced TOP2A- and TOP2B- DNA complexes were also significantly increased in the presence of MLN7243 following etoposide removal, indicating reduced TOP2 complex processing. Similarly to proteasome inhibition, levels of remaining TOP2A-DNA complexes were significantly increased at 0.5, 1 and 2 hours after etoposide removal ($p<0.01$), and levels of remaining TOP2B-DNA complexes were increased after 0.5 hours ($p<0.001$). To determine whether each inhibitor exerts its effects via the same pathway, etoposide-treated cells were also co-incubated with both 10 µM MG132 and 10 µM MLN7243. Levels of remaining TOP2A- and TOP2B- DNA complexes were not significantly increased by both inhibitors compared to each inhibitor alone, suggesting that the roles of the proteasome and ubiquitin activating enzymes are epistatic. Although levels of TOP2-DNA complexes were not affected after etoposide removal, administration of both inhibitors together did significantly increase the initial levels of TOP2A- and TOP2B- DNA complexes induced by etoposide immediately following 2 hours continuous exposure (0 hours after VP-16 removal, $p<0.01$ and $p<0.001$, respectively).

To further investigate the role of ubiquitin in the removal of TOP2-DNA complexes, the TARDIS assay was repeated following co-incubation of cells with etoposide and one of two additional UAE inhibitors, PYR-41 or PYZD-4409. K562 cells were treated with etoposide alone or in combination with 10 µM PYR-41, followed by the removal of etoposide and incubation in the continued presence of DMSO or PYR-41 for up to 2 hours. Levels of TOP2A- and TOP2B- DNA complexes were measured following 0, 0.5, 1 and 2 hours after etoposide removal. Consistently, levels of remaining TOP2A-DNA complexes were significantly higher in the presence of PYR-41 after 1 or 2 hours incubation in etoposide-free medium ($p<0.01$), and levels of TOP2B-DNA complexes were significantly higher after 1 hour ($p<0.05$) (Figure 3.5A). Similarly, treatment of cells with 10 µM PYZD-4409 also increased levels of remaining TOP2A-DNA complexes following 1 or 2 hours incubation in etoposide-free medium ($p<0.001$), and increased levels of remaining TOP2B-DNA complexes after 1 hour ($p<0.001$) (Figure 3.5B).

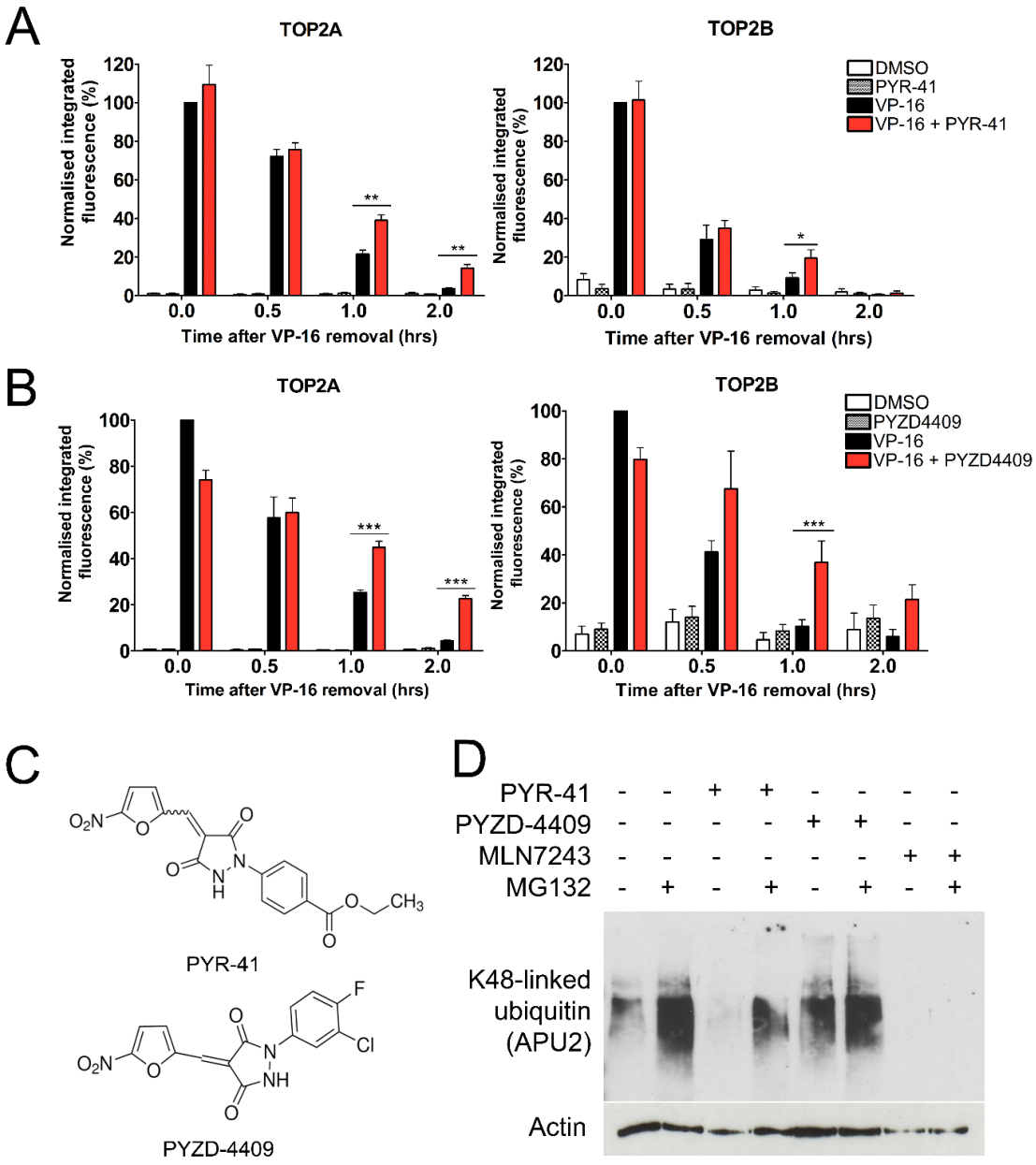

Figure 3.5. Effect of UAE inhibitors PYR-41 and PYZD-4409 on levels of etoposide-induced TOP2-DNA complexes. A) K562 cells were treated for 2 hours with 100 µM etoposide (VP-16) alone or in combination with 10 µM PYR-41. Cells were collected (0 hours after VP-16 removal) or incubated for 0.5, 1 or 2 hours in etoposide-free medium containing 0.1% v/v DMSO or 10 µM PYR-41 to maintain UAE inhibition. B) K562 cells were treated with 100 µM etoposide alone or in combination with 10 µM PYZD-4409 for 2 hours followed by up to 2 hours incubation in etoposide-free medium containing 0.1% v/v DMSO or 10 µM PYZD-4409. Levels of TOP2A- and TOP2B- DNA complexes were measured using the TARDIS assay, and statistical significance was determined by two-way ANOVA with Bonferroni post-test (n=3). Values represent the mean of median ± SEM, normalised to the average TOP2-DNA complex levels at 2 hours continuous exposure to 100 µM etoposide (0 hours after VP-16 removal). C) Chemical structures of UAE inhibitors, PYR-41 and PYZD-4409. D) Western blot to compare total levels of K48-linked ubiquitin conjugates (APU2 antibody) following treatment with PYR-41, PYZD-4409 or MLN7243. K562 cells were treated for 2 hours with 10 µM of PYR-41, PYZD-4409 or MLN7243 alone or in combination with 10 µM MG132, as indicated.

PYR-41 and PYZD-4409 are structurally distinct from MLN7243 (Figure 3.5C), and therefore the slowed removal of TOP2-DNA complexes by all three UAE inhibitors is unlikely to be due to the same off-target effect. To compare the efficacy of PYR-41 and PYZD-4409 with MLN7243, levels of K48-linked ubiquitin conjugates were measured by western blot as an indication of UAE inhibition. K562 cells were treated for 2 hours with 10 µM PYR-41, 10 µM PYZD-4409 or 10 µM MLN7243 alone or in combination with 10 µM MG132 (for enrichment of ubiquitinated proteins). As expected, levels of K48-linked ubiquitin were increased following MG132 treatment (Figure 3.5D). PYR-41 alone reduced levels of K48-linked ubiquitin compared to untreated control, though did not prevent the MG132-induced accumulation of ubiquitinated proteins. Ubiquitination was not noticeably affected by 10 µM PYZD-4409 alone, and PYZD-4409 did not affect the accumulation of ubiquitinated proteins upon MG132 treatment. Strikingly, K48-linked ubiquitination of proteins was not detectable following MLN7243 treatment alone or in combination with MG132. Therefore, MLN7243 is a highly effective UAE inhibitor which was used for the duration of this study.

3.4.1 *siRNA knockdown of ubiquitin activating enzymes*

The role of ubiquitin in the removal of TOP2-DNA complexes was also investigated following siRNA knockdown of the major UAE, UAE1. K562 cells were transfected with 500 nM non-coding (CON) siRNA or 500 nM UAE1 siRNA by electroporation, and levels of UAE1 protein were measured by western blot (Figure 3.6A). UAE1 levels were reduced to 1% in UAE1 siRNA knockdown cells after 72 hours compared to control siRNA-treated cells. Thus, all subsequent experiments were performed in UAE1 knockdown cells 72 hours after electroporation.

CON siRNA or UAE1 siRNA knockdown cells were treated with 100 µM etoposide for 2 hours, followed by etoposide washout and 2 hours further incubation in drug-free medium. Levels of TOP2A- and TOP2B- DNA complexes were measured by TARDIS assay at 0, 0.5, 1 and 2 hours after etoposide removal. Unlike chemical inhibition of UAE, levels of etoposide-induced TOP2A-DNA complexes were not significantly affected by UAE1 knockdown at any of the time points tested (Figure 3.6B). Initial levels of TOP2B-DNA complexes were significantly increased in UAE1 knockdown cells following 2 hours continuous exposure to etoposide ($p<0.001$, 0

hours after VP-16 removal), but returned to control levels at 0.5, 1 and 2 hours after etoposide removal. Figure 3.6C shows the level of UAE1 protein and K48-linked ubiquitin conjugates in control versus UAE1 knockdown cells from a single TARDIS experiment, measured by western blot. As in previous experiments (Figure 3.6A) siRNA knockdown was highly efficient, as UAE1 was not detectable in UAE1 knockdown cells (0%, Figure 3.6C). However, 39% of K48-linked ubiquitination still occurred suggesting the presence of remaining UAE activity.

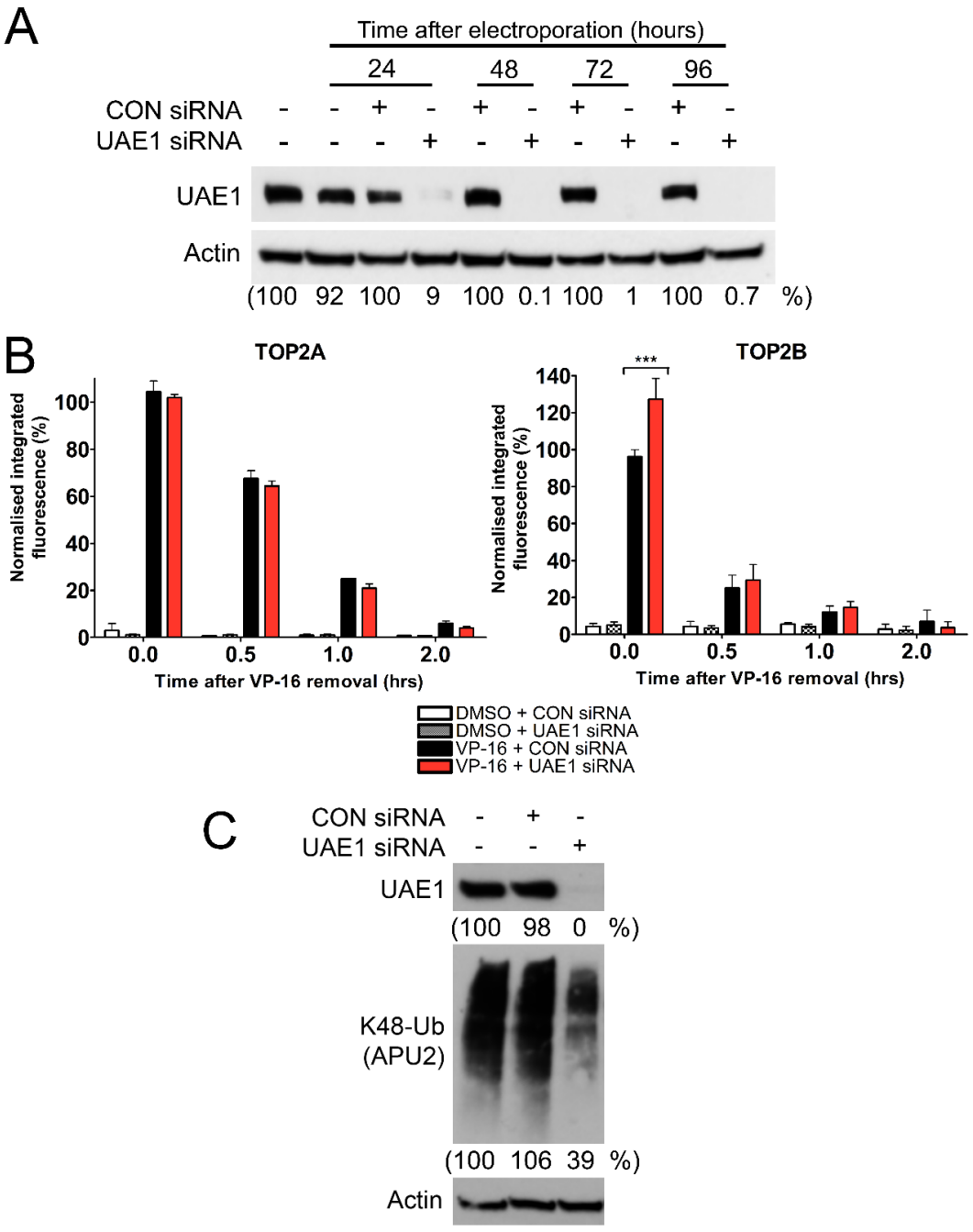

Figure 3.6. siRNA knockdown of ubiquitin activating enzyme 1 (UAE1) and the effect on TOP2-DNA complex levels measured by TARDIS assay. A) K562 cells were transfected with 500 nM non-coding siRNA (CON siRNA) or 500 nM UAE1 siRNA by electroporation. Cells were collected following 24, 48, 72 and 96 hours after electroporation and levels of UAE1 protein were tested by western blot. UAE1 levels were quantified and expressed as the percentage remaining compared to the corresponding CON siRNA control. B) CON siRNA or UAE1 siRNA knockdown cells were treated with 100 µM etoposide (VP-16) for 2 hours, followed by 2 hours incubation in etoposide-free medium. TOP2A- and TOP2B- DNA complex levels were measured by TARDIS assay at 0, 0.5, 1 and 2 hours after etoposide removal, and statistical comparisons were made by two-way ANOVA followed by Bonferroni post-test (n=3). C) Levels of UAE1 protein and K48-linked ubiquitin in CON siRNA and UAE1 siRNA knockdown cells from a single experiment in B were measured by western blot. Protein levels were quantified and expressed as the percentage remaining compared to a non-electroporated control, as described in Chapter 2, section 2.7.1.

UBA6 is a second and more recently discovered UAE enzyme which is also inhibited by MLN7243 (Hyer *et al.*, 2018). Like UAE1, UBA6 is essential in mice, suggesting that UAE1 and UBA6 are required for separate functions and are not simply redundant enzymes (Groettrup *et al.*, 2008). Interestingly, the E2 conjugating enzyme Use1 is charged by UBA6 but not UAE1, implying the existence of distinct ubiquitin activation pathways (Jin *et al.*, 2007). Furthermore, UBA6 is required for the ubiquitination of a defined set of substrates, indicating a level of specificity which exists at the level of ubiquitin activation (Liu *et al.*, 2017). Therefore, the effect of MLN7243, but not UAE1 siRNA, on the removal of TOP2-DNA complexes could be attributed to inhibition of UBA6-dependent ubiquitination. To test this, K562 cells were transfected with 500 nM UBA6 siRNA by electroporation. Figure 3.7A shows the levels of UBA6 in CON siRNA-treated versus UBA6 siRNA-treated cells at 24, 48, 72 and 96 hours after electroporation. UBA6 levels were reduced to 28% after 24 hours compared to CON-siRNA treated cells, and were undetectable after 72 hours (0%). Therefore, all experiments with UBA6 siRNA knockdown cells were performed 72 hours after electroporation.

CON siRNA or UBA6 siRNA knockdown cells were treated with 100 µM etoposide for 2 hours, followed by etoposide washout and incubation in drug-free medium. Levels of TOP2A- and TOP2B- DNA complexes were measured at 0, 0.5, 1 and 2 hours after etoposide removal using the TARDIS assay (Figure 3.7B). Levels of TOP2A-DNA complexes (both in the presence and absence of etoposide) were not affected by UBA6 knockdown at any of the time points tested. Unlike UAE1 knockdown cells in which the levels of TOP2B-DNA complexes were increased after 2 hours of etoposide exposure, TOP2B-DNA complex levels were unaffected in UBA6 knockdown cells at all time points tested. Therefore, the normal removal of TOP2-DNA complexes in UAE1 siRNA knockdown cells is not due to UBA6-dependent ubiquitination.

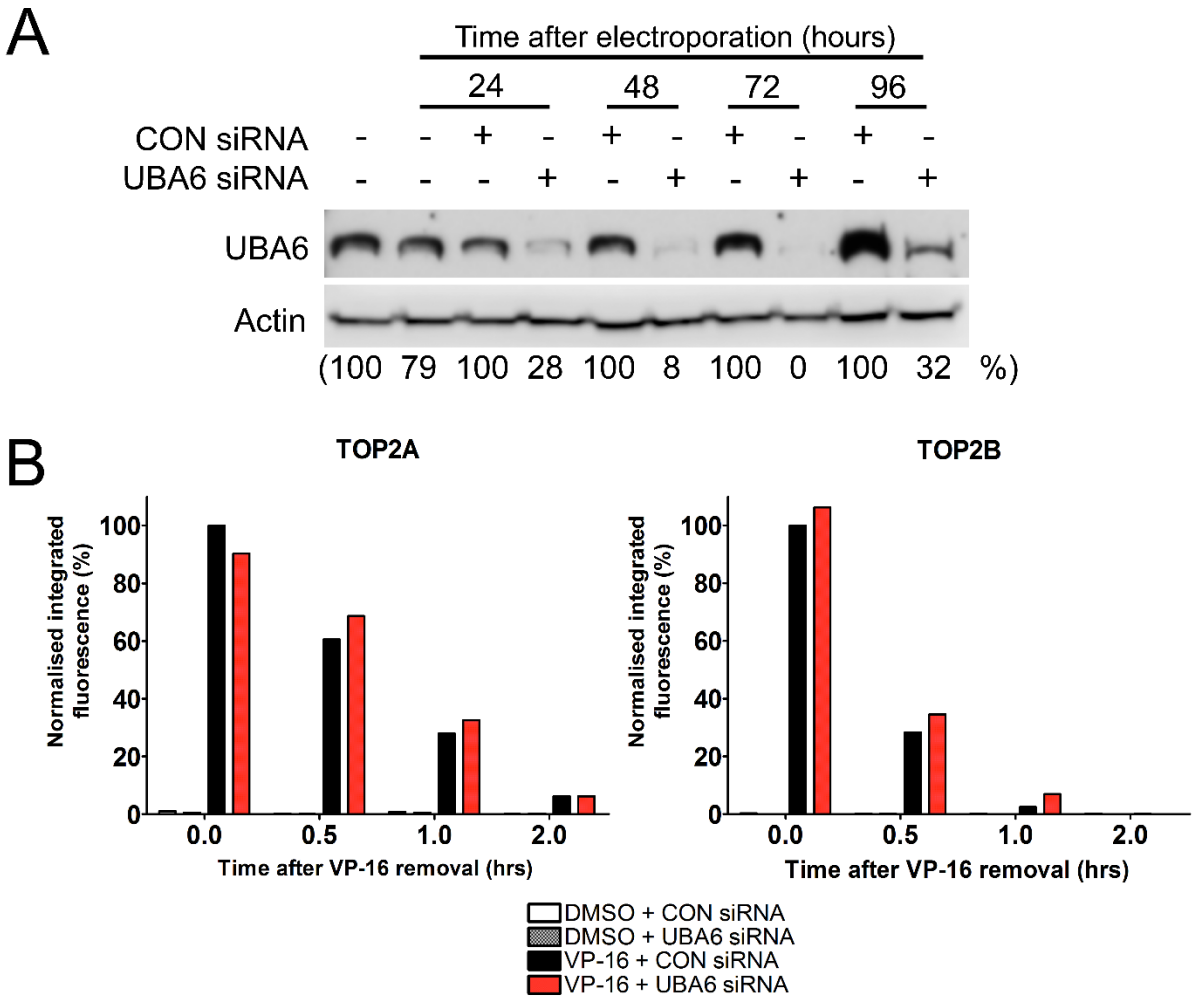

Figure 3.7. siRNA knockdown of ubiquitin activating enzyme UBA6 and the effect on TOP2-DNA complex levels measured by TARDIS assay. A) K562 cells were transfected with 500 nM non-coding siRNA (CON siRNA) or 500 nM UBA6 siRNA by electroporation. Western blotting was used to measure levels of UBA6 protein at 24, 48, 72 and 96 hours after electroporation. UBA6 levels were quantified and expressed as the percentage remaining compared to the corresponding CON siRNA control, as described in Chapter 2, section 2.7.1. B) CON siRNA and UBA6 siRNA knockdown cells were treated with 100 µM etoposide (VP-16) for 2 hours, followed by 2 hours incubation in etoposide-free medium. Levels of TOP2A- and TOP2B- DNA complexes were measured at 0, 0.5, 1 and 2 hours after etoposide removal. Averages represent the mean of median integrated fluorescence values from a single experiment (n=1), normalised to average TOP2-DNA complex levels at 2 hours continuous exposure to 100 µM etoposide (0 hours after VP-16 removal).

It is possible that the normal reversal of TOP2-DNA complexes in UAE1 knockdown or UBA6 knockdown cells is due to residual levels of activated ubiquitin or compensatory ubiquitin activation by the alternative UAE. To more completely knockdown levels of activated ubiquitin, the TARDIS assay was also performed in K562 cells following double siRNA knockdown of UAE1 and UBA6. CON siRNA and double UAE1/UBA6 siRNA knockdown cells were treated with 100 µM etoposide for 2 hours, followed by etoposide washout and incubation in drug-free medium. Levels

of TOP2A-DNA complexes were not affected by UAE1/UBA6 siRNA knockdown, while a small increase in TOP2B-DNA complexes was detectable 0 hours after etoposide removal in a single experiment (Figure 3.8A).

Despite what appears to be an efficient siRNA knockdown of both UAE1 and UBA6, and the subsequent reduction in levels of K48-linked ubiquitin conjugates (Figure 3.8B), it is plausible that some functional UAE activity remains in UAE1/UBA6 knockdown cells. In contrast, it is anticipated that chemical inhibition of UAE enzymes efficiently blocks the function of any protein present. To compare the effectiveness of double UAE1/UBA6 siRNA knockdown with chemical inhibition by MLN7243, total levels of ubiquitinated proteins were measured by western blot as an indication of UAE activity (Figure 3.8C). Total levels of ubiquitin conjugates were reduced in UAE1/UBA6 knockdown cells compared to control cells, as expected (compare lane 1 with lane 3). Cells were also treated for 2 hours with 10 µM MG132 (or 0.1% v/v DMSO) for the enrichment of ubiquitinated proteins upon proteasome inhibition. The MG132-induced accumulation of ubiquitin conjugates was substantially reduced but still detectable in UAE1/UBA6 knockdown cells (compare lane 2 with lane 4). UAE activity was also examined in non-transfected K562 cells (no siRNA) treated with 10 µM MG132 alone or in combination with 10 µM MLN7243. Unlike UAE1/UBA6 knockdown cells, no ubiquitin conjugates were detectable in MLN7243-treated cells even in the presence of MG132 (lane 7). Together, this suggests that chemical inhibition of UAE activity by MLN7243 is more complete than siRNA knockdown of UAE enzymes, which may explain the differences observed in the TARDIS assay.

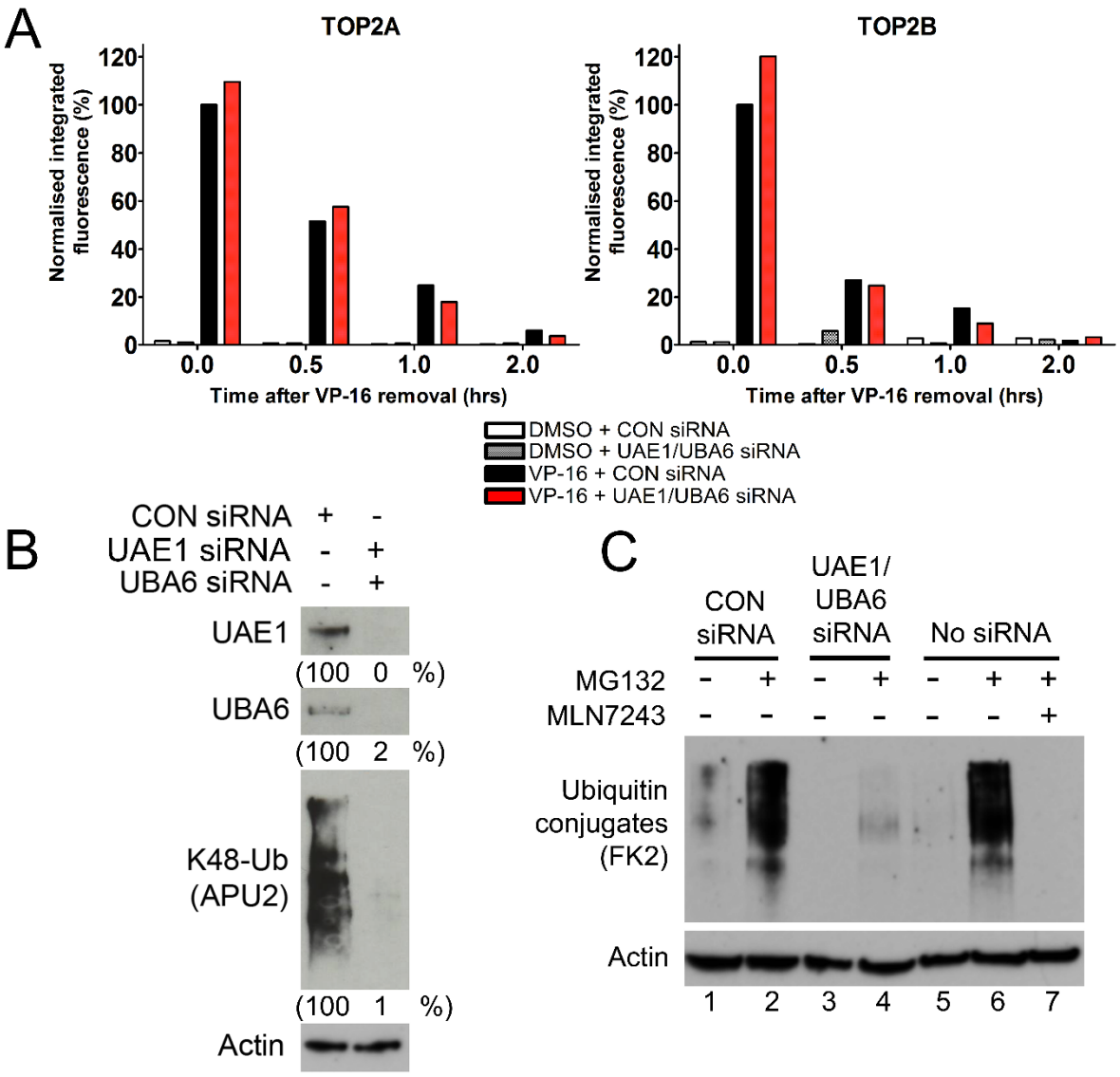

Figure 3.8. Investigating the effect of double siRNA knockdown of UAE1 and UBA6 on levels of TOP2-DNA complexes using the TARDIS assay. A) CON siRNA or double UAE1/UBA6 siRNA knockdown cells were treated with 100 µM etoposide (VP-16) for 2 hours followed by 2 hours incubation in etoposide-free medium. Levels of TOP2A- and TOP2B- DNA complexes were measured at 0, 0.5, 1 and 2 hours after etoposide removal. Averages represent the mean of median integrated fluorescence values from a single experiment (n=1), normalised to the average level of TOP2-DNA complexes at 2 hours continuous exposure to 100 µM etoposide (0 hours after VP-16 removal). B) Western blot to show UAE1 and UBA6 protein levels in CON siRNA and double UAE1/UBA6 siRNA knockdown cells. Blots were also probed for K48-linked ubiquitin as an indication of UAE activity. Protein levels were quantified and expressed as the percentage remaining compared to the corresponding CON siRNA control. C) Ubiquitination assay to compare UAE activity in double UAE1/UBA6 siRNA knockdown cells with MLN7243-treated cells. K562 cells treated with control siRNA or UAE1 and UBA6 siRNA were incubated with 10 µM MG132 to induce the accumulation of ubiquitinated proteins. Non-transfected cells were also treated with 10 µM MG132 alone or in combination with 10 µM MLN7243. Western blotting was used to compare total levels of ubiquitination by probing with anti-ubiquitin antibody clone FK2, which detects all conjugated ubiquitin (mono- and poly-ubiquitinated proteins).

3.4.2 *Effect of the Nedd8-activating enzyme inhibitor MLN4924 on levels of TOP2-DNA complexes*

The high selectivity of MLN7243 for ubiquitin activating enzymes was recently demonstrated by Misra et al. (Misra *et al.*, 2017). Nonetheless, other ubiquitin-like activating enzymes (such as the SUMO activating enzyme SAE, or Nedd8 activating enzyme, NAE) share similar structures to UAE and may therefore be inhibited by the relatively high dose of MLN7243 used in this study. However, treatment of cells with 10 µM MLN7243 did not affect the SUMOylation of TOP2-DNA complexes, as detailed in Chapter 4 (Figure 4.12). To test whether MLN7243 slows the removal of TOP2-DNA complexes through non-specific targeting of NAE, K562 cells were treated with 100 µM etoposide alone or in combination with 3 µM MLN4924, a highly specific NAE inhibitor (Soucy *et al.*, 2009). After 2 hours continuous exposure to etoposide, etoposide was removed from the culture medium and cells were incubated for up to 2 hours in the continued presence of 3 µM MLN4924 or DMSO. Levels of TOP2-DNA complexes were measured 0, 0.5, 1 and 2 hours after etoposide removal using the TARDIS assay.

Co-incubation of cells with MLN4924 did not significantly affect levels of TOP2A- or TOP2B- DNA complexes at any of the time points tested (Figure 3.9). This suggests that the accumulation of TOP2-DNA complexes observed with the UAE inhibitor MLN7243 is not due to inhibition of the Nedd8 activating enzyme. Neddylation is required for the ubiquitination of proteins by cullin-RING E3 ubiquitin ligases (Boh *et al.*, 2011). Therefore, this also suggests that ubiquitination by cullin-RING E3 ligases is not involved in the ubiquitin-dependent removal of TOP2-DNA complexes.

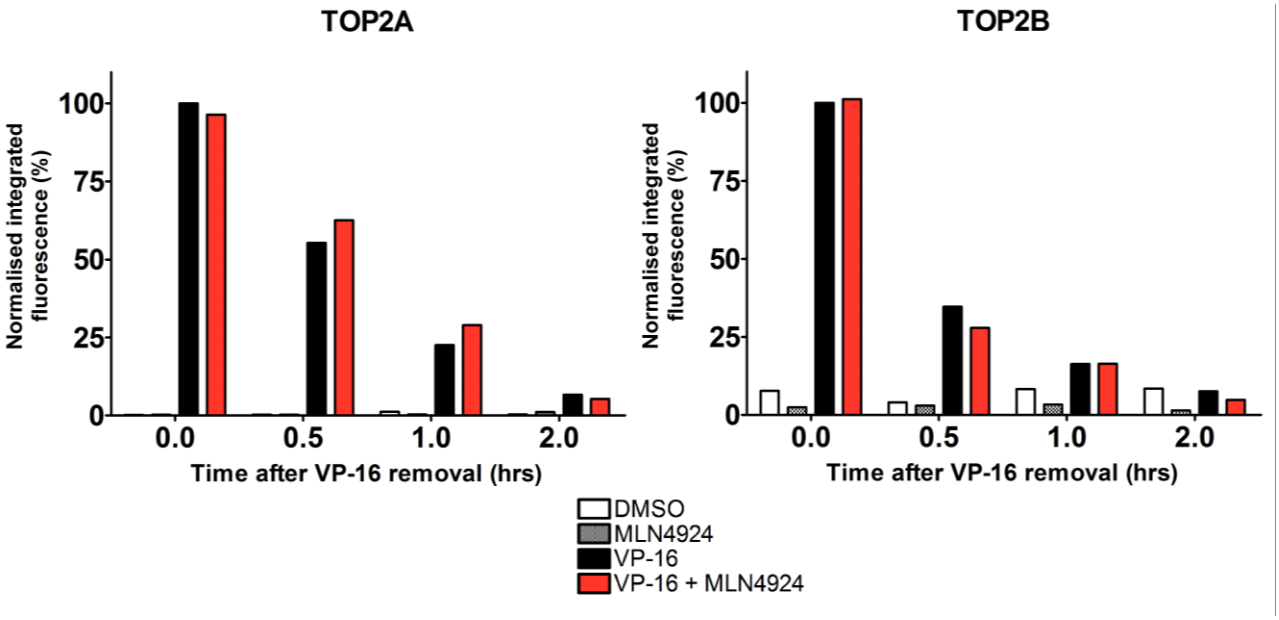

Figure 3.9. Effect of the Nedd8 activating enzyme (NAE) inhibitor MLN4924 on levels of TOP2-DNA complexes, measured using the TARDIS assay. K562 cells were treated with 100 µM etoposide alone or in combination with 3 µM MLN4924, a highly specific NAE inhibitor. After 2 hours etoposide treatment, cells were then incubated in etoposide-free media containing 0.1% DMSO or 3 µM MLN4924. Levels of TOP2A- and TOP2B-DNA complexes were measured by TARDIS assay up to 2 hours after etoposide removal (n=1).

In summary, the removal of TOP2A- and TOP2B- DNA complexes is significantly slowed following chemical inhibition of UAE1 and UBA6 in a manner that is epistatic with the proteasomal processing pathway. This effect was observed using three separate UAE inhibitors, the most potent of which was MLN7243. Furthermore, the ubiquitin-dependent removal of TOP2-DNA complexes does not involve a cullin-RING E3 ligase, as TOP2-DNA complex levels were unaffected by the neddylation inhibitor, MLN4924. Levels of etoposide-induced TOP2B-, but not TOP2A-, DNA complexes were increased both after single siRNA knockdown of UAE1 and combined knockdown of UAE1 and UBA6. Western blot analysis of total ubiquitination levels suggests that the normal reversal of TOP2-DNA complexes in UAE1/UBA6 knockdown cells after etoposide removal is due to residual UAE activity, which was present in siRNA knockdown cells but not in MLN7243-treated cells. Together, this indicates that the proteasomal pathway of TOP2-DNA complex processing is ubiquitin-dependent.

3.5 A study of TOP2 poison-induced proteasomal degradation of TOP2 isoforms following continuous drug exposure

The TOP2 poison-induced degradation of TOP2 was first demonstrated by western blot of total TOP2 protein, which showed a proteasome-dependent decrease in total TOP2 levels with continuous exposure to the TOP2 poison teniposide (Mao *et al.*, 2001) and was later demonstrated following etoposide treatment (Zhang *et al.*, 2006; Azarova *et al.*, 2007; Fan *et al.*, 2008; Ban *et al.*, 2013; Lee *et al.*, 2016). This approach was used here with the intention of testing the effect of UAE inhibition on the TOP2 poison-induced degradation of TOP2 isoforms.

3.5.1 *Effect of teniposide and etoposide on total TOP2 levels measured by western blot*

K562 cells were treated with 100 µM etoposide alone or in combination with 50 µM MG132 for up to 8 hours, and TOP2A levels were measured by western blot. Cell lysates were prepared with DNase I for the digestion of genomic DNA and extraction of TOP2-DNA complexes, which are otherwise unable to enter the gel for electrophoresis (leading to a band depletion effect (Mao *et al.*, 2001)). As reported in the literature, levels of TOP2A were reduced with time following exposure to etoposide compared to DMSO-treated solvent control cells (Figure 3.10A). While MG132 alone did not affect levels of TOP2A protein, proteasome inhibition prevented the etoposide-induced decrease in TOP2A levels. Therefore, the degradation of TOP2A upon continuous etoposide exposure appears to be proteasome dependent. However, although this result was observed in many technical replicates (western blots) of the biological sample shown in Figure 3.10, etoposide-induced degradation of TOP2A was not observed in another biological replicate (see Appendix Table 1 for details). Furthermore, levels of TOP2A were noticeably increased following exposure to 1% v/v DMSO compared to untreated (0 hour) control cells which may interfere with the accurate interpretation of data (Figure 3.10A). Therefore, higher stock concentrations of etoposide and MG132 were used in subsequent experiments to minimise the final solvent concentration. In addition to high variability, much of the data obtained could not be used due to technical issues such as actin failure or lack of antibody signal (see details in Appendix Table 1). In particular, little data was obtained regarding the effect of etoposide treatment on

TOP2B levels due to lack of signal with the TOP2B antibody, 4555. Because of this, only a single blot was acquired showing the levels of TOP2B following exposure to 100 µM etoposide, and is shown in Figure 3.10B. TOP2B levels were reduced in etoposide-treated cells compared to DMSO-treated cells (Figure 3.10B), as previously reported.

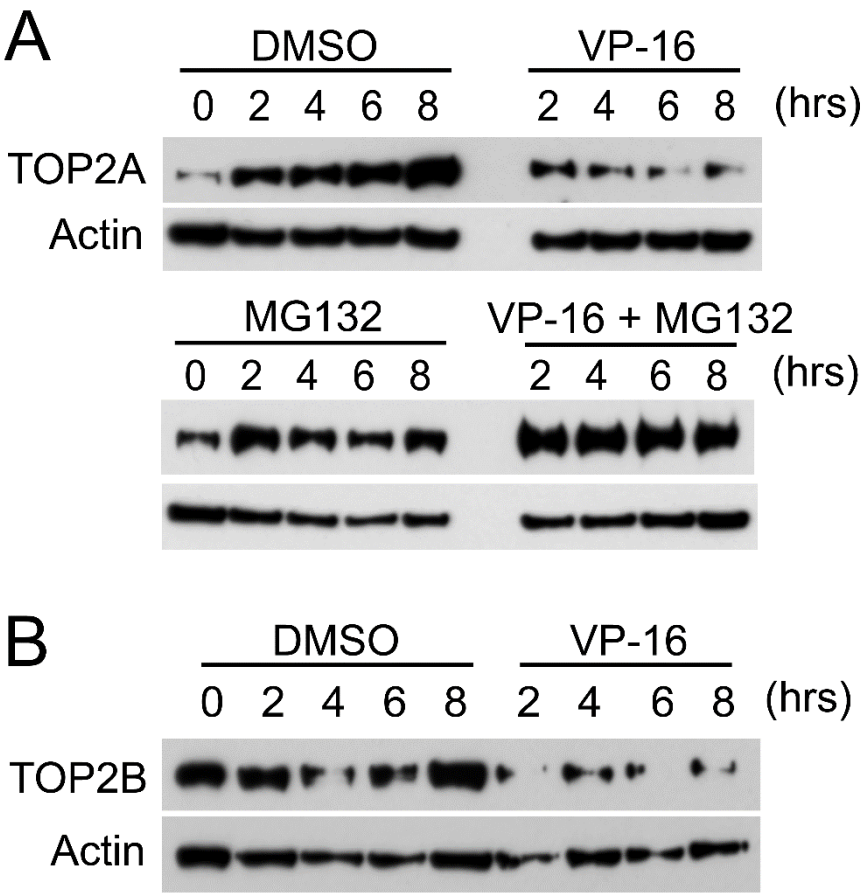

Figure 3.10. Effect of continuous etoposide exposure on TOP2 levels measured by western blot. A) K562 cells were treated for up to 8 hours with 100 µM etoposide (VP-16) alone or in combination with 50 µM MG132, and levels of TOP2A protein were measured by western blot (n=2). B) K562 cells were treated with 100 µM etoposide or 1% v/v DMSO, and TOP2B levels measured by western blot (n=1). During preparation of cell extracts in A and B, chromatin-associated proteins were extracted from DNA through the addition of DNase I.

The blots shown above were developed by standard ECL (enhanced chemiluminescence) methods, followed by detection on x-ray film. Detection of chemiluminescence is limited by the number of silver grains on the surface of x-ray film, which become activated in the presence of photons. Because of this, film has a narrow range of detection which can be rapidly saturated. In contrast, digital western blot scanners such as the LiCor C-DiGit blot scanner have a wide dynamic range which can be used to accurately quantify small changes in protein levels. The LiCor

C-DiGit was used in the current study to investigate the teniposide-induced degradation of TOP2 isoforms, previously demonstrated by others (Mao *et al.*, 2001; Alchanati *et al.*, 2009). Due to variable results obtained with the previously used TOP2B antibody (4555), antibody 30400 was used for the detection of TOP2B protein.

K562 cells were treated with 100 µM teniposide (VM-26) for up to 8 hours alone or in combination with 10 µM MG132. Whole cell lysates were prepared as above, and analysed by western blot. Blots were developed in ECL solution followed by detection using the Li-Cor C-DiGit western blot scanner for 12 minutes. A suitable 'exposure' (i.e. one which does not under- or overexpose the protein signal) was selected from a range of digital images. Triplicate blots were quantified and combined to give a mean band density, normalised to the actin loading control as described in Chapter 2, section 2.7.1.

Levels of TOP2A were not noticeably affected by continuous exposure to teniposide (Figure 3.11A), and quantification of triplicate blots did not reveal any significant differences between teniposide-treated cells and a 0 hour untreated control at any of the time points tested (Figure 3.11B). Neither were there any significant differences in TOP2A levels when teniposide-treated cells were co-incubated with MG132. In contrast, levels of TOP2B were reduced with time following continuous exposure to teniposide, consistent with the notion that TOP2B is degraded faster than TOP2A. Specifically, there was a statistically significant decrease in TOP2B levels following 8 hours teniposide treatment compared to the 0 hour untreated control (Figure 3.11B). However, there was no significant difference in levels of TOP2B following 8 hours teniposide exposure compared to untreated control when cells were also treated with MG132, showing that the teniposide-induced degradation of TOP2B is proteasome-dependent.

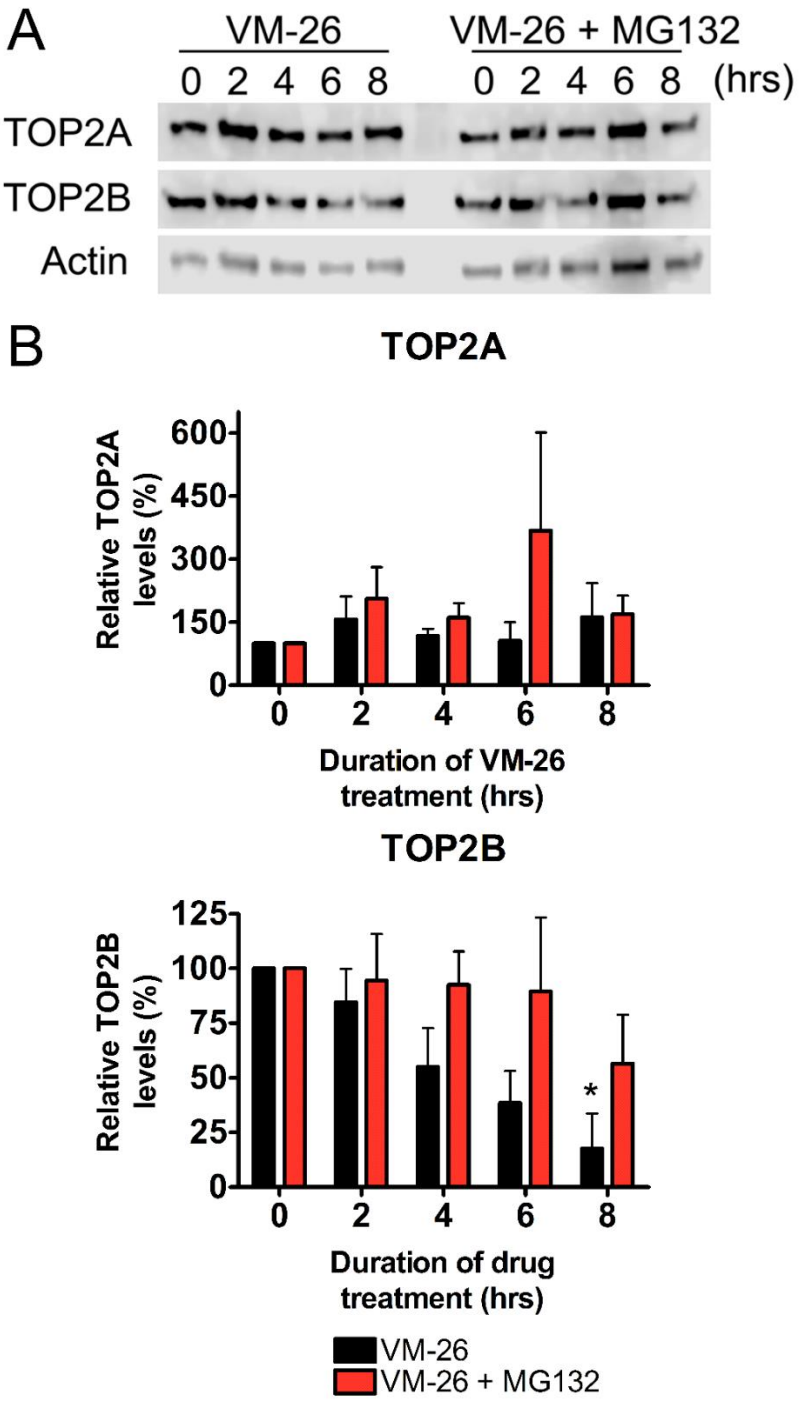

Figure 3.11. Proteasomal degradation of TOP2 isoforms following continuous teniposide exposure, as measured by western blot. A) K562 cells were treated for up to 8 hours with 100 µM teniposide (VM-26) alone or in combination with 10 µM MG132. During preparation of cell extracts, chromatin-associated proteins were extracted from DNA through the addition of DNase I to the lysate, followed by solubilisation and heating in buffer containing 2% SDS. Total TOP2 levels were measured by western blot, probing for TOP2A (antibody 3116) and TOP2B (antibody 30400). Blots were developed using the LiCor C-DiGit blot scanner. B) TOP2 levels from three separate experiments were quantified and normalised to the 0 hour untreated control. Statistical comparisons were made by unpaired t-test (n=3). Drug treatments and preparation of whole cell lysates were carried out by R. Swan. Western blotting and quantification was performed by E. Trofimowicz.

Although the blots presented in Figure 3.10 and Figure 3.11 are consistent with published literature, results obtained by western blotting were highly variable and susceptible to multiple technical issues. Quantitation can be improved by using the LiCor C-DiGit western blot detection system, although high variability between experiments remains an issue as demonstrated by the large standard error. While variability in protein loading can be accounted for through normalisation to the actin control, another important source of variation may be the extraction of drug-stabilised TOP2 complexes from DNA. Therefore, western blotting was not used to investigate the effect of UAE inhibition on the TOP2 poison-induced proteasomal degradation of TOP2 isoforms, as initially intended.

3.5.2 *Effect of teniposide and etoposide on total TOP2 levels measured by immunofluorescence*

The TOP2 poison-induced degradation of TOP2 isoforms was also investigated by immunofluorescence. Like western blotting, immunofluorescence measures total TOP2 levels (i.e. free and DNA-bound in TOP2-DNA covalent complexes). However, detection of DNA-bound TOP2 does not require the prior digestion of DNA with nucleases, and therefore does not depend on the complete extraction of TOP2 from DNA. In addition, immunofluorescence gives a cell-by-cell measure of TOP2 levels which can be easily quantified.

K562 cells were treated with 250 µM etoposide (VP-16) continuously for 0, 2, 4 or 6 hours alone or in combination with 10 µM MG132, and total TOP2 levels were measured by immunofluorescence. Levels of TOP2A and TOP2B were not significantly affected by incubation with 0.6% v/v DMSO or 10 µM MG132 alone (Figure 3.12A). TOP2A and TOP2B levels were also unaffected by etoposide treatment at any time point tested, either alone or in combination with MG132 (Figure 3.12B). Therefore, etoposide-induced degradation of TOP2 isoforms was not observed by immunofluorescence.

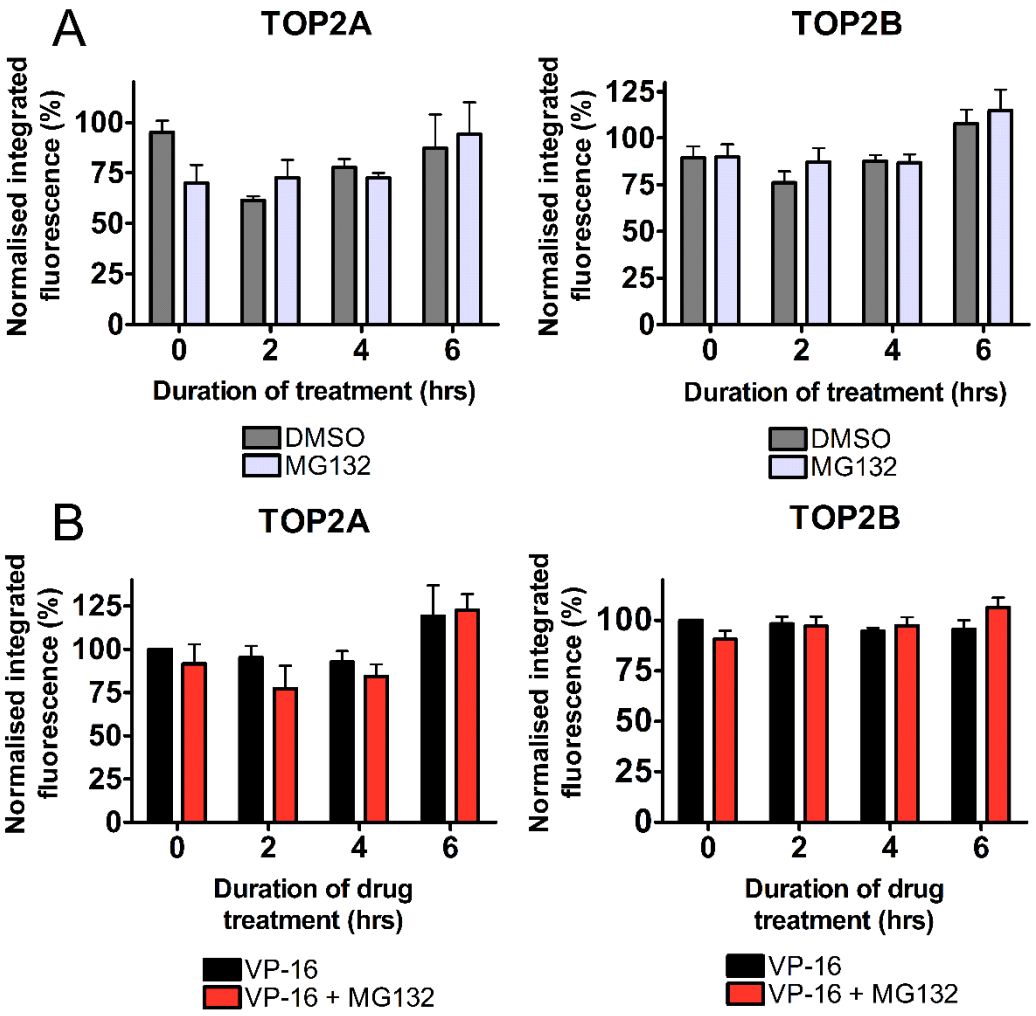

Figure 3.12. Effect of continuous etoposide exposure on total TOP2 levels measured by immunofluorescence. K562 cells were treated for 0, 2, 4 and 6 hours with A) 0.6% DMSO or 10 µM MG132, or B) 250 µM etoposide (VP-16) alone or in combination with 10 µM MG132. TOP2A and TOP2B levels were measured and quantified by standard immunofluorescence. Values represent the mean of medians ± SEM from 3 replicate experiments, and are normalised to an untreated (0 hour) control. To compare drug treatments within the same time point (e.g. VP-16 alone versus VP-16 in combination with MG132 at 6 hours drug exposure), statistical significance was tested by two way ANOVA followed by Bonferroni post-test. Where comparisons were made between drug treatment (i.e. VP-16 alone) and the 0 hour untreated control, statistical significance was determined by unpaired t-test (n=3).

Immunofluorescence was also used to investigate the effect of teniposide on total levels of TOP2A and TOP2B. K562 cells were treated continuously with 100 µM teniposide (VM-26) alone or in combination with 10 µM MG132 for 0, 2, 4 and 6 hours. Incubation with 0.3% v/v DMSO or 10 µM MG132 alone did not affect levels of TOP2A or TOP2B at any of the time points tested (Figure 3.13A). Consistent with the western blot data shown above (Figure 3.11), levels of TOP2A did not change at any of the time points tested following continuous exposure to 100 µM teniposide alone compared to the 0 hour untreated control (Figure 3.13B). Despite this, a statistically significant increase in TOP2A levels was detected when cells were co-treated with MG132 for 6 hours compared to teniposide alone ($p<0.01$, two way ANOVA). Given that MG132 alone does not affect levels of TOP2 (Figure 3.13A), this implicates a synergistic interaction between proteasome inhibition and teniposide.

Unlike TOP2A, TOP2B levels were significantly decreased following 6 hours exposure to teniposide alone compared to the 0 hour untreated control ($p=0.0268$, t-test). Co-treatment of cells with MG132 prevented the teniposide-induced decrease in TOP2B levels after 6 hours drug exposure, as TOP2B levels were significantly higher in the presence of MG132 compared to teniposide alone ($p<0.01$, two way ANOVA). Together, this supports the notion that TOP2B is degraded in a proteasome-dependent manner following teniposide exposure.

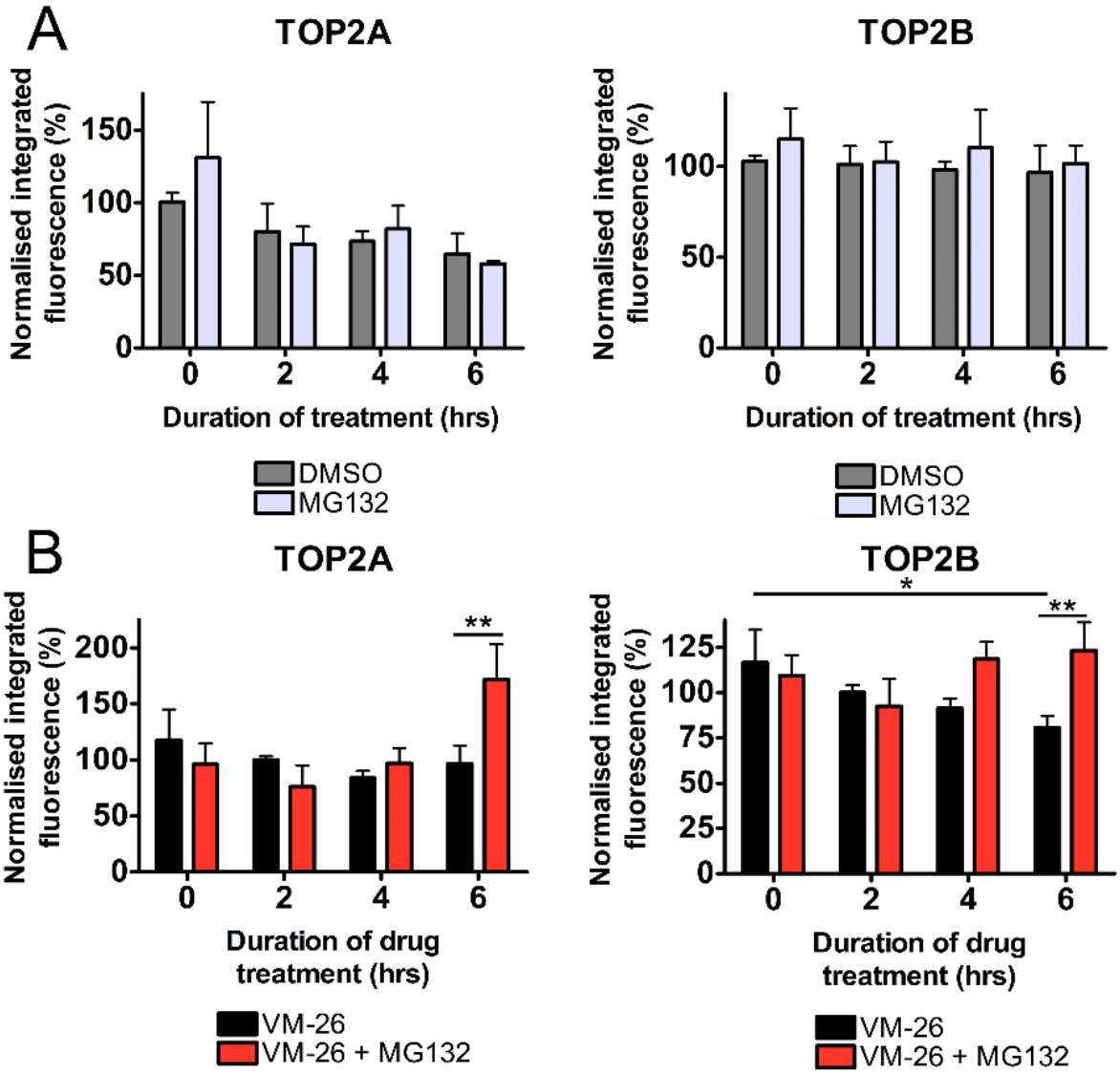

Figure 3.13. Effect of continuous teniposide exposure on total TOP2 levels measured by immunofluorescence. Total levels of TOP2A and TOP2B were measured by immunofluorescence. K562 cells were treated for 0, 2, 4 and 6 hours with A) 0.3% v/v DMSO or 10 µM MG132 as a negative control, or B) with 100 µM teniposide (VM-26) alone or in combination with 10 µM MG132. TOP2A and TOP2B levels were measured and quantified by standard immunofluorescence. Values represent the mean of medians ± SEM from 3 replicate experiments, and are normalised to an untreated (0 hour) control. To compare drug treatments within the same time point (e.g. VM-26 alone versus VM-26 in combination with MG132 at 6 hours drug exposure), statistical significance was tested by two way ANOVA followed by Bonferroni post-test. Where comparisons were made between drug treatment (i.e. VM-26 alone) and the 0 hour untreated control, statistical significance was determined by unpaired t-test (n=3).

It is presumed that the TOP2 poison-induced degradation of TOP2 isoforms represents the proteolysis of TOP2-DNA complexes, which is a key step in TOP2 complex repair. It is therefore plausible that western blotting or immunofluorescence of total TOP2 levels is not sensitive enough to detect changes in the proportion of DNA-bound TOP2 amidst a pool of non-covalently bound TOP2. Indeed, TOP2 is a highly abundant enzyme, with approximately 5.7 x 10^5 monomers of TOP2A, and 4.4 x 10^5 monomers of TOP2B in K562 cells (Padget *et al.*, 2000). Therefore, a more informative approach may be the direct measurement of TOP2-DNA complexes following prolonged exposure to TOP2 poisons. Studies using the TARDIS assay (Sunter *et al.*, 2010; Lee *et al.*, 2016) and ICE assay (Fan *et al.*, 2008; Alchanati *et al.*, 2009) have shown that DNA-bound TOP2 is degraded in a proteasome-dependent manner following treatment with TOP2 poisons. Specifically, proteasome inhibition slows the removal of etoposide-induced TOP2A- and TOP2B- complexes from DNA as shown in Figure 3.4. Here, the TARDIS assay was used to investigate the effect of continuous etoposide exposure on the degradation of TOP2-DNA complexes.

K562 cells were treated with 10 µM, 100 µM or 250 µM etoposide for 0, 1, 2, 4 or 6 hours, and levels of TOP2-DNA complexes were measured by TARDIS assay. Etoposide was dissolved in DMSO, and in each condition the final concentration of DMSO was 0.5% v/v. As shown previously in Figure 3.1 and Figure 3.2, TOP2A- and TOP2B- DNA complexes were detectable upon the exposure of cells to 10 µM etoposide, and became saturated at doses above 100 µM (Figure 3.14A). However, both TOP2A- and TOP2B- DNA complex levels remained elevated with continuous exposure to etoposide at all doses and all time points tested. Therefore, the proteasomal degradation of TOP2-DNA complexes is not detectable upon continuous etoposide exposure. This could be due to the steady turnover of complexes, whereby the rate of TOP2 complex formation is the same as the rate of complex processing. This is in contrast to the proteolytic removal of TOP2-DNA complexes which is observed following etoposide washout (Figure 3.4). Upon etoposide removal, the equilibrium between the formation of new complexes and TOP2-DNA complex repair exists in favour of increased complex removal, due to both reduced trapping of complexes and increased complex reversal upon etoposide withdrawal.

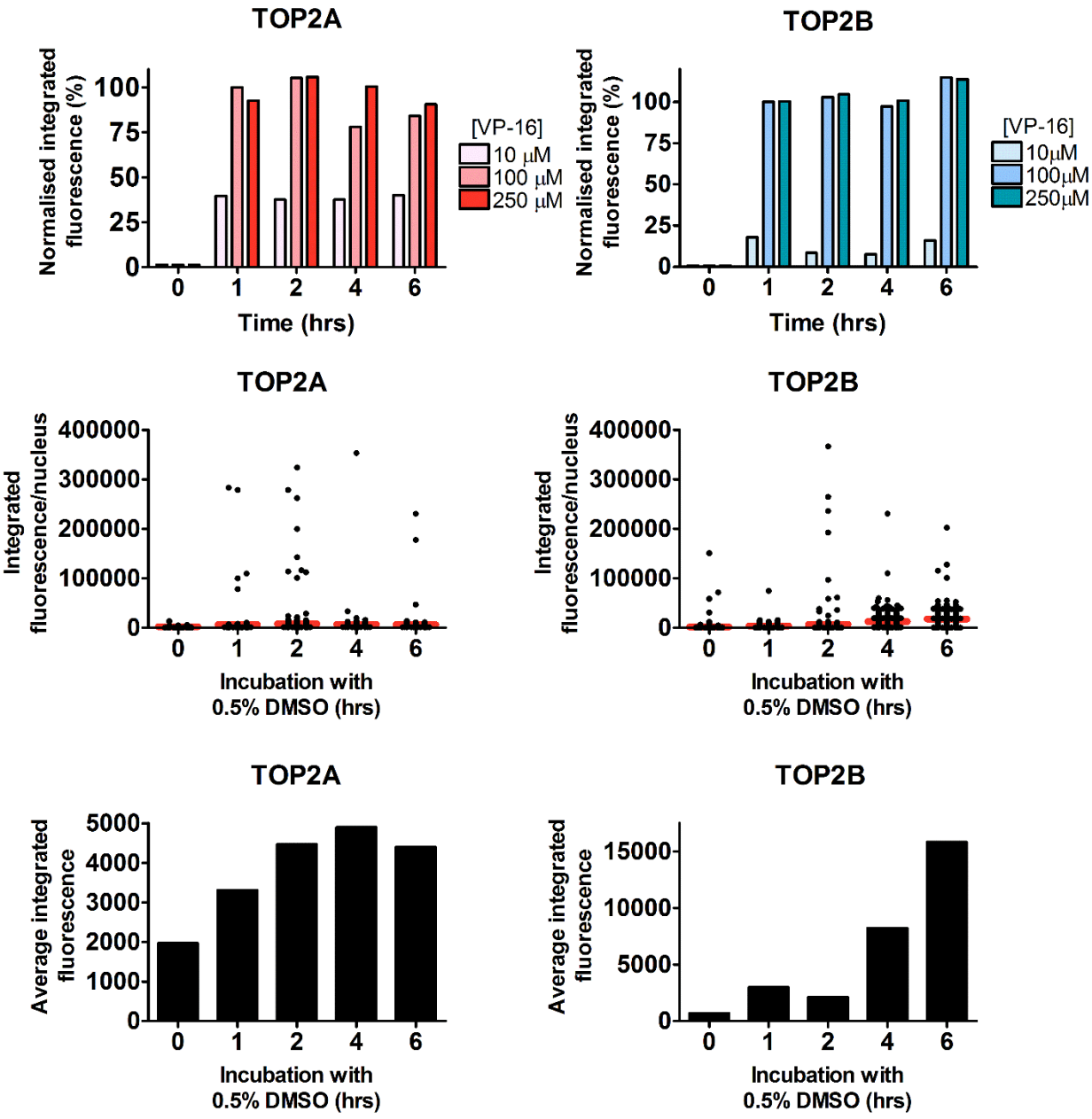

Figure 3.14. Effect of continuous etoposide exposure on levels of TOP2-DNA complexes measured using the TARDIS assay. A) K562 cells were treated with 10 μM, 100 μM or 250 μM etoposide (VP-16) (each containing 0.5% v/v DMSO) and levels of TOP2A- and TOP2B- DNA complexes were measured at 0, 1, 2, 4 and 6 hours of etoposide exposure. B) Effect of 0.5% v/v DMSO on levels of TOP2-DNA complexes. Scatter diagrams show raw integrated fluorescence values of TOP2 levels in individual nuclei, and histograms show the corresponding median values normalised to a 100 μM etoposide control (n=1).

Notably, levels of TOP2A- and TOP2B- DNA complexes increased with time following incubation in 0.5% v/v DMSO (Figure 3.14B, with individual values from a single experiment presented as a scatter diagram, and the corresponding medians as a histogram). While TOP2A-DNA complexes were increased to approximately 3% of the 100 μM etoposide signal after 4 hours, the induction of TOP2B-DNA

complexes was increased to approximately 15% of the 100 µM etoposide control after 6 hours. Therefore, DMSO concentration and duration of treatment were minimised in all subsequent TARDIS experiments.

3.6 Role of the ubiquitin-proteasome system in the processing of etoposide-induced TOP2-DNA complexes to protein-free DSBs

The repair of DSBs is orchestrated by multiple post-translational modifications which facilitate the recruitment of essential repair factors such as BRCA1 and 53BP1 to broken DNA (Bekker-Jensen and Mailand, 2010; Zhao *et al.*, 2014). The so-called DNA damage response (DDR) is initiated by kinases ATM and DNA-PK which are activated by DSBs, and phosphorylate histones surrounding the DNA break (Paull *et al.*, 2000; Burma *et al.*, 2001). Specifically, histone H2AX is phosphorylated at serine 139 (ɣH2AX) (Rogakou *et al.*, 1998). The phosphorylation of histone H2AX can be detected by immunofluorescence using an antibody specific to phospho-histone H2AX (Ser139), and this is termed the ɣH2AX assay. While not a direct measure of DSBs, the phosphorylation of histone H2AX is a surrogate marker which reflects one of the foremost steps in the recognition and repair of DSBs. However, TOP2 poison-induced DSBs are not recognised by DDR proteins until TOP2 has been removed from the TOP2-DNA complex (Martensson *et al.*, 2003; Zhang *et al.*, 2006; Fan *et al.*, 2008; Tammaro *et al.*, 2013). Therefore, the processing of TOP2-DNA complexes can also be studied through the appearance of protein-free DSBs. Here, the ɣH2AX assay was used to investigate the role of the ubiquitin-proteasome system in the appearance of etoposide-induced DSBs.

K562 cells were treated continuously with 10 µM etoposide alone or in combination with 10 µM MG132 for up to 4 hours, and levels of protein-free DSBs were measured by ɣH2AX assay. Phosphorylation of histone H2AX was detectable within 1 hour of etoposide treatment, and remained elevated for the duration of etoposide exposure (Figure 3.15A). Proteasomal inhibition significantly reduced etoposide-induced ɣH2AX levels following 2 and 4 hours drug exposure ($p<0.0001$), consistent with a role for the proteasome in the appearance of etoposide-induced DSBs (Zhang *et al.*, 2006; Fan *et al.*, 2008; Sunter, 2008; Tammaro *et al.*, 2013). Co-treatment with MG132 also significantly reduced the appearance of etoposide- and mitoxantrone-induced DSBs in Nalm-6 cells (see Appendix Figure 2 and 3).

To determine whether the appearance of etoposide-induced DSBs is ubiquitin-dependent, the ɣH2AX assay was also performed in K562 cells treated with 10 µM etoposide alone or in combination with 10 µM MLN7243 (UAE inhibitor) for up to 4

hours. Cells were also treated for 2 hours, followed by removal of etoposide from the cell culture medium and incubation in the continued presence of MLN7243 or 0.1% v/v DMSO for 2 hours (2+2hr washout, WO), as per the TARDIS assay. Similarly to proteasome inhibition, co-treatment of cells with MLN7243 significantly reduced the etoposide-induced phosphorylation of histone H2AX following 1, 2 and 4 hours drug exposure (Figure 3.15B & C, $p<0.05$), and after etoposide washout (Figure 3.15B, $p<0.05$). UAE inhibition also significantly reduced the appearance of etoposide- and mitoxantrone-induced DSBs in Nalm-6 cell lines (see Appendix Figure 4 and 5). Therefore, the processing of drug-stabilised TOP2-DNA complexes to protein-free DSBs is ubiquitin-dependent.

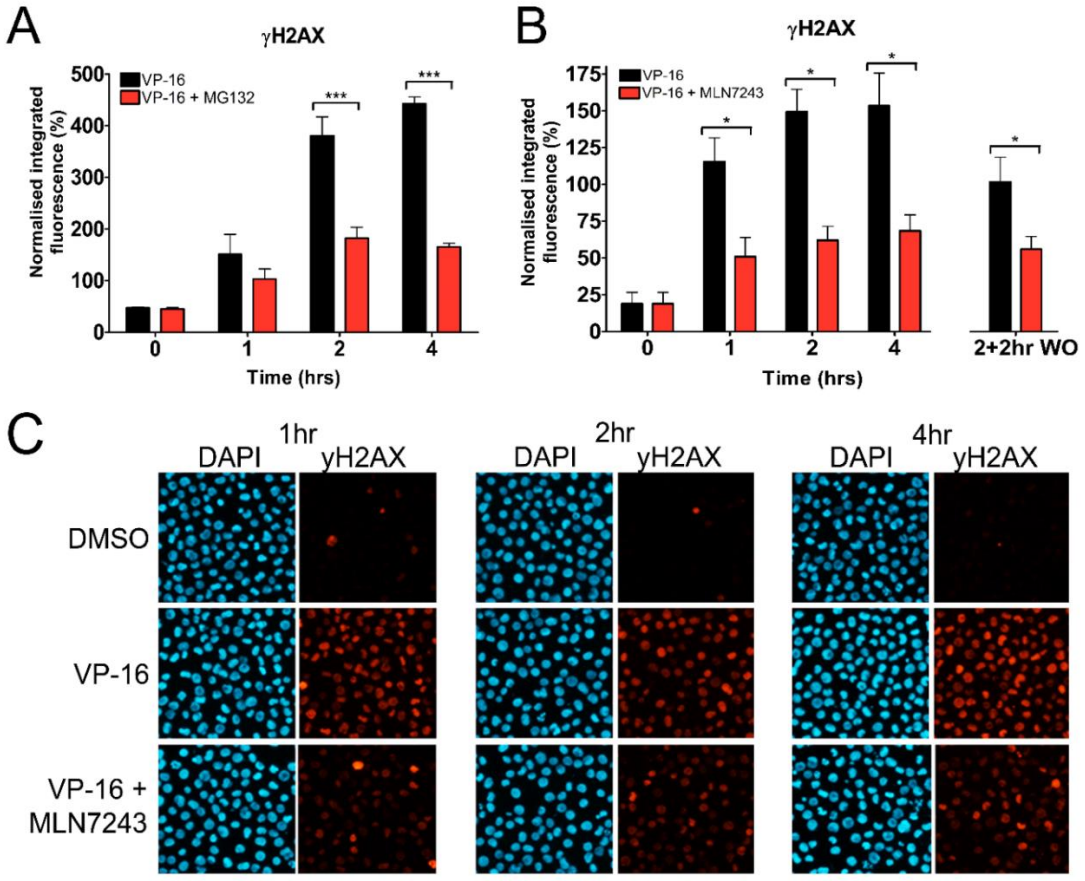

Figure 3.15. Inhibition of the ubiquitin-proteasome system and the effect on etoposide-induced histone H2AX phosphorylation. K562 cells were treated with 10 µM etoposide (VP-16) alone or in combination with A) 10 µM MG132 or B) 10 µM MLN7243 for up to 4 hours, and levels of protein-free DSBs were measured by γH2AX assay. B) Cells were also treated for 2 hours with 10 µM etoposide alone or in combination with 10 µM MLN7243, followed by etoposide washout and a further 2 hour incubation in medium containing 10 µM MLN7243 or 0.1% v/v DMSO (2+2hr washout, WO). All values represent the mean of triplicate experiments ± SEM, normalised to a 1 hour 10 µM etoposide control. Statistical comparisons were made by two-way ANOVA followed by Bonferroni post-test (n=3). C) Representative images of data shown in B.

To further investigate the role of UAE enzymes in the generation of etoposide-induced DSBs, the γH2AX assay was performed in double UAE1/UBA6 siRNA knockdown cells and control (CON) siRNA cells treated with 10 µM etoposide for up to 4 hours. Consistently, etoposide-induced phosphorylation of histone H2AX was significantly reduced in UAE1/UBA6 knockdown cells compared to control cells following 1 and 4 hours etoposide treatment (Figure 3.16, $p<0.05$ and $p<0.01$, respectively), although no significant difference was detected after 2 hours. This is in contrast to the TARDIS data shown in Figure 3.8, where siRNA knockdown of UAE1 and UBA6 did not affect the rate of TOP2-DNA complex removal following etoposide washout. While the reason for this is unclear, this could be explained by differences between the TARDIS assay and γH2AX assay. Firstly, detection of TOP2-DNA complexes in the TARDIS assay is isoform-specific, whereas DSBs detected using the γH2AX assay represent the processing of both TOP2A- and TOP2B- DNA complexes. This combined effect may enable the detection of smaller changes in levels of TOP2A- and TOP2B- induced DSBs, which are not significantly detected when measuring levels of TOP2A- and TOP2B- DNA complexes separately. Secondly, the TARDIS assay involves the measurement of TOP2-DNA complexes following etoposide removal, and therefore the removal of TOP2-DNA complexes upon etoposide washout is due to both active processing by the proteasome and spontaneous complex reversal upon completion of the TOP2 reaction cycle. In contrast, the γH2AX assay was performed following continuous etoposide exposure, where the etoposide-induced γH2AX signal is produced only upon active processing of TOP2-DNA complexes. Hence, the effect of UAE knockdown may be less detectable in the TARDIS assay where TOP2 removal occurs in parallel to TOP2 complex reversal. Nonetheless, this further supports a role for ubiquitination in the processing of etoposide-induced DNA damage.

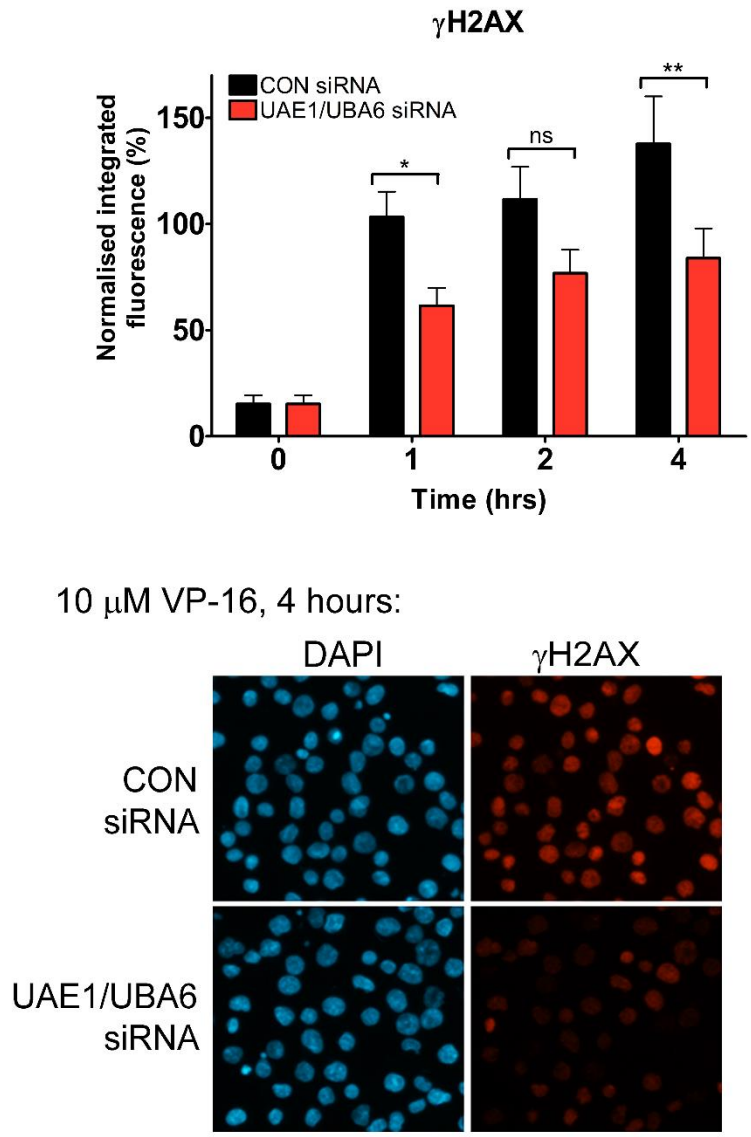

Figure 3.16. siRNA knockdown of ubiquitin activating enzymes and the effect on etoposide-induced phosphorylation of histone H2AX. CON siRNA or double UAE1/UBA6 siRNA knockdown cells were treated with 10 μM etoposide (VP-16) for up to 4 hours, and levels of protein-free DSBs were measured by γH2AX assay. Values represent the mean of triplicate experiments ± SEM, normalised to a 1 hour 10 μM etoposide control. Statistical comparisons were made by two-way ANOVA followed by Bonferroni post-test (n=3).

Histone phosphorylation is one of the earliest events in the DDR, occurring before the wave of ubiquitination which contributes to DNA repair (Bekker-Jensen and Mailand, 2010). To test whether ubiquitination is required for the DNA damage-induced phosphorylation of histone H2AX, the γH2AX assay was repeated in K562 cells following exposure to 2 Gy ionising irradiation in the presence and absence of MLN7243.

Levels of IR-induced DSBs were measured following 0.5, 1, 2 and 4 hours incubation in cell culture medium containing 0.1% v/v DMSO or 10 µM MLN7243. IR-induced histone H2AX phosphorylation increased up to 1 hours after irradiation, but began to decrease in DMSO-treated cells after 4 hours incubation in drug-free medium reflecting effective DNA repair and resolution of DSBs. γH2AX levels were not significantly affected by UAE inhibition within 2 hours after irradiation, but remained significantly higher in MLN7243-treated cells 4 hours post-irradiation ($p<0.01$, Figure 3.17). This shows that inhibition of ubiquitination prevents the repair of DSBs, consistent with published data (Moudry *et al.*, 2012). Furthermore, ubiquitination is not required for the phosphorylation of histone H2AX, supporting the conclusion from Figure 1.16 that the role of ubiquitin in the appearance of etoposide-induced DSBs is specific to TOP2-mediated damage.

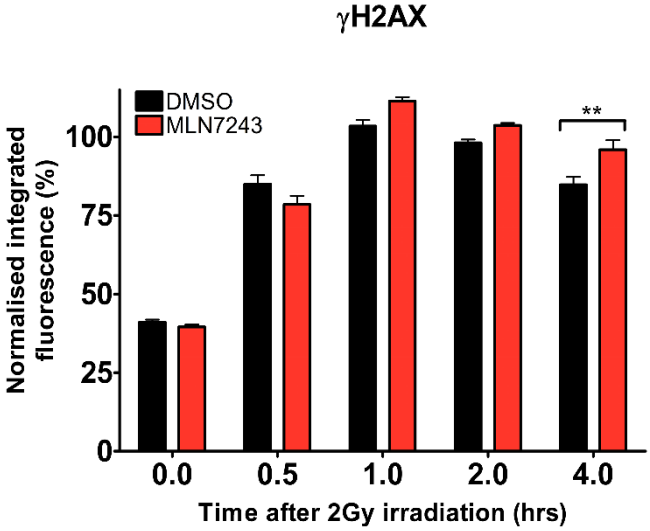

Figure 3.17. Effect of UAE1 inhibition on irradiation-induced γH2AX levels. K562 cells were treated with 10 µM MLN7243 (or 0.1% v/v DMSO) and exposed to 2Gy X-ray irradiation. The γH2AX assay was used to measure levels of DSBs at 0.5, 1, 2 and 4 hours after irradiation. Values represent the mean of triplicate experiments ±SEM, normalised to a 1 hour irradiation control. Statistical significance was determined by two-way ANOVA with Bonferroni post-test (n=3).

3.7 Investigating the role of the BMI1/RING1A E3 ubiquitin ligase in the processing of TOP2-DNA complexes

The BMI1/RING1A E3 ubiquitin ligase has been implicated in the proteasomal degradation of TOP2A-DNA complexes (Alchanati *et al.*, 2009). There are over 600 E3 ubiquitin ligases encoded in the human genome which interact directly with target proteins and therefore largely determine substrate specificity. Consequently, targeting of E3 ubiquitin ligases with small molecule inhibitors would offer more selectivity than upstream targeting of UAE in potential clinical applications. PRT4165 is a small molecule inhibitor shown to inhibit the self-ubiquitination of BMI1/RING1A and the proteasome-dependent degradation of TOP2A-DNA complexes (Alchanati *et al.*, 2009). Hence, the role of the BMI1/RING1A ubiquitin ligase in the removal of etoposide-induced TOP2 complexes from DNA was investigated using the TARDIS assay following treatment of cells with PRT4165. K562 cells were treated with 100 µM etoposide alone or in combination with 90 µM PRT4165 for 2 hours, followed by etoposide washout and incubation in etoposide-free medium containing DMSO or PRT4165. Levels of TOP2A- and TOP2B- DNA complexes were measured following 0, 0.5, 1 and 2 hours incubation in etoposide-free medium.

Levels of TOP2A-DNA complexes were not affected by co-incubation with PRT4165 immediately after 2 hours continuous exposure to etoposide (0 hours after VP-16 removal) (Figure 3.18). However, TOP2A-DNA complexes were significantly higher in the presence of PRT4165 1 hour after etoposide removal ($p<0.05$), in support of a role for BMI1/RING1A in the processing of TOP2A-DNA complexes. Levels of TOP2B-DNA complexes were also unaffected immediately following 2 hours continuous exposure to etoposide (0 hours after VP-16 removal), but were significantly increased in the presence of PRT4165 0.5 hours after etoposide removal ($p<0.05$). This indicates a role for BMI1/RING1A in the removal of TOP2B complexes from DNA, which was not previously reported by Alchanati et al.

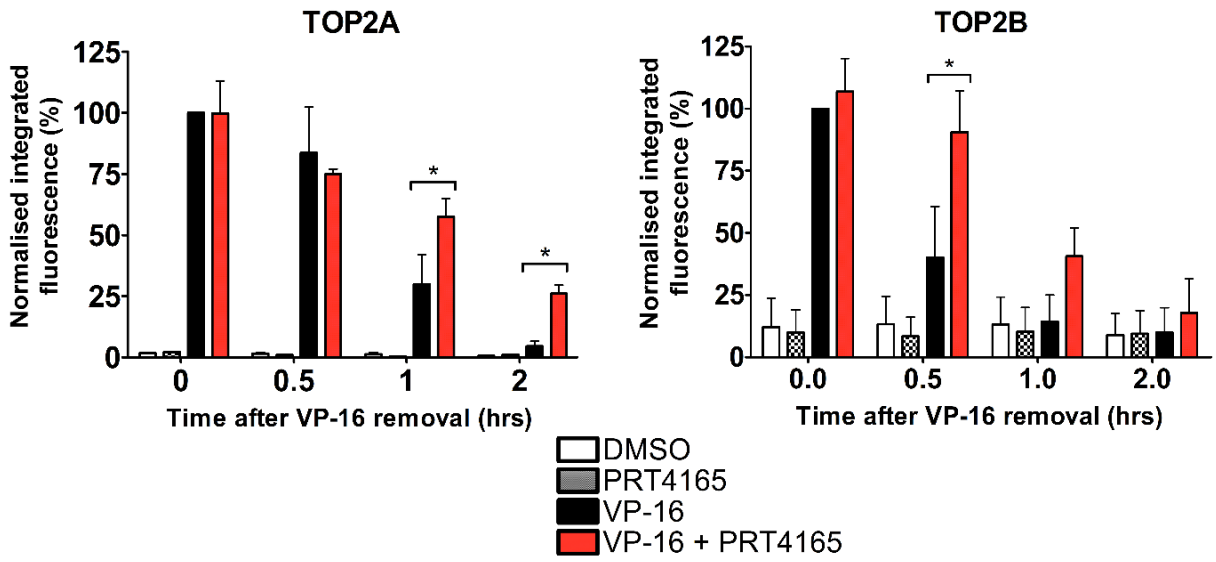

Figure 3.18. Effect of the BMI1/RING1A inhibitor PRT4165 on levels of etoposide-induced TOP2-DNA complexes. K562 cells were treated with 100 µM etoposide (VP-16) alone or in combination with 90 µM PRT4165 for 2 hours. Etoposide was removed from the culture medium and cells were incubated for a further 2 hours in medium containing 90 µM PRT4165 or 0.09% v/v DMSO. Levels of TOP2A- and TOP2B- DNA complexes were measured at 0, 0.5, 1 and 2 hours after etoposide removal using the TARDIS assay. Values represent the mean of medians ± SEM from triplicate experiments, normalised to a 100 µM etoposide control. Statistical comparisons were made by two-way ANOVA followed by Bonferroni post-test (n=3).

To further investigate the role of BMI1/RING1A in the processing of etoposide-induced TOP2-DNA complexes, the γH2AX assay was used to test the effect of PRT4165 on the appearance of etoposide-induced DSBs. K562 cells were treated with 10 µM etoposide alone or in combination with 90 µM PRT4165 for up to 4 hours. Notably, 4 hours incubation with PRT4165 alone induced a small but significant increase in histone H2AX phosphorylation ($p<0.01$). However, inhibition of BMI1/RING1A significantly reduced the appearance of etoposide-induced DSBs after 1, 2 and 4 hours drug exposure (Figure 3.19, $p<0.001$). Strikingly, histone H2AX phosphorylation was completely reduced to background levels after 1 and 2 hours of drug treatment. While this could suggest that the induction of etoposide-induced DSBs is largely BMI1/RING1A-dependent, it is important to note that PRT4165 has also been shown to inhibit the RING1A paralog, RING1B (Ismail *et al.*, 2013), and concerns exist regarding its lack of specificity. Nonetheless, PRT4165 does not affect the IR-induced phosphorylation of histone H2AX (Ismail *et al.*, 2013), suggesting that inhibition of the etoposide-induced γH2AX signal by PRT4165 is specific to TOP2-mediated damage.

Together, the effect of MLN7243 and PRT4165 ubiquitination inhibitors on the appearance of etoposide-induced DSBs demonstrates an important role for the ubiquitin system in the processing of TOP2 poison-induced DNA damage. While the role of the proteasome has already been shown by others, the role of ubiquitinating enzymes in the appearance of etoposide-induced DSBs has not yet been reported. Therefore, the role of ubiquitin is an important but currently underappreciated aspect of TOP2-DNA complex repair.

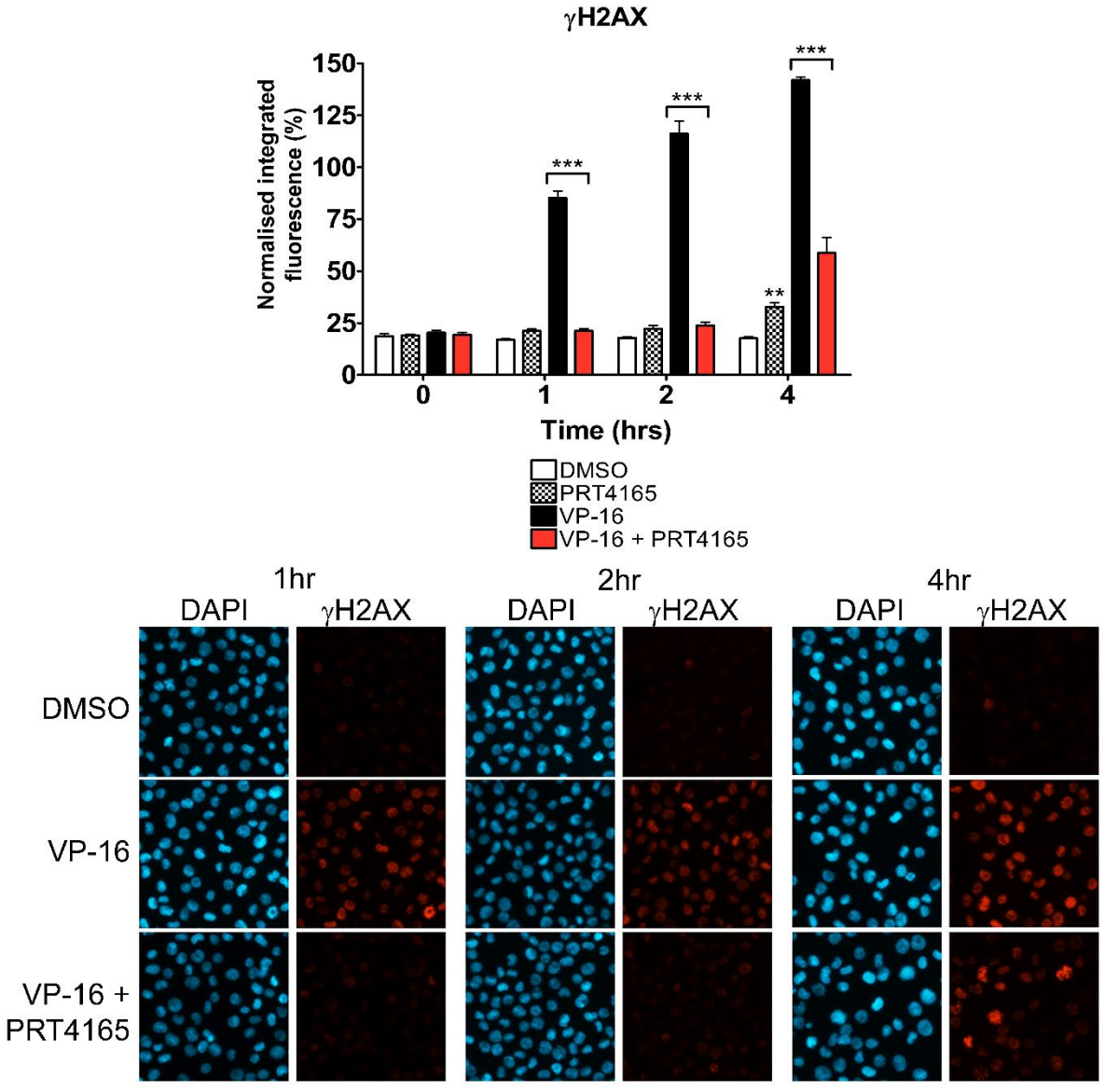

Figure 3.19. Effect of the BMI1/RING1A inhibitor PRT4165 on etoposide-induced histone H2AX phosphorylation. K562 cells were incubated with 10 µM etoposide (VP-16) alone or in combination with 90 µM PRT4165 for up to 4 hours, and protein-free DSBs were measured by γH2AX assay. Values are normalised to a 1 hour 10 µM etoposide control and represent the mean integrated fluorescence from triplicate experiments. Statistical significance was determined by two-way ANOVA with Bonferroni post-test (n=3).

3.8 Investigating the role of transcription in the processing of TOP2-DNA complexes

The proteasomal processing of TOP2-DNA complexes (or a component of it) may be transcription dependent, as inhibition of transcription has been reported to prevent proteasome-dependent degradation of TOP2-DNA complexes and the appearance of etoposide-induced DSBs (Mao *et al.*, 2001; Zhang *et al.*, 2006; Fan *et al.*, 2008; Ban *et al.*, 2013; Tammaro *et al.*, 2013). In the current study, the role of transcription in the processing of TOP2-DNA complexes was investigated following chemical inhibition of transcription. α-Amanitin inhibits transcription by binding to RNA polymerase II (RNAPII), and to a lesser extent RNAPIII, thereby preventing the incorporation of nucleotides into nascent RNA (Bensaude, 2011). In contrast, the major target of DRB (5,6-Dichloro-1-β-Ribo-furanosyl Benzimidazole) is the cyclin-dependent kinase CDK9, which is responsible for the hyper-phosphorylation of the RNAPII C terminal domain during transcription elongation. While α-Amanitin is a slow-acting, irreversible inhibitor at relatively low concentrations, DRB reversibly inhibits transcription within minutes of addition to cell culture medium but only at high working concentrations (Bensaude, 2011).

The effects of α-Amanitin and DRB on levels of transcription in K562 cells were measured by incorporation of 5-ethynyl uridine (EU) into newly synthesised RNA transcripts. K562 cells were treated with 10 µg/mL α-Amanitin for 2 or 4 hours, or 150 µM DRB for 30 minutes or 2 hours, then incubated for 1 hour in the presence of 1 mM EU. Unexpectedly, α-Amanitin (10 µg/mL) did not affect the production of nascent RNA transcripts after 2 or 4 hours incubation (Figure 3.20). This is surprising as 10 µg/mL α-Amanitin efficiently inhibits transcription according to previously published studies (Anindya *et al.*, 2007; Bensaude, 2011). In contrast, transcription was inhibited by approximately 50% following 30 minutes exposure to DRB. Inhibition was not further increased by 2 hours exposure to DRB, suggesting that 30 minutes is sufficient for maximum inhibition with 150 µM DRB.

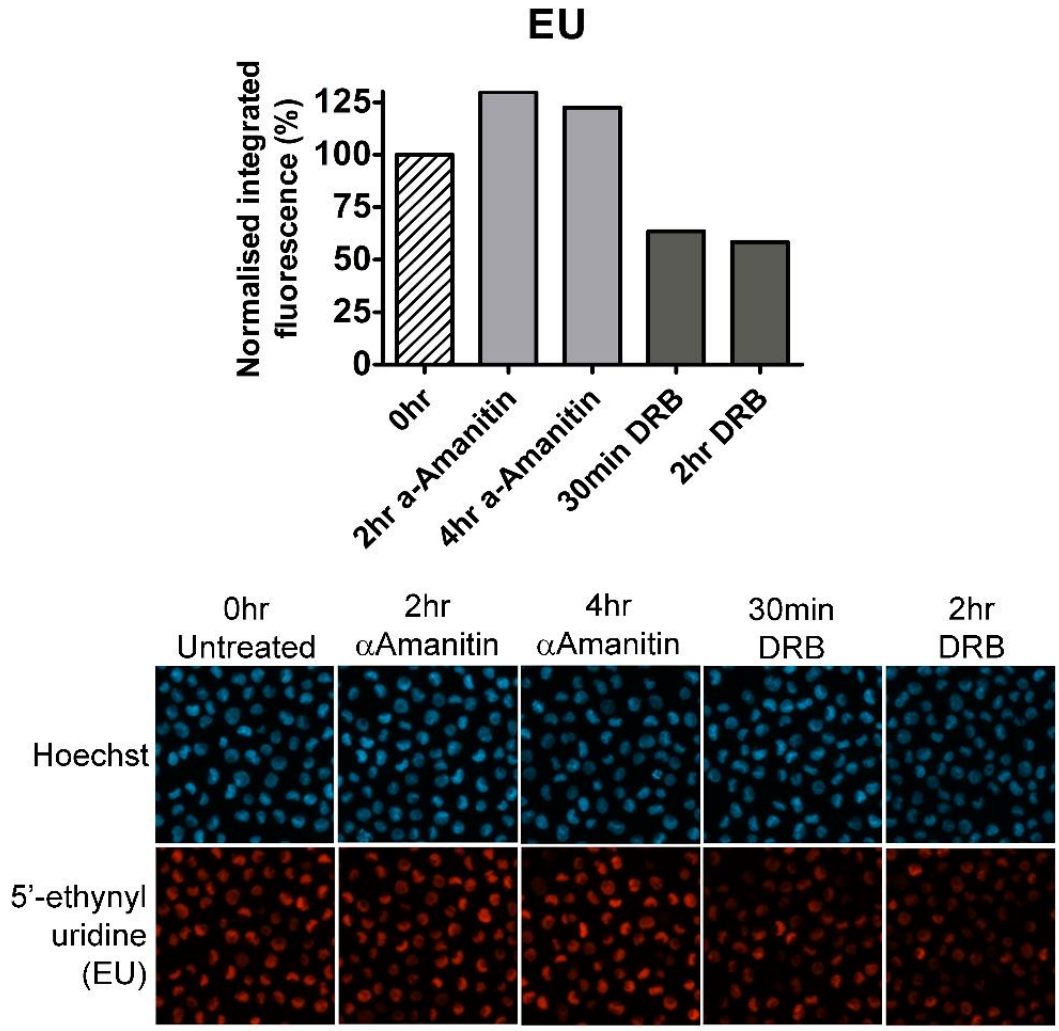

Figure 3.20. Transcription inhibition by α-Amanitin and DRB in K562 cells. K562 cells were incubated with 10 µg/mL α-Amanitin or 150 µM DRB for the time indicated. Cells were then incubated with 1 mM 5-ethynyl uridine (EU) for 1 hour in the continued presence of drug, and transcription inhibition was measured by incorporation of EU into nascent RNA. EU levels were quantified by integrated fluorescence per nucleus, and are represented as median values normalised to an untreated (0 hour) control (n=1).

The EU assay was also used to determine the effect of α-Amanitin and DRB on transcription in Nalm-6 cells. Nalm-6 cells were treated with 10 µg/mL α-Amanitin for 4 hours or the indicated concentration of DRB (100, 150 or 300 µM) for 30 minutes. As in K562 cells, α-Amanitin did not affect levels of transcription in Nalm-6 cells compared to an untreated (H_2O) control (Figure 3.21). However, transcription levels were reduced by at least 50% in cells treated with DRB at all concentrations tested. Therefore, DRB was used for the inhibition of transcription in all subsequent experiments.

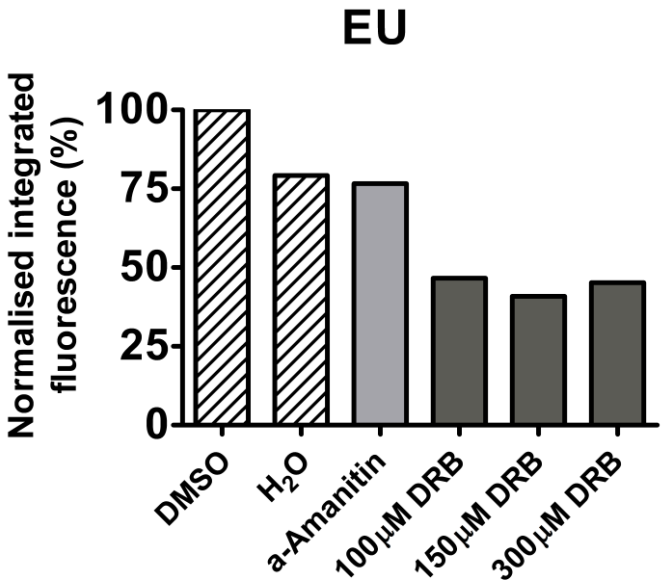

Figure 3.21. Transcription inhibition by α-Amanitin and DRB in Nalm-6 cells. Nalm-6 cells were treated with 10 µg/mL α-Amanitin for 4 hours, or increasing concentrations of DRB for 30 minutes. Cells were then incubated with 1 mM 5-ethynyl uridine (EU) for 1 hour in the continued presence of drug, and transcription inhibition was measured by incorporation of EU into nascent RNA. EU levels were quantified by integrated fluorescence per nucleus, and are represented as median values normalised to an untreated (0 hour) control (n=1).

The role of transcription in the removal of TOP2-DNA complexes was investigated using the TARDIS assay. As only 50% transcription inhibition was achieved with 150 µM DRB, K562 cells were treated with or without 300 µM DRB as used in other studies (Tammaro *et al.*, 2013) with the aim of increasing transcription inhibition. Cells from each replicate TARDIS experiment were collected for processing via the EU assay, which showed on average 75% inhibition of transcription in cells treated with 300 µM DRB (Figure 3.22).

K562 cells were treated with 100 µM etoposide (VP-16) alone or in combination with 300 µM DRB for 2 hours. Etoposide was then removed from the culture medium and cells were incubated for up to 2 hours in the continued presence of 300 µM DRB or DMSO. Levels of TOP2A-DNA complexes were not affected by transcription inhibition following 2 hours continuous exposure to etoposide (0 hours after VP-16 removal) (Figure 3.23A). However, levels of remaining TOP2A-DNA complex levels were significantly higher 0.5 and 1 hours after etoposide removal ($p<0.01$), suggesting that the removal of TOP2A complexes from DNA is partly transcription-dependent. Levels of etoposide-induced TOP2B-DNA complexes were not

significantly affected by transcription inhibition at any time point tested. This is in contrast to previous studies which have demonstrated a transcription-dependent mechanism of TOP2B complex processing (Mao *et al.*, 2001; Zhang *et al.*, 2006; Fan *et al.*, 2008; Ban *et al.*, 2013; Tammaro *et al.*, 2013). Together, this suggests that transcription is involved in the processing of TOP2A-DNA complexes under these conditions (where transcription is inhibited by 75%).

To test for cell-specific effects, the role of transcription was also investigated in the Nalm-6 cell line. Nalm-6 cells were treated with 100 µM etoposide alone or in combination with 150 µM DRB for 2 hours, followed by 2 hours incubation in medium containing DRB or DMSO. Levels of TOP2A- and TOP2B- DNA complexes were measured using the TARDIS assay. As shown in K562 cells, the level of etoposide-induced TOP2A-DNA complexes remaining 0.5 and 1 hours after etoposide removal were higher in the presence of DRB compared to DMSO-treated cells, while levels of TOP2B-DNA complexes were unaffected by transcription inhibition at all time points (Figure 3.23B). Therefore, transcription is involved in the processing of TOP2A-DNA complexes in myeloid and lymphoblastic cell lines.

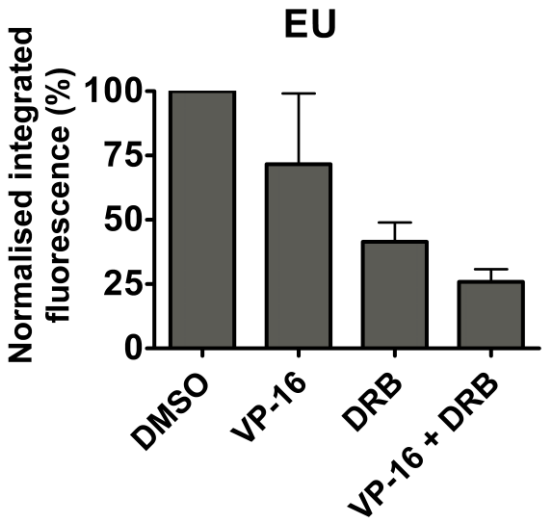

Figure 3.22. Transcription inhibition by DRB in K562 cells. K562 cells from each TARDIS experiment were collected following 2 hours exposure to 100 µM etoposide (VP-16) with or without 300 µM DRB, and inhibition of transcription was measured using the EU assay. Median integrated fluorescence (representing average EU levels per nucleus) were normalised to the DMSO negative control. Averages represent the mean of medians ± SEM from triplicate experiments (n=3)

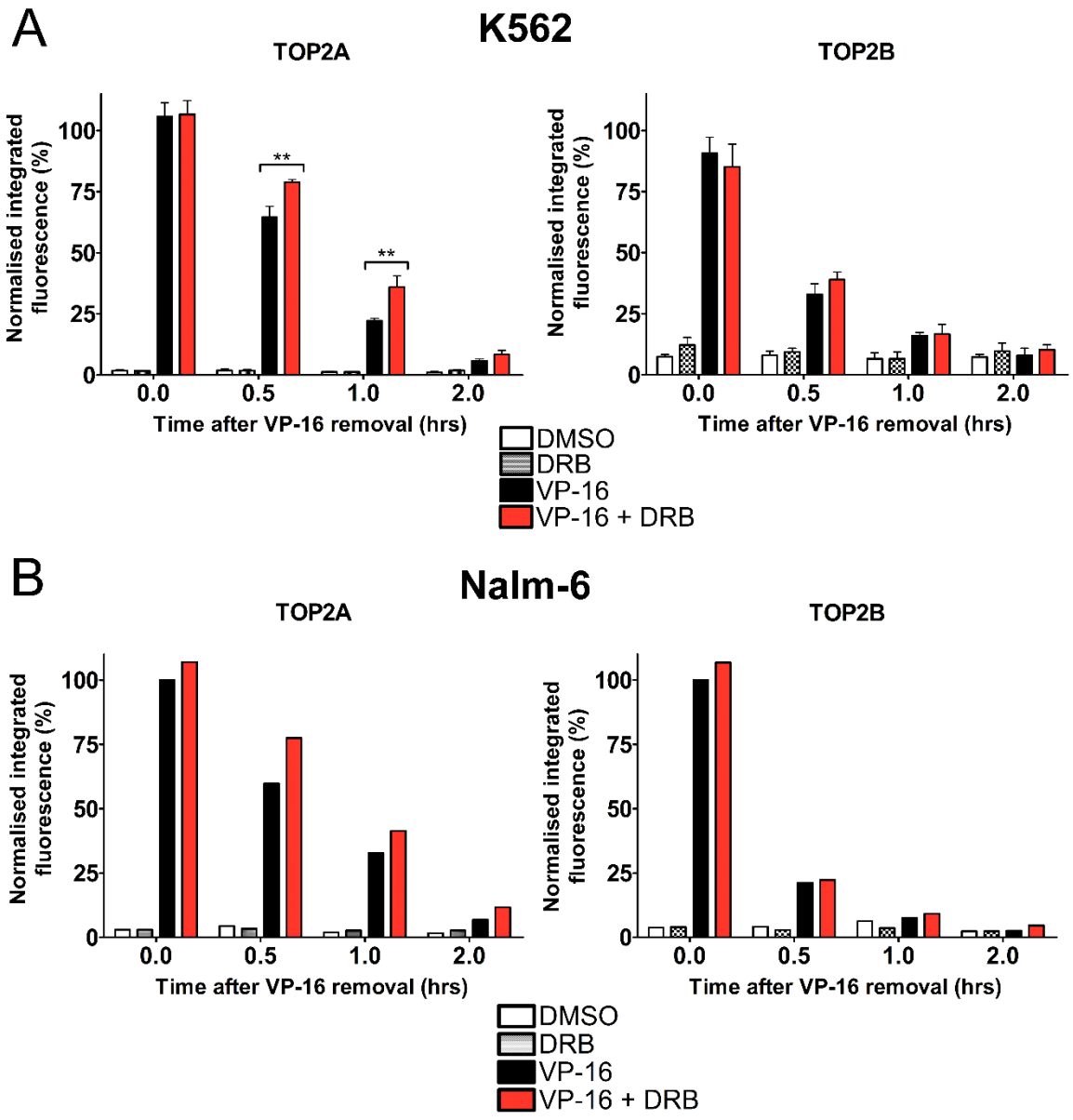

Figure 3.23. Effect of transcription inhibition on levels of etoposide-induced TOP2-DNA complexes, measured using the TARDIS assay. A) K562 cells were treated with 100 µM etoposide (VP-16) alone or in combination with 300 µM DRB for 2 hours. Etoposide was removed from the culture medium and cells were collected (0 hours after VP-16 removal) or incubated for a further 2 hours in etoposide-free medium containing 300 µM DRB or 0.4% v/v DMSO. TOP2A- and TOP2B- DNA complexes were measured at 0, 0.5, 1 and 2 hours after etoposide removal using the TARDIS assay. Median integrated fluorescence was normalised to a 100 µM etoposide control, and statistical comparisons were made by two-way ANOVA followed by Bonferroni post-test (n=3). B) Nalm-6 cells were treated with 100 µM etoposide alone or in combination with 150 µM DRB for 2 hours, followed by a further 2 hour incubation in etoposide-free medium containing 150 µM DRB or 0.2% DMSO. TOP2A- and TOP2B- DNA complexes were measured at 0, 0.5, 1 and 2 hours after etoposide removal using the TARDIS assay (n=1).

To further investigate the role of transcription in the processing of TOP2-DNA complexes, the γH2AX assay was used to test the effect of transcription inhibition on the appearance of etoposide-induced DSBs. K562 cells were treated with 10 μM etoposide (VP-16) alone or in combination with 300 μM DRB continuously for up to 4 hours, and DSBs were measured following 0, 1, 2 and 4 hours of drug treatment. Alternatively, cells were treated for 2 hours with etoposide alone or in combination with DRB for 2 hours, followed by etoposide removal and 2 hours incubation in the continued presence of DMSO or DRB, respectively. Exposure of cells to DRB alone did not affect levels of phosphorylated histone H2AX. Furthermore, co-incubation of cells with DRB and etoposide did not significantly affect levels of etoposide-induced DSBs following 1 or 2 hours drug exposure, nor after etoposide washout (Figure 3.24). However, after 4 hours continuous drug exposure there was a statistically significant decrease in levels of etoposide-induced DSBs in the presence of DRB compared to etoposide alone ($p<0.001$). Therefore, the appearance of DSBs is partly transcription-dependent following 4 hours continuous exposure to etoposide, consistent with a role for transcription in the processing of TOP2-DNA complexes to DSBs.

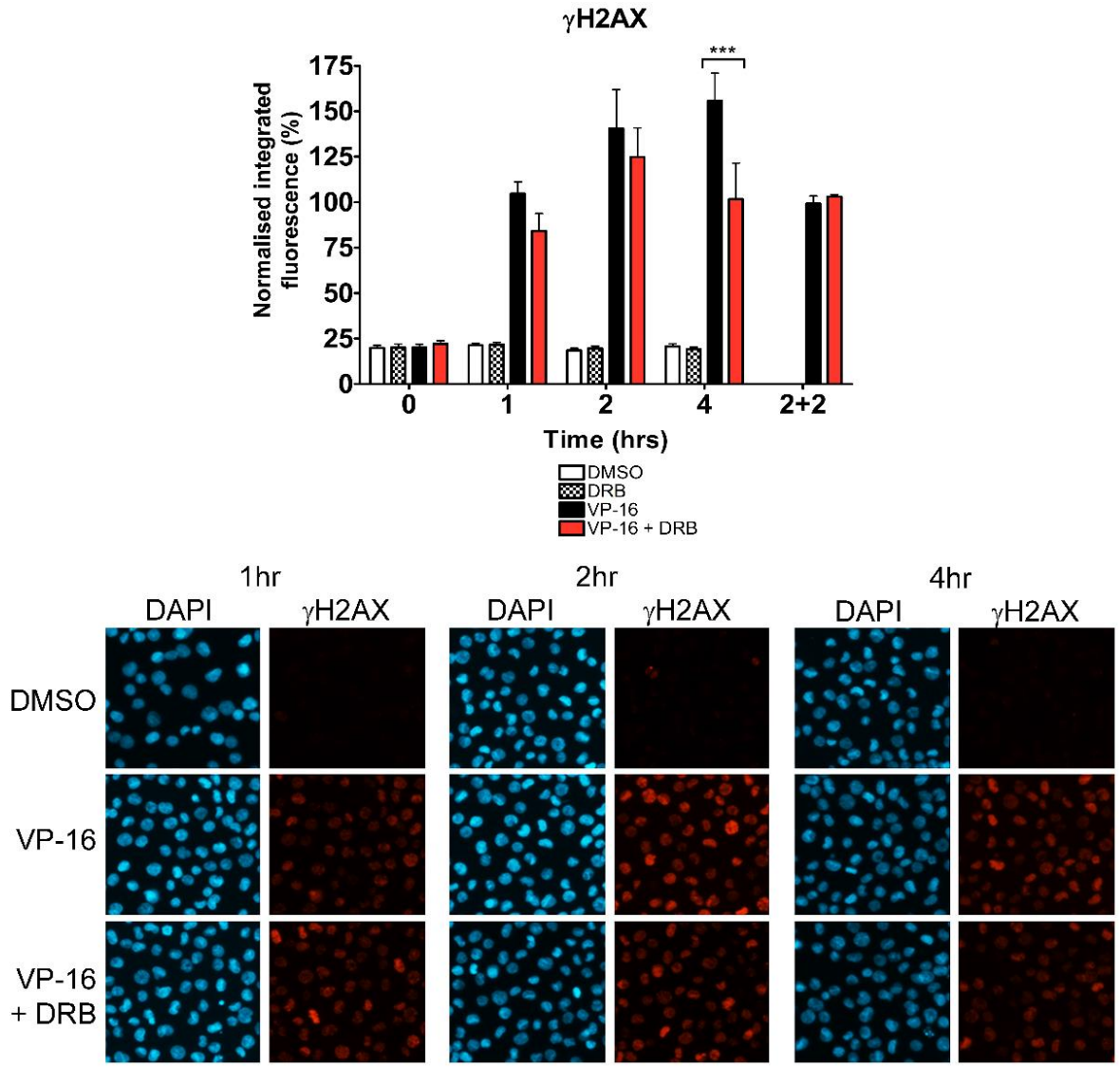

Figure 3.24. Effect of transcription inhibition on the etoposide-induced phosphorylation of histone H2AX. K562 cells were treated with 10 µM etoposide (VP-16) alone or in combination with 300 µM DRB for up to 4 hours. Alternatively, cells were treated with etoposide for 2 hours followed by a further 2 hour incubation in etoposide-free medium containing DRB or 0.4% v/v DMSO (2+2). Protein-free DSBs were measured by γH2AX assay, and all data normalised to a 1 hour 10 µM etoposide control. Values represent the mean of median integrated fluorescence from at least 3 replicate experiments. Statistical comparisons were made by two-way ANOVA with Bonferroni post-test ($n<8$).

3.9 Investigating other mechanisms of TOP2-DNA complex processing

Studies using the TARDIS assay have shown that inhibition of the proteasome does not completely prevent the removal of TOP2-DNA complexes (Lee *et al.*, 2016) (also see Figure 3.4). In this assay, the ongoing removal of TOP2 from DNA under conditions of proteasome inhibition could be attributed to the reversible nature of TOP2-DNA complexes (upon the removal of etoposide) or the active removal of TOP2 by alternative mechanisms. Besides the proteasomal pathway, other mechanisms have been described which can remove covalently bound TOP2 from DNA, and these are outlined in Chapter 1. In this section, the contribution of these pathways to the processing of TOP2-DNA complexes is investigated using TARDIS and the ɣH2AX assay.

3.9.1 *The nucleolytic processing pathway*

TOP2-DNA complexes can be removed via a nuclease-dependent pathway involving Mre11 of the MRN complex or CtIP, which cleaves the DNA (Hartsuiker *et al.*, 2009; Lee *et al.*, 2012; Aparicio *et al.*, 2016). To better understand the contribution of the nucleolytic pathway to the removal of TOP2-DNA complexes, the TARDIS assay was performed in etoposide-treated cells in the presence and absence of mirin, an inhibitor of the Mre11 nuclease.

K562 cells were treated with 100 µM etoposide (VP-16) alone or in combination with 100 µM mirin and/or 10 µM MG132 for 2 hours. Etoposide was removed from the culture medium and cells were incubated for up to 2 hours in the continued presence of mirin, MG132, mirin and MG132, or DMSO as indicated. Levels of TOP2A- and TOP2B- DNA complexes were measured at 0, 0.5, 1 and 2 hours after etoposide removal. As previously demonstrated, levels of remaining TOP2A-DNA complexes were increased in the presence of MG132 at 0.5, 1 and 2 hours after etoposide removal (Figure 3.25). In addition, levels of TOP2B-DNA complexes were increased 0.5 hours after etoposide removal when the proteasome was inhibited. However, levels of etoposide-induced TOP2A- and TOP2B- DNA complexes were unaffected by the treatment of cells with mirin, and this was true at all time points tested. Furthermore, no additive effect was observed when etoposide-treated cells were incubated with both mirin and MG132, suggesting that Mre11 does not significantly contribute to the removal of TOP2-DNA complexes as measured by the TARDIS

assay. This is in contrast to previously published data, whereby incubation of TARDIS slides with recombinant Mre11 significantly reduced levels of etoposide-induced TOP2-DNA complexes, indicating Mre11-dependent removal of drug-induced TOP2 complexes *in vitro* (Lee *et al.*, 2012). Lee et al. also demonstrated an increase in basal levels of TOP2-DNA complexes in the absence of TOP2 poison following treatment of K562 cells with 100 µM mirin, which was not observed in the current study. An important difference between these studies is the duration of mirin incubation, which was a maximum of 4 hours in the present study and 24 hours in the aforementioned study (Lee *et al.*, 2012). Therefore, prolonged exposure of cells with mirin may be required to inhibit Mre11 nuclease activity.

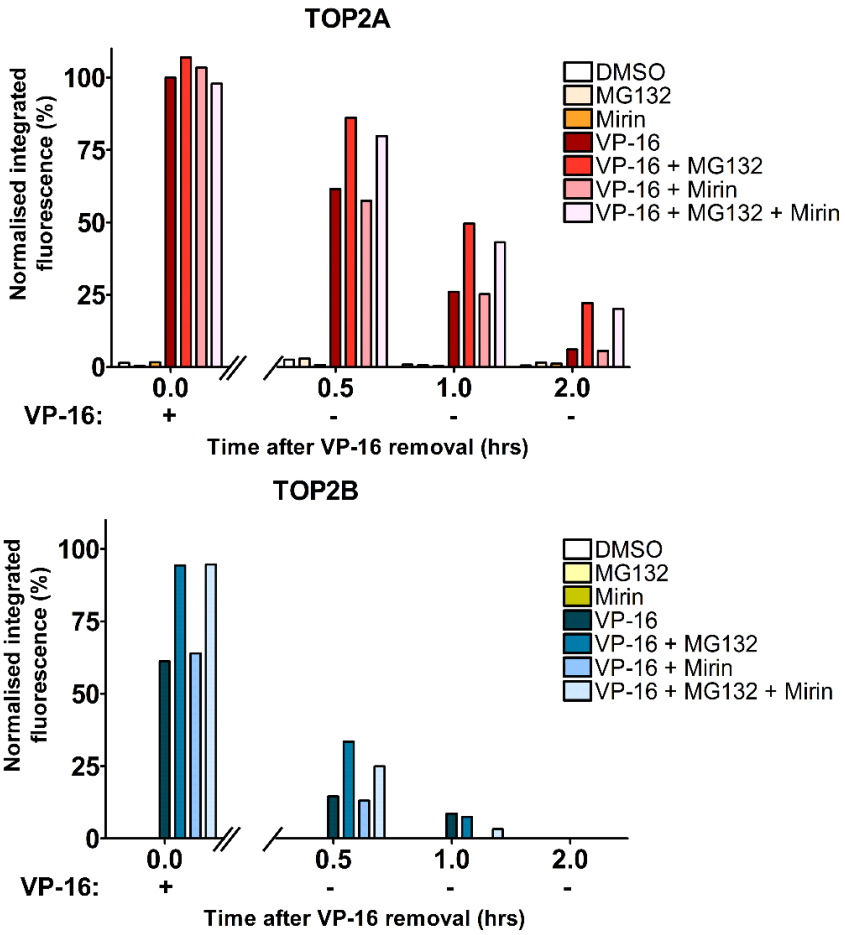

Figure 3.25. Effect of Mre11 inhibition on levels of etoposide-induced TOP2-DNA complexes. K562 cells were treated with 100 µM etoposide (VP-16) alone or in combination with 10 µM MG132 and/or 100 µM mirin for 2 hours. Etoposide was removed from the culture medium and cells were collected (0 hours after VP-16 removal) or incubated for up to 2 hours in the continued presence of 10 µM MG132 and/or 100 µM mirin. Levels of TOP2-DNA complexes were determined using the TARDIS assay. Values represent the median integrated fluorescence from a single experiment, and are normalised to a 100 µM etoposide control (n=1).

The role of Mre11 in the processing of TOP2-DNA complexes to protein-free DSBs was also investigated using the γH2AX assay. K562 cells were treated with 10 µM etoposide (VP-16) alone or in combination with 100 µM mirin for up to 4 hours. Alternatively, cells were treated with etoposide alone or in combination with mirin for 2 hours, followed by incubation in etoposide-free medium containing DMSO or mirin, respectively. Co-incubation of cells with mirin did not affect the appearance of etoposide-induced γH2AX signal with continuous drug exposure, suggesting that Mre11 does not contribute significantly to the processing of TOP2-DNA complexes to DSBs. In contrast, levels of etoposide-induced DSBs were significantly increased in the presence of mirin following 2 hours incubation in etoposide-free medium (2+2hr washout, $p>0.01$), indicating inhibition of DSB repair. This is consistent with the role of Mre11 in homologous recombination, which is partly involved in the repair etoposide-induced DNA damage (de Campos-Nebel *et al.*, 2010; Liu and Huang, 2016). Furthermore, this suggests that exposure of cells to mirin for 4 hours is sufficient to inhibit Mre11, although this should be confirmed in future studies.

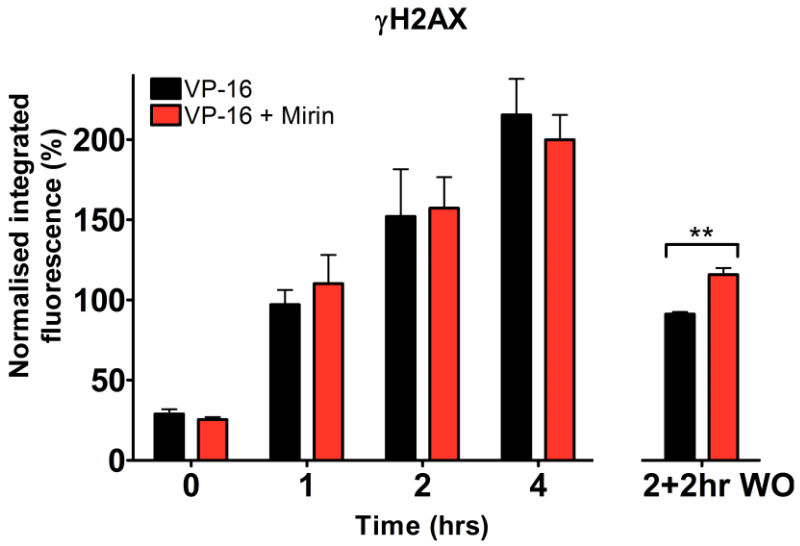

Figure 3.26. Effect of Mre11 inhibition on etoposide-induced γH2AX levels. K562 cells were treated with 10 µM etoposide (VP-16) alone or in combination with 100 µM mirin for up to 4 hours. Alternatively, cells were treated with 10 µM etoposide alone or in combination with 100 µM mirin for 2 hours, followed by 2 hours incubation in etoposide-free medium containing DMSO or mirin, respectively (2+2hr washout, WO). Cells were collected following 0, 1, 2 and 4 hours of drug treatment, and levels of histone H2AX phosphorylation were measured by γH2AX assay. Values represent the mean of triplicate experiments ± SEM, normalised to a 1 hour 10 µM etoposide control. Statistical comparisons were made by two-way ANOVA followed by Bonferroni post-test (n=3).

3.9.2 *Proteasome-independent processing by TDP2*

TDP2 is a 5'-phosphodiesterase which directly cleaves the 5'-phosphotyrosyl bond between DNA and the TOP2 active site tyrosine (Cortes Ledesma *et al.*, 2009; Zeng *et al.*, 2011; Schellenberg *et al.*, 2012; Gao *et al.*, 2014). This bond becomes accessible once the bulk of the TOP2 protein has been degraded by the proteasome, and is subsequently cleaved by TDP2 to produce ligatable ends for NHEJ (Gómez-Herreros *et al.*, 2013; Gao *et al.*, 2014). However, a proteasome-independent mechanism of removal was also recently described whereby TDP2 removes TOP2-DNA complexes in cooperation with the ZATT SUMO ligase (formerly known as ZNF451) (Schellenberg *et al.*, 2017), which is expressed in K562 cells (see Appendix Figure 6). To determine the relative contribution of TDP2-mediated TOP2 removal from DNA, the TARDIS assay was performed in TDP2 siRNA knockdown cells in the presence and absence of the proteasome inhibitor MG132.

K562 cells were electroporated in the presence of 500 nM non-coding (CON siRNA) or 500 nM TDP2 siRNA, and levels of TDP2 protein were measured by western blot after 24, 48 and 72 hours (Figure 3.27). TDP2 protein was reduced at all time points tested, but most notably after 48 hours after electroporation where only 2% TDP2 protein remained compared to control siRNA-treated cells. TDP2 levels began to recover after 72 hours, and therefore all experiments with TDP2 knockdown cells were performed 48 hours after electroporation.

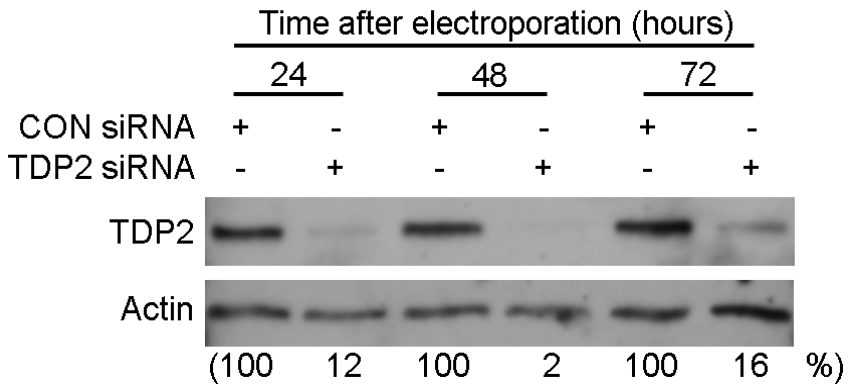

Figure 3.27. siRNA knockdown of TDP2 in K562 cells. K562 cells were transfected with 500 nM non-coding siRNA (CON siRNA) or 500 nM TDP2 siRNA by electroporation. Western blotting was used to measure levels of TDP2 protein at 24, 48 and 72 hours after electroporation. TDP2 levels were quantified and expressed as the percentage remaining compared to the corresponding CON siRNA control.

CON siRNA or TDP2 siRNA knockdown cells were treated with 100 µM etoposide (VP-16) alone or in combination with 10 µM MG132 for 2 hours. Etoposide was removed from the culture medium, and levels of TOP2A- and TOP2B- DNA complexes were measured following 0, 0.5, 1 and 2 hours incubation in etoposide-free medium containing MG132 or DMSO. Figure 3.28A shows the siRNA-mediated knockdown of TDP2 in cells from each replicate experiment. The efficiency of siRNA knockdown was variable between experiments, with levels of detectable TDP2 protein ranging from 0% to 27% (compared to control siRNA-treated cells).

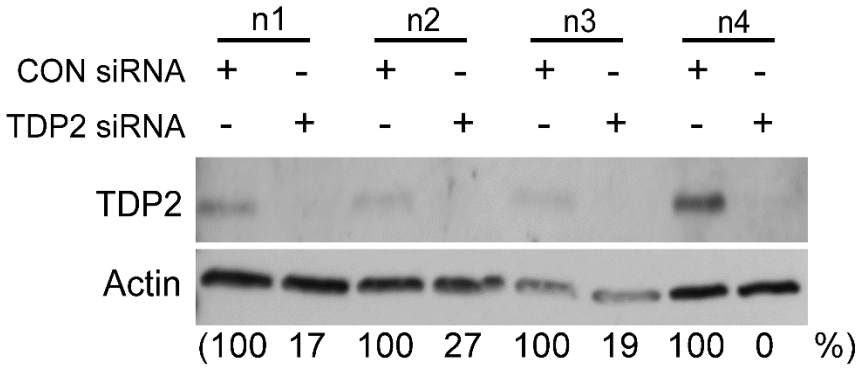

Figure 3.28. siRNA knockdown of TDP2 in cells from replicate TARDIS experiments. CON siRNA and TDP2 siRNA knockdown cells were collected from 4 replicate TARDIS experiments, and TDP2 levels were tested by western blot. TDP2 levels were quantified and expressed as the percentage remaining compared to the corresponding CON siRNA control, as described in Chapter 2, section 2.7.1.

As previously shown, inhibition of the proteasome did not significantly affect levels of TOP2A- or TOP2B- DNA complexes following 2 hours continuous exposure to etoposide (0 hours after VP-16 removal, Figure 3.29), but did increase remaining TOP2 complex levels after etoposide removal. This was true in cells treated with both control siRNA and TDP2 siRNA. Importantly, TDP2 knockdown did not significantly affect levels of etoposide-induced TOP2A- or TOP2B-DNA complexes at any of the time points tested, suggesting that TDP2 alone does not contribute significantly to the removal of TOP2-DNA complexes in K562 cells. Furthermore, TDP2 knockdown did not affect levels of etoposide-induced TOP2A- or TOP2B- DNA complexes when the proteasome was inhibited. Therefore, proteasome-independent removal of TOP2-DNA complexes by TDP2 was not detected in K562 cells using the TARDIS assay.

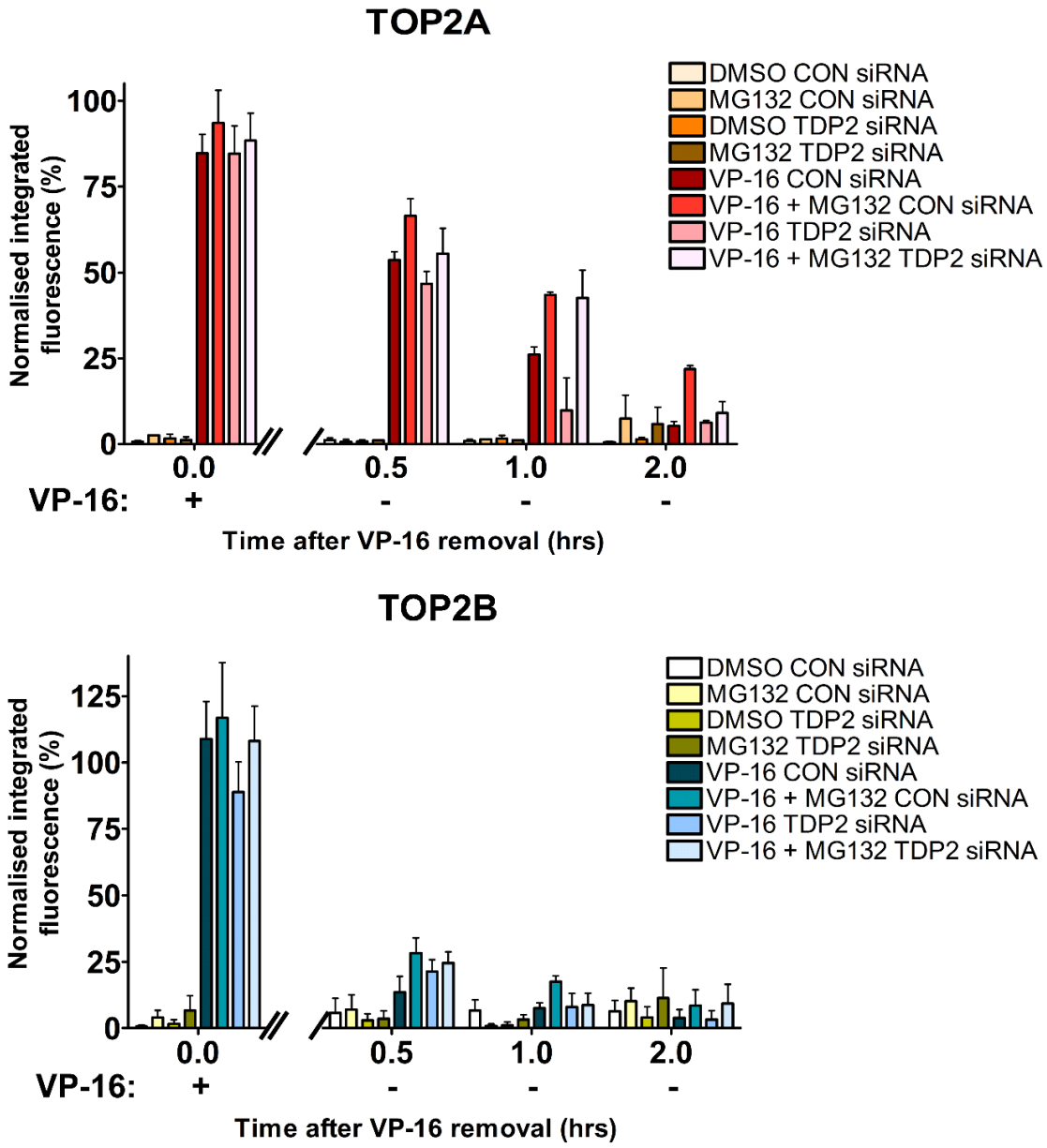

Figure 3.29. Effect of TDP2 knockdown on the proteasome-independent removal of TOP2-DNA complexes measured using the TARDIS assay. CON siRNA or TDP2 siRNA knockdown cells were treated with 100 µM etoposide (VP-16) alone or in combination with 10 µM MG132 for 2 hours. Following etoposide washout, cells were collected or incubated for a further 2 hours in etoposide-free medium containing 10 µM MG132 or 0.1% v/v DMSO. TOP2-DNA complex levels were measured at 0, 0.5, 1 and 2 hours after etoposide removal. Replicate experiments were normalised to a 2 hour 100 µM etoposide control, and compared by two-way ANOVA with Bonferroni post-test (n=3 for TOP2A, and n=4 for TOP2B).

Schellenberg et al. report that TDP2 specifically targets SUMOylated TOP2-DNA complexes, which accumulate in TDP2 knockout cells when the proteasome is inhibited (Schellenberg *et al.*, 2017). It is therefore possible that changes in levels of SUMO-modified TOP2-DNA complexes could be detected by measuring only TOP2 complexes that are SUMOylated. To test this, TARDIS slides were also probed for SUMO-2/3 conjugates. The stringent conditions utilised during the TARDIS lysis procedure effectively remove all non-covalently bound proteins from DNA whilst TOP2 complexes remain covalently attached in the presence of etoposide (see Figure 3.3). Therefore, it is anticipated that the only SUMO conjugates present on TARDIS slides are SUMOylated TOP2-DNA complexes. Consistent with this, SUMO-2/3 conjugates were not detectable on TARDIS slides in the absence of etoposide, but were readily detectable in control siRNA and TDP2 siRNA knockdown cells following 2 hours incubation in 100 µM etoposide (0 hours after VP-16 removal, Figure 3.30).

While probing of TARDIS slides for TOP2A or TOP2B reveals a proteasome-dependent increase in remaining TOP2-DNA complex levels after etoposide removal (Figure 3.4), levels of SUMOylated TOP2-DNA complexes were not significantly affected by co-incubation of control cells with MG132 when TARDIS slides were probed for SUMO-2/3 conjugates. This was true both after continuous etoposide exposure (0 hours after VP-16 removal) and at all time points after etoposide removal. This suggests that the proteasome is not involved in the regulation of SUMOylated TOP2-DNA complexes. Furthermore, levels of SUMOylated TOP2 were not affected by TDP2 knockdown compared to control cells, suggesting that TDP2 alone does not remove SUMO-2/3-TOP2 from DNA. TDP2 knockdown did not affect levels of SUMOylated TOP2-DNA complexes even when the proteasome was inhibited. Therefore, the proteasome-independent removal of SUMOylated TOP2-DNA complexes was not observed in K562 cells following TDP2 knockdown. This is in contrast to what has been previously reported in TDP2 knockout MEFs using the ICE assay, whereby TDP2 knockout led to the accumulation of SUMO-2/3-TOP2 complexes within 30 minutes of etoposide washout (Schellenberg *et al.*, 2017).

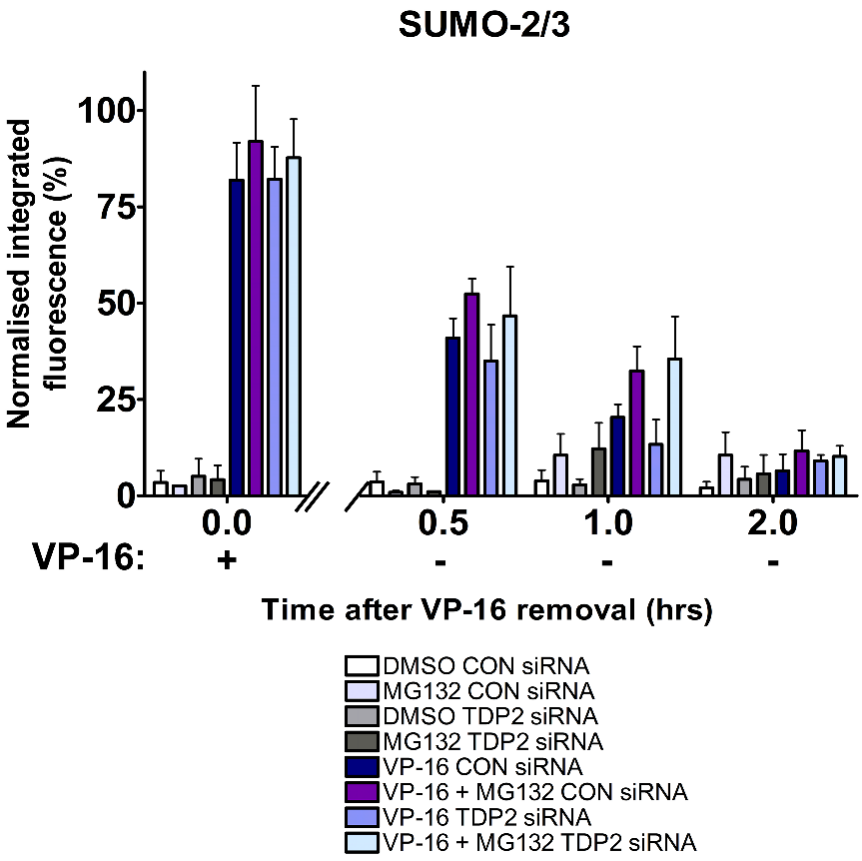

Figure 3.30. Effect of TDP2 knockdown on the proteasome-independent removal of SUMOylated TOP2-DNA complexes measured using the TARDIS assay. CON siRNA or TDP2 siRNA knockdown cells were treated with 100 µM etoposide (VP-16) alone or in combination with 10 µM MG132 for 2 hours. Following etoposide washout, cells were collected or incubated for a further 2 hours in etoposide-free medium containing 10 µM MG132 or 0.1% v/v DMSO. Levels of SUMO conjugates were measured at 0, 0.5, 1 and 2 hours after etoposide removal. The TARDIS assay was performed as previously described, except for the inclusion of 10 mM NEM in lysis buffers to inhibit DUB enzymes, and probing of slides with anti-SUMO-2/3 antibody. Replicate experiments were normalised to a 2 hour 100 µM etoposide control, and compared by two-way ANOVA with Bonferroni post-test (n=3).

The role of TDP2 in the proteasome-independent removal of TOP2-DNA complexes was also investigated using the γH2AX assay. Previous publications have shown that TDP2 knockout does not affect the appearance of etoposide-induced DSBs but significantly slows DSB repair (Gómez-Herreros *et al.*, 2013). However, in the presence of MG132, the number of etoposide-induced γH2AX foci were reported to be significantly reduced by TDP2 knockout, suggesting that TDP2 removes TOP2-DNA complexes in the absence of proteasomal activity (Schellenberg *et al.*, 2017).

To investigate this, CON siRNA or TDP2 siRNA cells (shown in Figure 3.29A) were treated with 100 µM etoposide alone or in combination with 10 µM MG132 for 2 hours. Etoposide was removed from the culture medium and cells were incubated in the continued presence of MG132 or DMSO. γH2AX levels were measured at 0, 0.5, 1, 2 and 3 hours after etoposide removal. In control cells, the level of etoposide-induced DSBs (as measured by γH2AX fluorescence) are gradually decreased with time following incubation in etoposide-free medium, reflecting DNA repair (Figure 3.31). siRNA knockdown of TDP2 did not significantly affect the appearance of etoposide-induced DSBs, further supporting the notion that TDP2 alone does not remove TOP2 complexes from DNA. Surprisingly, the rate of DSB repair (as measured by the disappearance of γH2AX signal) was also unaffected in TDP2 knockdown cells, in contrast to published data in TDP2 knockout cells (Gómez-Herreros *et al.*, 2013).

In the presence of MG132, the appearance of etoposide-induced DSBs were greatly reduced in both CON siRNA and TDP2 siRNA knockdown cells (Figure 3.31), as previously shown. However, TDP2 knockdown did not affect levels of etoposide-induced histone H2AX phosphorylation in the presence of MG132. Therefore, the proteasome-independent removal of TOP2-DNA complexes by TDP2 was not detected in TDP2 knockdown cells using the γH2AX assay. An important difference between this study and others (Gómez-Herreros *et al.*, 2013; Schellenberg *et al.*, 2017) is the use of TDP2 knockdown and TDP2 knockout cells, respectively. Indeed, low levels of TDP2 protein may still be present in knockdown cells, which may be sufficient for TOP2 complex removal. Furthermore, histone H2AX phosphorylation is quantified here by integrated fluorescence per nucleus, whereas quantification of γH2AX by Schellenberg et al. is achieved by counting foci numbers. Unlike IR-

induced γH2AX foci which are relatively uniform and easy to count in an automated manner, etoposide-induced γH2AX foci vary in size and fluorescence intensity. Therefore, it is plausible that the numbers of foci are affected without affecting the overall fluorescence of the nucleus. This would suggest that small changes in levels of γH2AX foci are not detected by integrated fluorescence. Nonetheless, measurement of integrated fluorescence is an automated process and therefore less susceptible to human error or investigator bias.

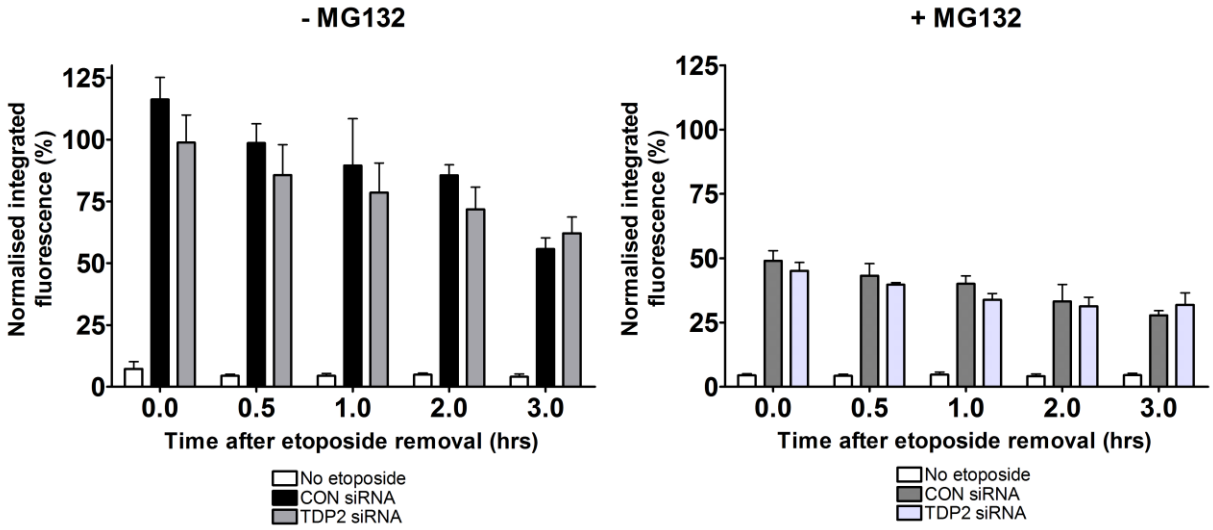

Figure 3.31. Effect of TDP2 siRNA knockdown on etoposide-induced γH2AX levels. CON siRNA and TDP2 siRNA knockdown cells were treated with 100 µM etoposide (VP-16) alone or in combination with 10 µM MG132. Cells were collected after 2 hours continuous drug exposure (0 hours after VP-16 removal) or incubated for up to 3 hours in etoposide-free medium containing 10 µM MG132 or 0.1% v/v DMSO. Levels of protein-free DSBs were measured using the γH2AX assay. Values represent mean of medians ± SEM, normalised to a 1 hour 100 µM etoposide control and compared by two-way ANOVA with Bonferroni post-test (n=3).

3.10 Discussion

In this chapter, the role of the ubiquitin-proteasome system in the processing of etoposide-induced TOP2-DNA complexes was investigated by small molecule inhibition and siRNA knockdown of ubiquitin activating enzymes. While current evidence suggests that TOP2A-DNA complexes are degraded in a ubiquitin-dependent manner (Alchanati *et al.*, 2009), conflicting reports exist regarding the role of ubiquitin in the processing of TOP2B-DNA complexes (Mao *et al.*, 2001; Ban *et al.*, 2013). Here, the removal of both TOP2A- and TOP2B- DNA complexes was slowed in the presence of UAE inhibitor MLN7243, suggesting that the processing of both TOP2A- and TOP2B- DNA complexes is partly ubiquitin-dependent. Furthermore, chemical inhibition or siRNA knockdown of UAE1 and UBA6 significantly reduced the appearance of etoposide-induced DSBs in a manner specific to topoisomerase-mediated damage.

Although western blotting and immunofluorescence could be used to examine the proteasomal degradation of TOP2B, the processing of TOP2-DNA complexes was further investigated using the TARDIS assay. This approach is more informative as it enables the direct measurement of TOP2-DNA complexes in an easily quantifiable manner. Moreover, the proteasomal degradation of TOP2A-DNA complexes was observed using the TARDIS assay but not by western blot or immunofluorescence, suggesting changes in levels of TOP2-DNA complexes are difficult to detect in a pool of total TOP2 protein. TOP2A is removed at a slower rate than TOP2B, which is also indicated by the longer half-life of TOP2A complexes in the TARDIS assay.

Combination studies with MLN7243 and MG132 show that UAE and the proteasome operate via the same pathway in the removal of TOP2-DNA complexes, thereby supporting the role of ubiquitin-dependent proteolysis. However, these data do not exclude the possibility that UAE activity is required for the ubiquitination of another protein involved in TOP2-DNA complex repair rather than TOP2 itself. Indeed, it is important to note that inhibition of UAE will induce widespread disruption of the ubiquitin-proteasome system, and will affect the ubiquitination of many proteins. Because of this, a more favourable approach is the inhibition of specific E3 ubiquitin ligases, which restricts inhibition to a more defined group of substrates. Strikingly, inhibition of the BMI1/RING1A ubiquitin ligase greatly reduced the appearance of

etoposide-induced DSBs and slowed the removal of both TOP2A- and TOP2B-complexes from DNA, suggesting that TOP2-DNA complex processing can be targeted downstream of UAE enzymes.

The TARDIS assay was also used to investigate other pathways contributing to TOP2-DNA complex removal. For example, the role of transcription was addressed by the co-treatment of cells with DRB. Surprisingly, inhibition of transcription slowed the removal of TOP2A- but not TOP2B- DNA complexes. This is in contrast to published data which has shown a transcription-dependent mechanism for the removal of both TOP2A- and TOP2B- DNA complexes (Mao *et al.*, 2001; Fan *et al.*, 2008; Ban *et al.*, 2013; Tammaro *et al.*, 2013). Numerous studies have shown that like proteasome inhibition, treatment of cells with DRB prevents the etoposide- or teniposide- induced degradation of TOP2A and TOP2B as measured by western blotting (Mao *et al.*, 2001; Zhang *et al.*, 2006; Fan *et al.*, 2008; Ban *et al.*, 2013). Transcription inhibition, but not replication inhibition, also prevents the phosphorylation of DNA damage-dependent proteins such as histone H2AX, RPA, Chk1 and Chk2 following etoposide treatment (Fan *et al.*, 2008; Tammaro *et al.*, 2013). Ban et al. propose that the collision of TOP2B complexes with RNA polymerase II leads to the proteasomal degradation of TOP2 via RNA polymerase II-associated AAA ATPases (Ban *et al.*, 2013). However, the data presented in Figure 3.23 and Figure 3.24 suggest that TOP2B complexes can be removed by the proteasome even in the absence of ongoing transcription. However, it cannot be fully excluded that the transcription-dependent removal of TOP2B complexes may still have occurred in DRB-treated cells due to incomplete inhibition of transcriptional activity.

Importantly, inhibition of the proteasome, UAE or transcription did not completely prevent the removal of TOP2 complexes from DNA. The TARDIS assay was used to examine the role of other processing pathways including the nuclease-dependent removal of TOP2 by Mre11 and proteasome-independent removal by TDP2. However, disruption of these alternative pathways did not significantly affect TOP2-DNA complex processing as measured by TARDIS or γH2AX assay. While this may be due to incomplete inhibition of these pathways (for example by mirin or TDP2 knockdown), this suggests that the proteasome- and ubiquitin- independent removal

of TOP2 complexes observed using the TARDIS assay is largely due to the spontaneous reversal of complexes and completion of the TOP2 reaction mechanism upon etoposide removal. This further indicates that the ubiquitin- and proteasome- dependent processing of TOP2-DNA complexes is a major repair pathway.

In summary, this study shows that ubiquitination is partly required for the processing of both TOP2A- and TOP2B- DNA complexes, and is therefore an important layer of regulation in the repair of etoposide-induced DNA damage. Inhibition of the ubiquitin-proteasome system with proteasome inhibitors or UAE inhibitors significantly increases the half-life of TOP2-DNA complexes, which may increase drug cytotoxicity (see Chapter 6). In addition, the appearance of protein-free DSBs is significantly reduced. While protein-free DSBs can lead to cell death, aberrant NHEJ repair of these breaks are associated with leukaemogenic chromosome translocations. Therefore, combination therapies of ubiquitin-proteasome inhibitors with TOP2 poisons could prove beneficial in a clinical setting by maintaining drug efficacy whilst also reducing genotoxicity.

Chapter 4 Studying the post-translational modifications of TOP2-DNA complexes

4.1 Introduction

Ubiquitination involves the conjugation of ubiquitin to the lysine residues of target proteins. Whilst most typically associated with proteasomal degradation, there are many consequences of ubiquitination including changes in enzymatic activity, protein localisation and protein-protein interactions. As described in Chapter 1, ubiquitin is involved in the regulation of multiple cellular pathways. In the previous chapter, it was shown that ubiquitination is required for the efficient removal of TOP2-DNA complexes and the subsequent appearance of etoposide-induced DSBs. This effect was epistatic with the role of the proteasome, suggesting that the proteasomal degradation of TOP2-DNA complexes is ubiquitin dependent. It was hypothesised that UAE activity facilitates the processing of TOP2-DNA complexes through the ubiquitination of TOP2. However, these data do not eliminate the possibility that UAE activity could be required for the ubiquitination of another protein involved in removal or repair. Therefore, the principle aim of the current chapter was to investigate the ubiquitination of TOP2 following etoposide treatment.

The ubiquitin-dependent degradation of TOP2A has been shown in response to various stresses, including glucose starvation (Yun *et al.*, 2004), HDAC inhibition (Chen *et al.*, 2011) and treatment with teniposide (Alchanati *et al.*, 2009). In the latter study, an increase in TOP2A molecular weight (presumed to be TOP2A ubiquitination) was observed in HeLa cells following teniposide treatment. This was further increased in cells overexpressing the E3 ubiquitin ligase BMI1/RING1A, which was thereby identified as the E3 ubiquitin ligase required for the proteasomal degradation of TOP2A-, but not TOP2B-, DNA complexes. Consistently, TOP2A ubiquitination was also observed *in vitro* when Flag-TOP2A immunoprecipitates were incubated with recombinant BMI1/RING1A (Alchanati *et al.*, 2009). Chen et al. also show a decrease in TOP2A electrophoretic mobility when cells are treated with HDAC inhibitors (Chen *et al.*, 2011). However, TOP2 poison-induced ubiquitination of TOP2 has not been adequately demonstrated using more recently developed methods which are now available for the study of protein ubiquitination. In particular, overexpression of tagged ubiquitin or ubiquitinating enzymes may lead to the

artificial ubiquitination of proteins which would not otherwise be ubiquitinated, or may disrupt normal ubiquitin physiology (Emmerich and Cohen, 2015). Indeed, Ban et al. were not able to detect ubiquitinated TOP2B in cells expressing HA-tagged ubiquitin either in the presence and absence of etoposide, while TOP2A ubiquitination was not investigated in this study (Ban *et al.*, 2013). However, at least 32 TOP2B ubiquitination sites have been detected by mass spectrometry in the absence of TOP2 poison (Kim *et al.*, 2011). Known ubiquitination sites in TOP2A and TOP2B are displayed in Chapter 1, Figure 1.7.

The study of protein ubiquitination is particularly challenging due to rapid reversal by deubiquitinase enzymes (DUBs) and the potential degradation of ubiquitinated proteins by the proteasome. Furthermore, ubiquitination of small subpopulations of protein can be difficult to detect due to low stoichiometry. Consequently, changes in levels of ubiquitinated protein may escape detection by measuring total protein levels, for example by western blot (Kim *et al.*, 2011). Nonetheless, western blotting can be used to specifically study ubiquitinated proteins by first isolating and enriching ubiquitinated proteins using antibodies or Tandem Ubiquitin Binding Entities (TUBEs). TUBEs contain multiple ubiquitin binding domains which bind ubiquitinated proteins with high affinity (Hjerpe *et al.*, 2009; Wilson *et al.*, 2012). This is preferable to immunoprecipitation, as binding of TUBEs to ubiquitinated proteins has also been shown to protect proteins from deubiquitination and proteasomal degradation (Hjerpe *et al.*, 2009; Wilson *et al.*, 2012; Emmerich and Cohen, 2015). This approach was used here to investigate the conjugation of TOP2 with endogenous ubiquitin before and after exposure of cells to etoposide.

Closely related to ubiquitin is the ubiquitin-like (UBL) protein known as SUMO (small ubiquitin-like modifier). There are four SUMO isoforms in human cells (SUMO-1, SUMO-2/3 and SUMO-4) which are also conjugated to target lysines in a 3-step enzymatic cascade (Geiss-Friedlander and Melchior, 2007). While not initially associated with proteasomal degradation, SUMOylation can lead to protein degradation through the regulation of protein ubiquitination. For example, SUMO-targeted ubiquitin ligases (STUbLs) are E3 ubiquitin ligases containing a SUMO-interacting motif which binds non-covalently to SUMOylated proteins, leading to their ubiquitination (Geoffroy and Hay, 2009).

SUMOylation of TOP2A is essential for proper chromosome segregation (Bachant *et al.*, 2002; Azuma *et al.*, 2003; Takahashi *et al.*, 2006; Higgins, 2012). Specifically, SUMOylation of the TOP2A C terminal domain leads to the recruitment of Claspin and Haspin to mitotic centromeres, which are involved in the activation and localisation of Aurora B, respectively (Ryu *et al.*, 2015; Clarke and Azuma, 2017). However, studies have also shown that TOP2A and TOP2B are SUMOylated following treatment with etoposide or teniposide (Mao *et al.*, 2000; Agostinho *et al.*, 2008; Schellenberg *et al.*, 2017). Importantly, TOP2 poison-induced SUMOylation of TOP2 may not be related to the formation of TOP2-mediated DNA damage but due to changes in protein confirmation, as TOP2 SUMOylation is also observed following exposure to the catalytic inhibitors, ICRF-193 and ICRF-187 which trap TOP2 on DNA without stabilising TOP2-DNA covalent complexes (Mao *et al.*, 2000; Isik *et al.*, 2003; Agostinho *et al.*, 2008; Schellenberg *et al.*, 2017). Consistent with this, the accessibility of a known SUMOylation site in TOP2A (Lys662) is increased upon DNA binding, leading to more efficient SUMOylation by the E3 SUMO ligase, PIASɣ (Ryu *et al.*, 2010; Wendorff *et al.*, 2012). TOP2 SUMOylation has been implicated in the proteasome-independent removal and repair of TOP2-DNA complexes through direct removal by TDP2 (Schellenberg *et al.*, 2017). In the current study, the ubiquitination and SUMOylation of TOP2-DNA complexes was investigated using the TARDIS assay. Given the highly quantifiable nature of TARDIS, this provided a useful platform to test the effects of various ubiquitin-proteasome system inhibitors on levels of ubiquitinated and SUMOylated TOP2-DNA complexes.

4.2 Aims

Multiple ubiquitination sites have been identified on both TOP2A and TOP2B (Kim *et al.*, 2011) (Figure 1.7, Chapter 1), but little is known about their function. In particular, evidence is lacking regarding the ubiquitination of TOP2 in response to TOP2 poisons like etoposide. Therefore, TOP2 ubiquitination was investigated here using TUBEs and by immunoprecipitation of endogenous ubiquitin. Furthermore, the ubiquitination and SUMOylation of TOP2-DNA complexes was investigated using the TARDIS assay.

4.3 TOP2-DNA complexes are ubiquitinated

In this study, the TARDIS assay was adapted to investigate the post-translational modifications of TOP2-DNA complexes including ubiquitination and SUMOylation. As shown in Chapter 3, the stringent lysis conditions used during the TARDIS assay effectively remove non-covalently bound proteins from DNA, including RNA polymerase II and Ku70/80. Therefore only covalently-bound TOP2 is present on TARDIS slides in the presence of etoposide, which can be probed using anti-ubiquitin and anti-SUMO antibodies.

To investigate whether etoposide-induced TOP2-DNA complexes are conjugated to ubiquitin, K562 cells were treated with 100 μM etoposide (or 0.2% v/v DMSO) for 2 hours, and ubiquitinated TOP2-DNA complexes were visualised using the TARDIS assay. Slides were probed using linkage-specific anti-ubiquitin antibodies which detect K48-linked ubiquitin or K63-linked ubiquitin chains. Alternatively, all conjugated ubiquitin (mono- and poly- ubiquitin) was detected using anti-ubiquitin monoclonal antibody (clone FK2). No ubiquitin conjugates were detected in DMSO-treated cells, further corroborating that all ubiquitinated proteins (such as histones) are effectively removed from TARDIS slides (Figure 4.1). However, ubiquitin conjugates were easily detected on TARDIS slides following etoposide exposure, indicating the presence of ubiquitinated TOP2-DNA complexes. Specifically, K48-linked and K63-linked ubiquitin chains were detected, which are typically associated with proteasomal degradation and signalling pathways, respectively.

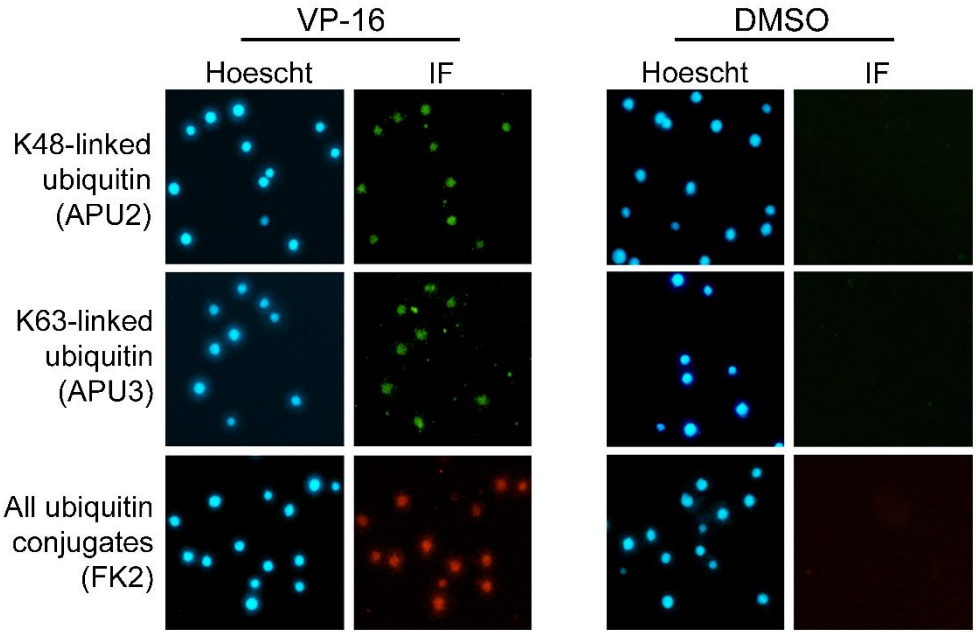

Figure 4.1. Detection of ubiquitin conjugates on TARDIS slides following etoposide treatment. K562 cells were treated with 100 µM etoposide (VP-16) or 0.2% v/v DMSO for 2 hours. TOP2-DNA complexes were isolated as per the TARDIS assay and probed for K48-linked ubiquitin (APU2), K63-linked ubiquitin (APU3) and all conjugated ubiquitin (FK2). *IF* indicates where specific proteins were detected by immunofluorescence.

Like TOP2A and TOP2B, levels of ubiquitinated TOP2-DNA complexes can be quantified by integrated fluorescence. This was used to examine the effect of the UAE inhibitor MLN7243 on the ubiquitination of TOP2-DNA complexes. K562 cells were treated with 100 µM etoposide alone or in combination with 10 µM MLN7243 for 2 hours, and ubiquitinated TOP2-DNA complexes were quantified using the TARDIS assay. As shown above, levels of ubiquitinated TOP2-DNA complexes were significantly increased when cells were treated with etoposide compared to untreated DMSO control. However, in the presence of MLN7243 the etoposide-induced ubiquitin signal was significantly reduced ($p=0.0003$) and no longer significantly different from background levels. This suggests that UAE activity is completely abolished in cells treated with MLN7243, consistent with western blot data shown in Chapter 3 (Figure 3.4B and Figure 3.5D). Therefore, MLN7243 is a highly effective UAE inhibitor which completely inhibits TOP2 ubiquitination.

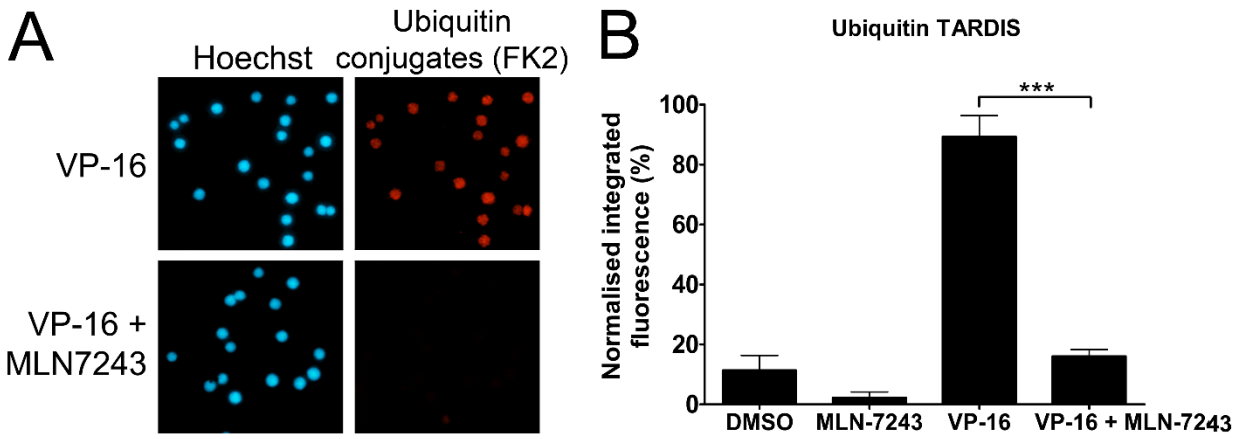

Figure 4.2. Effect of UAE inhibitor MLN7243 on levels of ubiquitinated TOP2-DNA complexes. K562 cells were treated with 100 µM etoposide (VP-16) alone or in combination with 10 µM MLN7243 for 2 hours, and levels of ubiquitinated TOP2-DNA complexes were measured using the TARDIS assay. A) Representative images of TARDIS slides probed for all conjugated ubiquitin (anti-ubiquitin antibody clone FK2). B) Quantification of ubiquitinated TOP2-DNA complexes. Values represent mean of medians ± SEM from triplicate experiments and are normalised to a 2 hour 100 µM etoposide control. Statistical comparisons were made by unpaired t-test (n=3).

In the previous chapter, it was also shown that residual levels of ubiquitination remain in UAE1/UBA6 siRNA knockdown cells which are not present in cells treated with MLN7243. To further investigate this, CON siRNA or double UAE1/UBA6 siRNA knockdown cells were treated with 100 µM etoposide or 0.2% v/v DMSO for 2 hours, and the TARDIS assay was used to measure levels of ubiquitinated TOP2-DNA complexes. Ubiquitinated TOP2-DNA complexes were significantly induced in CON siRNA cells treated with etoposide ($p=0.0007$, Figure 4.3), as expected. Moreover, levels of ubiquitin conjugates were significantly reduced in UAE1/UBA6 siRNA knockdown cells ($p=0.0041$), indicating inhibition of UAE activity. Although reduced, etoposide still induced ubiquitinated TOP2-DNA complexes in knockdown cells, which remained significantly above background levels ($p=0.0005$) indicating incomplete knockdown of UAE activity. This supports the notion that chemical inhibition of UAE by MLN7243 is more effective than siRNA knockdown.

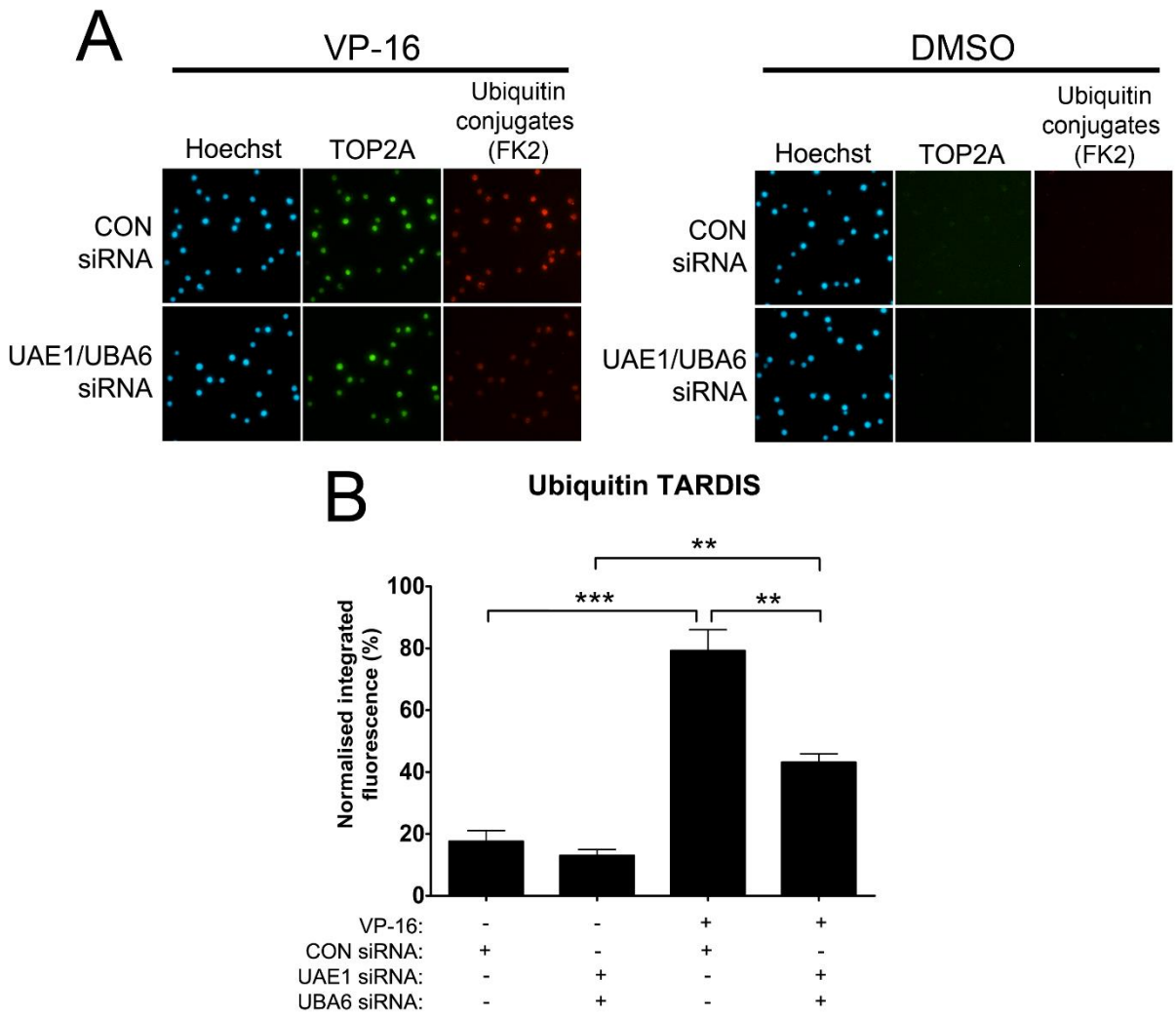

Figure 4.3. Effect of double UAE1 and UBA6 siRNA knockdown on levels of ubiquitinated TOP2-DNA complexes. CON siRNA or double UAE1/UBA6 siRNA knockdown cells were treated with 100 µM etoposide (VP-16) or 0.2% DMSO for 2 hours, and levels of ubiquitinated TOP2-DNA complexes were measured by TARDIS assay. A) Representative images of TARDIS slides probed for TOP2A or conjugated ubiquitin (anti-ubiquitin antibody clone FK2). B) Quantification of ubiquitinated TOP2-DNA complexes. Values represent mean of medians ± SEM from triplicate experiments and are normalised to a 2 hour 100 µM etoposide control. Statistical comparisons were made by unpaired t-test (n=3).

Finally, the TARDIS assay was used to test the effect of the BMI1/RING1A inhibitor PRT4165 on the ubiquitination of TOP2-DNA complexes. BMI1/RING1A is an E3 ubiquitin ligase shown to ubiquitinate TOP2A *in vitro*, and in response to teniposide treatment in cells overexpressing BMI1/RING1A (Alchanati *et al.*, 2009). K562 cells were treated with 100 µM etoposide alone or in combination with 90 µM PRT4165 for 2 hours. As shown above, levels of ubiquitinated TOP2-DNA complexes on TARDIS slides were significantly increased in the presence of etoposide (Figure 4.4A). In the presence of PRT4165, levels of ubiquitinated TOP2-DNA complexes were

significantly reduced compared to etoposide alone (p=0.0026, Figure 4.4B), though remained significantly higher than background levels (p=0.0257). This suggests that other E3 ubiquitin ligases are also involved in the ubiquitination of TOP2-DNA complexes. Notably, the ubiquitin TARDIS assay does not distinguish between ubiquitinated TOP2A- and ubiquitinated TOP2B- DNA complexes. It is reported by Alchanati et al. that BMI1 is not required for the proteasomal degradation of TOP2B after teniposide treatment (Alchanati *et al.*, 2009). Therefore, residual levels of ubiquitinated TOP2 complexes could be due to the ubiquitination of TOP2B-DNA complexes. Nonetheless, this shows that PRT4165 inhibits the ubiquitination of TOP2, whether TOP2A, TOP2B or both. Thus, ubiquitination is partly BMI1/RING1A-dependent.

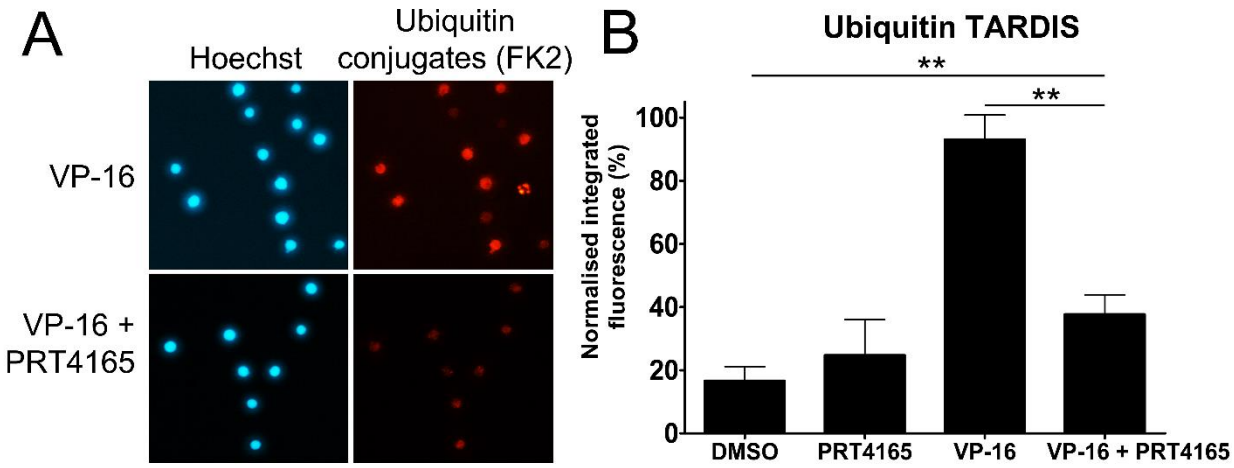

Figure 4.4. Effect of the BMI1/RING1A inhibitor PRT4165 on levels of ubiquitinated TOP2-DNA complexes. K562 cells were treated with 100 µM etoposide (VP-16) alone or in combination with 90 µM PRT4165 for 2 hours, and levels of ubiquitinated TOP2-DNA complexes were measured using the TARDIS assay. A) Representative images of TARDIS slides probed for all conjugated ubiquitin (anti-ubiquitin antibody clone FK2). B) Quantification of ubiquitinated TOP2-DNA complexes. Values represent mean of medians ± SEM from triplicate experiments and are normalised to a 2 hour 100 µM etoposide control. Statistical comparisons were made by unpaired t-test (n=3).

4.4 Effect of proteasome inhibition on levels of ubiquitinated TOP2-DNA complexes

Proteasome inhibition leads to the accumulation of ubiquitinated proteins which are otherwise degraded. To investigate whether ubiquitinated TOP2-DNA complexes are degraded by the proteasome, K562 cells were treated with 100 µM etoposide alone or in combination with 10 µM MG132 for 2 hours, and levels of ubiquitinated TOP2-DNA complexes were measured by TARDIS assay.

Paradoxically, there was a significant decrease in levels of ubiquitinated TOP2-DNA complexes when cells were co-treated with MG132 compared to etoposide alone ($p = 0.0352$, Figure 4.5A). This is contrary to the proteasome inhibitor-induced accumulation of ubiquitin conjugates which is anticipated when ubiquitinated proteins are normally degraded by the proteasome. However, proteasome inhibition can also lead to inhibition of ubiquitination due to depletion of the free ubiquitin pool, which is no longer recycled from degraded ubiquitin conjugates (Xu *et al.*, 2004). Furthermore, proteasome inhibition leads to the redistribution of ubiquitin from the nucleus to the cytoplasm, which is largely attributed to the deubiquitination of highly abundant monoubiquitinated proteins such as histone H2A (Dantuma *et al.*, 2006). Interestingly, mass spectrometry analysis of the ubiquitin-modified proteome has shown that many proteins are deubiquitinated in response to proteotoxic stress (Kim *et al.*, 2011; Udeshi *et al.*, 2012). It is therefore plausible that TOP2 is deubiquitinated in response to proteasome inhibition.

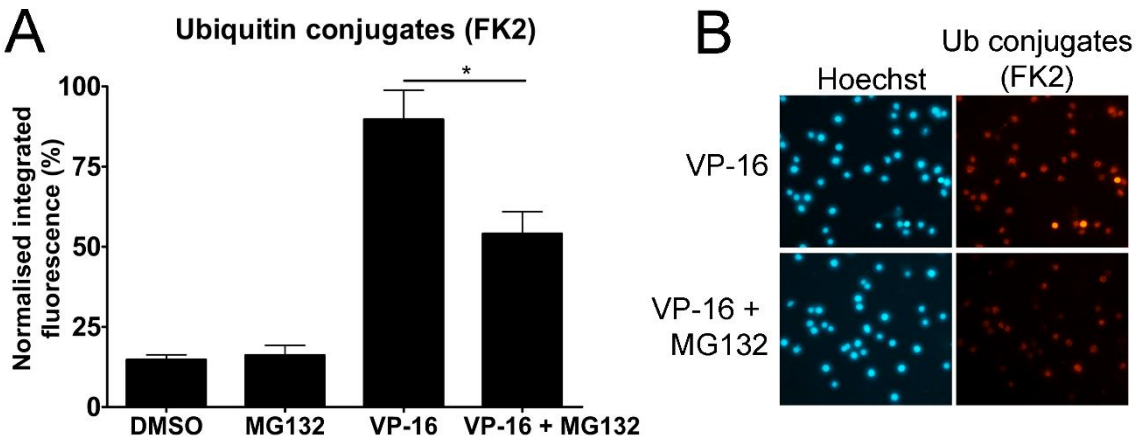

Figure 4.5. Effect of proteasome inhibition on levels of ubiquitinated TOP2-DNA complexes, investigated using the TARDIS assay. K562 cells were treated with 100 µM etoposide (VP-16) alone or in combination with 10 µM MG132 for 2 hours, and levels of ubiquitinated TOP2-DNA complexes measured using the TARDIS assay. A) Quantification of ubiquitinated TOP2-DNA complexes. Values represent mean of medians ± SEM from triplicate experiments and are normalised to a 2 hour 100 µM etoposide control. Statistical comparisons were made by unpaired t-test (n=3). B) Representative images of TARDIS slides probed for all conjugated ubiquitin (anti-ubiquitin antibody clone FK2).

To investigate the potential role of deubiquitinase enzymes (DUBs) in the MG132-induced decrease in ubiquitinated TOP2-DNA complexes, cells were treated with PR-619, a broad-spectrum DUB inhibitor (Tian *et al.*, 2011; Seiberlich *et al.*, 2012). Firstly, a PR-619 dose-response experiment was conducted to determine the concentration of PR-619 required to efficiently inhibit DUB enzymes, indicated by the accumulation of ubiquitin conjugates on a western blot. While levels of ubiquitin conjugates were not significantly affected in the presence of 2 µM PR-619, there was a 141% increase in levels of ubiquitinated proteins when K562 cells were treated for 2 hours with 5 µM PR-619 compared to untreated control (Figure 4.6), and therefore 5 µM PR-619 was used to inhibit DUBs in subsequent experiments.

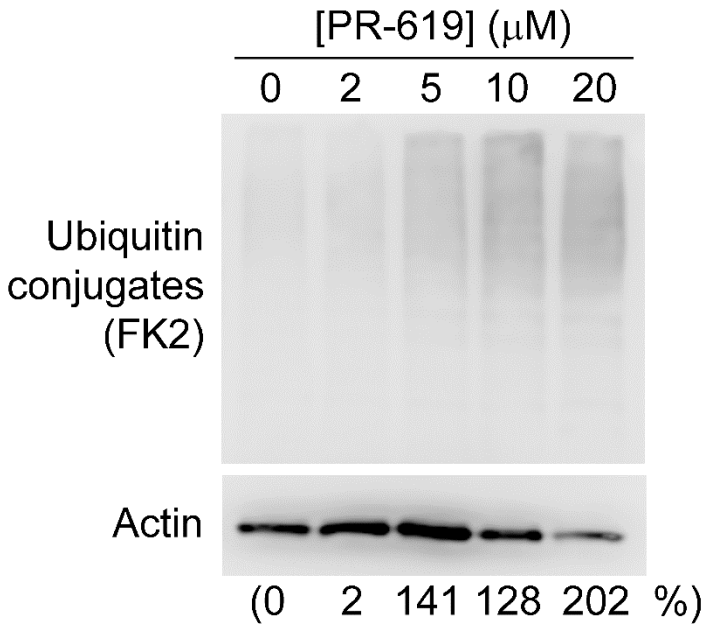

Figure 4.6. Inhibition of deubiquitinases (DUBs) by PR-619 shown by western blot. K562 cells were treated with 0, 2, 5, 10 or 20 μM PR-619 (each containing equivalent volumes of DMSO), and levels of ubiquitinated proteins were determined by western blot. Blots were probed for all conjugated ubiquitin using the anti-ubiquitin antibody clone FK2, and developed using the LiCor C-DiGit western blot scanner. Levels of ubiquitin conjugates were quantified and expressed as a percentage increase compared to untreated control.

To investigate the effect of DUB inhibition on levels of ubiquitinated TOP2-DNA complexes, K562 cells were treated with 100 μM etoposide alone or in combination with 10 μM MG132 and 5 μM PR-619 for 2 hours. Intriguingly, treatment of cells with 5 μM PR-619 alone induced a small but significant increase in TOP2A-DNA complexes ($p=0.0108$), suggesting PR-619 itself can poison TOP2 (Figure 4.7A). Consistently, there was also a small but significant increase in ubiquitin signal following PR-619 treatment ($p=0.0059$) (Figure 4.7B). However, PR-619 did not affect levels of etoposide-induced ubiquitinated TOP2-DNA complexes, suggesting that etoposide-induced TOP2-DNA complexes are not deubiquitinated in the absence of MG132.

As previously shown, co-treatment of cells with MG132 reduced the levels of etoposide-induced ubiquitinated TOP2-DNA complexes (Figure 4.7B). However, when etoposide-treated cells were incubated with both PR-619 and MG132, PR-619 prevented the MG132-induced decrease in ubiquitinated TOP2-DNA complexes. In fact, levels of ubiquitinated TOP2-DNA complexes were significantly increased compared to etoposide alone, suggesting that DUB inhibition not only prevents the

MG132-induced deubiquitination of TOP2-DNA complexes, but also reveals the MG132-dependent accumulation of ubiquitinated TOP2-DNA complexes. Therefore, ubiquitinated TOP2-DNA complexes are deubiquitinated upon proteasome inhibition, but are also degraded by the proteasome. Notably, the MG132-induced accumulation of TOP2-DNA complexes was not observed when TARDIS slides were probed for total TOP2A-DNA complex levels (Figure 4.7A), suggesting that only a small proportion of TOP2-DNA complexes are ubiquitinated and degraded by the proteasome.

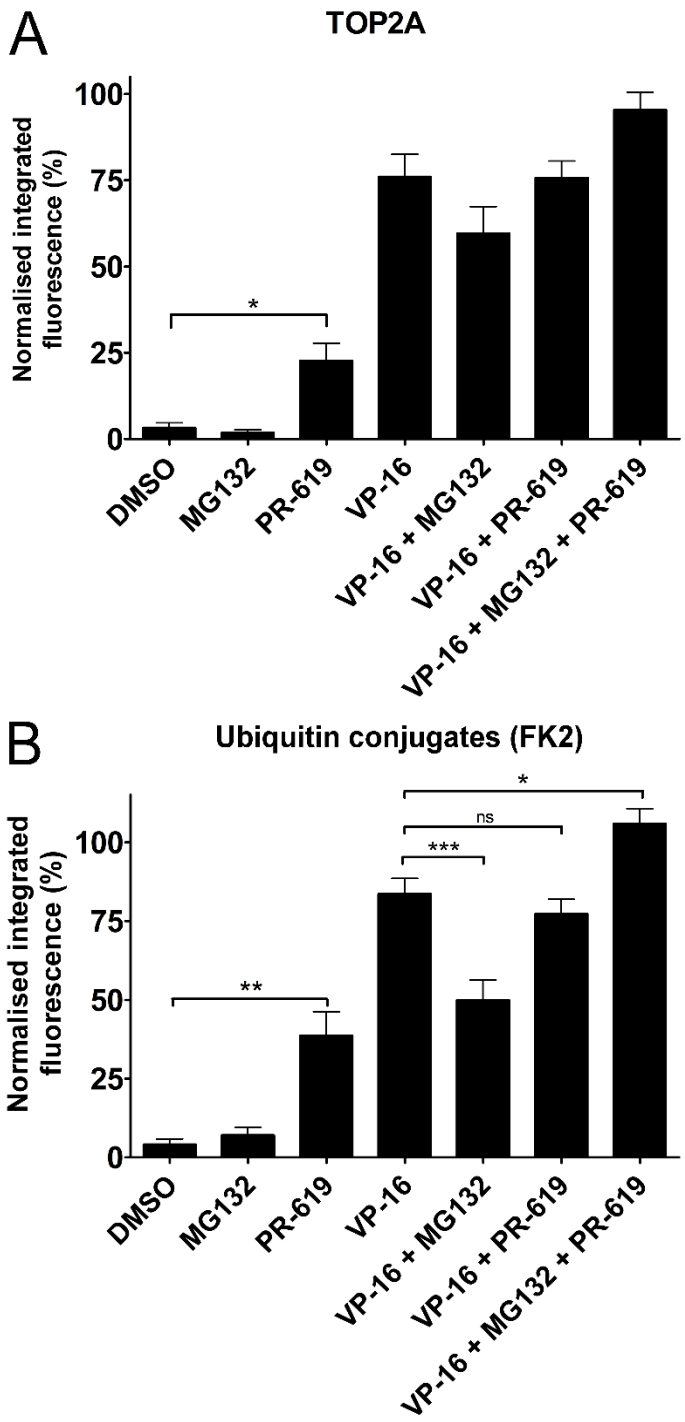

Figure 4.7. Effect of proteasome inhibition and DUB inhibition on levels of ubiquitinated TOP2-DNA complexes. K562 cells were treated with 100 µM etoposide (VP-16) alone or in combination with 10 µM MG132 and/or 5 µM PR-619. TARDIS slides were probed for A) TOP2A and B) all conjugated ubiquitin (anti-ubiquitin antibody clone FK2). Values represent the mean of medians ± SEM of triplicate experiments, normalised to a 2 hour 100 µM etoposide control. Statistical comparisons were made by unpaired t-test (n=3).

Studies have shown that the deubiquitination of histone H2A occurs within 5 minutes of MG132 addition, with approximately half of the monoubiquitinated histone H2A pool remaining after 30 minutes (Dantuma *et al.*, 2006). Therefore, MG132-induced deubiquitination is time-dependent, suggesting that shorter incubations with MG132 could be used to inhibit the proteasome without inducing the deubiquitination of TOP2-DNA complexes. To investigate this, K562 cells were treated with 10 µM MG132 for 30, 60 or 120 minutes, and proteasome inhibition was assessed by the accumulation of ubiquitinated proteins, detected by western blot. Probing of blots with the anti-ubiquitin antibody clone FK2 also reveals a 23 kDa band corresponding to a highly abundant monoubiquitinated protein, likely to be histone H2A (Mimnaugh *et al.*, 1997). Although not a direct measure of monoubiquitinated histone H2A, this was used as an indication of MG132-induced deubiquitination.

Figure 4.8A shows the accumulation of ubiquitin conjugates within 30 minutes of MG132 exposure, demonstrating proteasomal inhibition. Levels of the 23kDa monoubiquitinated protein were gradually decreased with time of MG132 treatment, reflecting MG132-induced deubiquitination. Consistent with Dantuma et al., levels of this protein were reduced but still present following 30 minutes MG132 treatment (18% remaining compared to untreated control), and further reduced to 9% and 3% following 1 and 2 hours of proteasome inhibition, respectively (Figure 4.8A). Therefore, the MG132-induced deubiquitination of histone H2A is time-dependent.

To investigate the potential time-dependent effect of MG132 on levels of etoposide-induced ubiquitinated TOP2-DNA complexes, the ubiquitin TARDIS assay was performed where 10 µM MG132 was added at various time points during a 2 hour incubation of cells with 100 µM etoposide. Specifically, MG132 was added simultaneously with etoposide as previously in Figure 4.5 (i.e. MG132 was present for the full 2 hour incubation with etoposide), or MG132 was added in the final hour or final 30 minutes of incubation with etoposide.

Levels of etoposide-induced ubiquitinated TOP2-DNA complexes were significantly reduced following 2 hours co-incubation with MG132, as previously shown ($p=0.0444$) (Figure 4.8B). This was also true when MG132 was added in the final hour of etoposide treatment ($p=0.0007$), indicating that the deubiquitination of TOP2-DNA complexes occurs within 1 hour of incubation with MG132. In contrast, levels of

etoposide-induced ubiquitinated TOP2-DNA complexes were not affected when MG132 was added in the final 30 minutes of drug incubation. Therefore, the deubiquitination of TOP2-DNA complexes is not detectable within 30 minutes of proteasome inhibition. This delay is likely due to the time-dependent depletion of free ubiquitin following proteasome inhibition, and the subsequent redistribution of ubiquitin from the nucleus. Notably, MG132-induced deubiquitination reportedly occurs within 5 minutes of drug addition (Dantuma *et al.*, 2006) and therefore the rate of TOP2 deubiquitination at 30 minutes MG132 exposure may be undetectable due to an equivalent rate of MG132-induced accumulation of ubiquitinated TOP2-DNA complexes. This suggests that, like histone H2A, TOP2 is deubiquitinated in response to proteotoxic stress in order to replenish the free ubiquitin pool. It is therefore possible that proteasomal inhibition may prevent the processing of TOP2-DNA complexes through the inhibition of TOP2 ubiquitination, rather than by inhibition of TOP2 degradation.

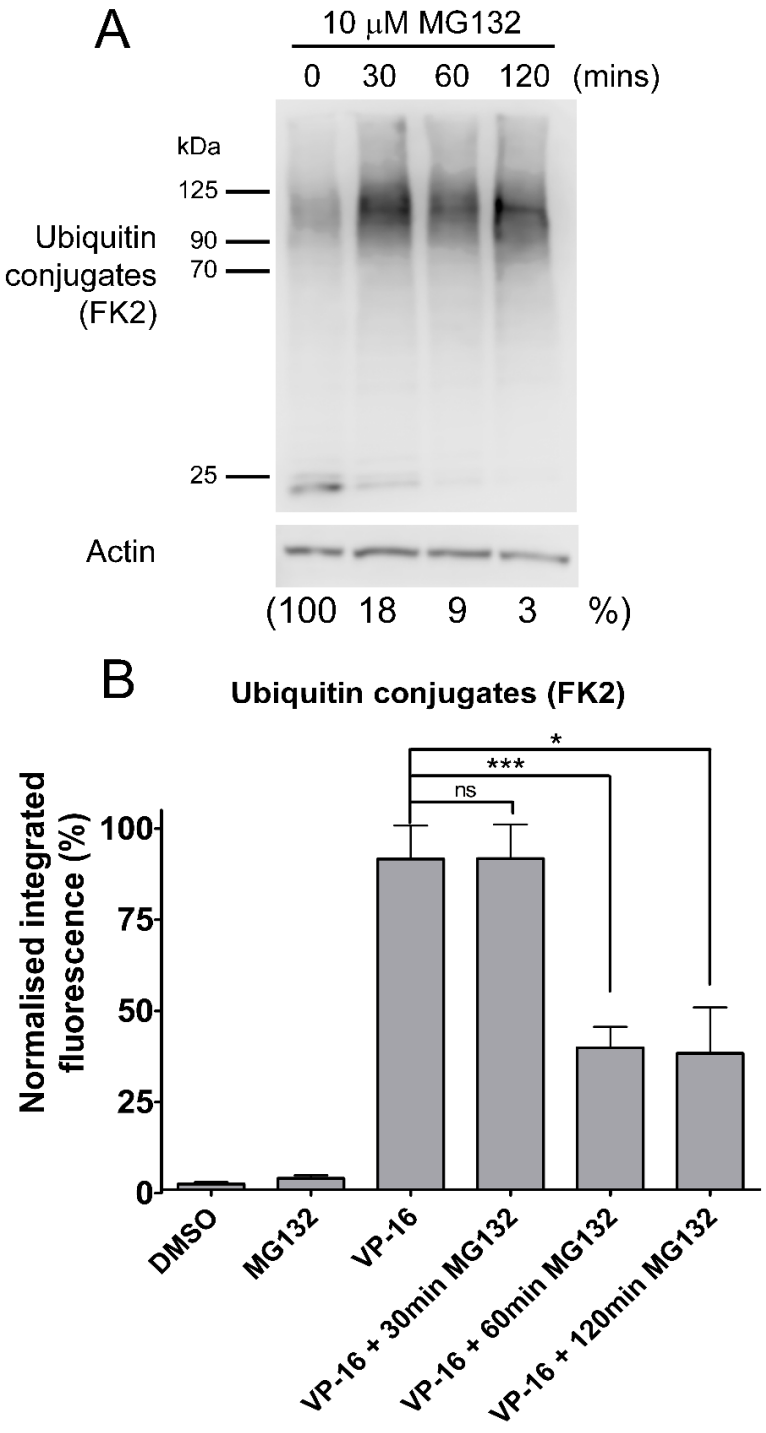

Figure 4.8. Investigating the effect of increasing MG132 exposure on levels of ubiquitinated TOP2-DNA complexes using the TARDIS assay. A) K562 cells were treated with 10 μM MG132 for 30, 60 or 120 minutes, and total levels of ubiquitinated proteins were measured by western blot. Levels of the 23 kDa monoubiquitinated protein (presumed to be histone H2A) were quantified and expressed as percentage remaining compared to untreated control. B) K562 cells were treated with 100 μM etoposide alone or in combination with 10 μM MG132 for 30, 60 or 120 minutes, and levels of ubiquitinated TOP2-DNA complexes were measured by TARDIS assay. Values represent mean of medians ± SEM from triplicate experiments and are normalised to a 2 hour 100 μM etoposide control. Statistical comparisons were made by unpaired t-test (n=3).

As shown in Figure 4.7A, treatment with PR-619 alone induced stable TOP2A-DNA complexes. Therefore a PR-619 dose-response experiment was performed to investigate the effect of PR-619 as a potential TOP2 poison. K562 cells were treated with increasing concentrations of PR-619 for 2 hours, and levels of TOP2-DNA complexes were measured by the TARDIS assay. Strikingly, PR-619 induced TOP2A-DNA complexes in a dose-dependent manner (Figure 4.9A). Indeed, the induction of TOP2A-DNA complexes by 10 μM PR-619 was even greater than TOP2A complex levels induced by 100 μM etoposide. PR-619 also induced a dose-dependent increase in levels of ubiquitinated TOP2-DNA complexes (Figure 4.9B). Interestingly, PR-619-induced TOP2-DNA complexes appear unevenly distributed across the nuclei (Figure 4.9C), unlike the diffuse, pan-nuclear pattern that is observed upon etoposide treatment (not shown). These TOP2A foci colocalise with ubiquitin conjugates, further demonstrating that PR-619-induced TOP2-DNA complexes are ubiquitinated.

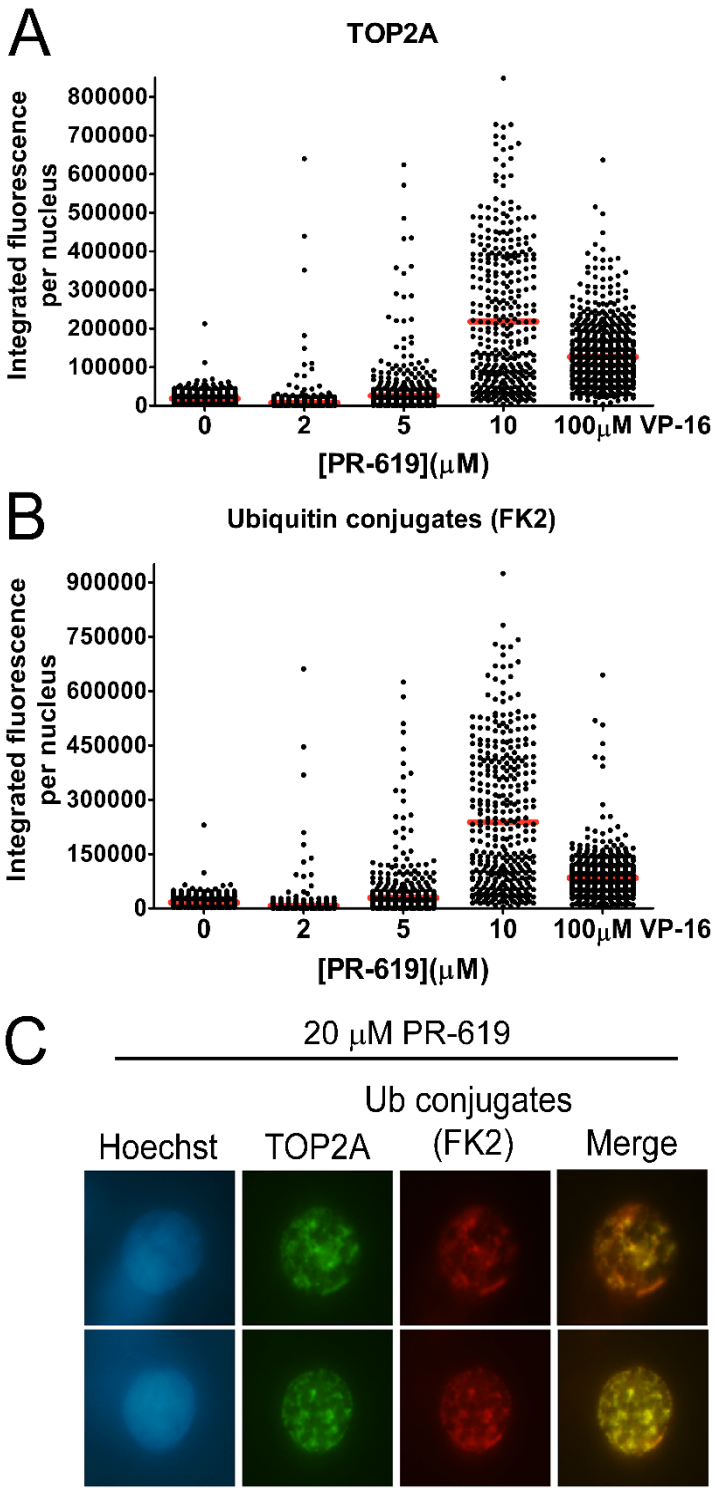

Figure 4.9. Stabilisation of TOP2A-DNA complexes by PR-619. K562 cells were treated with the indicated concentration of PR-619 for 2 hours (or 100 μM etoposide for comparison), and levels of TOP2-DNA complexes were quantified using the TARDIS assay (n=1). Scatter diagrams in A) and B) show the raw integrated fluorescence per nucleus of TOP2A and all conjugated ubiquitin (anti-ubiquitin antibody clone FK2), respectively. C) Representative images (40x objective) of ubiquitinated TOP2-DNA complexes in the presence of 20 μM PR-619.

4.4.1 Effect of transcription inhibition on the ubiquitination of TOP2-DNA complexes

It is suggested that the proteasome-dependent processing of TOP2-DNA complexes is transcription-dependent (Mao *et al.*, 2001; Fan *et al.*, 2008; Ban *et al.*, 2013; Tammaro *et al.*, 2013). Indeed, while inhibition of transcription did not significantly affect the formation of TOP2-DNA complexes, co-incubation of cells with DRB significantly slowed the removal of etoposide-induced TOP2A-DNA complexes, as shown in Chapter 3 (Figure 3.23). To investigate whether the ubiquitination of TOP2-DNA complexes is also transcription-dependent, K562 cells were treated for 2 hours with 100 µM etoposide alone or in combination with 300 µM DRB. Strikingly, the ubiquitination of etoposide-induced TOP2-DNA complexes was significantly reduced in the presence of DRB compared to etoposide alone ($p=0.0381$, Figure 4.10). This suggests that the ubiquitination of TOP2-DNA complexes is partly transcription-dependent. Notably, levels of ubiquitinated TOP2-DNA complexes remained significantly above background even in the presence of DRB, which could be due to incomplete inhibition of transcription or other pathways leading to TOP2 ubiquitination. Nonetheless, this indicates that transcription is involved in the ubiquitination of TOP2.

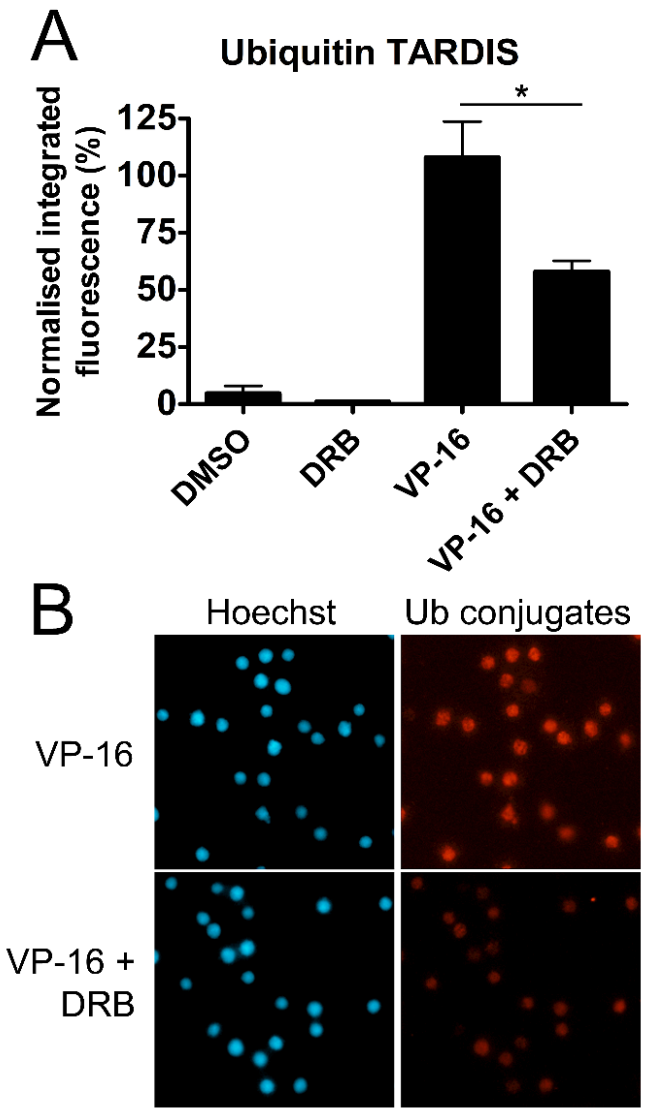

Figure 4.10. Effect of transcription inhibition on levels of TOP2-DNA complexes. K562 cells were treated with 100 µM etoposide (VP-16) alone or in combination with 300 µM DRB for 2 hours. Levels of ubiquitinated TOP2-DNA complexes were determined by TARDIS assay. A) Quantification of ubiquitinated TOP2-DNA complexes. Values represent mean of medians ± SEM of triplicate experiments, normalised to a 100 µM etoposide control. Statistical comparisons were made by unpaired t-test (n=3). B) Representative images of data presented in A.

4.5 TOP2-DNA complexes are SUMOylated

TOP2-DNA complexes are SUMOylated in response to TOP2 poisons (Mao *et al.*, 2000; Agostinho *et al.*, 2008; Schellenberg *et al.*, 2017), and this was investigated using the TARDIS assay. SUMO-2 and SUMO-3 are 97% identical, and thereby referred to as SUMO-2/3 (Geiss-Friedlander and Melchior, 2007). K562 cells were treated with 100 µM etoposide or 0.2% v/v DMSO, and levels of SUMOylated TOP2-DNA complexes were measured by probing TARDIS slides with anti-SUMO-2/3 antibodies. Indeed, SUMO-2/3 conjugates were readily detectable on TARDIS slides following the treatment of cells with etoposide (Figure 4.11). SUMO-2/3 conjugates were not detected in the absence of etoposide, demonstrating that other chromatin-associated SUMO conjugates are removed during TARDIS lysis. The presence of etoposide-induced SUMO-1 conjugates on TARDIS slides was not investigated in the current study, but has been shown by others (Jobson, 2004).

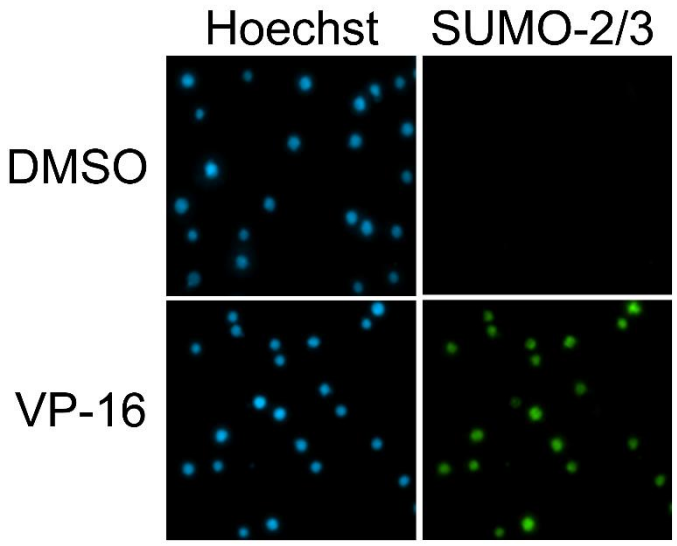

Figure 4.11. Detection of SUMO-2/3 conjugates on TARDIS slides following etoposide treatment. K562 cells were treated with 100 µM etoposide for 2 hours, and processed according to the TARDIS assay. Levels of SUMOylated TOP2-DNA complexes were visualised and quantified by probing slides with anti-SUMO-2/3 antibody.

While the specificity of MLN7243 for ubiquitin activating enzymes over other UBL-like enzymes has been demonstrated by others (Misra *et al.*, 2017), the TARDIS assay was used to test the effect of the UAE inhibitor MLN7243 on the SUMOylation of TOP2-DNA complexes. K562 cells were treated with 100 µM etoposide alone or in combination with 10 µM MG132 or 10 µM MLN7243 for 2 hours. Notably, co-incubation of cells with MG132 did not significantly affect levels of SUMOylated

TOP2-DNA complexes, suggesting SUMOylated TOP2-DNA complexes are not regulated by the proteasome. Furthermore, MLN7243 treatment did not affect levels of SUMOylated TOP2-DNA complexes, suggesting that MLN7243 selectively inhibits UAE activity without affecting SUMO activating enzyme (SAE) activity. This confirms that the effect of MLN7243 on the removal of TOP2-DNA complexes (shown in Chapter 3) is not due to targeting of SUMO.

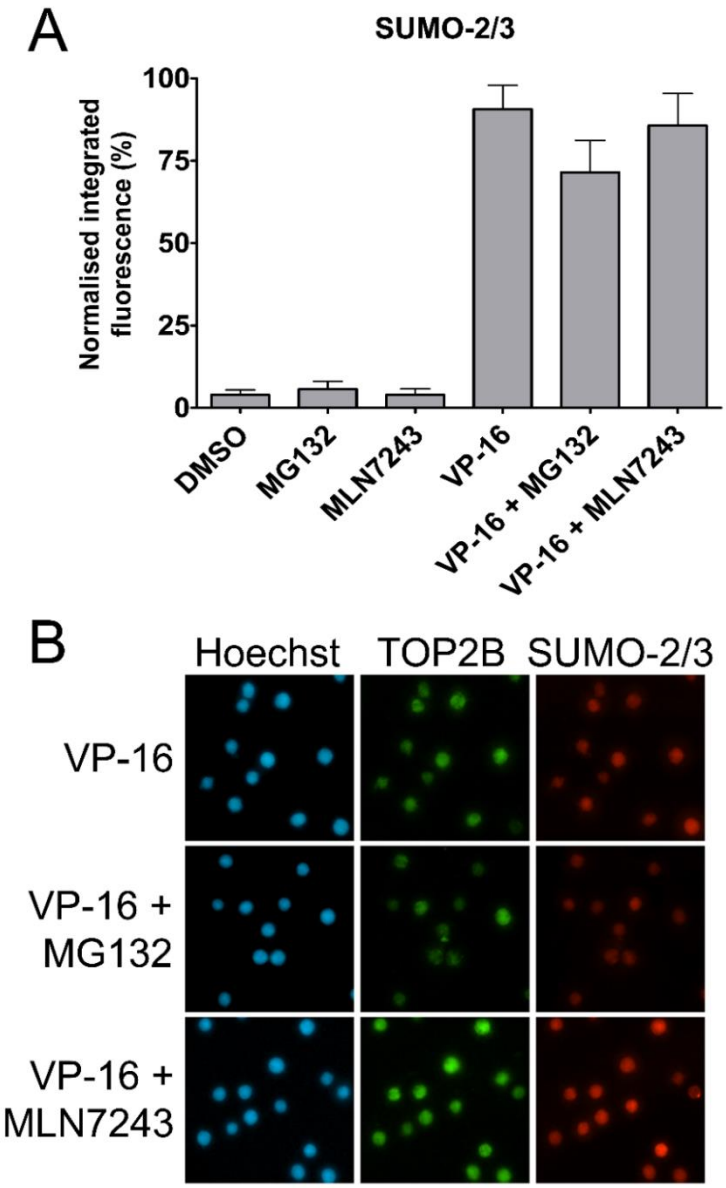

Figure 4.12. Effect of proteasome inhibition and the UAE inhibitor MLN7243 on levels of SUMOylated TOP2-DNA complexes. A) K562 cells were treated with 100 µM etoposide (VP-16) alone or in combination with 10 µM MG132 or 10 µM MLN7243 for 2 hours. Levels of SUMOylated TOP2-DNA complexes were determined by TARDIS assay. Values represent the mean of medians ± SEM of triplicate experiments, normalised to a 2 hour 100 µM etoposide control. Statistical comparisons were made by unpaired t-test (n=3). B) Representative images of data shown in A.

4.6 Investigating the ubiquitination of TOP2 using Tandem Ubiquitin Binding Entities (TUBEs)

A major limitation of the TARDIS assay is the inability to compare the ubiquitination of etoposide-induced TOP2-DNA complexes with the ubiquitination of non-covalently bound TOP2 in untreated cells. Therefore, it is not possible to deduce whether TOP2 is ubiquitinated in response to etoposide, or if TOP2 is already ubiquitinated before it is trapped in the TOP2-DNA complex. To address this, TOP2 ubiquitination was investigated before and after etoposide treatment using Tandem Ubiquitin Binding Entities (TUBEs).

4.6.1 Using TUBEs to study the ubiquitination of Rpb1 upon transcription inhibition

TUBEs contain multiple repeats of ubiquitin binding domains which bind ubiquitinated proteins with high affinity (Hjerpe *et al.*, 2009; Wilson *et al.*, 2012). Commercially available TUBEs also contain an affinity tag such as GST or biotin, which can be pulled down by affinity purification, followed by analysis of ubiquitinated proteins by western blot. Anindya et al. used this approach to demonstrate that Rpb1, the large subunit of RNA polymerase II, is ubiquitinated in response to transcription inhibition by α-Amanitin (Anindya *et al.*, 2007). This experiment was replicated here in order to optimise an effective TUBE protocol using TUBE2 linked to GST (GST-TUBE2).

K562 cells were treated with α-Amanitin (or H_2O solvent control) for 4 hours, and whole cell lysates were prepared with the addition of DNase I and sonication to facilitate the release of chromatin-associated proteins from DNA. Ubiquitinated proteins were then isolated by incubation of the lysate with GST-TUBE2 and analysed by western blotting. Equal volumes of whole cell lysate before (input) and after ubiquitin pulldown (flow-through) were probed for all ubiquitinated proteins (FK2 antibody) to test pulldown efficiency. Indeed, ubiquitinated proteins were detectable in the input of both untreated and α-Amanitin-treated cells but were completely undetectable in the flow-through, indicating highly efficient isolation of ubiquitinated proteins by GST-TUBE2 (Figure 4.13). Notably, a significant proportion of Rpb1 remained in the flow-through, suggesting that not all Rpb1 is ubiquitinated upon transcription inhibition. Alternatively, transcription inhibition may be incomplete.

Following elution from glutathione beads, levels of ubiquitinated Rpb1 were measured by probing ubiquitinated proteins with anti-Rpb1 antibody. Blots were also probed with anti-ubiquitin FK2 antibody as a loading control (Figure 4.13). As previously shown (Anindya *et al.*, 2007), Rpb1 ubiquitination was increased in α-Amanitin-treated cells compared to untreated cells. Therefore, TUBEs can be used to reliably study protein ubiquitination.

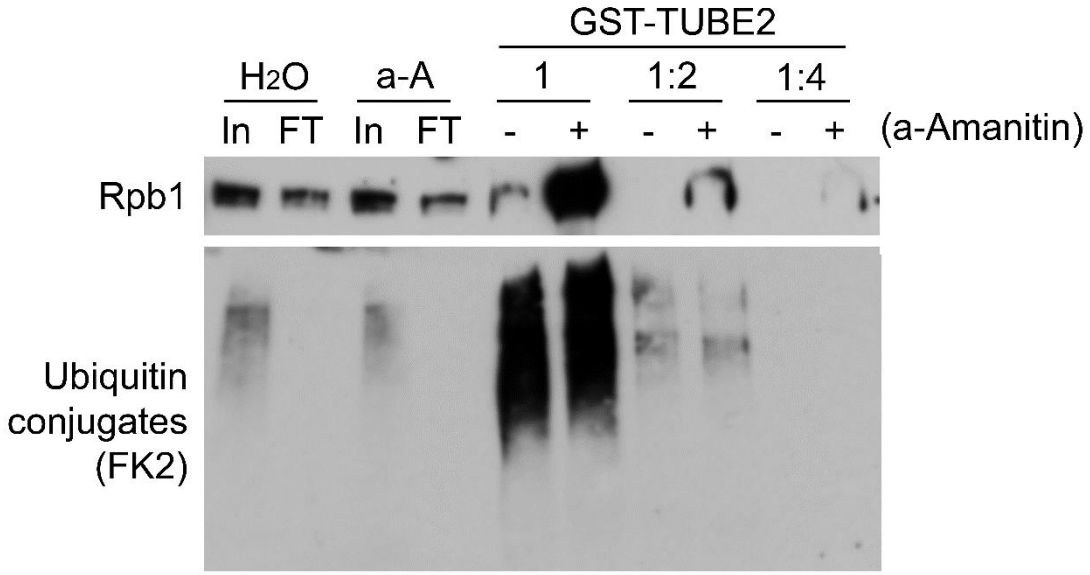

Figure 4.13. Ubiquitination of RNA polymerase II in response to transcription inhibition. K562 cells were treated with 10 µg/mL α-Amanitin or H_2O for 4 hours, and ubiquitinated proteins were isolated by incubating cell lysates with GST-TUBE2. Western blotting was used to measure levels of ubiquitinated proteins and ubiquitinated Rpb1 (RNA polymerase II large subunit) following GST-TUBE pulldown. Levels of Rpb1 and ubiquitin conjugates were also measured in whole cell lysates before and after ubiquitin pulldown, indicated by In (input) and FT (flow-through), respectively.

The α-Amanitin-induced ubiquitination of Rpb1 was then used to examine the effect of double UAE1/UBA6 siRNA knockdown and MLN7243 treatment on the ubiquitination of a known substrate. Figure 4.14A shows that total levels of ubiquitin conjugates are reduced in whole cell lysates (input) of UAE1/UBA6 siRNA knockdown and MLN7243-treated cells compared to control cells. However, ubiquitin conjugates are still detectable in UAE1/UBA6 siRNA knockdown cells, indicating incomplete knockdown of ubiquitination. Consistently, UAE1 levels were reduced but still detectable in UAE1/UBA6 siRNA knockdown cells. Nonetheless, incubation of lysates with GST-TUBE2 efficiently isolated ubiquitinated proteins in control and UAE1/UBA6 knockdown cells, which were depleted in the flow-through.

Ubiquitinated proteins were then eluted from glutathione beads and levels of ubiquitinated Rpb1 were measured by western blot. As expected, levels of ubiquitinated Rpb1 were increased in CON siRNA cells following treatment with α-Amanitin (Figure 4.14B). However, Rpb1 ubiquitination was abrogated in both UAE1/UBA6 siRNA knockdown cells and cells treated with MLN7243. Therefore, inhibition of UAE activity by both siRNA knockdown or acute chemical inhibition is sufficient to inhibit α-Amanitin-induced Rpb1 ubiquitination.

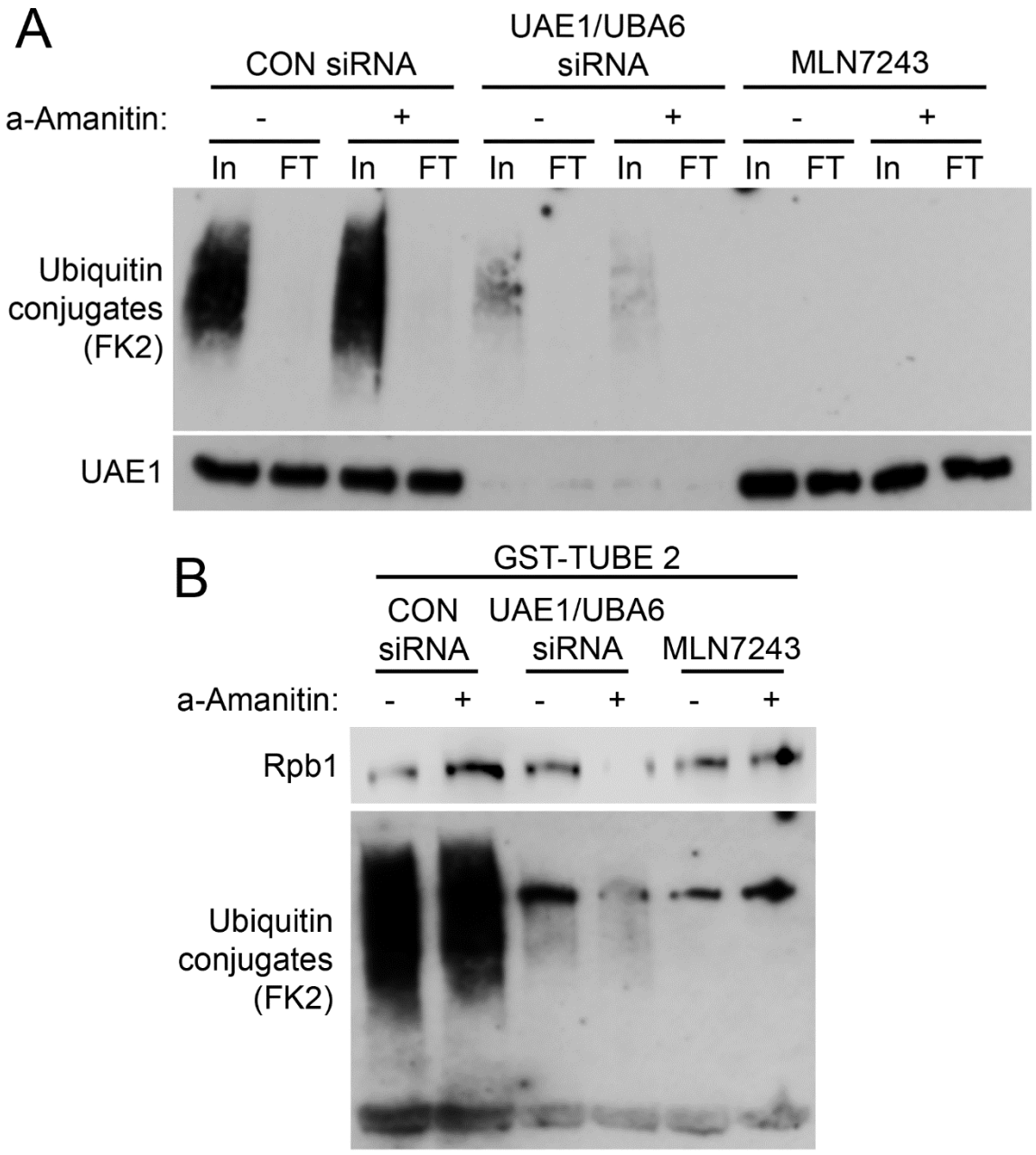

Figure 4.14. Ubiquitination of RNA polymerase II in double UAE1/UBA6 siRNA knockdown cells and MLN7243-treated cells. K562 cells (no siRNA) were treated with 10 µM MLN7243 alone or in combination with 10 µg/mL α-Amanitin for 2 hours. CON siRNA and double UAE1/UBA6 siRNA cells were also treated with 10 µg/mL α-Amanitin or H_2O for 2 hours, and ubiquitinated proteins were isolated by GST-TUBE pulldown. A) Western blot to show levels of ubiquitin conjugates in CON siRNA, UAE1/UBA6 siRNA knockdown and MLN7243-treated K562 cells before (In) and after (FT) ubiquitin pulldown. B) Ubiquitin conjugates in CON siRNA, UAE1/UBA6 siRNA knockdown and MLN7243-treated K562 cells were isolated by GST-TUBE pulldown and levels of ubiquitinated Rpb1 were measured by western blot.

4.6.2 Using TUBEs to study TOP2 ubiquitination

This approach was used to investigate the ubiquitination of TOP2 in the presence and absence of 100 µM etoposide. Whole cell lysates were prepared in the presence of DNase I (and the DUB inhibitor, NEM) for the release of etoposide-induced TOP2 covalent complexes from DNA and analysis by western blot. Overall ubiquitination was markedly increased in the whole cell lysate of etoposide-treated cells, likely reflecting DNA damage-induced ubiquitination (Figure 4.15). However, levels of TOP2A were reduced in whole cell lysates from etoposide-treated cells compared to untreated cells, indicating incomplete extraction of TOP2 from DNA. This suggests that a more effective method of TOP2 extraction is required for the analysis of TOP2-DNA complexes by western blotting. Various conditions were investigated to optimise the extraction of TOP2-DNA complexes, such as the inclusion of a sonication step and adjustment of sonication conditions. However, sonication did not increase the yield of TOP2 in etoposide-treated cells (see Appendix Table 2 and 3 for details). Because of this, experiments were commenced using DNase I, though in the future should be performed using a more efficient nuclease such as benzonase (Turbonuclease). Alternatively, the decrease of TOP2A levels in etoposide-treated cells could be due to the TOP2 poison-induced proteasomal degradation of TOP2A previously shown by others using western blotting techniques (Fan *et al.*, 2008; Alchanati *et al.*, 2009). While etoposide-induced degradation of TOP2A was not observed within 2 hours treatment in K562 cells by western blotting (Chapter 3, Figure 3.10), it is possible that proteasomal degradation is more readily detectable in a pool of ubiquitinated TOP2A as opposed to total TOP2A levels.

As above, whole cell lysates were subjected to ubiquitin pulldown with GST-TUBE1 and levels of total ubiquitin conjugates were measured in lysates before (input) and after (flow-through) ubiquitin pulldown. While levels of ubiquitinated proteins were slightly reduced in the flow-through, many ubiquitin conjugates remained indicating a poor ubiquitin pulldown (Figure 4.15). Despite an apparently inefficient pulldown, ubiquitinated TOP2A (Ub-TOP2A) was still detected when eluted proteins were probed for TOP2A. Notably, an additional band (corresponding to GST) was observed in samples containing GST-TUBE1, as the TOP2A antibody used was raised to a GST-fusion protein. To prevent this from interfering with the interpretation of results, proteins were adequately separated by running gradient gels for longer,

and ~178 kDa Ub-TOP2A was identified by comparison with a ladder of protein standards with known molecular weight. Ub-TOP2A was present in both untreated and etoposide-treated cells, suggesting that TOP2A is ubiquitinated before the addition of etoposide. Paradoxically, no ubiquitin conjugates were detected when eluted proteins were probed with anti-ubiquitin FK2 antibody. This may be due to low pulldown efficiency, whereby levels of isolated ubiquitinated proteins are below the range of detection.

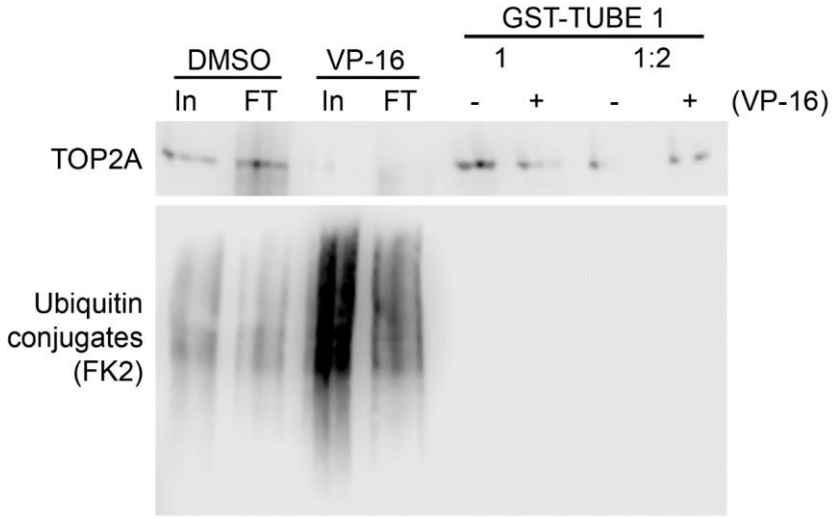

Figure 4.15. Investigating the ubiquitination of TOP2 with GST-TUBEs. K562 cells were treated with 100 µM etoposide (VP-16) or 0.2% DMSO for 2 hours. Ubiquitin conjugates were isolated from K562 cell lysates by incubation with GST-TUBE1, and analysed by western blotting (with serial dilution of the sample indicated by 1:2). Ubiquitinated proteins bound to GST-TUBE1 (as well as whole cell lysates before (In) and after (FT) ubiquitin pulldown) were probed for all conjugated ubiquitin and TOP2A. Blots were developed using the LiCor C-DiGit western blot scanner.

MultiDsk2 is another ubiquitin binding reagent which can be used to isolate ubiquitinated proteins while also protecting them from DUBs and proteasomal degradation (Wilson *et al.*, 2012). Like TUBEs, MultiDsk2 contains a tandem ubiquitin binding domain (Dsk2) which binds all ubiquitin chains with high affinity, and a GST tag which can be pulled down with glutathione beads. MultiDsk2 was also used to investigate the ubiquitination of TOP2 in the presence and absence of 100 µM etoposide.

Whole cell lysates were prepared from DMSO- or etoposide- treated cells and probed for all ubiquitin conjugates before and after ubiquitin pulldown with MultiDsk2. Levels of ubiquitinated proteins were not noticeably reduced in the flow-through

compared to input samples, indicating an inefficient ubiquitin pulldown (Figure 4.16A). Furthermore, TOP2A was not readily detectable in whole cell lysates using the LiCor C-DiGit western blot scanner, but could be detected upon prolonged exposure on film (Figure 4.16B). Despite this, Ub-TOP2A was detectable after the elution of ubiquitinated proteins from glutathione beads (Figure 4.16A). As shown previously using GST-TUBE1, Ub-TOP2A was detected in both untreated and etoposide-treated cells, with levels appearing slightly reduced after etoposide treatment. Together, studies using TUBEs and MultiDsk2 show that TOP2A is ubiquitinated before etoposide treatment. However, the efficiency of ubiquitin pulldown was poor, and therefore a large proportion of ubiquitinated TOP2A may have been lost in the supernatant. Because of this and various other technical issues (detailed in Appendix Tables 2 and 3), TOP2 ubiquitination was also investigated by immunoprecipitation.

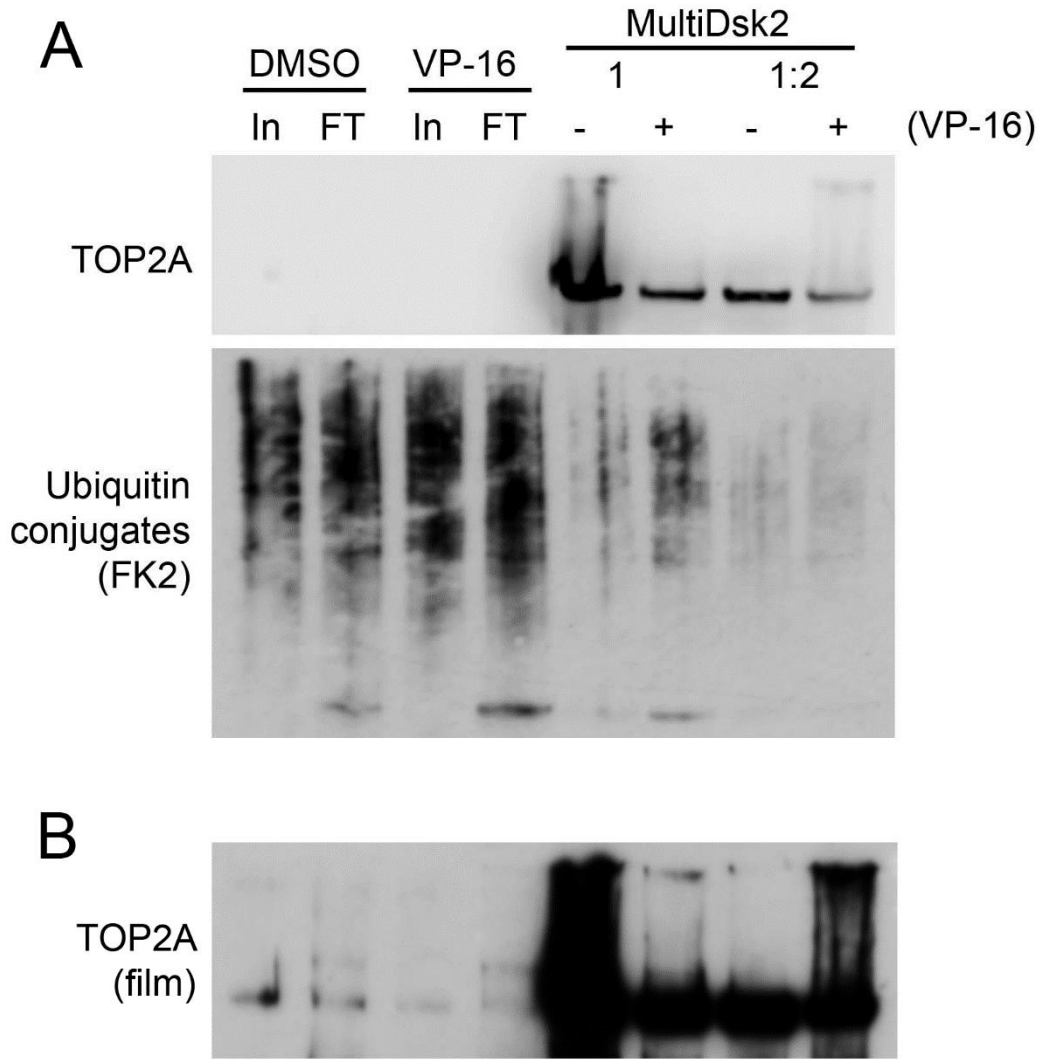

Figure 4.16. Investigating the ubiquitination of TOP2 with MultiDsk2. A) K562 cells were treated with 100 µM etoposide (VP-16) or 0.2% DMSO for 2 hours, and ubiquitinated proteins were isolated by incubation of cell lysate with MultiDsk2. Levels of ubiquitin conjugates and TOP2A were measured by western blot, and developed using the LiCor C-DiGit western blot scanner. Whole cell lysate before and after ubiquitin pulldown are indicated by In (input) and FT (flow-through), respectively, and 1:2 indicates serial dilution of the sample. B) Prolonged film exposure of TOP2A blot shown in A.

4.7 Investigating the ubiquitination of TOP2 by immunoprecipitation

K562 cells were treated with 100 μM etoposide for 2 hours, and whole cell lysate was prepared with the inclusion of DNase I. All ubiquitinated proteins were then immunoprecipitated by incubating lysates with anti-ubiquitin FK2 antibody, and analysed by western blotting. Figure 4.17A shows the levels of ubiquitinated proteins present in whole cell lysate (input) and the highly efficient depletion of ubiquitin conjugates in whole cell lysate after ubiquitin IP (flow-through). Ubiquitin IPs were then probed for TOP2A to examine levels of Ub-TOP2A in untreated and etoposide-treated cells from three individual experiments (Figure 4.17B). Consistent with TUBE data, ubiquitinated TOP2A was detected in both untreated and etoposide-treated cells, suggesting that TOP2A is ubiquitinated before etoposide addition. However, levels of ubiquitinated TOP2A appeared to be decreased in the presence of etoposide. This could be due to the inefficient extraction of TOP2 from DNA, or due to the proteasomal degradation of TOP2A reported by others (Zhang *et al.*, 2006; Fan *et al.*, 2008; Alchanati *et al.*, 2009). Alternatively, TOP2 ubiquitination may be decreased in response to etoposide treatment.

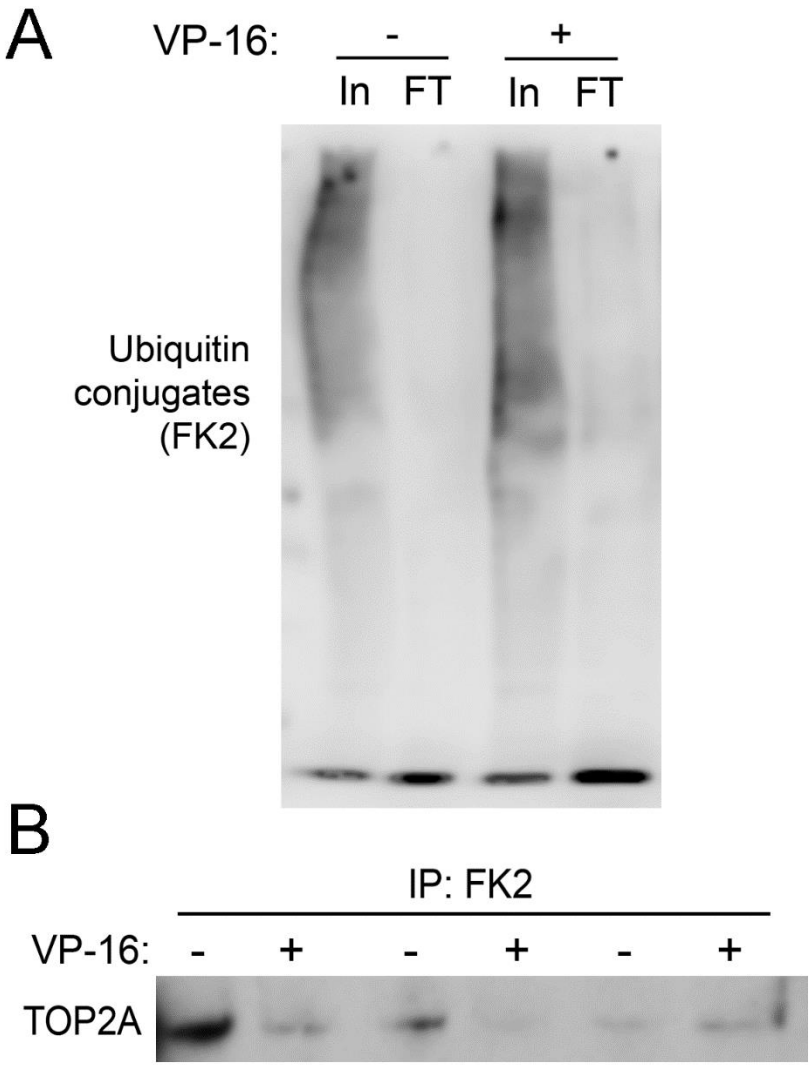

Figure 4.17. Effect of etoposide treatment on levels of ubiquitinated TOP2A, measured by immunoprecipitation. K562 cells were treated with 100 µM etoposide or 0.2% v/v DMSO for 2 hours. Whole cell lysates were prepared in the presence of DNase I to facilitate the release of TOP2 complexes from DNA, and subjected to immunoprecipitation with anti-ubiquitin FK2 antibody. A) Levels of ubiquitinated proteins in whole cell lysates before and after ubiquitin IP were measured by western blot. B) Levels of TOP2A in ubiquitin IPs with and without etoposide treatment were measured by western blot. Blot shows three biological replicates ran on a precast 4-20% gradient gel (n=3).

However, when probing IPs for TOP2A, there was an accumulation of TOP2A at the top of the blot which suggested that not all protein was able to enter the precast 4-20% gradient gel. Therefore, the same lysates were subjected to another immunoprecipitation with anti-ubiquitin FK2 antibody and run on a self-cast 5% gel, which allows better separation of large proteins. No TOP2A protein was detected at the top of the blot, suggesting all protein had effectively migrated into the gel. Figure 4.18A shows the successful immunodepletion of ubiquitinated proteins from whole cell lysates after ubiquitin IP. In contrast to Figure 4.17B, levels of Ub-TOP2A were increased in the presence of etoposide (Figure 4.18B). Therefore, the amount of Ub-TOP2A detected in etoposide-treated cells depends on the gel running conditions used. Specifically, more Ub-TOP2A is detected when a 5% gel is used, suggesting that larger pore sizes are required for the entry of large (>170 kDa) ubiquitinated proteins into the gel. In addition, the composition of the stacking gel in commercially available precast gels is unknown, and may interfere with the migration of larger proteins. Because of this variability and the substantial differences in results from separate IPs with the same lysate, it is not possible to conclude how levels of Ub-TOP2A change in the presence of etoposide without further experimentation. Nonetheless, these studies show that at least a proportion of TOP2A is ubiquitinated without etoposide treatment.

Ub-TOP2A is detected as a discrete band rather than the canonical polyubiquitinated smear which is typically associated with proteasomal degradation. Indeed, while K48-linked ubiquitin and K63-linked ubiquitin chains were detected on TOP2-DNA complexes using linkage-specific antibodies in the TARDIS assay (Figure 4.1), ubiquitin chains were not detectable by western blot. Therefore, the proteasomal processing of TOP2-DNA complexes may not involve canonical K48-linked ubiquitination of TOP2.

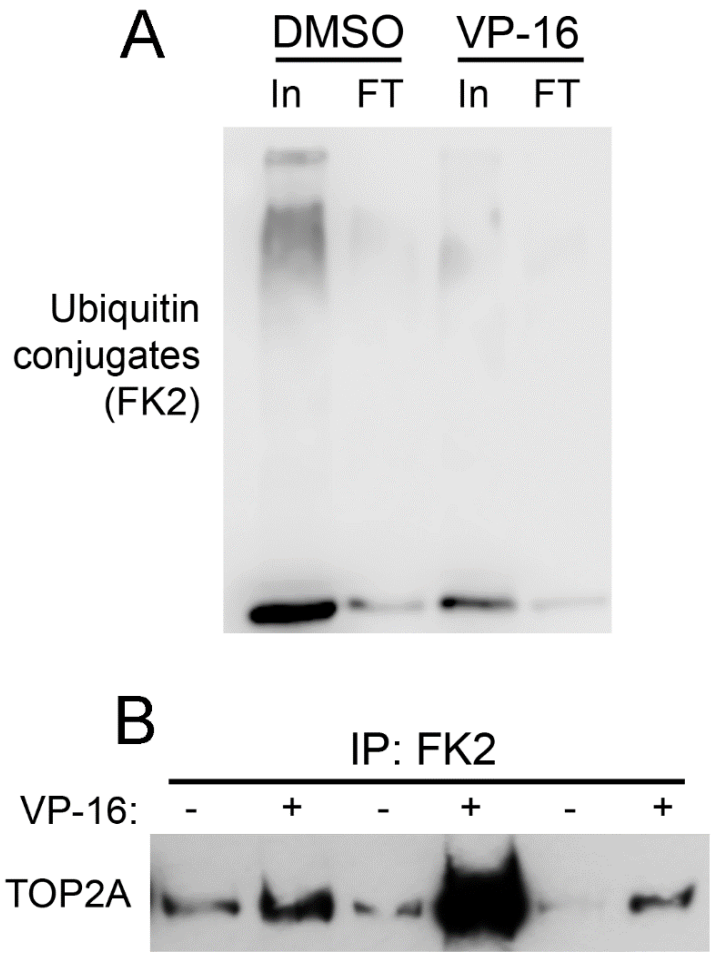

Figure 4.18. Effect of etoposide treatment on levels of ubiquitinated TOP2A, measured by immunoprecipitation. K562 cells were treated with 100 µM etoposide or 0.2% v/v DMSO for 2 hours. Whole cell lysates were prepared in the presence of DNase I to facilitate the release of TOP2 complexes from DNA, and subjected to immunoprecipitation with anti-ubiquitin FK2 antibody. A) Levels of ubiquitinated proteins in whole cell lysates before and after ubiquitin IP were measured by western blot. B) Levels of TOP2A in ubiquitin IPs with and without etoposide treatment were measured by western blot. Blot shows three biological replicates run on a 5% gel (n=3).

While some of the blots presented above were also probed for TOP2B, ubiquitinated TOP2B was not successfully detected by any of the approaches used. However, TOP2B was also undetectable in whole cell lysates before ubiquitin pulldown, suggesting the possibility of various technical issues which are outlined in Appendix Tables 2 and 3. Therefore, it was not possible to investigate the ubiquitination of TOP2B before and after etoposide treatment.

4.8 Discussion

In the current chapter, the ubiquitination of TOP2 was investigated using multiple approaches. Firstly, the TARDIS assay was adapted to detect and quantify ubiquitin and SUMO chains on TOP2-DNA complexes. In doing so, both ubiquitin and SUMO-2/3 was detected on TOP2, the latter of which has been previously shown in response to etoposide and catalytic TOP2 inhibitors such as ICRF-187 and ICRF-193 (Isik *et al.*, 2003; Agostinho *et al.*, 2008; Schellenberg *et al.*, 2017). Secondly, the ubiquitination of TOP2 was investigated through the isolation of ubiquitinated proteins using TUBEs. Unlike the TARDIS assay, this allowed the visualisation of TOP2 ubiquitination before the addition of etoposide, and suggested that TOP2A is also ubiquitinated before etoposide treatment. Thirdly, TOP2 ubiquitination was investigated by immunoprecipitation.

Studies with TUBEs suggested that levels of Ub-TOP2A do not change significantly with etoposide treatment. However, the pulldown of ubiquitin with TUBEs and MultiDsk2 was highly variable (see Appendix Tables 2 and 3 for details), and therefore a significant proportion of ubiquitinated proteins were lost in the supernatant. Because of this, levels of Ub-TOP2A may not be representative of the entire Ub-TOP2A pool. These experiments were also susceptible to other technical issues, such as the potentially incomplete extraction of TOP2 complexes from etoposide-treated cells even after digestion of the lysate with DNase I. Indeed, these conditions may be sufficient to extract RNA polymerase II but not covalently-bound TOP2. It is also difficult to adequately conclude the effect of etoposide on the ubiquitination of TOP2A following ubiquitin IP, as two separate analyses of the same biological samples generated opposing results depending on the percentage gel used. Probing blots for TOP2B was also problematic due to absence of TOP2B signal and other technical issues. Thus, it is difficult to conclude how levels of Ub-TOP2 change (if at all) after etoposide treatment. However, these experiments show that TOP2A is ubiquitinated both before and after etoposide exposure.

Alchanati et al. show the polyubiquitination of TOP2A in response to teniposide treatment, which is significantly increased when BMI1 and RING1A were overexpressed in HeLa cells (Alchanati *et al.*, 2009). However, polyubiquitination of TOP2A (denoted by a high molecular weight smear on a western blot) was not

observed in the current study with any of the approaches used. Indeed, polyubiquitinated TOP2 was not detectable even after the enrichment of all ubiquitin chains with TUBEs or MultiDsk2. Therefore, the teniposide-induced polyubiquitination of TOP2 may be a teniposide-specific effect, or a non-physiological consequence of protein overexpression which is driven by an excess of BMI1/RING1A protein. Instead, Ub-TOP2A was observed in the present study as a discrete band which may correspond to monoubiquitination, multi-monoubiquitination (i.e. monoubiquitination at multiple lysine residues) or short ubiquitin chains (e.g. di-ubiquitin). This is in contrast to TARDIS data which showed the presence of K48- and K63-linked ubiquitin chains on TOP2-DNA complexes. Notably, the detection of ubiquitin chains by fluorescence microscopy required long exposure times (>1 second), suggesting that K48- and K63-linked ubiquitin chains are present on TOP2-DNA complexes at low levels. While it is difficult to accurately compare signals with different antibodies, visualisation of all conjugated ubiquitin (using the anti-ubiquitin antibody clone FK2) on TARDIS slides required shorter exposure times (~400 msec), which could be due to the detection of other, more abundant ubiquitin chains such as monoubiquitin on TOP2-DNA complexes. Therefore, it is possible that the western blotting techniques used are not sensitive enough to detect the polyubiquitination of TOP2. Alternatively, the ubiquitin-dependent processing of TOP2-DNA complexes may not involve the polyubiquitination of TOP2, which typically leads to proteasomal degradation.

The TARDIS assay was also used to test the effect of various ubiquitin-proteasome system inhibitors on levels of ubiquitinated etoposide-induced TOP2-DNA complexes. Co-treatment of cells with etoposide and MG132 revealed a dynamic regulation of TOP2 ubiquitination by deubiquitinase enzymes, which occurs upon proteasome inhibition. This suggests that, like histone H2A, TOP2 is a highly abundant monoubiquitinated protein which can be deubiquitinated to provide free ubiquitin during proteotoxic stress. When DUBs were inhibited, there was a proteasome-dependent accumulation of ubiquitinated TOP2-DNA complexes which may be due to ubiquitin-dependent proteasomal degradation of TOP2 complexes. In the absence of MG132, the ubiquitination of etoposide-induced TOP2-DNA complexes was partly transcription-dependent. Transcription has already been implicated in the processing of drug-stabilised TOP2-DNA complexes, as inhibition of

transcription prevents the degradation of TOP2 following etoposide treatment (Mao *et al.*, 2001; Fan *et al.*, 2008; Ban *et al.*, 2013; Tammaro *et al.*, 2013) and slows the removal of TOP2A-DNA complexes (Chapter 3, Figure 3.23).

In summary, these results indicate that ubiquitinated TOP2-DNA complexes are degraded by the proteasome, but not via canonical K48-linked polyubiquitination. Instead, TOP2A is monoubiquitinated both before and after etoposide treatment. TUBE experiments show that levels of Ub-TOP2A do not change in response to etoposide treatment, but do not show whether the nature of TOP2A ubiquitination changes in response to etoposide. For example, mass spectrometry could be used to test for changes in the ubiquitination of specific lysine residues before and after etoposide treatment. Indeed, trapping of TOP2 on DNA may reveal an otherwise concealed ubiquitination site, as previously shown for the SUMOylation of TOP2A at Lys662 (Ryu *et al.*, 2010; Wendorff *et al.*, 2012). In addition, protein ubiquitination can lead to many consequences besides degradation by the proteasome. Indeed, TOP2 ubiquitination may not lead directly to proteasomal degradation but to the recruitment of other proteins involved in removal or repair. For example, VCP/p97 is an AAA ATPase which binds and extracts ubiquitinated proteins from chromatin, thereby facilitating their proteasomal degradation (Verma *et al.*, 2011; Meyer *et al.*, 2012; Dantuma *et al.*, 2014; van den Boom *et al.*, 2016). The potential role of VCP/p97 in the removal of TOP2-DNA complexes is investigated in Chapter 5.

Chapter 5 A role for VCP/p97 in the proteasomal processing of TOP2-DNA complexes

5.1 Introduction

VCP/p97 is a AAA ATPase (ATPase associated with diverse cellular activities) which is increasingly recognised as an important mediator of the ubiquitin-proteasome system. Proteasomal degradation involves the translocation of proteins through the narrow core of the 20S catalytic subunit, which requires protein unfolding. While this is largely mediated by the ATPases associated with the 19S regulatory subunit, some (but not all) proteins require the additional unfoldase activity of VCP/p97 (Beskow *et al.*, 2009; Heidelberger *et al.*, 2018). Indeed, VCP/p97 is transiently associated with the proteasome (Besche *et al.*, 2009), and this interaction is stabilised in conditions of proteotoxic stress, including proteasome inhibition (Isakov and Stanhill, 2011).

Each protomer of the hexameric VCP/p97 complex contains two highly conserved ATPase domains (D1 and D2), which utilise energy from ATP binding and hydrolysis to induce conformational changes in the substrate, leading to protein unfolding and remodelling (Rouiller *et al.*, 2000; DeLaBarre and Brunger, 2005). While VCP/p97 itself can bind ubiquitin (Pye *et al.*, 2007), the N terminal domain of VCP/p97 mediates important interactions with the major ubiquitin adaptor proteins, p47 and Ufd1 (Meyer *et al.*, 2012). Both p47 and Ufd1 bind ubiquitinated proteins but form structurally distinct complexes with VCP/p97, directing VCP/p97 to separate functional pathways (Meyer *et al.*, 2000; Pye *et al.*, 2007). For example, while p47 is most associated with membrane fusion events at the endoplasmic reticulum, Ufd1 (together with Npl4) mediates the degradative functions of VCP/p97. Consistently, knockdown of Ufd1 reduces the association between VCP/p97 and the proteasome (Isakov and Stanhill, 2011).

In addition to the role of VCP/p97 at the proteasome, VCP/p97 is a protein segregase that can extract proteins from protein complexes and cellular structures, thereby facilitating their proteasomal degradation (Meyer *et al.*, 2012). This is particularly evident during the DNA damage response, where VCP/p97 (in complex with Ufd1-Npl4) ensures the timely removal and degradation of various repair factors

from chromatin, including CSB, L3MBTL1 and Rad52 (Acs *et al.*, 2011; Bergink *et al.*, 2013; Dantuma *et al.*, 2014; He *et al.*, 2016). In particular, VCP/p97 enables the extraction of stalled RNA polymerase II (RNAPII) following UV-induced DNA damage, leading to RNAPII proteolysis (Verma *et al.*, 2011; Lafon *et al.*, 2015; He *et al.*, 2017a). Intriguingly, VCP/p97 can extract proteins which are sterically trapped on DNA, including the Ku70/80 complex (van den Boom *et al.*, 2016).

Inactivation of a temperature-sensitive Cdc48 (the yeast VCP/p97 homolog) increases levels of ubiquitinated TOP2 (Wei *et al.*, 2017), suggesting that Cdc48 is involved in the proteasomal degradation of TOP2 in yeast. Furthermore, Cdc48 co-operates together with the non-specific protease Wss1 in the degradation of DNA-protein crosslinks including topoisomerase I (TOP1) covalent complexes (Stingele *et al.*, 2014; Balakirev *et al.*, 2015). Interestingly, other AAA ATPase activities have been implicated in the proteasomal processing of TOP2-DNA complexes. Specifically, Ban *et al* propose that the clearance of etoposide-induced TOP2B-DNA complexes involves the unfolding of TOP2B by 19S AAA ATPases associated with elongating RNAPII, leading to TOP2B proteolysis (Ban *et al.*, 2013). It was therefore hypothesised that VCP/p97 could facilitate the proteasomal degradation of TOP2-DNA complexes by unfolding and extracting TOP2 from DNA.

5.2 Aims

The aim of the current chapter was to investigate the potential role of VCP/p97 as a protein segregase in the removal of etoposide-induced TOP2-DNA complexes. This was achieved using the TARDIS assay to measure the removal of TOP2 complexes from DNA following chemical inhibition or siRNA knockdown of VCP/p97. In addition, the role of VCP/p97 in the processing of TOP2-DNA complexes to protein-free DSBs was examined using the ɣH2AX assay.

5.3 Chemical inhibition or siRNA knockdown of VCP/p97 increases levels of etoposide-induced TOP2-DNA complexes

The role of VCP/p97 in the processing of TOP2-DNA complexes was investigated using NMS-873, an allosteric inhibitor of VCP/p97. NMS-873 binds VCP/p97 between the D1 and D2 ATPase domains, thereby inhibiting the conformational change in VCP/p97 which occurs upon ATP binding (Rouiller *et al.*, 2000; Magnaghi *et al.*, 2013). This conformational change is required for the unfolding and remodelling of substrate proteins, and NMS-873 is therefore a potent inhibitor of ATPase activity.

The effect of NMS-873 on the removal of TOP2 complexes from DNA was investigated using the TARDIS assay. K562 cells were treated with 100 µM etoposide (VP-16) alone or in combination with 5 µM NMS-873 and/or 10 µM MG132. After 2 hours, etoposide was removed from the cell culture medium and cells were incubated for a further 2 hours in the continued presence of DMSO, NMS-873 or MG132. Levels of TOP2A- and TOP2B- DNA complexes were measured immediately after 2 hours continuous exposure to etoposide (0 hours after VP-16 removal), and 0.5, 1 and 2 hours after etoposide removal. As previously shown in Chapter 3, co-incubation of cells with MG132 did not affect overall levels of etoposide-induced TOP2A- or TOP2B- DNA complexes following 2 hours continuous etoposide exposure (Figure 5.1). However, proteasome inhibition significantly increased remaining levels of TOP2A- and TOP2B- DNA complexes after etoposide removal, reflecting the role of proteasomal degradation in the removal of TOP2-DNA complexes.

Interestingly, levels of both TOP2A- and TOP2B- DNA complexes were significantly increased in the presence of NMS-873 following 2 hours continuous exposure to etoposide ($p<0.05$ and $p<0.001$, respectively). Levels of remaining TOP2A-DNA complexes were also significantly higher in the presence of NMS-873 0.5 and 1 hour after etoposide removal ($p<0.001$ and $p<0.01$, respectively). In contrast, no significant differences were observed in levels of TOP2B-DNA complexes at any time point after etoposide removal. Therefore, inhibition of VCP/p97 increases TOP2A- and TOP2B- DNA complex levels.

To further investigate whether VCP/p97 is involved in the proteasomal processing of TOP2-DNA complexes, etoposide-treated cells were incubated with both 10 µM MG132 and 5 µM NMS-873. Dual inhibition of the proteasome and VCP/p97 did not additively increase levels of TOP2A- or TOP2B- DNA complexes compared to each inhibitor alone, suggesting that these pathways are epistatic. Together, this suggests that VCP/p97 is involved in the proteasomal processing of TOP2A- and TOP2B-DNA complexes.

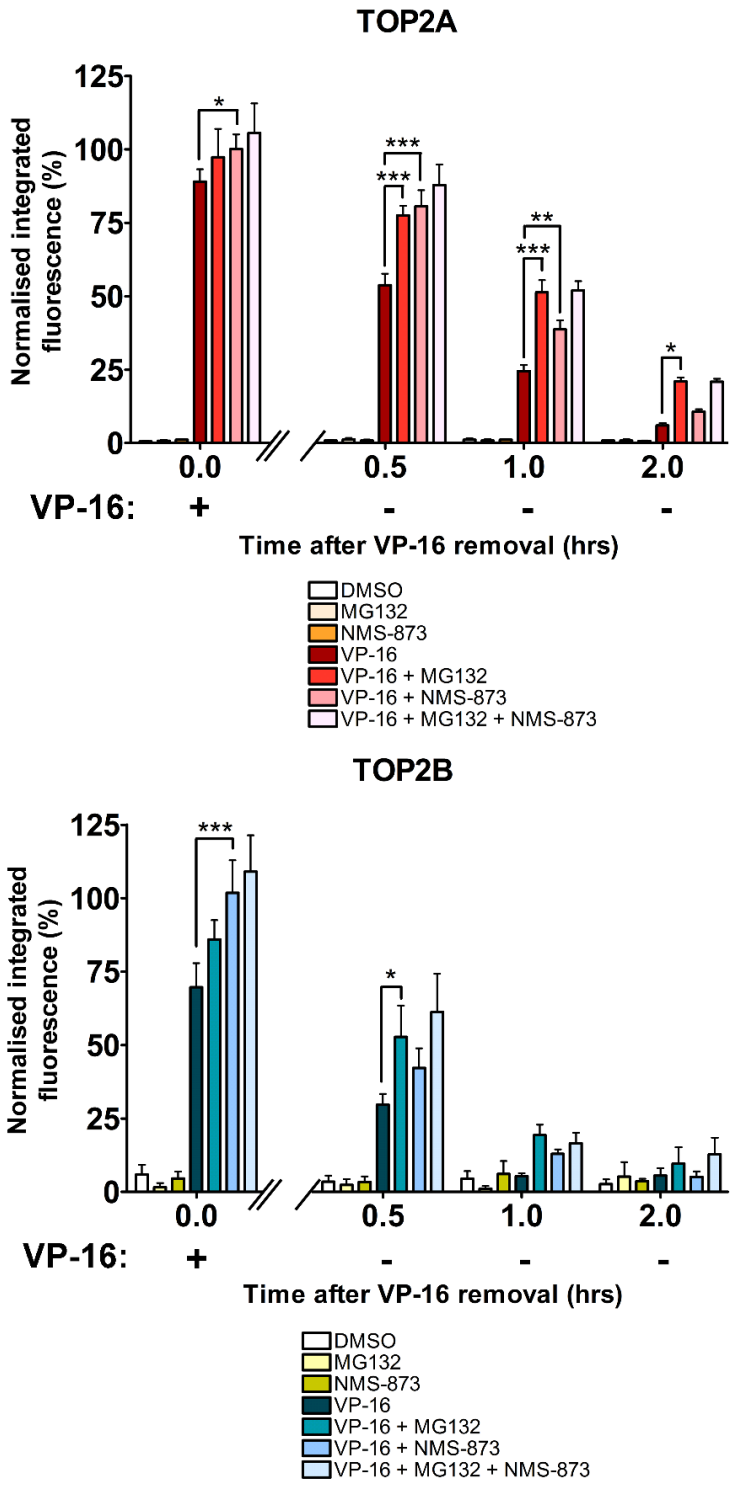

Figure 5.1. Effect of the VCP/p97 inhibitor NMS-873 on levels of TOP2-DNA complexes. K562 cells were treated with 100 µM etoposide (VP-16) alone or in combination with 10 µM MG132 and/or 5 µM NMS-873 for 2 hours. Cells were collected after 2 hours continuous drug exposure (0 hours after VP-16 removal), or following 0.5, 1 and 2 hours further incubation in etoposide-free medium containing MG132, NMS-873 or DMSO. Levels of TOP2A- and TOP2B- DNA complexes were measured using the TARDIS assay. Values represent the mean of medians ± SEM from triplicate experiments, normalised to a 2 hour 100 µM etoposide control. Statistical significance was determined by two-way ANOVA with Bonferroni post-test (n=3).

As shown in Chapter 4, the TARDIS assay can also be used to visualise and quantify ubiquitinated TOP2-DNA complexes. To investigate the effect of VCP/p97 inhibition on levels of ubiquitinated TOP2-DNA complexes, K562 cells were treated with 100 µM etoposide (VP-16) alone or in combination with 5 µM NMS-873 for 2 hours. Levels of ubiquitinated TOP2-DNA complexes were then measured by probing TARDIS slides with anti-ubiquitin FK2 antibody (which detects mono- and poly- ubiquitin). Inhibition of VCP/p97 led to the significant accumulation of ubiquitinated TOP2-DNA complexes on DNA (Figure 5.2), although this may simply be a consequence of increased TOP2 complex levels irrespective of ubiquitination status, as shown in Figure 5.1.

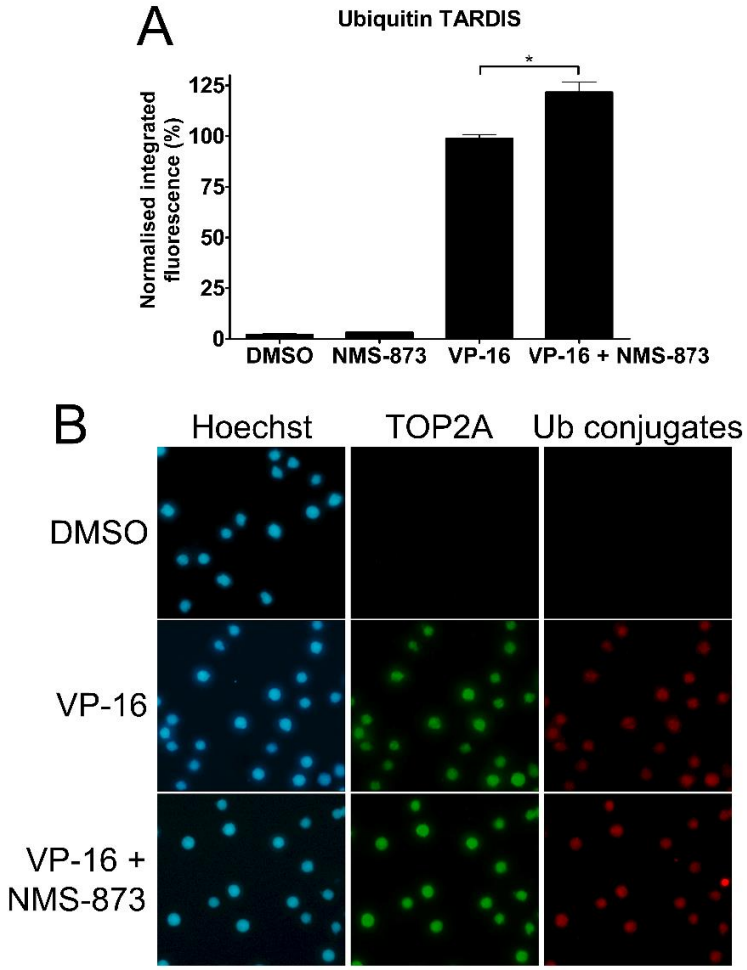

Figure 5.2. Effect of VCP/p97 inhibition on levels of ubiquitinated TOP2-DNA complexes.A) K562 cells were treated with 100 µM etoposide (VP-16) alone or in combination with 5 µM NMS-873 for 2 hours, and levels of ubiquitinated TOP2-DNA complexes were measured using the TARDIS assay. Values represent the mean of medians ± SEM from 3 independent experiments, normalised to a 2 hour 100 µM etoposide control. Statistical comparisons were made by unpaired t-test (n=3). B) Representative images of data shown in A.

The role of VCP/p97 in the processing of etoposide-induced TOP2-DNA complexes was also investigated following siRNA knockdown of VCP/p97. K562 cells were electroporated with 500 nM non-coding (CON siRNA) or VCP/p97 siRNA, and levels of VCP/p97 were measured after 24, 48, 72 and 96 hours. Levels of VCP/p97 were reduced to 38% within 24 hours of transfection with VCP/p97 siRNA compared to CON siRNA, and further reduced to 22% after 72 hours (Figure 5.3). All subsequent experiments in VCP/p97 knockdown cells were performed 72 hours after electroporation.

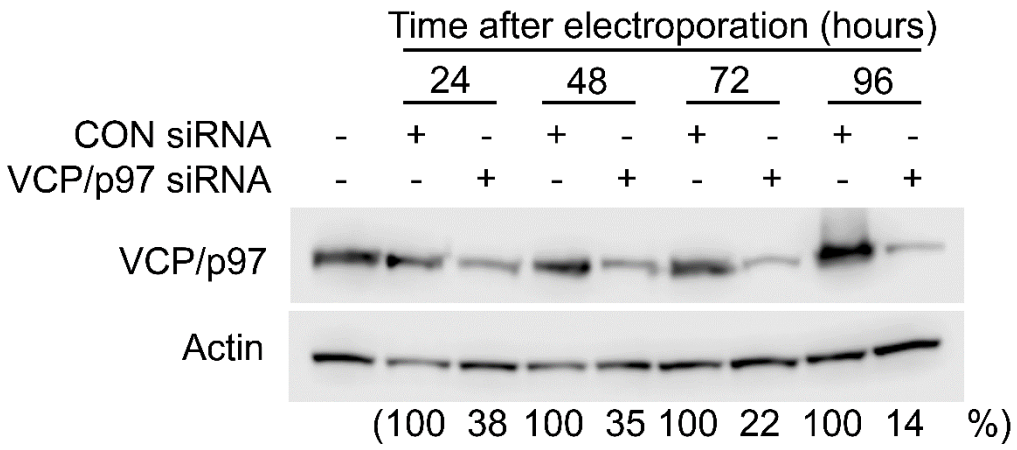

Figure 5.3. siRNA knockdown of VCP/p97. K562 cells were transfected with 500 nM non-coding (CON) siRNA or VCP/p97 siRNA by electroporation. Cells were collected 24, 48, 72 and 96 hours after electroporation, and VCP/p97 protein levels were measured by western blot. VCP/p97 levels were quantified and expressed as percentage remaining compared to the corresponding CON siRNA-treated control.

The effect of VCP/p97 knockdown on the removal of TOP2-DNA complexes was investigated using the TARDIS assay. CON siRNA or VCP/p97 siRNA knockdown cells were treated with 100 µM etoposide (VP-16) for 2 hours, then incubated for a further 2 hours in etoposide-free medium. Levels of TOP2A- and TOP2B- DNA complexes were measured following 0, 0.5, 1 and 2 hours after etoposide removal. As shown in Figure 5.4A, VCP/p97 protein levels were reduced by at least 83% in VCP/p97 siRNA knockdown cells compared to control siRNA-treated cells in all triplicate TARDIS experiments. However, levels of TOP2A-DNA complexes were not significantly affected at any of the time points tested (Figure 5.4B). In contrast, levels of TOP2B-DNA complexes were significantly increased in VCP/p97 knockdown cells following 2 hours continuous exposure to etoposide (0 hours after VP-16 removal, $p<0.01$), as previously shown following chemical inhibition of VCP/p97.

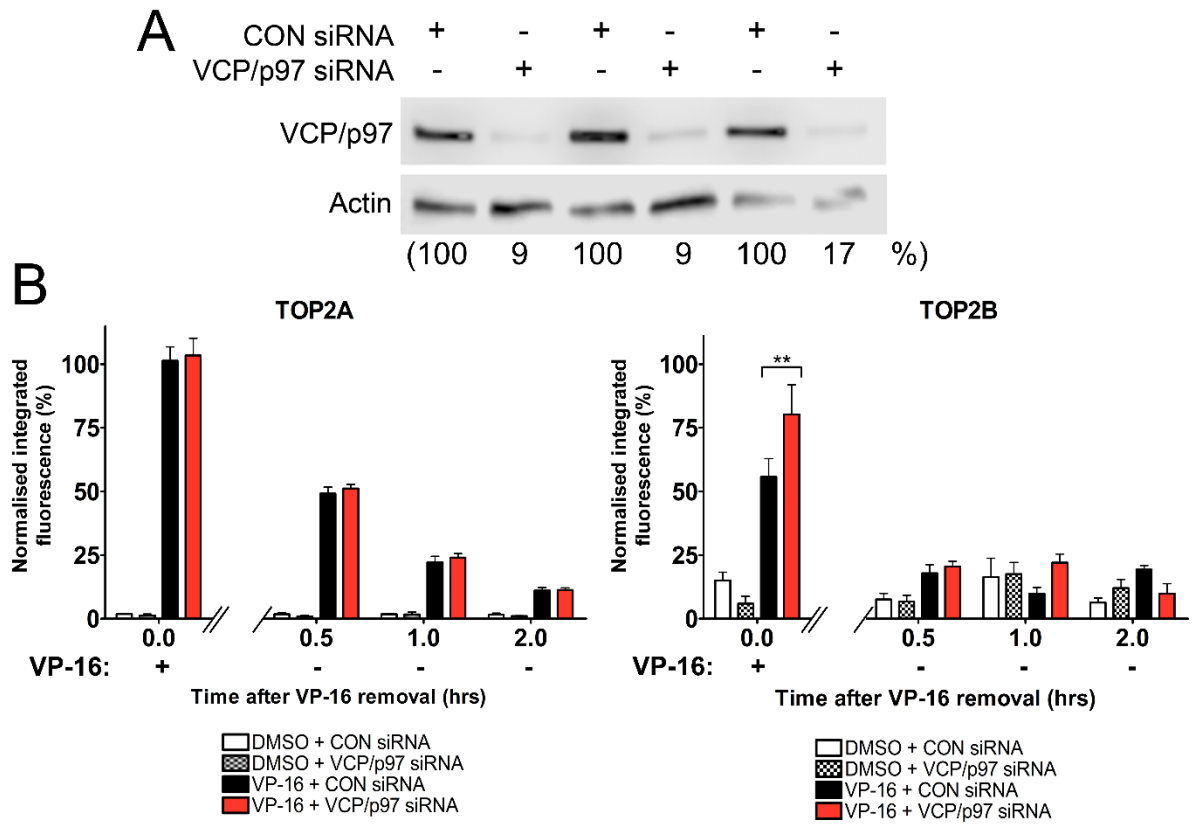

Figure 5.4. siRNA knockdown of VCP/p97 and the effect on levels of etoposide-induced TOP2-DNA complexes. A) The siRNA knockdown of VCP/p97 in cells from triplicate TARDIS experiments was tested by western blot. VCP/p97 levels were quantified and expressed as percentage remaining compared to the corresponding CON siRNA-treated control. B) CON siRNA or VCP/p97 siRNA knockdown cells were treated with 100 µM etoposide (VP-16) for 2 hours. Cells were collected or incubated for up to 2 hours in etoposide-free medium, and levels of TOP2A- and TOP2B- DNA complexes were measured following 0, 0.5, 1 and 2 hours after etoposide removal using the TARDIS assay. Values represent mean of medians ± SEM from 3 separate experiments, normalised to a 2 hour 100 µM etoposide control. Statistical significance was determined by two-way ANOVA with Bonferroni post-test (n=3).

5.4 Investigating the role of VCP/p97 in the appearance of etoposide-induced DSBs

As detailed in Chapter 3, removal of TOP2 from drug-stabilised TOP2-DNA complexes is required before the enzyme-mediated DSB can be detected by DNA damage response proteins. Therefore, to further examine the role of VCP/p97 in the removal of TOP2-DNA complexes, the γH2AX assay was used to test the effect of VCP/p97 inhibition on the appearance of etoposide-induced DSBs.

K562 cells were treated continuously with 10 µM etoposide alone or in combination with 5 µM NMS-873 for up to 4 hours. As expected, incubation of cells with etoposide

alone led to the significant induction of protein-free DSBs (Figure 5.5). However, in the presence of NMS-873 the appearance of etoposide-induced DSBs was significantly reduced following 1 and 2 hours drug exposure ($p<0.001$ and $p<0.05$, respectively), though were not significantly different at later time points. This suggests that VCP/p97 is involved in the processing of TOP2-DNA complexes to protein-free DSBs.

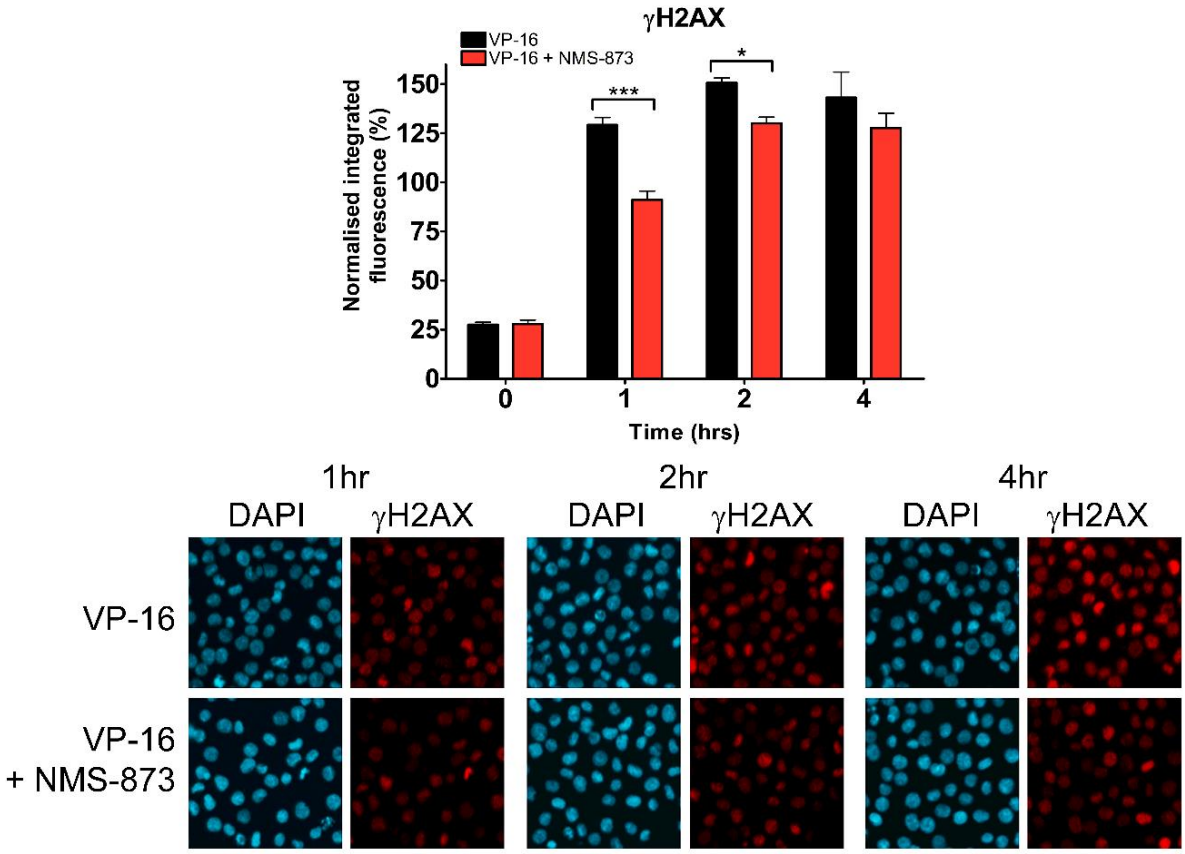

Figure 5.5. Effect of VCP/p97 inhibition on levels of etoposide-induced phosphorylation of histone H2AX. A) K562 cells were treated with 10 µM etoposide (VP-16) alone or in combination with 5 µM NMS-873 for up to 4 hours, and levels of protein-free DSBs were measured by γH2AX assay. Values represent mean of medians ± SEM of triplicate experiments, normalised to a 1 hour 10 µM etoposide control. Statistical comparisons were made by two-way ANOVA followed by Bonferroni post-test (n=3). B) Representative images of data shown in A.

The γH2AX assay was also performed using the VCP/p97 siRNA knockdown cells shown in Figure 5.4A. Consistently, levels of etoposide-induced histone H2AX phosphorylation were significantly reduced in VCP/p97 knockdown cells compared to control cells, and this was true at all time points tested (Figure 5.6, $p<0.001$). Levels of etoposide-induced DSBs in VCP/p97 knockdown cells were 50% lower than control cells within 2 hours of etoposide exposure, compared to only 10% in NMS-873-treated cells. This may suggest that VCP/p97 activity is more efficiently inhibited by siRNA knockdown than small molecule inhibition. Notably, VCP/p97 knockdown did not completely prevent the appearance of etoposide-induced DSBs, which could be due to VCP/p97-independent pathways of TOP2 complex removal or incomplete knockdown of VCP/p97 (Figure 5.4A).

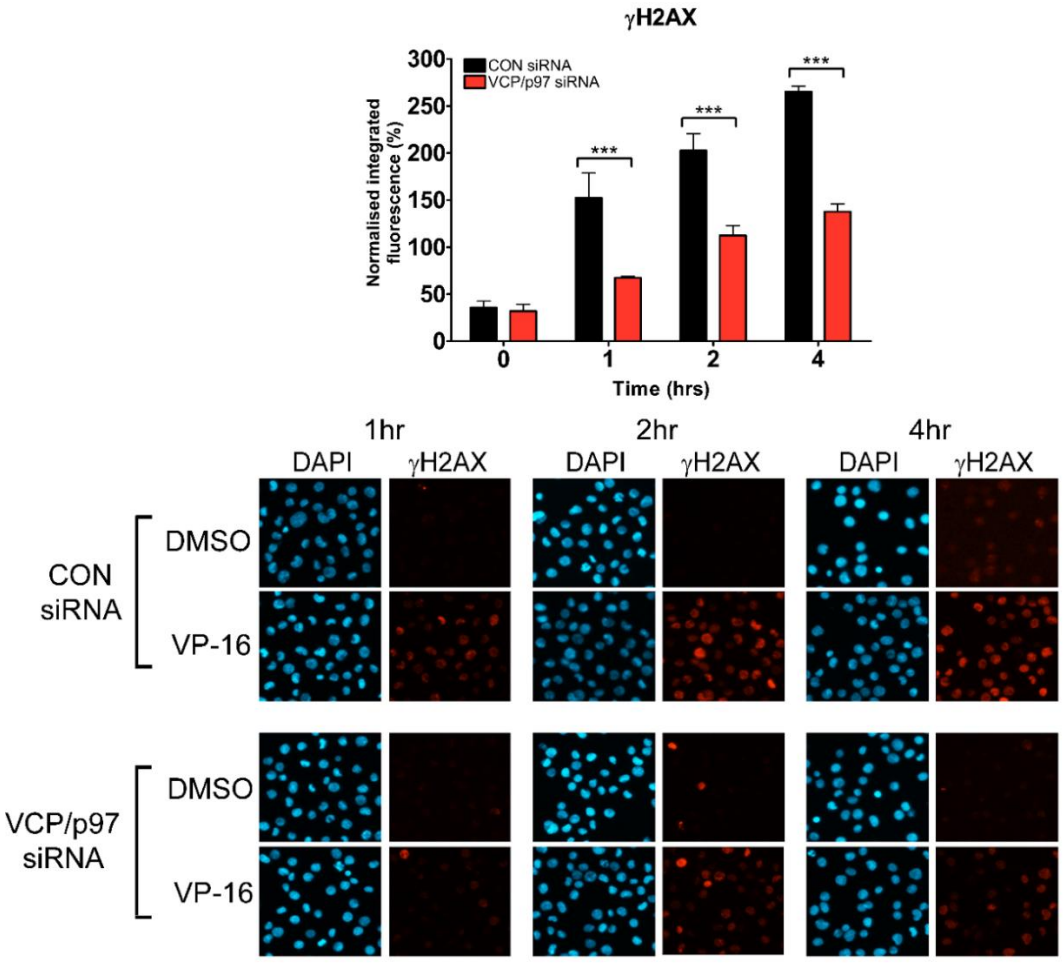

Figure 5.6. Effect of siRNA-mediated VCP/p97 knockdown on etoposide-induced phosphorylation of histone H2AX. K562 cells transfected with 500 nM control (CON) siRNA or 500 nM VCP/p97 siRNA were treated with 10 µM etoposide (VP-16) for up to 4 hours. Levels of protein-free DSBs were measured after 0, 1, 2 or 4 hours continuous etoposide exposure using the γH2AX assay. Values represent mean of medians ± SEM from 3 separate experiments, normalised to a 1 hour 10 µM etoposide non-electroporated control. Statistical comparisons were made by two-way ANOVA with Bonferroni post-test (n=3).

VCP/p97-dependent extraction of proteins from chromatin is regulated by ubiquitination. Specifically, VCP/p97 is directed to ubiquitinated substrates by ubiquitin adaptor proteins, such as Ufd1-Npl4 or p47. While p47 is mostly associated with membrane fusion events, Ufd1-Npl4 has been implicated in many VCP/p97-dependent processes, including chromatin-associated degradation (CAD) (Acs *et al.*, 2011; Verma *et al.*, 2011; Vaz *et al.*, 2013; van den Boom *et al.*, 2016; He *et al.*, 2017a; Stach and Freemont, 2017). In particular, Ufd1-Npl4 is involved in the removal of sterically trapped Ku70/80 and stalled RNAPII from DNA (Verma *et al.*, 2011; van den Boom *et al.*, 2016; He *et al.*, 2017a). Thus, the potential role of Ufd1-Npl4 in the VCP/p97-dependent processing of etoposide-induced TOP2-DNA complexes was investigated by siRNA knockdown.

K562 cells were electroporated in the presence of 500 nM Ufd1 siRNA and 500 nM Npl4 siRNA, or 1 µM non-coding (CON) siRNA as a negative control. Cells were collected after 24, 48 and 72 hours after electroporation, and levels of Ufd1 and Npl4 protein were analysed by western blotting (Figure 5.7A). Ufd1 levels were reduced to 24% after 24 hours, and were undetectable after 48 hours. Npl4 levels were also reduced, with 30% of Npl4 protein remaining after 48 hours. All subsequent experiments with dual Ufd1/Npl4 siRNA knockdown cells were performed 48 hours after electroporation.

The effect of Ufd1/Npl4 siRNA knockdown on the processing of etoposide-induced TOP2-DNA complexes to protein-free DSBs was then investigated by ɣH2AX assay. CON siRNA or double Ufd1/Npl4 siRNA knockdown cells were treated with 10 µM etoposide for up to 4 hours, and levels of ɣH2AX signal were measured following 0, 1, 2 and 4 hours continuous etoposide exposure. Alternatively, cells were treated with 10 µM etoposide for 2 hours, followed by 2 hours incubation in etoposide-free medium (2+2hr washout, WO). Levels of etoposide-induced DSBs were unaffected by Ufd1/Npl4 knockdown at any of the time points tested (Figure 5.7B). This suggests that Ufd1-Npl4 is not involved in the VCP/p97-dependent processing of TOP2-DNA complexes to DSBs. Alternatively, siRNA knockdown of Ufd1 and Npl4 may be incomplete.

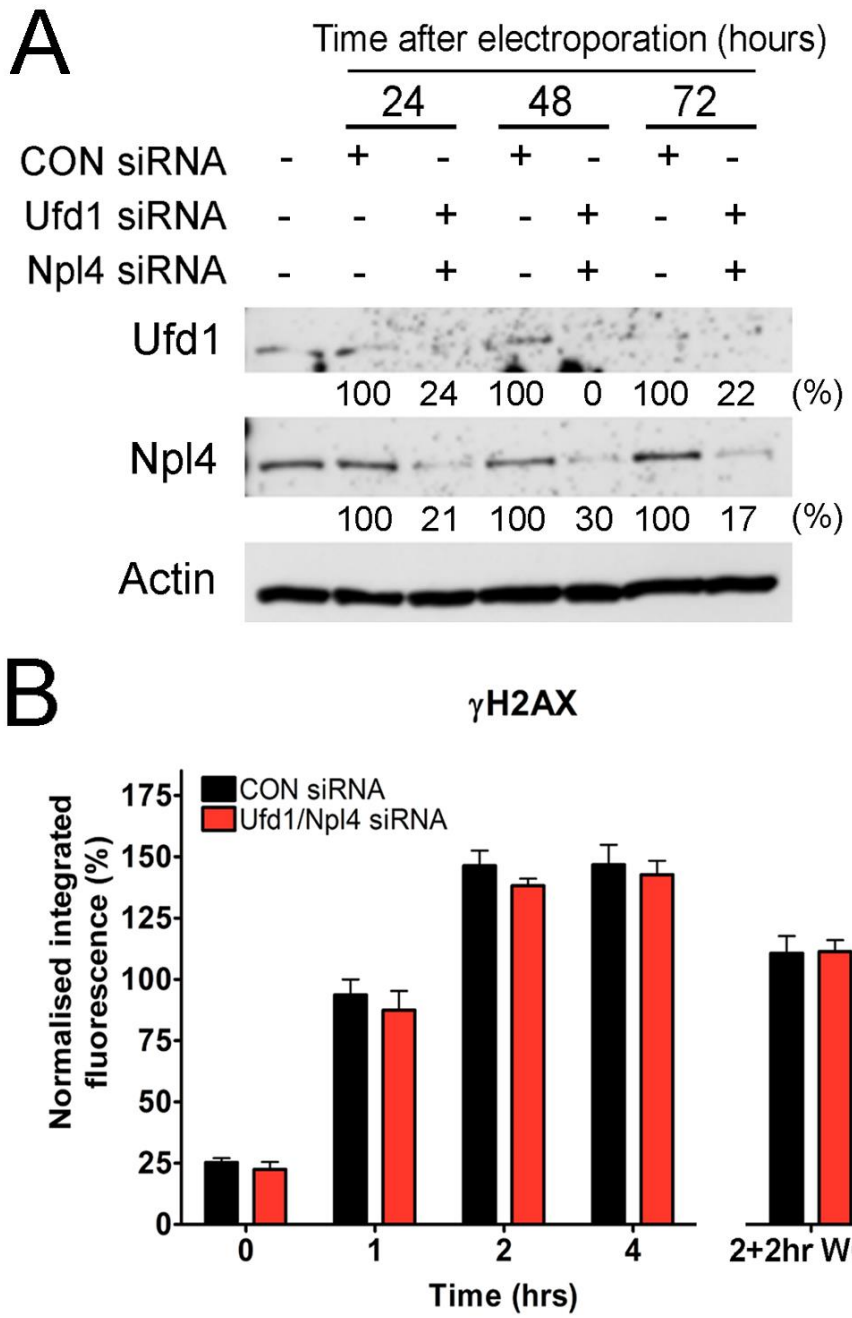

Figure 5.7. Dual siRNA knockdown of Ufd1 and Npl4 and the effect on etoposide-induced phosphorylation of histone H2AX. A) K562 cells were transfected with 500 nM Ufd1 siRNA and 500 nM Npl4 siRNA, or 1 µM control (CON) siRNA by electroporation. Cells were collected 24, 48 and 72 hours after electroporation, and Ufd1 and Npl4 protein levels were measured by western blot. Protein levels were quantified and expressed as percentage remaining compared to the corresponding CON siRNA-treated control. B) 48 hours after electroporation, Ufd1-Npl4 siRNA knockdown cells were treated with 10 µM etoposide (VP-16) or DMSO for up to 4 hours. Levels of protein-free DSBs were measured after 0, 1, 2 and 4 hours continuous etoposide exposure using the γH2AX assay. Alternatively, cells were treated with 10 µM etoposide for 2 hours, followed by incubation in etoposide-free medium for a further 2 hours (2+2hr washout, WO). Values represent mean of medians ± SEM from 3 separate experiments, normalised to a 1 hour 10 µM etoposide non-electroporated control. Statistical comparisons were made by two-way ANOVA with Bonferroni post-test (n=3).

5.5 VCP/p97 interacts with TOP2A and TOP2B

The functional association between TOP2 and VCP/p97 was further investigated by immunoprecipitation. VCP/p97 was efficiently immunoprecipitated from the lysates of DMSO- and etoposide- treated K562 cells, as shown by the depletion of VCP/p97 in whole cell lysate after IP (i.e. flow through, Figure 5.8A). TOP2A was detectable in the input of both untreated and etoposide-treated cells, indicating that TOP2-DNA complexes were extracted during the preparation of lysates with DNase I.

VCP/p97 IPs were performed in triplicate and analysed by western blotting (Figure 5.8B). As expected, VCP/p97 was readily detectable by western blot, as well as the known VCP/p97-interacting protein, YOD1. Interestingly, TOP2A was consistently detected following VCP/p97 IP in untreated cells, while TOP2B was occasionally but not always detected. Importantly, this association was not due to non-specific binding of TOP2 to the IP antibody or protein-G sepharose beads, as TOP2A was not detectable following a mock actin IP (Figure 5.8C). This suggests that VCP/p97 interacts with both TOP2 isoforms in cells.

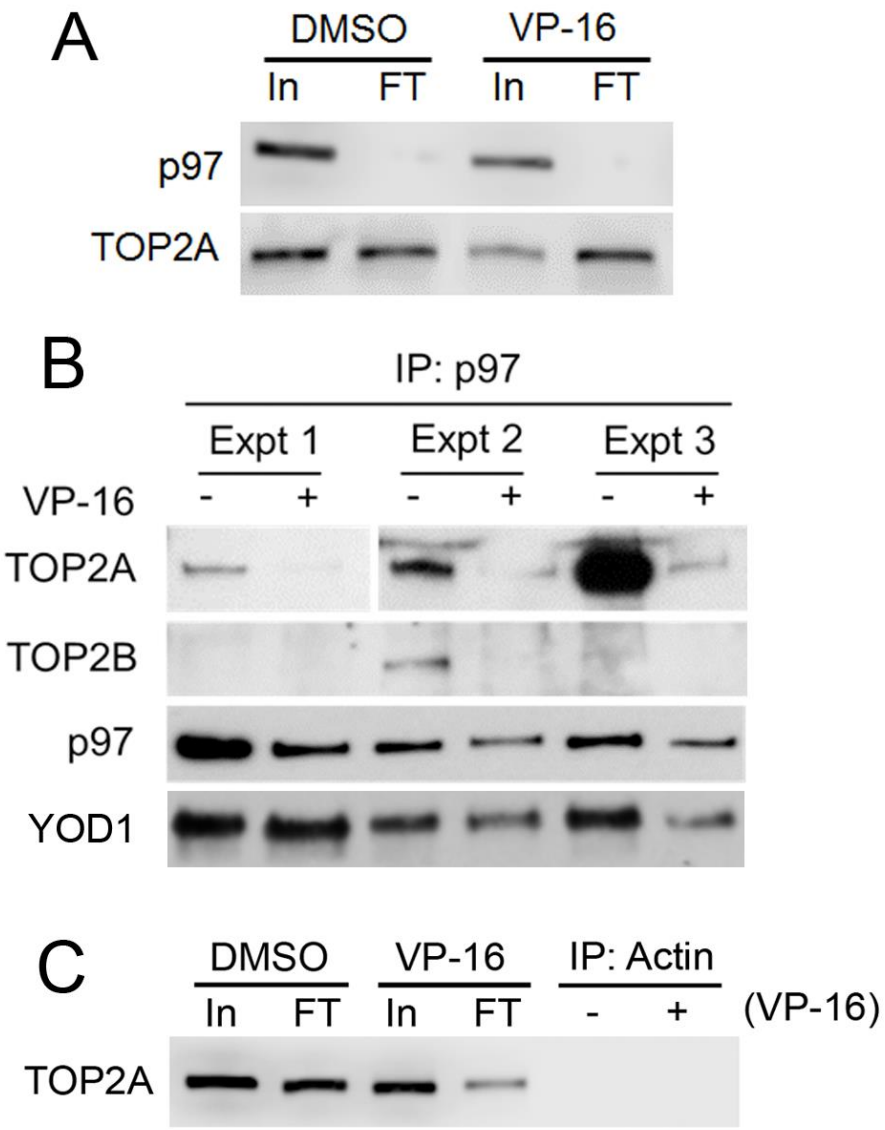

Figure 5.8. Co-immunoprecipitation of VCP/p97 and TOP2 isoforms. K562 cells were treated with 100 µM etoposide (VP-16) or 0.2% v/v DMSO for 2 hours. VCP/p97 and VCP/p97-interacting proteins were isolated from cell lysates by immunoprecipitation with anti-VCP/p97 antibody. A) Levels of VCP/p97 and TOP2A in whole cell extract before (input) and after (flow through, FT) VCP/p97 IP were measured by western blotting. B) Triplicate VCP/p97 IPs were analysed by SDS-PAGE followed by western blotting to test for the presence of TOP2 isoforms. IPs were probed for TOP2A, TOP2B, VCP/p97 and YOD1 (a known interactor of VCP/p97). C) Cell lysates from A and B were also subjected to actin IP. Western blot shows TOP2A levels in actin immunoprecipitates, and in whole cell lysates before (input) and after (flow through, FT) actin IP.

Surprisingly, the interaction between VCP/p97 and TOP2 was reduced in etoposide-treated cells in all three experiments. During the preparation of whole cell extracts, DNase I was added to the lysate to digest the DNA and release chromatin-associated proteins including TOP2. Levels of TOP2A in the whole cell extract (input) of etoposide-treated cells shown in Figure 5.8A are slightly reduced compared to untreated cells. In contrast, the level of TOP2A in the input samples shown in Figure 5.8C appear to be the same in both DMSO- and etoposide- treated cells. This suggests that the extraction of TOP2-DNA complexes with DNase I is highly variable, and may not be sufficient to remove all covalently bound TOP2 from DNA in the presence of etoposide. Therefore, the absence of TOP2 in the VCP/p97 IPs of etoposide-treated cells may be due to a band depletion effect, whereby not all TOP2 is able to enter the gel.

To further investigate this, VCP/p97 IPs were repeated following treatment of cell lysate with benzonase, an alternative nuclease with 34-fold greater activity than DNase I (Benedik and Strych, 1998). Indeed, addition of benzonase instantly reduced the viscosity of the lysate indicating highly efficient digestion of DNA. Other amendments were made to further optimise the IP experiment, including separation of proteins on a non pre-cast 8% gel (where the composition of the stacking gel is known) and co-treatment of cells with the DUB inhibitor PR-619 (to enrich ubiquitinated proteins without inhibiting the proteasome, which otherwise leads to deubiquitination of TOP2-DNA complexes, see Chapter 4, Figure 4.7). Lysates were subjected to VCP/p97 IP and analysed by western blotting (Figure 5.9). TOP2A (and VCP/p97) was equally detectable in the input of both untreated and etoposide-treated cells, suggesting all drug-stabilised TOP2-DNA complexes were successfully extracted from DNA following digestion with benzonase. Furthermore, levels of VCP/p97 were reduced in the flow through, indicating successful immunoprecipitation of VCP/p97. Levels of TOP2A were also reduced in the flow through compared to the input, suggesting that some TOP2A protein was pulled out together with VCP/p97. However, TOP2A was not detectable following VCP/p97 IP in this experiment, in contrast to Figure 5.8.

Therefore, VCP/p97 IPs are highly variable, with TOP2A detected in only 3 of 4 experiments and TOP2B detected in only 2 of 3 replicate experiments. Furthermore, VCP/p97 was not detectable following TOP2A or TOP2B IP in a reciprocal IP experiment (data not shown). This could be due to the unstable nature of the VCP/p97 interaction with protein substrates. Because of this, detection of VCP/p97-protein interactions frequently requires the expression of a "substrate-trapping" VCP/p97 mutant (p97-E578Q), in which mutation of the D2 ATPase domain prevents the release of protein substrates. Indeed, the interaction of VCP/p97 with other proteins such as RNAPII and Ku70/80 was not observed with wild-type VCP/p97 but was readily detectable with the p97-EQ mutant (van den Boom *et al.*, 2016; He *et al.*, 2017a). Therefore, the interaction between VCP/p97 and TOP2 should be verified using another experimental approach.

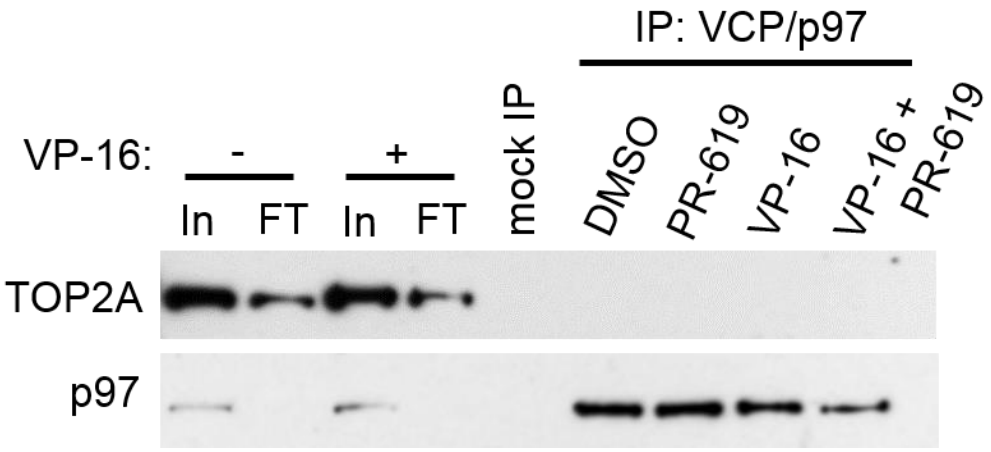

Figure 5.9. Immunoprecipitation of VCP/p97 following preparation of lysates with benzonase. K562 cells were treated with 100 µM etoposide (VP-16) or 0.2% v/v DMSO for 2 hours, alone or in combination with 5 µM PR-619 (a DUB inhibitor). Cell lysates were prepared using benzonase to extract chromatin-associated proteins from DNA, followed by immunoprecipitation with anti-VCP/p97 antibody. Levels of VCP/p97 and TOP2A in whole cell extract before (input) and after (flow through, FT) VCP/p97 IP, and in VCP/p97 immunoprecipitates were analysed by SDS-PAGE followed by western blotting. A mock IP was also performed using an actin IP antibody as a control.

5.6 Discussion

While initially identified as a chaperone for the delivery of ubiquitinated proteins to the proteasome (Dai and Li, 2001), VCP/p97 also facilitates proteasomal degradation by unfolding and extracting proteins from cellular structures, including chromatin (Beskow *et al.*, 2009; Meyer *et al.*, 2012). Here, inhibition of VCP/p97 increased levels of drug-stabilised TOP2A- and TOP2B- DNA complexes suggesting that VCP/p97 is involved in the removal of TOP2 complexes from DNA. This effect was epistatic with the role of the proteasome, indicating that VCP/p97 partakes in the proteasomal processing of TOP2-DNA complexes. Consistently, VCP/p97 inhibition or siRNA knockdown significantly reduced the appearance of etoposide-induced DSBs. Furthermore, immunoprecipitation experiments suggested a previously unreported interaction between VCP/p97 and TOP2. Therefore, VCP/p97 is an important factor involved in the processing of drug-stabilised TOP2-DNA complexes to protein-free DSBs.

The suggestion that AAA ATPases could be involved in the proteasomal processing of TOP2-DNA complexes was first made by Ban et al., who propose that the clearance of TOP2B-DNA complexes involves 19S AAA ATPases associated with elongating RNAPII (Ban *et al.*, 2013). In this model, collision of RNAPII with stabilised TOP2B-DNA complexes leads to the activation of RNAPII-associated 19S AAA ATPases and subsequent recruitment of the 20S proteasome. Importantly, this model does not involve the ubiquitination of TOP2B, as the proteasome is directly recruited to the stalled RNAPII which serves as the primary DNA damage signal.

In contrast, VCP/p97 is a ubiquitin-dependent enzyme which is recruited to ubiquitinated proteins through ubiquitin adaptor proteins such as p47 and Ufd1-Npl4. In Chapter 4, it was shown that TOP2A is ubiquitinated in both the presence and absence of etoposide. While K48- and K63- linked chains were detected on TOP2-DNA complexes using the TARDIS assay, ubiquitin pulldown experiments suggested that TOP2A is largely monoubiquitinated. Polyubiquitin and monoubiquitin chains are known to bind VCP/p97 and Ufd1-Npl4 (Park *et al.*, 2005; Pye *et al.*, 2007; Song *et al.*, 2015). Indeed, Ufd1 contains two ubiquitin binding sites which can bind both poly- and mono- ubiquitin (Park *et al.*, 2005; Pye *et al.*, 2007). However, double siRNA knockdown of Ufd1 and Npl4 did not affect the appearance (or

disappearance) of etoposide-induced DSBs, suggesting that Ufd1-Npl4 is not required for the VCP/p97-dependent removal of TOP2-DNA complexes. Many VCP/p97-associated ubiquitin adaptor proteins have been described which could be involved in the processing of TOP2-DNA complexes (Stach and Freemont, 2017). FAF1 is another ubiquitin adaptor protein which has been recently implicated in chromatin-associated degradation (Franz *et al.*, 2016; van den Boom *et al.*, 2016; Stach and Freemont, 2017). Like Ufd1-Npl4, FAF1 can also contribute to the removal of trapped Ku70/80 rings from DNA (van den Boom *et al.*, 2016). While Ufd1 was identified as the principle adaptor protein involved in the VCP/p97-dependent removal of Ku70/80 from chromatin, van den Boom et al. show that FAF1 can also extract Ku70/80 from DNA when levels of Ufd1 are depleted. The potential role of other VCP/p97-associated adaptor proteins should be investigated in future studies.

VCP/p97 can also bind SUMOylated proteins both directly and via Ufd1, including the chromatin-associated DNA damage response protein Rad52 (Nie *et al.*, 2012; Bergink *et al.*, 2013). It is known that TOP2-DNA complexes are SUMOylated in response to TOP2 poisons (Mao *et al.*, 2000; Agostinho *et al.*, 2008; Schellenberg *et al.*, 2017), and therefore VCP/p97 could be involved in the processing of SUMOylated TOP2-DNA complexes. Cdc48 (the yeast VCP/p97 homolog) functions together with the non-specific protease Wss1 in the degradation of SUMOylated protein-DNA adducts, including TOP1 (Balakirev *et al.*, 2015). The effect of VCP/p97 inhibition on levels of SUMOylated TOP2-DNA complexes was not tested in this study, but could be investigated using the TARDIS assay to measure levels of SUMOylated TOP2-DNA complexes in the presence and absence of the VCP/p97 inhibitor, NMS-873. However, given that levels of SUMOylated TOP2-DNA complexes are not affected by proteasome inhibition (Chapter 3, Figure 1.29 and Chapter 4, Figure 4.12), SUMOylation of TOP2 is unlikely to be involved in the regulation of the VCP/p97- and proteasome- dependent processing pathway.

It is unclear exactly how VCP/p97 facilitates the proteasomal degradation of TOP2-DNA complexes. However, levels of TOP2-DNA complexes were increased following inhibition of VCP/p97 with the allosteric inhibitor NMS-873, directly implicating a role for VCP/p97 ATPase activity. Therefore, VCP/p97 is not required simply as a scaffold for the delivery of ubiquitinated TOP2 to the proteasome but is likely

required for protein unfolding. TOP2 unfolding by VCP/p97 may facilitate the translocation of TOP2 through the narrow 20S core, or may enable TOP2 proteolysis by extracting TOP2 from DNA. The data presented here indicate a new model of TOP2-DNA complex processing by the proteasome, involving the prior unfolding of ubiquitinated TOP2-DNA complexes by VCP/p97.

Chapter 6 Effect of ubiquitin-proteasome system inhibitors on the response to TOP2 poisons

6.1 Introduction

Proteasome inhibitors increase the cytotoxicity of TOP2 poisons (Ogiso *et al.*, 2000; Congdon *et al.*, 2008b; von Metzler *et al.*, 2009; Lee *et al.*, 2016), and are now FDA- and EMA-approved for the treatment of multiple myeloma in combination with other chemotherapeutic drugs, including the TOP2 poison doxorubicin. The proteasome is involved in many cellular processes including NFκB activation, cell cycle control and DNA repair, and this contributes to the potentiation of TOP2 poisons with proteasome inhibitors (Ceruti *et al.*, 2006; Jacquemont and Taniguchi, 2007; Congdon *et al.*, 2008a; Takeshita *et al.*, 2009; von Metzler *et al.*, 2009). However, the proteasome is also involved in the regulation of TOP2 levels and in the removal and repair of TOP2-DNA complexes (Ogiso *et al.*, 2000; Congdon *et al.*, 2008b; Lee *et al.*, 2016). Therefore, proteasome inhibition may also improve TOP2 poison efficacy by prolonging the half-life of drug-induced TOP2-DNA complexes.

While TOP2B levels remain relatively constant throughout the cell cycle, TOP2A levels are regulated by the proteasome in a cell-cycle dependent manner (Woessner *et al.*, 1991; Salmena *et al.*, 2001; Eguren *et al.*, 2014). Specifically, levels of TOP2A are increased during G2/M phase, where TOP2A mediates the decatenation of sister chromatids (DiNardo *et al.*, 1984; Uemura *et al.*, 1987; Clarke *et al.*, 1993; Sumner, 1995; Porter and Farr, 2004; Bower *et al.*, 2010). After chromosome segregation, TOP2A is rapidly degraded in a proteasome-dependent manner, with most TOP2A protein degraded during early G1 phase (Salmena *et al.*, 2001). TOP2A is also degraded by the proteasome in response to various stresses, including glucose starvation, hypoxia and treatment with TOP2 poisons (Mao *et al.*, 2001; Yun *et al.*, 2004; Alchanati *et al.*, 2009). In each instance, TOP2A degradation occurs in a ubiquitin-dependent manner but involves different E3 ubiquitin ligases. For example, TOP2A is ubiquitinated by the APC/C complex during early G1 phase (Salmena *et al.*, 2001; Eguren *et al.*, 2014), the ECV ligase in response to glucose starvation (Yun *et al.*, 2009), Fbw7 in response to HDAC inhibition (Chen *et al.*, 2011), and BMI1/RING1A in response to TOP2 poisons (Alchanati *et al.*, 2009).

In Chapter 3, it was shown that the proteasomal degradation of etoposide-induced TOP2A- and TOP2B- DNA complexes is ubiquitin dependent. Therefore, inhibition of relevant E3 ubiquitin ligases may also improve the efficacy of TOP2 poisons by preventing the processing and removal of TOP2-DNA complexes. Consistently, others have shown that inhibition of the BMI1/RING1A ubiquitin ligase increases the cytotoxicity of teniposide in a synergistic manner (Alchanati *et al.*, 2009). HDM2 is a RING ubiquitin ligase also implicated in the proteasomal degradation of TOP2A, as overexpression of Mdm2 (the murine homolog of human HDM2) is associated with increased TOP2A degradation and reduced sensitivity to the TOP2 poison etoposide (Nayak *et al.*, 2007). In the current chapter, the XTT assay was used to test the effects of BMI1/RING1A inhibition and HDM2 inhibition on the growth-inhibitory effects of four clinically relevant TOP2 poisons.

The processing of TOP2-DNA complexes by the proteasome leads to the liberation of protein-free DSBs (Zhang *et al.*, 2006; Fan *et al.*, 2008; Tammaro *et al.*, 2013) (see also Figure 3.15). Importantly, TOP2 poison-induced DSBs can participate in oncogenic chromosomal translocations following aberrant NHEJ repair, which lead to the development of therapy-related leukaemia (Malik *et al.*, 2006; Kantidze and Razin, 2007; Cowell and Austin, 2012; Cowell *et al.*, 2012). This suggests that proteasomal inhibition may also reduce TOP2 poison genotoxicity by reducing the appearance of protein-free DSBs and the likelihood of abnormal DSB repair. In support of this, proteasome inhibition significantly reduced etoposide-induced plasmid integration (Azarova *et al.*, 2007), and reduced levels of mitoxantrone-induced micronuclei in K562 cells (Lee, 2016). In Chapter 3, it was shown that the appearance of etoposide-induced DSBs is also ubiquitin-dependent (Figure 3.15 and Figure 3.16), suggesting that TOP2 poison genotoxicity could also be modulated by targeting ubiquitinating enzymes upstream of proteasomal degradation. Hence, another aim of the current study was to test the effect of UAE inhibition on the overall genotoxicity of etoposide, investigated using the micronucleus assay.

6.2 Aims

The aim of the current study was to investigate the effect of specific ubiquitination inhibitors on the growth inhibitory effects of four clinically relevant TOP2 poisons; mitoxantrone (an anthracenedione), mAMSA (an acridine), etoposide (an epipodophyllotoxin) and doxorubicin (an anthracycline). Additionally, Nalm-6$^{TOP2A+/-}$ and Nalm-6$^{TOP2B-/-}$ cells were used to investigate the role of each TOP2 isoform in the potentiation of TOP2 poisons with specific E3 ubiquitin ligase inhibitors. The micronucleus assay was also used to investigate the effect of the UAE inhibitor MLN7243 on the overall genotoxicity of etoposide.

6.3 TOP2 expression in Nalm-6 cell lines

Nalm-6 cells are a human pre-B ALL cell line in which genes can be efficiently inactivated by gene targeting (Toyoda *et al.*, 2008). Therefore, Nalm-6 cell lines with reduced TOP2A or null for TOP2B expression were used to investigate the roles of each TOP2 isoform in the potentiation of TOP2 poisons with ubiquitination inhibitors. As Nalm-6$^{TOP2A-/-}$ cells are non-viable, Nalm-6 cells heterozygous for TOP2A (Nalm-6$^{TOP2A+/-}$ cells) were used to examine the effect of reduced TOP2A expression on the response to TOP2 poisons, while TOP2B is absent in Nalm-6$^{TOP2B-/-}$ cells. TOP2 expression in each cell line was confirmed by immunofluorescence (Figure 6.1).

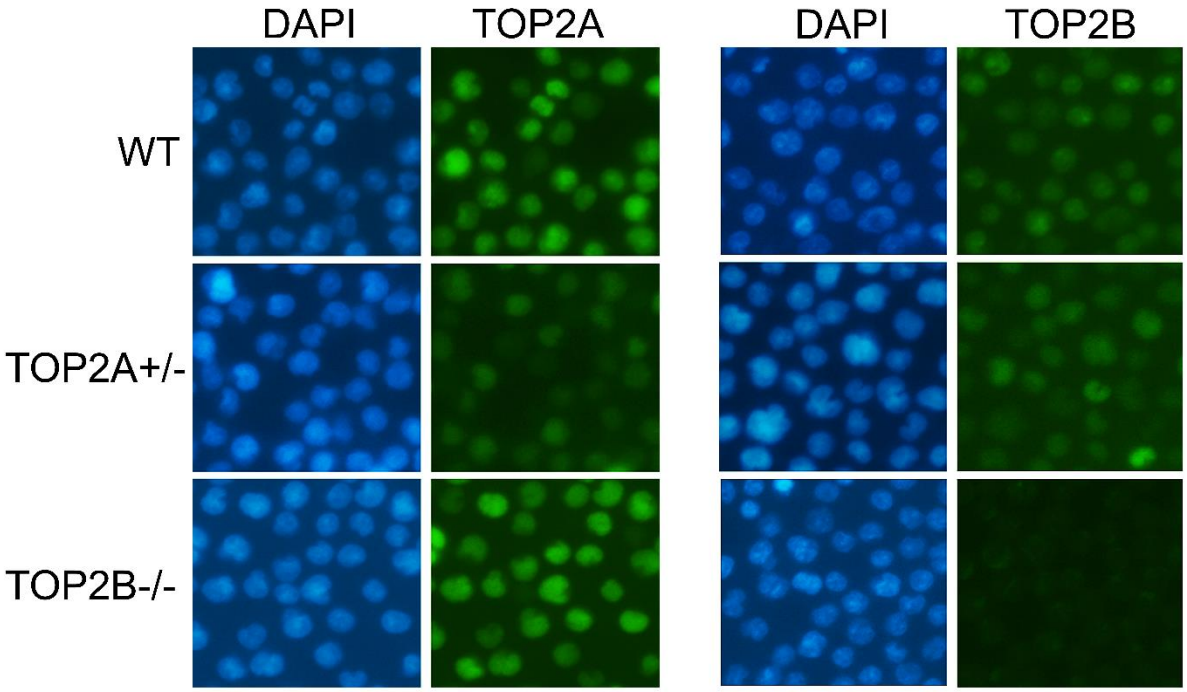

Figure 6.1. Expression of TOP2 isoforms in Nalm-6 cell lines. Levels of TOP2A and TOP2B in Nalm-6 wild-type (WT), Nalm-6$^{TOP2A+/-}$ and Nalm-6$^{TOP2B-/-}$ cells, measured by immunofluorescence.

6.4 Effect of UAE inhibition on the growth-inhibitory effects of TOP2 poisons

As shown in Chapter 3, inhibition of ubiquitin activating enzyme (UAE) activity prevents the removal and repair of etoposide-induced TOP2-DNA complexes. To investigate the effect of UAE inhibition on the growth inhibitory effects of TOP2 poisons, the XTT assay was first used to determine a sub-lethal dose of the UAE inhibitor MLN7243 (equivalent to 20% growth inhibition (Willmore *et al.*, 2004)) for use in combination assays.

The IC_{20} (concentration at 20% growth inhibition) of MLN7243 was determined by treating K562 or Nalm-6 wild type cells with increasing concentrations of MLN7243 alone. Cells were seeded in 96 well plates and incubated for 24 hours prior to drug treatment. Cells were incubated in the presence of MLN7243 for 120 hours, followed by staining with XTT reagent. The optical density (OD_{450nm}) of each well was measured using the Biorad 550 microplate reader, and used to plot a MLN7243 dose-response curve. MLN7243 inhibited the growth of both K562 and Nalm-6 cells in a dose-dependent manner (Figure 6.2A and B, respectively). The growth of K562 cells was inhibited by 20% following 120 hours exposure to 47 nM MLN7243. Nalm-6 cells were significantly less sensitive to MLN7243, with an average IC_{20} of 400 nM.

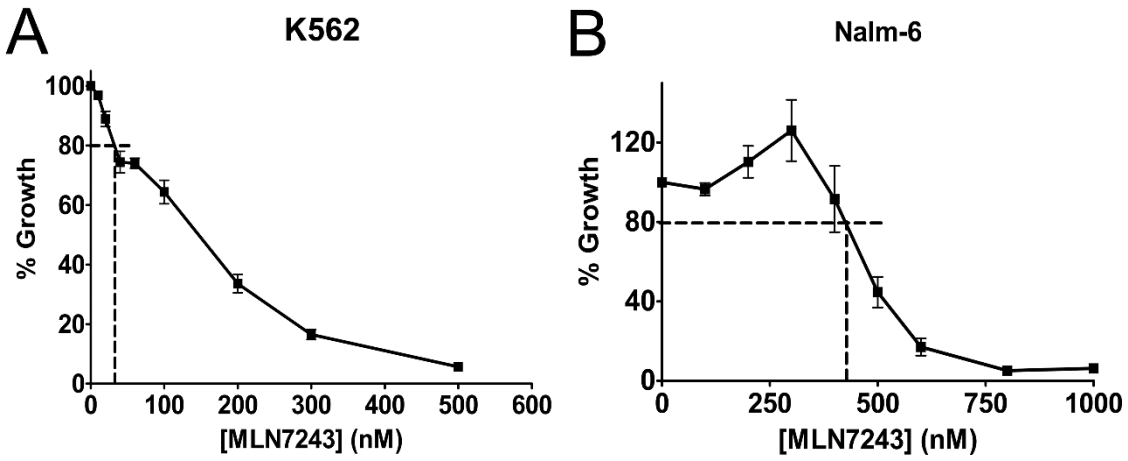

Figure 6.2. MLN7243 IC_{20} determination in Nalm-6 and K562 cells. K562 cells (A) or Nalm-6 wild-type cells (B) were treated with increasing concentrations of MLN7243 for 120 hours. Inhibition of growth was measured by XTT assay and a dose-response curve was plotted to determine the IC_{20} (concentration at 20% growth inhibition) of MLN7243 in each cell line. Error bars represent the mean ± SEM of 3 separate experiments.

To examine the effect of MLN7243 on the growth inhibitory effects of TOP2 poisons, Nalm-6 wild type cells were treated with increasing concentrations of TOP2 poison alone or in combination with 400 nM MLN7243. TOP2 poisons included mitoxantrone (MTX), etoposide (VP-16), mAMSA and doxorubicin. The effect of MLN7243 on the growth inhibitory effects of each TOP2 poison was quantified by a potentiation factor (Pf_{50}), which was calculated as a ratio of the IC_{50} of TOP2 poison alone and the IC_{50} of TOP2 poison in combination with MLN7243 (Equation 1). Therefore, a Pf_{50} value of 2 indicates a two-fold decrease in the TOP2 poison IC_{50}. Potentiation was deemed statistically significant if there was a significant difference between the IC_{50} of TOP2 poison alone versus IC_{50} of TOP2 poison in combination with MLN7243, as determined by unpaired t-test.

Equation 1

$$Potentiation\ factor\ (Pf_{50}) = \frac{IC_{50}\ of\ TOP2\ poison\ alone}{IC_{50}\ of\ TOP2\ poison + MLN7243}$$

Strikingly, co-incubation of Nalm-6 wild type cells with MLN7243 significantly reduced the IC_{50} of all TOP2 poisons tested (Figure 6.3). For example, the IC_{50} of mitoxantrone was reduced from 5.23 nM to 1.70 nM in the presence of MLN7243, equating to a Pf_{50} of 3.26 (p=0.0004). Individual IC_{50} and Pf_{50} values from triplicate experiments are displayed in Table 1. The potentiation of doxorubicin with MLN7243 was noticeably lower than other TOP2 poisons (with a Pf_{50} of 2.20), but was nonetheless statistically significant (p=0.0006). This shows that the growth inhibitory effects of TOP2 poisons are substantially increased following UAE inhibition.

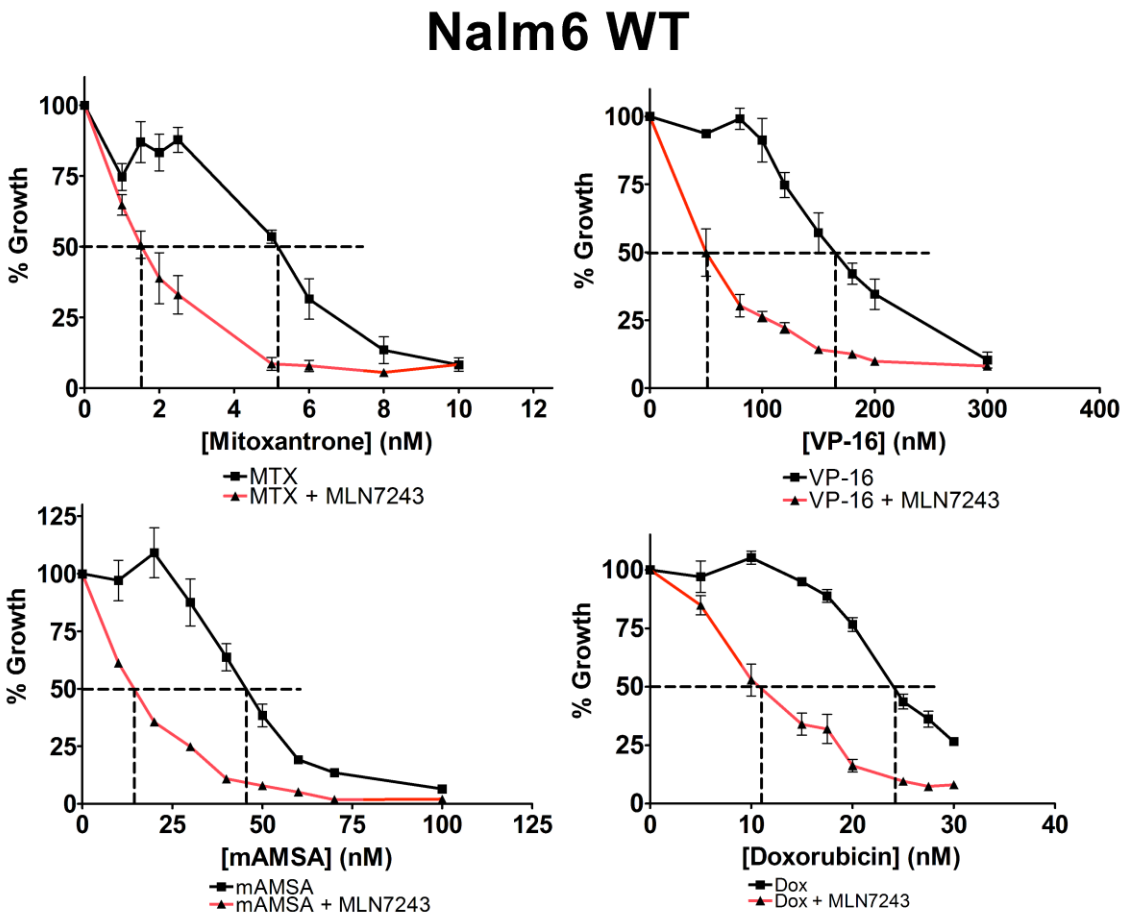

Figure 6.3. Effect of MLN7243 on the growth inhibitory effects of TOP2 poisons in Nalm-6 WT cells. Nalm-6 wild-type (WT) cells were treated with increasing concentrations of TOP2 poison alone or in combination with 400 nM MLN7243 for 120 hours, and growth inhibition was measured by XTT assay. The IC_{50} (concentration at 50% growth inhibition) of each TOP2 poison alone or in combination with MLN7243 was determined by plotting dose-response curves. Error bars represent the mean ± SEM of at least 3 separate experiments.

		IC_{50} (nM)			
	n	**TOP2 poison alone**	**TOP2 poison + MLN7243**	**Pf_{50}**	***p* value**
Mitoxantrone	1	5.25	2.3	2.28	
	2	5.45	1.35	4.04	
	3	5	1.45	3.45	***
	Mean	5.23	1.70	3.26	0.0004
Etoposide	1	144	38	3.79	
	2	172	63	2.73	
	3	175	58	3.02	***
	Mean	163.67	53.00	3.18	0.0009
mAMSA	1	41	14	2.93	
	2	44	13.5	3.26	
	3	48	13.5	3.56	***
	Mean	44.33	13.67	3.25	0.0001
Doxorubicin	1	25	13.3	1.88	
	2	23.6	11.3	2.09	
	3	23.7	9	2.63	***
	Mean	24.10	11.20	2.20	0.0006

Table 1. IC_{50} of TOP2 poisons and the effect of MLN7243 in Nalm-6 wild type cells. IC_{50} values of TOP2 poisons alone or in combination with 400 nM MLN7243 are shown from three replicate experiments. Individual replicates were used to calculate the Pf_{50} values from each experiment, which were then used to calculate the mean Pf_{50}. Statistical significance was determined using an unpaired t-test to compare the IC_{50} of TOP2 poison alone and the IC_{50} of TOP2 poison in combination with MLN7243 (n=3).

To investigate the role of TOP2B in the potentiation of TOP2 poisons with MLN7243, the XTT assay was repeated in Nalm-6$^{TOP2B-/-}$ cells. Nalm-6$^{TOP2B-/-}$ cells were treated with increasing concentrations of mitoxantrone (MTX), etoposide (VP-16), mAMSA or doxorubicin for 120 hours, alone or in combination with 400 nM MLN7243. As shown in Nalm-6 wild type cells, MLN7243 significantly reduced the IC_{50} of all TOP2 poisons tested in Nalm-6$^{TOP2B-/-}$ cells (Figure 6.4, Table 2). For example, the IC_{50} of etoposide was reduced from 169 nM to 104.33 nM in the presence of MLN7243, giving a Pf_{50} of 1.63 (p=0.0001). However, the Pf_{50} values of mitoxantrone, etoposide and mAMSA were significantly smaller in Nalm-6$^{TOP2B-/-}$ cells compared to the respective Pf_{50} values in Nalm-6 wild type cells (p=0.0342, p=0.0086, and p=0.0008). For example, the Pf_{50} of mAMSA is almost 2-fold greater in Nalm-6 wild type cells compared to Nalm-6$^{TOP2B-/-}$ cells (Pf_{50} = 3.25 in wild type cells, compared to Pf_{50} = 1.25 in Nalm-6$^{TOP2B-/-}$ cells). In contrast, the potentiation of doxorubicin by MLN7243 treatment was not significantly affected by TOP2B knockout, suggesting that the potentiation of doxorubicin by MLN7243 is mediated via TOP2-independent

mechanisms. Alternatively, the potentiation of doxorubicin with MLN7243 may be mediated by TOP2A. With the exception of doxorubicin, this suggests that the potentiation of MLN7243 is mediated by both TOP2A and TOP2B. Importantly, the concentration of MLN7243 used in combination assays with Nalm-6$^{TOP2B-/-}$ cells corresponds to the IC_{20} of MLN7243 previously determined in Nalm-6 wild type cells. Indeed, the IC_{20} of MLN7243 in Nalm-6$^{TOP2B-/-}$ cells was not measured in this study, and so we cannot eliminate the possibility that Nalm-6$^{TOP2B-/-}$ cells are simply less sensitive to MLN7243.

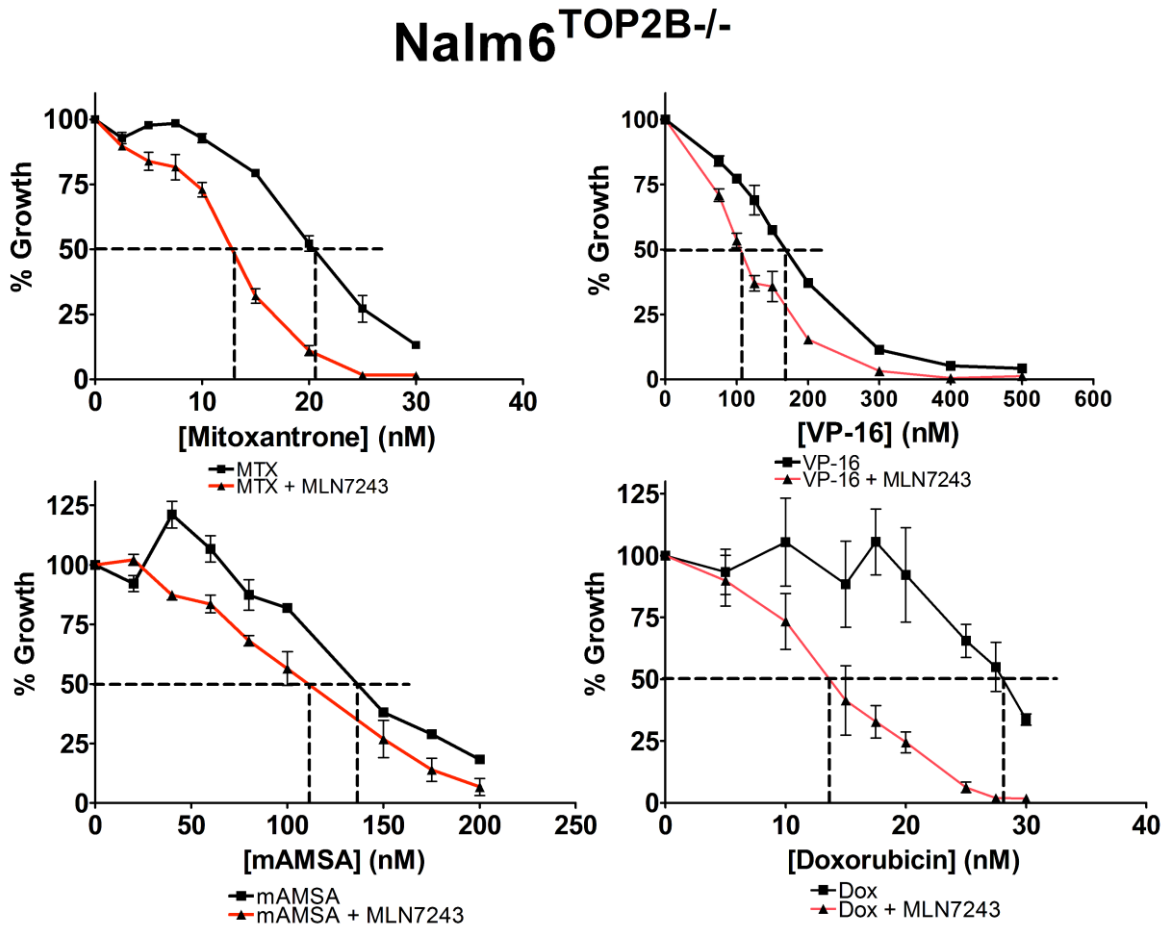

Figure 6.4. Effect of MLN7243 on the growth inhibitory effects of TOP2 poisons in Nalm-6$^{TOP2B-/-}$ cells. Nalm-6$^{TOP2B-/-}$ cells were treated with increasing concentrations of TOP2 poison alone or in combination with 400 nM MLN7243 for 120 hours, and growth inhibition was measured by XTT assay. The IC_{50} (concentration at 50% growth inhibition) of each TOP2 poison alone or in combination with MLN7243 was determined by plotting dose-response curves. Error bars represent the mean ± SEM of at least 3 separate experiments.

		IC_{50} (nM)				
	n	**TOP2 poison alone**	**TOP2 poison + MLN7243**	**Pf_{50}**	***p* value**	**Pf_{50} TOP2B-/- vs WT**
Mitoxantrone	1	20.8	13.5	1.54		
	2	19	12	1.58		
	3	21	12.2	1.72	***	*
	Mean	20.27	12.57	1.62	0.0006	0.0342
Etoposide	1	168	113	1.49		
	2	170	100	1.70		
	3	169	100	1.69	***	**
	Mean	169.00	104.33	1.63	0.0001	0.0086
mAMSA	1	136	136	1.00		
	2	138	100	1.38		
	3	136	99	1.37	NS	***
	Mean	136.67	111.67	1.25	0.1095	0.0008
Doxorubicin	1	28.5	17	1.68		
	2	28.8	10.3	2.80		
	3	25.4	13.7	1.85	**	NS
	Mean	27.57	13.67	2.11	0.0033	0.8385

Table 2. IC_{50} of TOP2 poisons and the effect of MLN7243 in Nalm-6$^{TOP2B-/-}$ cells. IC_{50} values of TOP2 poisons alone or in combination with 400 nM MLN7243 are shown from three replicate experiments. Individual replicates were used to calculate the Pf_{50} values from each experiment, which were then used to calculate the mean Pf_{50}. Statistical significance was determined using an unpaired t-test to compare the IC_{50} of TOP2 poison alone and the IC_{50} of TOP2 poison in combination with MLN7243 (n=3). Unpaired t-test was also used to compare the Pf_{50} values of each TOP2 poison in Nalm-6$^{TOP2B-/-}$ cells with that of Nalm-6 wild type cells.

Nalm-6 cells contain wild type p53 (Adachi *et al.*, 2006), which mediates cell cycle arrest or apoptosis in response to DNA damage through the transcriptional activation of various genes, including p21 and Bcl-2. p53 is degraded by the proteasome in a ubiquitin-dependent manner, and therefore inhibition of ubiquitination may increase TOP2 poison cytotoxicity through the upregulation of p53. In contrast, K562 cells are null for p53 (Law *et al.*, 1993). To test the effect of MLN7243 in the absence of functional p53, the XTT potentiation assay was also performed in K562 cells.

K562 cells were treated with increasing concentrations of mitoxantrone (MTX), etoposide (VP-16), mAMSA or doxorubicin alone or in combination with 47 nM MLN7243 (the IC_{20} of MLN7243 in these cells), and growth inhibition was measured by XTT assay (Figure 6.5). MLN7243 significantly reduced the IC_{50} of mitoxantrone from 14.33 nM to 8.17 nM, giving a Pf_{50} value of 1.74 (p=0.0275) (Table 3). In

addition, the IC_{50} of mAMSA was significantly reduced from 49 to 36 nM (p=0.0193, Pf_{50}=1.4). While statistically significant, the Pf_{50} values of mitoxantrone and mAMSA with MLN7243 in K562 cells are noticeably smaller than those observed in Nalm-6 wild type cells. Furthermore, MLN7243 did not significantly affect the IC_{50} of etoposide or doxorubicin in K562 cells but did in Nalm-6 wild type cells. Therefore, the effect of MLN7243 on the growth inhibitory effects of TOP2 poisons varies in different cell lines. While this could be due to other cell-specific differences, the sensitivity of Nalm-6 cells to the combination of TOP2 poisons with MLN7243 may be attributed to the upregulation of functional p53 protein, which is no longer proteasomally degraded. However, the potential upregulation of p53 following MLN7243 treatment was not determined in this study.

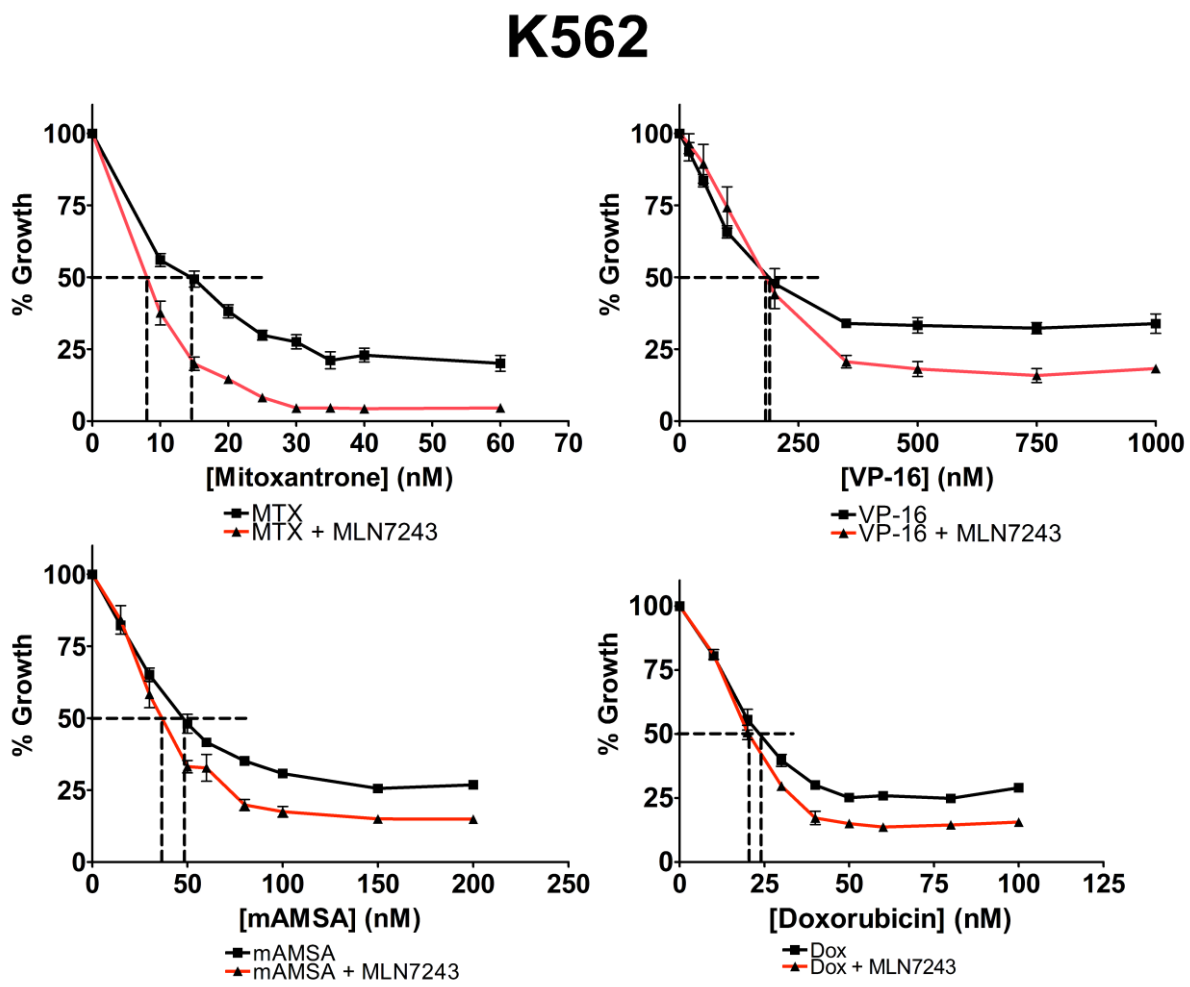

Figure 6.5. Effect of MLN7243 on the growth inhibitory effects of TOP2 poisons in K562 cells. K562 cells were treated with increasing concentrations of TOP2 poison alone or in combination with 47 nM MLN7243 for 120 hours, and growth inhibition was measured by XTT assay. The IC_{50} (concentration at 50% growth inhibition) of each TOP2 poison alone or in combination with MLN7243 was determined by plotting dose-response curves. Error bars represent the mean ± SEM of at least 3 separate experiments.

		IC_{50} (nM)			
	n	**TOP2 poison alone**	**TOP2 poison + MLN7243**	**Pf_{50}**	***p* value**
Mitoxantrone	1	17	9	1.89	
	2	15	8	1.88	
	3	11	7.5	1.47	*
	Mean	14.33	8.17	1.74	0.0275
Etoposide	1	252	195	1.29	
	2	177	198	0.89	
	3	160	140	1.14	NS
	Mean	196.33	177.67	1.11	0.6119
mAMSA	1	45	39	1.15	
	2	55	30	1.83	
	3	47	39	1.21	*
	Mean	49	36	1.40	0.0193
Doxorubicin	1	20	19	1.05	
	2	24	22	1.09	
	3	27	20.5	1.32	NS
	Mean	23.67	20.50	1.15	0.2243

Table 3. IC_{50} of TOP2 poisons and the effect of MLN7243 in K562 cells. IC_{50} values of TOP2 poisons alone or in combination with 47 nM MLN7243 are shown from three replicate experiments. Individual replicates were used to calculate the Pf_{50} values from each experiment, which were then used to calculate the mean Pf_{50}. Statistical significance was determined using an unpaired t-test to compare the IC_{50} of TOP2 poison alone and the IC_{50} of TOP2 poison in combination with MLN7243 (n=3).

6.1 Effect of specific E3 ubiquitin ligase inhibition on the growth-inhibitory effects of TOP2 poisons

BMI1/RING1A is directly implicated in the ubiquitin-dependent degradation of TOP2A following teniposide treatment, and inhibition of BMI1/RING1A increases the cytotoxicity of teniposide in a synergistic manner (Alchanati *et al.*, 2009). HDM2 is another E3 ubiquitin ligase implicated in the downregulation of TOP2A upon etoposide treatment, although this may be due to the HDM2-dependent export of TOP2A from the nucleus, as previously described for p53 (Nayak *et al.*, 2007). Inhibition of E3 ubiquitin ligases may improve the efficacy of TOP2 poisons without inhibiting proteasomal activity. To investigate this, the XTT potentiation assay was performed in Nalm-6 cells following treatment with TOP2 poisons alone or in combination with specific E3 ubiquitin ligase inhibitors.

6.1.1 Effect of BMI1/RING1A inhibition on the growth-inhibitory effects of TOP2 poisons

PRT4165 is a small molecule inhibitor of the E3 ubiquitin ligase BMI1/RING1A which was shown to inhibit the teniposide-induced degradation of TOP2A-DNA complexes and the auto-ubiquitination of BMI1/RING1A (Alchanati *et al.*, 2009). The IC_{20} of PRT4165 (concentration at 20% growth inhibition) in each cell line was determined by XTT assay. As these values were not significantly different between cell lines, the average IC_{20} of PRT4165 (35µM) was used in all subsequent experiments.

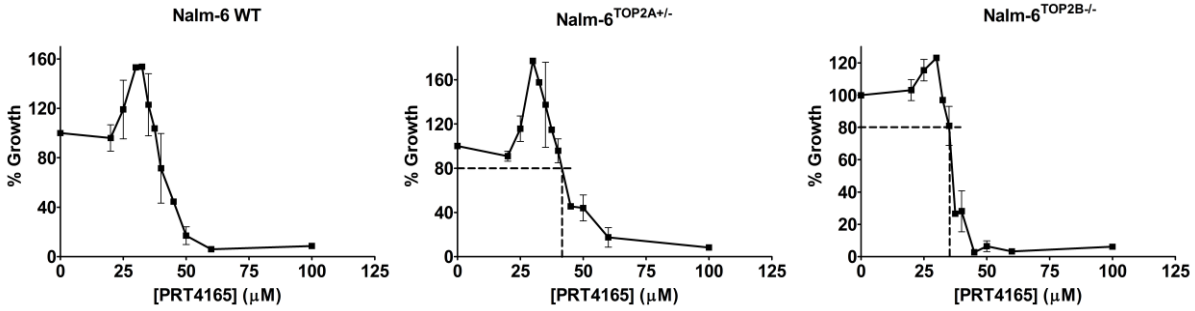

Figure 6.6. PRT4165 IC_{20} determination in Nalm-6 cell lines. Nalm-6 wild-type (WT), Nalm-6$^{TOP2A+/-}$ and Nalm-6$^{TOP2B-/-}$ cells were treated with increasing concentrations of PRT4165 for 120 hours. Inhibition of growth was measured by XTT assay and a dose-response curve was plotted to determine the IC_{20} (concentration at 20% growth inhibition) of PRT4165 in each cell line. Error bars represent the mean ± SEM of 3 separate experiments.

Nalm-6 cells were treated with increasing concentrations of TOP2 poison alone or in combination with 35 µM PRT4165, and growth inhibition was measured by XTT assay (Table 4, see also Figure 6.7 – Figure 6.10). Incubation of cells with PRT4165 significantly reduced the IC_{50} of mitoxantrone (p=0.0454), mAMSA (p=0.0021) and etoposide (p=0.0263). This effect was greatest with mAMSA, producing a mean Pf_{50} of 1.83 (Table 4). In contrast, the IC_{50} of doxorubicin was not significantly affected by BMI1/RING1A inhibition (IC_{50} = 13.8nM compared to 12.9nM with doxorubicin alone). This suggests that the growth inhibitory effect of TOP2 poisons (excluding doxorubicin) can be increased by inhibition of the BMI1/RING1A ubiquitin ligase.

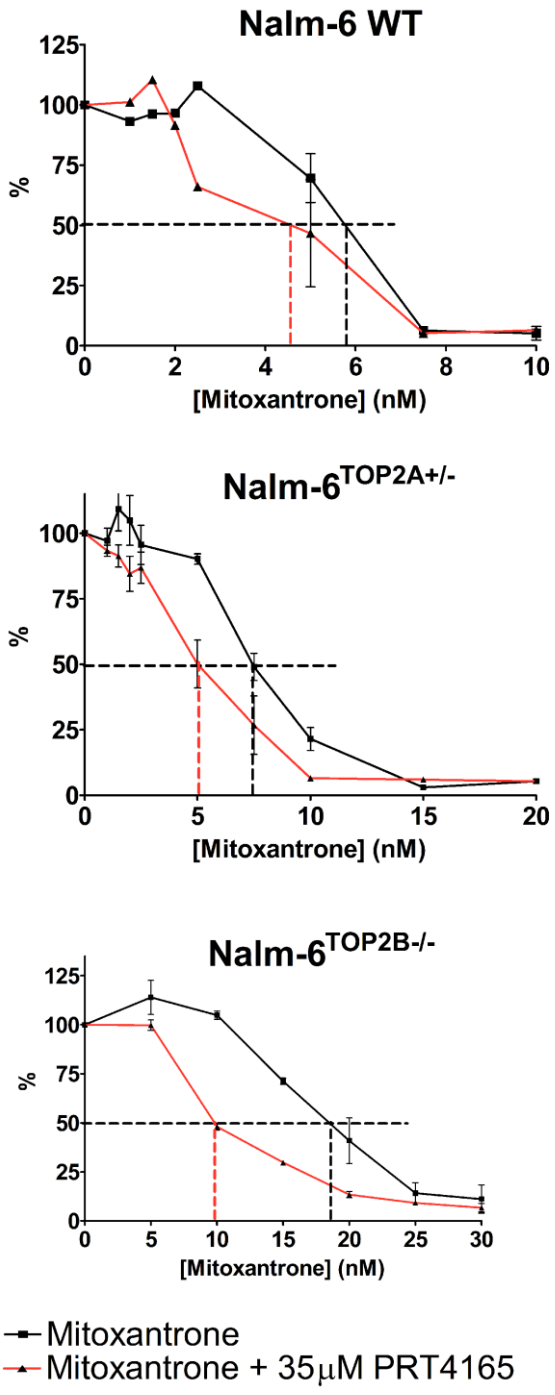

Figure 6.7. Effect of BMI1/RING1A inhibition on the growth inhibitory effect of mitoxantrone in Nalm-6 cell lines. Nalm-6 wild-type (WT), Nalm-6$^{TOP2A+/-}$ and Nalm-6$^{TOP2B-/-}$ cells were treated with increasing concentrations of mitoxantrone alone or in combination with 35 μM PRT4165 for 120 hours, and growth inhibition was measured by XTT assay. The IC_{50} (concentration at 50% growth inhibition) of mitoxantrone alone or in combination with PRT4165 was determined by plotting dose-response curves. Error bars represent the mean ± SEM of at least 3 separate experiments.

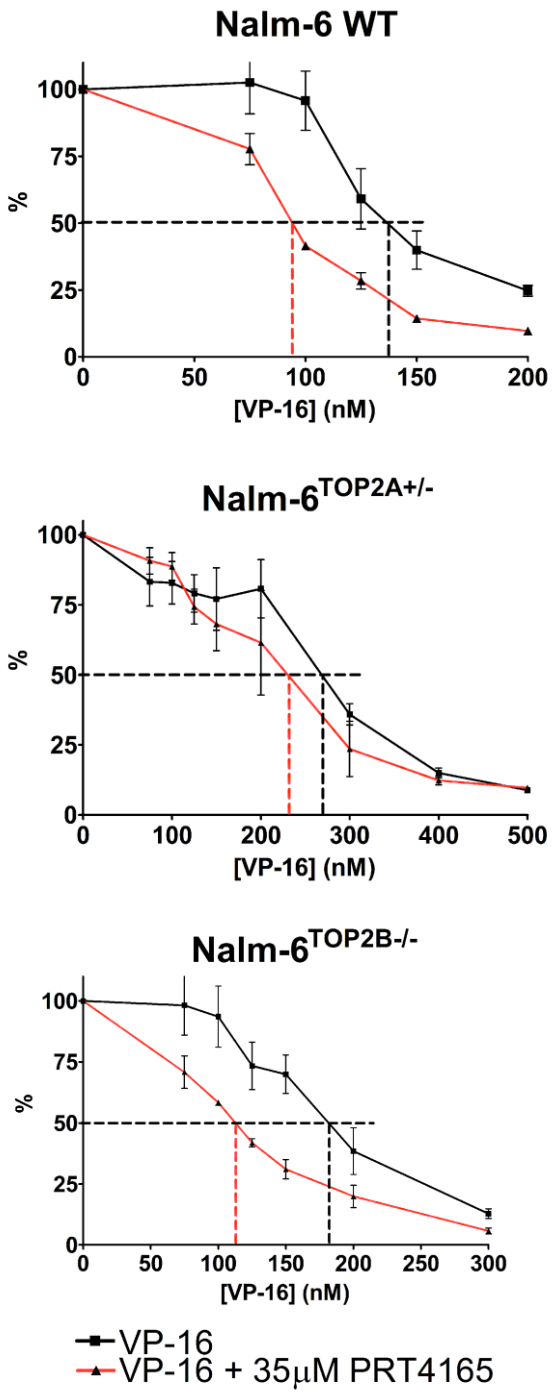

Figure 6.8. Effect of BMI1/RING1A inhibition on the growth inhibitory effect of etoposide (VP-16) in Nalm-6 cell lines. Nalm-6 wild-type (WT), Nalm-6$^{TOP2A+/-}$ and Nalm-6$^{TOP2B-/-}$ cells were treated with increasing concentrations of etoposide (VP-16) alone or in combination with 35 µM PRT4165 for 120 hours, and growth inhibition was measured by XTT assay. The IC_{50} (concentration at 50% growth inhibition) of etoposide alone or in combination with PRT4165 was determined by plotting dose-response curves. Error bars represent the mean ± SEM of at least 3 separate experiments.

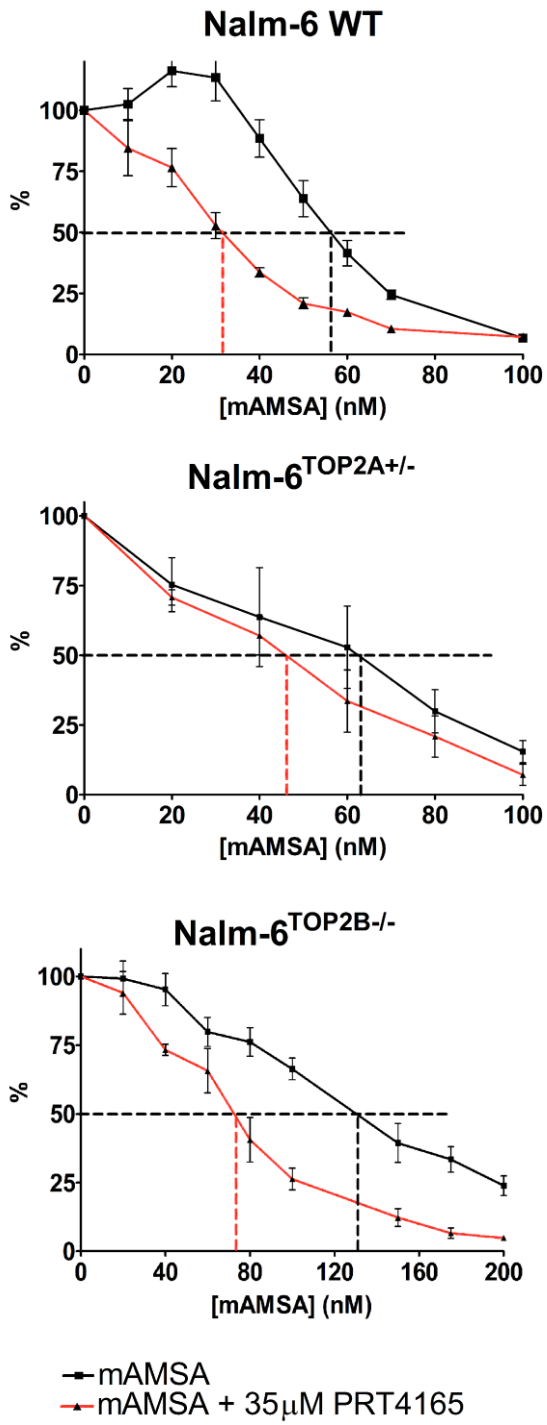

Figure 6.9. Effect of BMI1/RING1A inhibition on the growth inhibitory effect of mAMSA in Nalm-6 cell lines. Nalm-6 wild-type (WT), Nalm-6$^{TOP2A+/-}$ and Nalm-6$^{TOP2B-/-}$ cells were treated with increasing concentrations of mAMSA alone or in combination with 35 μM PRT4165 for 120 hours, and growth inhibition was measured by XTT assay. The IC_{50} (concentration at 50% growth inhibition) of mAMSA alone or in combination with PRT4165 was determined by plotting dose-response curves. Error bars represent the mean ± SEM of at least 3 separate experiments.

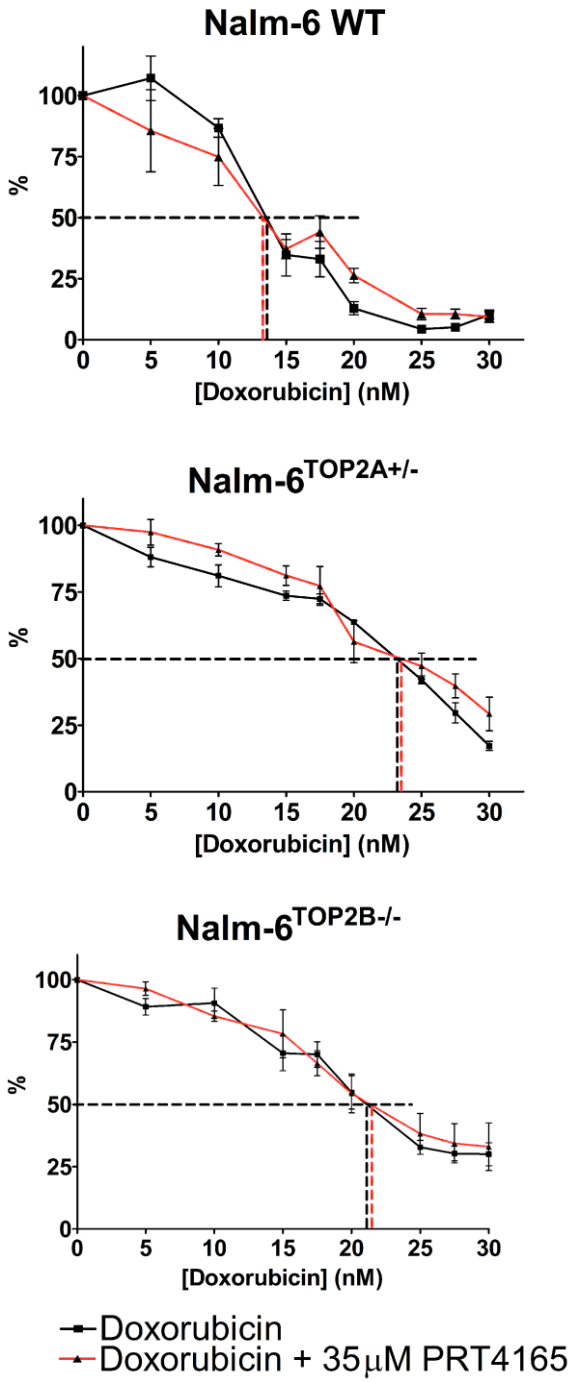

Figure 6.10. Effect of BMI1/RING1A inhibition on the growth inhibitory effect of doxorubicin in Nalm-6 cell lines. Nalm-6 wild-type (WT), Nalm-6$^{TOP2A+/-}$ and Nalm-6$^{TOP2B-/-}$ cells were treated with increasing concentrations of doxorubicin alone or in combination with 35 μM PRT4165 for 120 hours, and growth inhibition was measured by XTT assay. The IC_{50} (concentration at 50% growth inhibition) of doxorubicin alone or in combination with PRT4165 was determined by plotting dose-response curves. Error bars represent the mean ± SEM of at least 3 separate experiments.

In order to examine the role of each TOP2 isoform in the potentiation of TOP2 poisons with PRT4165, growth inhibition assays were also performed Nalm-6$^{TOP2A+/-}$ and Nalm-6$^{TOP2B-/-}$ cells (Figure 6.7 – Figure 6.10). Nalm-6$^{TOP2A+/-}$ and Nalm-6$^{TOP2B-/-}$ cells are more resistant to TOP2 poisons, as demonstrated by an increase in TOP2 poison IC_{50}. Consistent with published data, knockout of TOP2B conferred greater resistance to mAMSA and mitoxantrone (MTX), while Nalm-6$^{TOP2A+/-}$ cells were most resistant to etoposide (VP-16) and doxorubicin compared to wild type cells (Toyoda *et al.*, 2008; Lee *et al.*, 2016). Therefore, both TOP2A and TOP2B are important drug targets which mediate TOP2 poison-induced growth inhibition.

PRT4165 did not significantly affect the IC_{50} of mAMSA in Nalm-6$^{TOP2A+/-}$ cells ($p=0.6755$, $Pf_{50} = 1.33$), but significantly reduced the IC_{50} of mAMSA in Nalm-6$^{TOP2B-/-}$ cells similarly to wild-type ($p=0.0129$, $Pf_{50} = 1.85$) (Table 4). This suggests that TOP2B is dispensable for the potentiation of mAMSA with PRT4165. In contrast, the potentiation of etoposide with PRT4165 remained significant in both Nalm-6$^{TOP2A+/-}$ cells and Nalm-6$^{TOP2B-/-}$ cells ($p=0.0165$ and $p=0.0119$, respectively). Similarly, potentiation of mitoxantrone with PRT4165 was also observed in Nalm-6$^{TOP2A+/-}$ cells and Nalm-6$^{TOP2B-/-}$ cells (Pf_{50}=1.67 and 1.76, respectively, compared to 1.45 in Nalm-6 wild type cells). As in Nalm-6 wild-type cells, PRT4165 did not affect the IC_{50} of doxorubicin in Nalm-6$^{TOP2A+/-}$ or Nalm-6$^{TOP2B-/-}$ cells ($p=0.1933$, 0.5640, respectively).

	Nalm-6 WT		**Nalm-6$^{TOP2A+/-}$**		**Nalm-6$^{TOP2B-/-}$**	
	Pf_{50}	**SEM**	**Pf_{50}**	**SEM**	**Pf_{50}**	**SEM**
Mitoxantrone (n=6)	1.45	0.16	1.36	0.17	1.76	0.15
mAMSA (n=3)	1.83	0.20	1.33	0.48	1.85	0.21
VP-16 (n=3)	1.42	0.11	1.58	0.08	1.62	0.12
Doxorubicin (n=3)	0.94	0.03	0.89	0.03	0.94	0.03

Table 4. Potentiation factor (Pf_{50}) values of TOP2 poisons in combination with PRT4165 in Nalm-6 cell lines. Potentiation factors were calculated by dividing the IC_{50} of TOP2 poison alone by the IC_{50} of TOP2 poison in combination with PRT4165. Pf_{50} values represent the mean Pf_{50} from at least three biological replicates.

6.1.2 Effect of HDM2 inhibition on the growth-inhibitory effects of TOP2 poisons

While best known for its role in the ubiquitin-dependent proteasomal degradation of p53, HDM2 has also been implicated in the downregulation of TOP2A following etoposide treatment (Nayak *et al.*, 2007). The effect of HDM2 inhibition of the growth inhibitory effects of TOP2 poisons was investigated using the XTT assay following co-treatment of cells with HLI373. HLI373 is a small molecule HDM2 inhibitor of the HLI98 class of compounds shown to inhibit the ubiquitination and proteasomal degradation of p53, leading to p53-dependent cell death (Kitagaki *et al.*, 2008). While many HDM2 inhibitors target the HDM2-p53 interaction, the HLI98 class of HDM2 inhibitors specifically inhibit the E3 ubiquitin ligase activity of HDM2 (Yang *et al.*, 2005), and hence will affect the ubiquitination of other HDM2 substrates. The precise mechanism of inhibition by the HLI98 family of inhibitors is unclear, but may involve the inhibition of the HDM2 RING finger domain (which is essential for E3 ligase activity) or inhibition of the interaction of HDM2 with E2 conjugating enzymes (Yang *et al.*, 2005).

Firstly, the IC_{20} of HLI373 in Nalm-6 wild type, Nalm-6$^{TOP2A+/-}$ and Nalm-6$^{TOP2B-/-}$ cells was determined by XTT assay for use in combination experiments. Cells were treated with increasing concentrations of HLI373 for 120 hours. As expected, HLI373 efficiently inhibited the growth of each Nalm-6 cell line (Figure 6.11). There were no significant differences between the IC_{20} of HLI373 in each cell line, and so an average concentration of 2.7 µM HLI373 was used in all subsequent potentiation experiments in Nalm-6 cell lines.

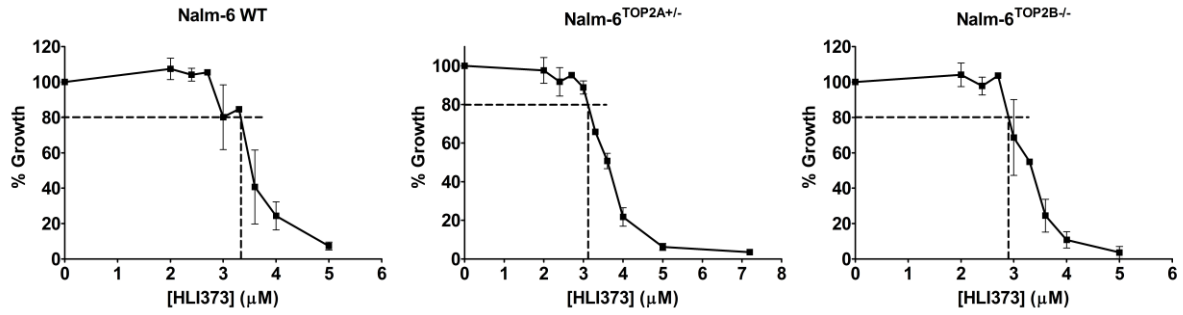

Figure 6.11. HLI373 IC_{20} determination in Nalm-6 cell lines. Nalm-6 wild-type (WT), Nalm-$6^{TOP2A+/-}$ and Nalm-$6^{TOP2B-/-}$ cells were treated with increasing concentrations of HLI373 for 120 hours. Inhibition of growth was measured by XTT assay and a dose-response curve was plotted to determine the IC_{20} (concentration at 20% growth inhibition) of HLI373 in each cell line. Error bars represent the mean ± SEM of 3 separate experiments.

Nalm-6 wild-type cells were treated with increasing concentrations of TOP2 poison alone or in combination with 2.7 μM HLI373 (see Figure 6.12 – Figure 6.15). The IC_{50} of mAMSA was significantly reduced in the presence of HLI373 (p=0.0135), while HDM2 inhibition did not affect the IC_{50} of any other TOP2 poison tested (Table 5). The potentiation of mAMSA by HLI373 was also observed in Nalm-$6^{TOP2A+/-}$ cells (p=0.0002), but was abolished in Nalm-$6^{TOP2B-/-}$ cells (p=0.3262). This suggests that TOP2B is required for the HLI373-mediated potentiation of mAMSA in Nalm-6 cells.

While HDM2 inhibition did not significantly affect the IC_{50} of mitoxantrone or etoposide in wild type cells, the growth inhibitory effects of mitoxantrone and etoposide were significantly increased by HLI373 treatment in Nalm-$6^{TOP2A+/-}$ cells (p=0.0009 and p=0.038), with Pf_{50} values of 1.69 and 1.34, respectively (Table 5, see also Figure 6.12 – Figure 6.15). Mitoxantrone and etoposide were also significantly potentiated by HLI373 in Nalm-$6^{TOP2B-/-}$ cells (Pf_{50} = 1.95 and 1.48, respectively), suggesting that TOP2B is not involved in the potentiation of mitoxantrone and etoposide with HLI373. However, this also shows that HDM2 inhibition increases mitoxantrone and etoposide sensitivity in cells expressing lower levels of TOP2, which is associated with TOP2 poison resistance (Ogiso *et al.*, 2000; Congdon *et al.*, 2008a). Therefore, HDM2 inhibitors may be clinically useful in combination with TOP2 poisons to reduce TOP2 poison resistance.

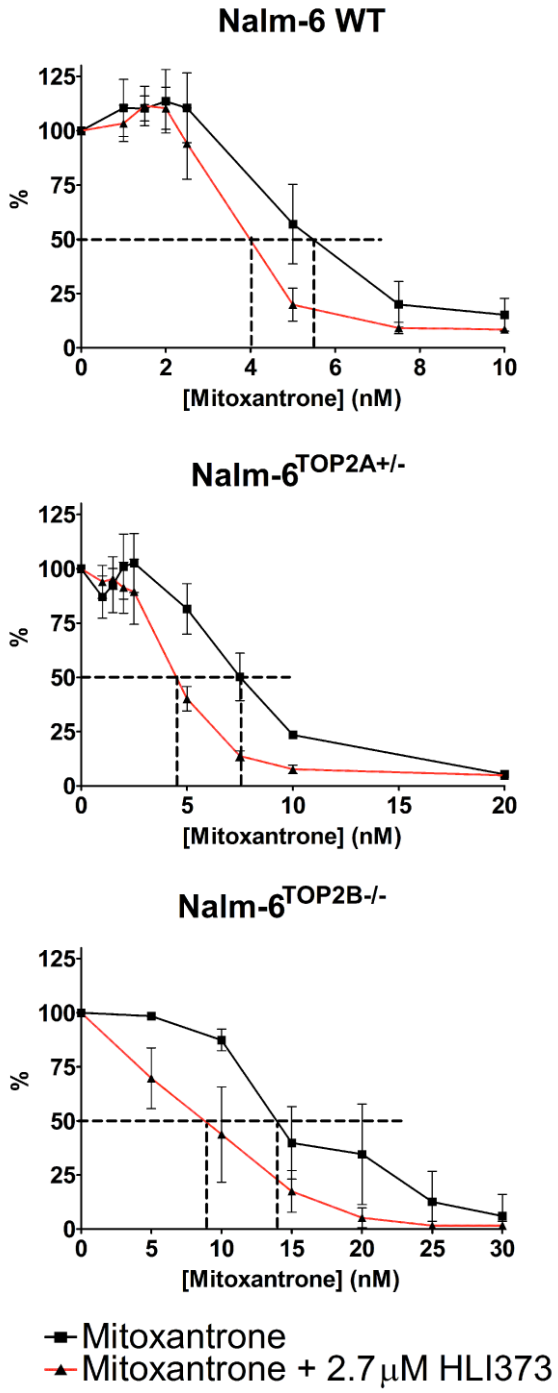

Figure 6.12. Effect of HDM2 inhibition on the growth inhibitory effect of mitoxantrone in Nalm-6 cell lines. Nalm-6 wild-type (WT), Nalm-6$^{TOP2A+/-}$ and Nalm-6$^{TOP2B-/-}$ cells were treated with increasing concentrations of mitoxantrone alone or in combination with 2.7 μM HLI373 for 120 hours, and growth inhibition was measured by XTT assay. The IC_{50} (concentration at 50% growth inhibition) of mitoxantrone alone or in combination with HLI373 was determined by plotting dose-response curves. Error bars represent the mean ± SEM of at least 3 separate experiments.

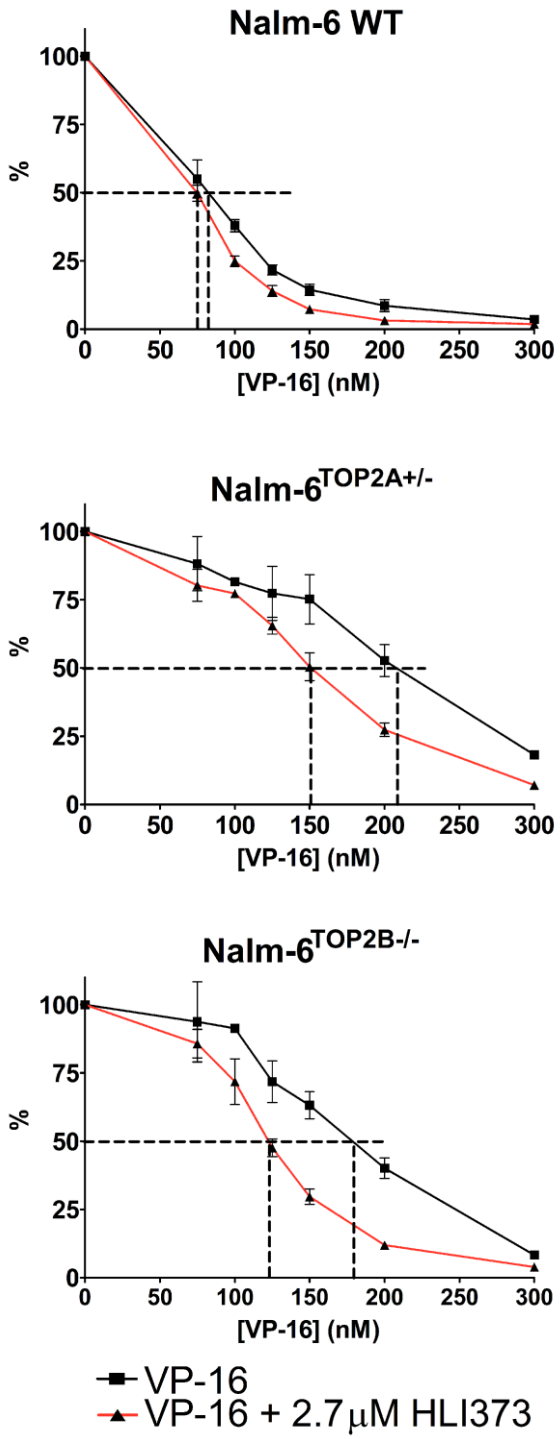

Figure 6.13. Effect of HDM2 inhibition on the growth inhibitory effect of etoposide (VP-16) in Nalm-6 cell lines. Nalm-6 wild-type (WT), Nalm-6$^{TOP2A+/-}$ and Nalm-6$^{TOP2B-/-}$ cells were treated with increasing concentrations of etoposide (VP-16) alone or in combination with 2.7 μM HLI373 for 120 hours, and growth inhibition was measured by XTT assay. The IC_{50} (concentration at 50% growth inhibition) of etoposide alone or in combination with HLI373 was determined by plotting dose-response curves. Error bars represent the mean ± SEM of at least 3 separate experiments.

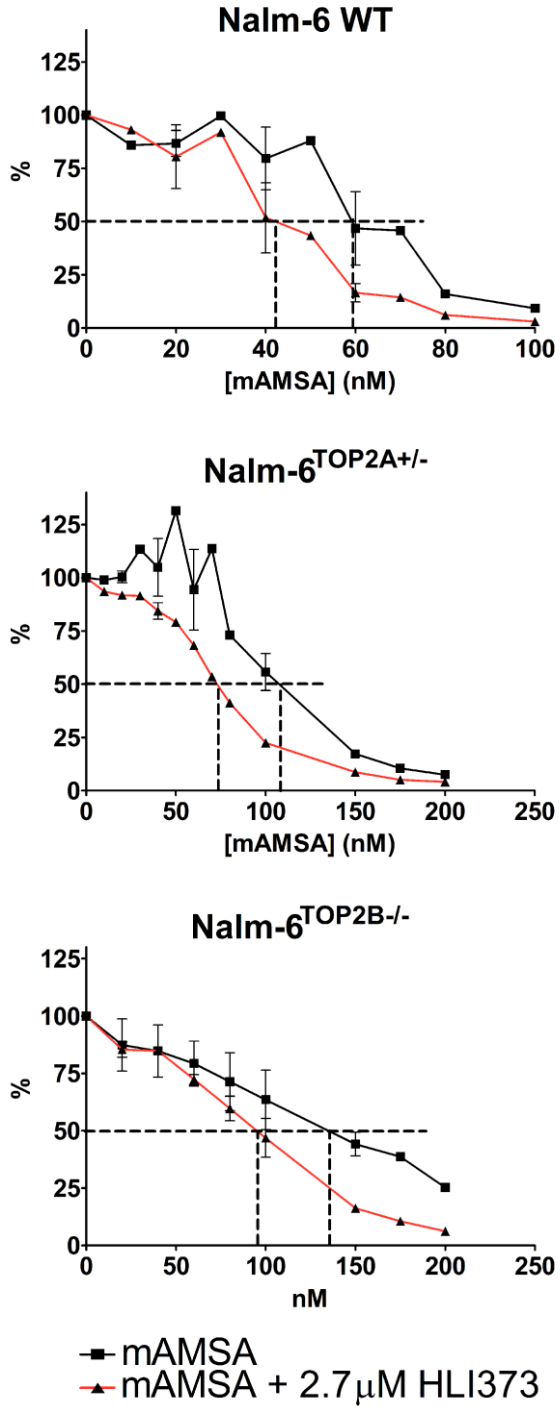

Figure 6.14. Effect of HDM2 inhibition on the growth inhibitory effect of mAMSA in Nalm-6 cell lines. Nalm-6 wild-type (WT), Nalm-6$^{TOP2A+/-}$ and Nalm-6$^{TOP2B-/-}$ cells were treated with increasing concentrations of mAMSA alone or in combination with 2.7 μM HLI373 for 120 hours, and growth inhibition was measured by XTT assay. The IC_{50} (concentration at 50% growth inhibition) of mAMSA alone or in combination with HLI373 was determined by plotting dose-response curves. Error bars represent the mean ± SEM of at least 3 separate experiments.

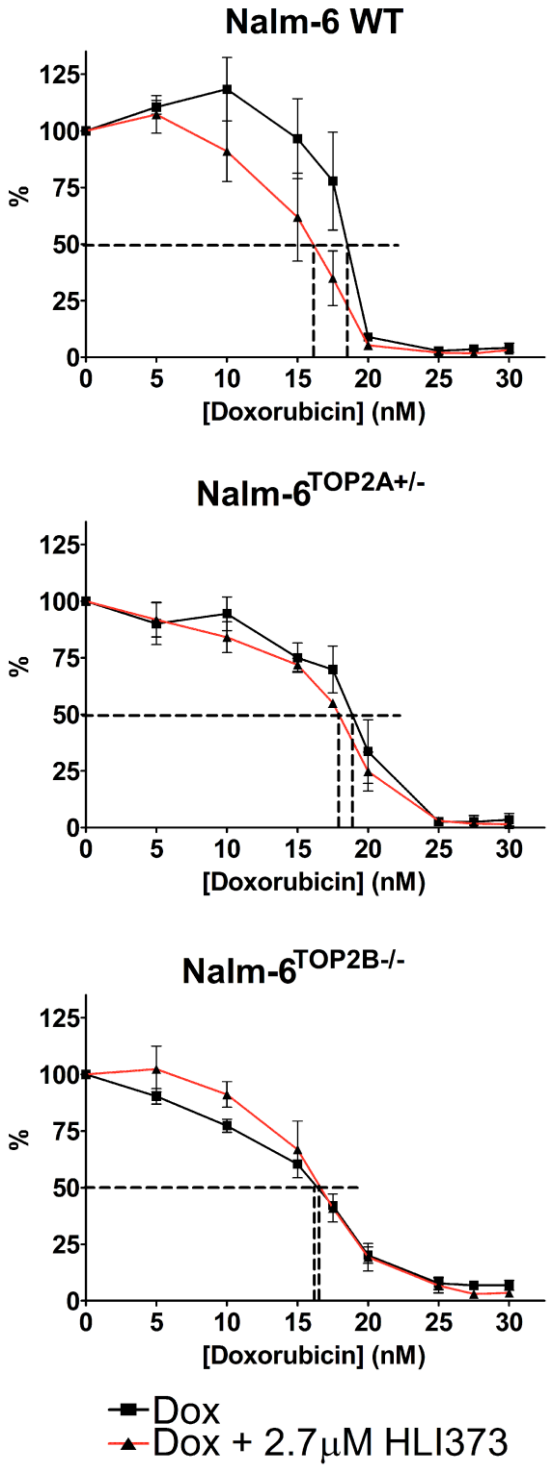

Figure 6.15. Effect of HDM2 inhibition on the growth inhibitory effect of doxorubicin in Nalm-6 cell lines. Nalm-6 wild-type (WT), Nalm-6$^{TOP2A+/-}$ and Nalm-6$^{TOP2B-/-}$ cells were treated with increasing concentrations of doxorubicin alone or in combination with 2.7 μM HLI373 for 120 hours, and growth inhibition was measured by XTT assay. The IC_{50} (concentration at 50% growth inhibition) of doxorubicin alone or in combination with HLI373 was determined by plotting dose-response curves. Error bars represent the mean ± SEM of at least 3 separate experiments.

	Nalm-6 WT		Nalm-6$^{TOP2A+/-}$		Nalm-6$^{TOP2B-/-}$	
	Pf_{50}	**SEM**	**Pf_{50}**	**SEM**	**Pf_{50}**	**SEM**
Mitoxantrone n=6	1.20	0.17	1.69	0.11	1.95	0.14
mAMSA n=3	1.52	0.08	1.33	0.02	1.18	0.14
VP-16 n=6	1.09	0.04	1.34	0.06	1.48	0.15
Doxorubicin n=3	1.21	0.10	1.06	0.04	1.02	0.07

Table 5. Potentiation factor (Pf_{50}) values of TOP2 poisons in combination with HLI373 in Nalm-6 cell lines. Potentiation factors were calculated by dividing the IC_{50} of TOP2 poison alone by the IC_{50} of TOP2 poison in combination with HLI373. Pf_{50} values represent the mean Pf_{50} from at least three biological replicates.

6.2 Effect of MLN7243 on the overall genotoxicity of etoposide

UAE inhibition prevents the processing of etoposide-induced TOP2-DNA complexes to DSBs (Chapter 3). It was therefore hypothesised that UAE inhibition would reduce the likelihood of oncogenic chromosome translocations which arise due to mis-repair of protein-free DSBs following treatment with a TOP2 poison. As a surrogate for specific chromosome translocations which occur at a very low frequency, the micronucleus assay was used to test the effect of UAE inhibitor MLN7243 on overall etoposide genotoxicity.

The following experiments were designed according to the OECD guidelines for the testing of potentially genotoxic chemicals. For example, cells were incubated with test substance for 48 hours to ensure that all cells have completed at least one round of mitosis. Another important consideration is the cytotoxicity of etoposide alone and in combination with MLN7243, as false positive results can arise due to secondary cytotoxic effects (Galloway, 2000). Therefore, cells were treated with a sub-lethal concentration of etoposide and MLN7243 which corresponds to the IC_{20} as determined previously by XTT assay. In addition, apoptotic and necrotic cells were identified through incubation of cells with 2 µg/mL ethidium monoazide bromide (EMA). EMA is a cell-impermeable nucleic acid dye which labels the DNA of cells with damaged membranes. EMA-stained cells were detected by fluorescence microscopy and excluded from the analysis.

K562 cells were treated with 120 nM etoposide (VP-16) alone or in combination with 47 nM MLN7243 for 48 hours. Cells were also incubated with 20 µM or 50 µM methyl methanesulfonate (MMS), a known clastogen, as a positive control. According to the OECD guidelines, it is important to demonstrate that all cells have completed at least one round of cell division, and to monitor the cytotoxicity of drug treatments. Thus, cells were counted before and after drug treatment, and cell counts were used to calculate the Relative Increase in Cell Count (RICC). RICC is expressed as a percentage of cell growth in treated cells compared to untreated cells (Equation 2).

Equation 2

$$RICC = \frac{(Increase\ in\ number\ of\ cells\ in\ treated\ cultures(finish - starting))}{(Increase\ in\ number\ of\ cells\ in\ untreated\ control\ (finish - starting))} \times 100$$

As expected, MMS reduced the RICC in a dose-dependent manner, which was reduced to 51% following exposure to 20 µM MMS and 31% following 50 µM MMS (Figure 6.16). Consistently, treatment of cells with 120 nM etoposide also reduced the RICC by approximately 50%. MLN7243 alone reduced cell viability by 54%, while co-treatment with both etoposide and MLN7243 further reduced the RICC to 26%. According to the OECD guidelines, compounds are considered cytotoxic when the RICC is reduced to less than 40%. Therefore, due to the cytotoxicity of etoposide in combination with MLN7243 the following micronuclei data should be interpreted with caution. In contrast, no significant changes in cell viability were detected by trypan blue exclusion (Figure 6.16).

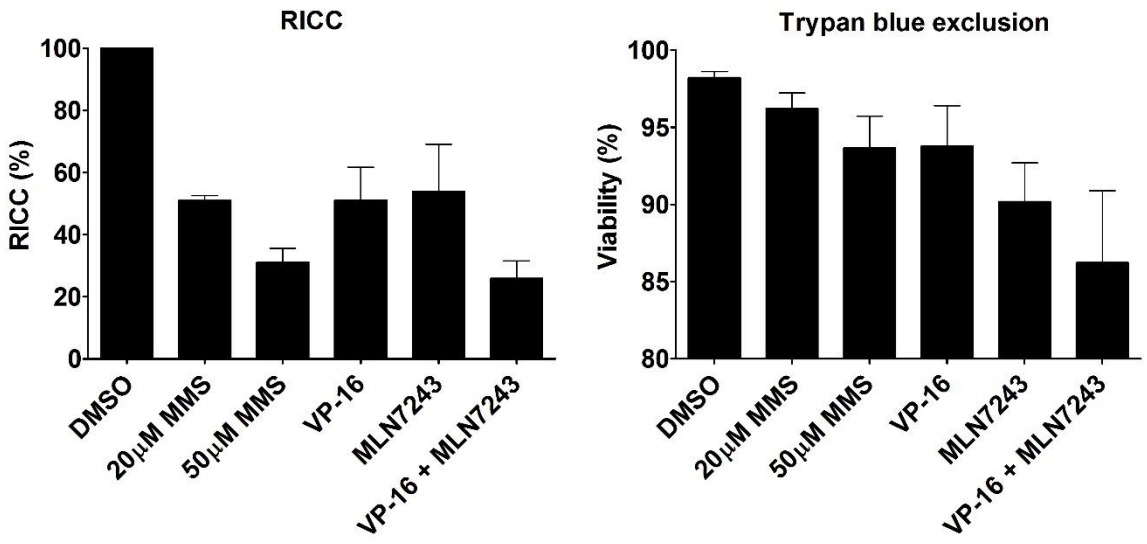

Figure 6.16. Cell viability of cells treated with etoposide alone or in combination with MLN7243. K562 cells were treated with 120 nM etoposide (VP-16) alone or in combination with 47 nM MLN7243 (or 20 µM and 50 µM MMS as a positive control) for 48 hours. Cell viability was measured by Relative Increase in Cell Count (RICC) and trypan blue exclusion. Error bars represent the mean ± SEM of 3 separate experiments. Statistical comparisons were made by unpaired t-test (n=3).

Cells were incubated with EMA prior to fixing on microscope slides. Micronuclei were detected by staining of cells with Hoechst DNA stain, and quantified by manual counting of at least 2000 cells per condition. The induction of micronuclei was expressed by percentage of cells containing micronuclei (% micronuclei, Equation 3), which was then used to determine the fold change in % micronuclei as shown in Equation 4.

Equation 3

$$\frac{Number\ cells\ with\ micronuclei}{Total\ number\ of\ cells\ counted} \times 100 = \%\ micronuclei$$

Equation 4

$$\frac{Drug\ treated\ (Average\ micronuclei\ \%)}{Untreated\ control\ (Average\ micronuclei\ \%)} = Fold\ change$$

As expected, the number of cells containing micronuclei were significantly increased in the presence of 50 µM MMS (p=0.0047), though were not significantly affected following exposure to 20 µM MMS (Figure 6.17). In addition, 3% of etoposide-treated cells contained micronuclei compared to 0.6% of untreated cells (p= 0.0138), while MLN7243 alone did not significantly induce micronuclei (p= 0.1208). According to the

OECD guidelines, a substance is classified as genotoxic when the % micronuclei is increased by a 2-fold change over untreated control. Etoposide induced an approximately 23-fold increase in micronuclei levels compared to untreated control (Figure 6.17). Micronuclei were induced by 10-fold when etoposide-treated cells were also co-incubated with MLN7243, although this was not significantly different to etoposide alone. Furthermore, MLN7243 did not significantly affect levels of etoposide-induced micronuclei when measured by percentage of cells containing micronuclei (% micronuclei, p=0.1850). Therefore contrary to the hypothesised effect, UAE inhibition does not significantly affect etoposide genotoxicity, as measured by micronucleus assay. However, it is important to note that these experiments did not meet strict OECD conditions due to the high cytotoxicity of etoposide in combination with MLN7243. Therefore, some micronuclei induced in these conditions may be due to secondary cytotoxic effects, thereby skewing the interpretation of results.

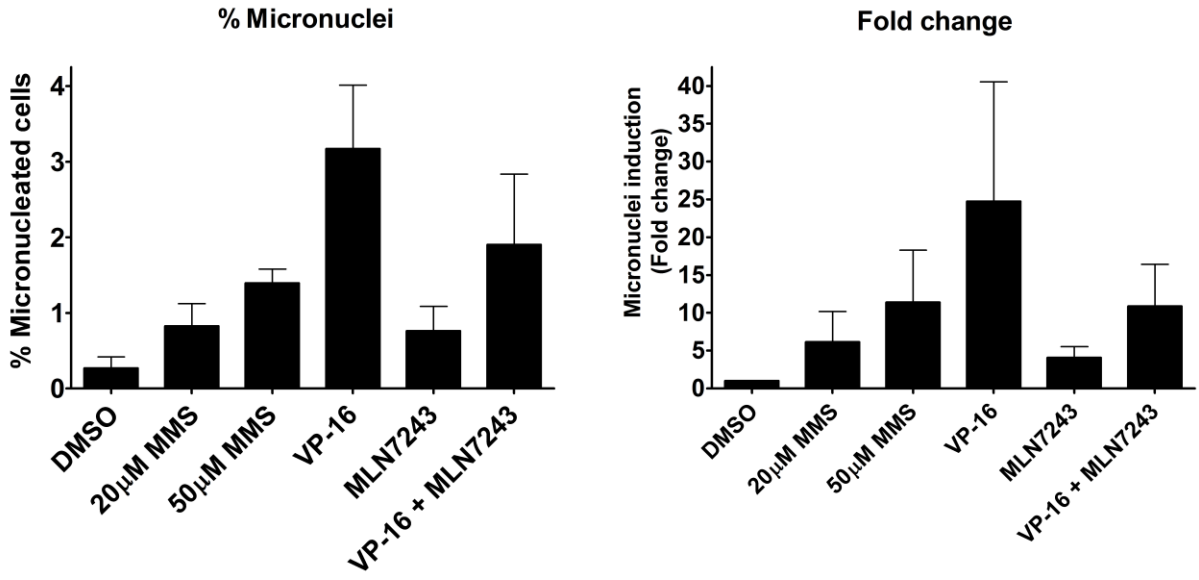

Figure 6.17. Effect of MLN7243 on etoposide-induced micronucleus formation. K562 cells were treated with 120 nM etoposide (VP-16) alone or in combination with 47 nM MLN7243 (or 20 μM and 50 μM MMS as a positive control) for 48 hours. After staining of cells with EMA to identify apoptotic cells, cells were fixed in paraformaldehyde and DNA was stained with Hoechst 33258. Micronuclei were counted manually and expressed as % micronucleated cells and fold change in micronuclei induction (compared to the 50 μM MMS control). Statistical comparisons were made by unpaired t-test (n=3).

6.3 Discussion

The ubiquitin-proteasome system is involved in the regulation of many cellular processes and is implicated in various diseases. This has stimulated a widespread clinical interest in the development of specific inhibitors targeting multiple steps in the ubiquitin-proteasome pathway, especially following the regulatory body approval of the proteasome inhibitor bortezomib (Velcade). In the current chapter, inhibition of UAE activity significantly increased the growth-inhibitory effects of four clinically used TOP2 poisons. Like proteasome inhibition, UAE inhibition leads to the upregulation of key proteins involved in cell cycle arrest and apoptosis, including the tumour suppressor p53. Indeed, the potentiation of TOP2 poisons with MLN7243 was greater in the wild type p53 Nalm-6 cell line than in p53-null K562 cells, suggesting that increased growth inhibition may be partly due to p53 upregulation. However, UAE inhibition also reduces the processing and repair of TOP2-DNA complexes (Chapter 3), and the potentiation of TOP2 poisons with MLN7243 was reduced in Nalm-6$^{TOP2B-/-}$ cells compared to wild type cells. This suggests that TOP2B is involved in the potentiation of TOP2 poisons by MLN7243 due to reduced repair of TOP2B-DNA complexes.

While proteasome inhibitors are surprisingly well tolerated in patients, the proteasome is involved in the regulation of many proteins, and a potentially superior approach may be the inhibition of specific ubiquitinating enzymes. There are over 600 E3 ubiquitin ligases in human cells, which mediate the proteasomal degradation of specific substrates. While the identification of relevant E3 ubiquitin ligases for a particular target is challenging, multiple E3 enzymes have been shown to regulate the proteasomal degradation of TOP2A, including the ECV ligase, Fbw7 and Hdm2 (Nayak *et al.*, 2007; Yun *et al.*, 2009; Chen *et al.*, 2011). Specifically, BMI1/RING1A is involved in the ubiquitination and proteasomal degradation of TOP2A-DNA complexes following teniposide treatment (Alchanati *et al.*, 2009), and inhibition of BMI1/RING1A slows the processing of TOP2-DNA complexes to DSBs (Chapter 3). In the current study, inhibition of BMI1/RING1A also increased the growth-inhibitory effects of three TOP2 poisons, including mitoxantrone, etoposide, and mAMSA. Similarly, HDM2 inhibition increased the growth-inhibitory effects of mAMSA in Nalm-6 wild type cells, and sensitised Nalm-6$^{TOP2A+/-}$ and Nalm-6$^{TOP2B-/-}$ cells to

mitoxantrone and etoposide. Therefore, the efficacy of TOP2 poisons can be increased through inhibition of specific E3 ubiquitin ligases.

However, PRT4165 may potentiate TOP2 poisons in ways other than through reduced processing of TOP2A covalent complexes. Importantly, PRT4165 also inhibits BMI1/RING1B (Ismail *et al.*, 2013), which functions as part of the polycomb repressive complex (PRC1) to mediate the ubiquitination of histones during the DNA damage response (Facchino *et al.*, 2010; Ismail *et al.*, 2010; Ginjala *et al.*, 2011; Pan *et al.*, 2011). Consequently, PRT4165 inhibits ubiquitin signalling at DSBs which is ultimately required for DNA repair (Ismail *et al.*, 2013). Therefore, the potentiation of TOP2 poisons with PRT4165 may be at least partly due to inhibition of repair of the TOP2-mediated DSB.

Similarly, HDM2 is involved in the ubiquitin-dependent degradation of essential tumour suppressor proteins such as p53 and the retinoblastoma (Rb) protein (Sdek *et al.*, 2005; Uchida *et al.*, 2005; Miwa *et al.*, 2006). Therefore, the upregulation of these proteins upon HDM2 inhibition may also account for increased cell cycle arrest and inhibition of growth in Nalm-6 cell lines. However, the reduced etoposide sensitivity of cells overexpressing Mdm2 is independent of p53 (Nayak *et al.*, 2007; Senturk *et al.*, 2017). Furthermore, the Mdm2 inhibitor PXN822 increases the sensitivity of murine PDAC cells to etoposide regardless of p53 status (Conradt *et al.*, 2013). Nayak et al. suggest that HDM2 mediates the export of TOP2A from the nucleus, as previously described for p53. Therefore, HDM2 inhibition may increase the efficacy of TOP2 poisons by increasing the levels of TOP2A in the nucleus.

Although effective anticancer agents, TOP2 poisons are also associated with the development of secondary leukaemias, which are thought to arise following the aberrant NHEJ repair of the enzyme-induced DSB. In addition to increasing drug cytotoxicity, inhibition of the ubiquitin-proteasome system may reduce TOP2 poison genotoxicity by preventing the processing of TOP2-DNA complexes to protein-free DSBs. The micronucleus assay is routinely used as a measure of overall genotoxicity, and was used here to investigate the effect of UAE inhibition on the genotoxicity of etoposide. Using this approach, micronuclei induction was successfully detected following treatment of cells with two known genotoxic compounds (MMS and etoposide). Levels of etoposide-induced micronuclei were not

significantly affected by the co-treatment of cells with MLN7243, suggesting that inhibition of ubiquitination does not dramatically affect TOP2 poison genotoxicity. However, the number of cells containing micronuclei varied significantly between individual experiments, as indicated by the large standard error. Therefore, this method may not be suitable for detecting small changes between different conditions. In addition, micronuclei were counted manually and are therefore subject to investigator bias and human error. Because of these technical limitations, the effect of UAE inhibition on the genotoxicity of TOP2 poisons warrants further investigation.

In summary, the growth inhibitory effects of TOP2 poisons can be increased upon co-treatment of cells with small molecule inhibitors of the ubiquitin-proteasome system. Given the clinical availability of proteasome inhibitors and the ongoing investigation of MLN7243 in phase I clinical trials, combination therapies with UPS inhibitors may present an easily translatable approach to the improvement of therapy with TOP2 poisons.

Chapter 7 Discussion

The processing of drug-stabilised TOP2-DNA complexes is a major step in the repair of TOP2 poison-mediated DNA damage. The removal of covalently bound TOP2 from DNA liberates the otherwise concealed DSB, which is then repaired predominantly by NHEJ. Multiple pathways have been shown to remove TOP2 complexes from DNA, but the appearance of etoposide-induced DSBs is largely proteasome-dependent (see Chapter 3, Figure 3.15A). Despite this, the regulation of the proteasomal processing pathway is poorly understood. In particular, conflicting studies have reported both ubiquitin-dependent and ubiquitin-independent pathways of TOP2B-DNA complex processing following inactivation of UAE1 (the primary ubiquitin activating enzyme) in temperature-sensitive ts85 cells (Mao *et al.*, 2001; Ban *et al.*, 2013), while the proteasome-dependent processing of TOP2A-DNA complexes was shown to involve the E3 ubiquitin ligase, BMI1/RING1A (Alchanati *et al.*, 2009). A major aim of this project was therefore to clarify the ubiquitin-dependence of TOP2A- and TOP2B- DNA complex processing following etoposide treatment. This was investigated primarily through targeting of both UAE in human cells, namely UAE1 and UBA6, by small molecule inhibition and siRNA knockdown. The effect of UAE inhibition on the processing of drug-stabilised TOP2-DNA complexes was assessed by the direct measurement of TOP2-DNA complexes using the TARDIS assay, and through the appearance of etoposide-induced DSBs via the ɣH2AX assay. This work showed that ubiquitination is partly required for the removal of both TOP2A- and TOP2B- DNA complexes, in a manner epistatic to the proteasomal processing pathway. Like proteasomal inhibition, inhibition of UAE (by both small molecule inhibition and siRNA knockdown) greatly reduced the appearance of etoposide-induced DSBs, thereby demonstrating a previously underappreciated role for ubiquitination in the repair of TOP2 poison-mediated DNA damage.

The ubiquitin-dependent processing of TOP2-DNA complexes was also evident when cells were treated with the BMI1/RING1A E3 ligase inhibitor, PRT4165. BMI1/RING1A is an E3 ubiquitin ligase associated with the polycomb repressive complex, which is also implicated in the degradation of TOP2A- (but not TOP2B-) DNA complexes (Alchanati *et al.*, 2009). However, inhibition of BMI1/RING1A slowed

the removal of both TOP2A- and TOP2B- DNA complexes following etoposide exposure, further supporting a ubiquitin-dependent processing pathway which is common to both TOP2 isoforms. While it is possible that other E3 ubiquitin ligases can also mediate the ubiquitin-dependent processing of TOP2-DNA complexes, PRT4165 completely abolished the etoposide-induced γH2AX response, suggesting that BMI1/RING1A is a major component of the ubiquitin-dependent processing pathway. Given that the BMI1/RING1A-dependent processing of TOP2B-DNA complexes was not reported by Alchanati et al. following siRNA-mediated knockdown of BMI1 in HeLa cells, it is important to consider that the effect of PRT4165 on TOP2B-DNA complex processing could be due to off-target inhibitor effects. This could be tested by repeating the above experiments following siRNA knockdown of BMI1/RING1A.

Role of transcription in TOP2-DNA complex processing

Multiple publications demonstrate a transcription-dependent mechanism of TOP2 complex processing which is implicated as part of the proteasome-dependent pathway. While initially described for TOP2B-DNA complexes (Mao *et al.*, 2001; Xiao *et al.*, 2003; Zhang *et al.*, 2006), transcription is also involved in the processing of TOP2A-DNA complexes (Fan *et al.*, 2008; Tammaro *et al.*, 2013). Surprisingly, studies using the TARDIS assay could detect transcription-dependent removal of TOP2A-DNA complexes, but not TOP2B-DNA complexes (Chapter 3, Figure 3.23). This corresponded to the reduced appearance of etoposide-induced DSBs in transcription-inhibited cells following 4 hours etoposide exposure (Figure 3.24). This supports a transcription-dependent mechanism of TOP2-DNA complex processing, although it is not possible to conclude whether this mechanism is part of the proteasome- (and ubiquitin-) dependent pathway, as suggested by others. This could be addressed by repeating the TARDIS assay with DRB alone or in combination with MG132 or MLN7243. Interestingly, inhibition of transcription reduced levels of etoposide-induced ubiquitinated TOP2-DNA complexes, suggesting that transcription could be involved in the regulation of the ubiquitin-dependent pathway. For example, collision of RNAPII with TOP2-DNA complexes could provide the DNA damage signal required for the ubiquitination of TOP2 complexes, and subsequent degradation of TOP2 by the proteasome.

TOP2A ubiquitination

Given the epistatic effect of proteasome and UAE inhibition on the removal of TOP2-DNA complexes, it was hypothesised that TOP2 is ubiquitinated in response to poisoning by etoposide, leading to its ubiquitin-dependent proteasomal degradation. In support of this, BMI1/RING1A has been shown to directly bind and ubiquitinate TOP2A *in vitro*, and in cells following teniposide exposure (Alchanati *et al.*, 2009). Furthermore, the ubiquitination of TOP2A has been demonstrated in response to other stimuli such as glucose starvation and HDAC inhibition, which leads to proteasomal degradation (Yun *et al.*, 2009; Chen *et al.*, 2011). Another aim of the current project was therefore to investigate the ubiquitination of TOP2A and TOP2B in the presence and absence of etoposide following pulldown of ubiquitinated proteins with TUBEs or by immunoprecipitation.

Mass spectrometry analysis has identified numerous ubiquitination sites within TOP2A and TOP2B in the absence of TOP2 poison (Kim *et al.*, 2011) and consistently, ubiquitinated TOP2 was detected in both untreated and etoposide-treated cells. Surprisingly, the polyubiquitination of TOP2A (previously reported by Alchanati et al. following teniposide exposure) was not observed in etoposide-treated cells. Instead, TOP2A was detected as a discrete band following western blot analysis both before and after etoposide treatment, likely corresponding to monoubiquitination. While the polyubiquitination of TOP2A reported by Alchanati et al. could be a teniposide-specific effect, K48- and K63-linked ubiquitin chains were detected on etoposide-induced TOP2-DNA complexes using the TARDIS assay, albeit at low levels. Therefore, it is possible that etoposide-induced polyubiquitination of TOP2A is below the level of detection, and may require the overexpression of ubiquitin or ubiquitinating proteins.

Alternatively, the ubiquitin-dependent proteasomal processing of TOP2-DNA complexes may not involve the canonical polyubiquitination of TOP2. Instead, TOP2 monoubiquitination could lead to the removal of complexes through the recruitment of other repair proteins to TOP2-DNA complexes. For example, TDP2 contains a ubiquitin binding domain which is required for the repair of TOP2-DNA complexes (Rao *et al.*, 2016). However, unlike UAE, inhibition of TDP2 does not affect the removal of TOP2 complexes or the appearance of etoposide-induced DSBs in the

presence of functional proteasomes (Gómez-Herreros *et al.*, 2013; Schellenberg *et al.*, 2017) (see also Chapter 3, Figure 3.30). Therefore the potential role of ubiquitin in the regulation of TDP2-mediated repair is distinct from the ubiquitin-dependent pathway described here. Interestingly, SUMOylation of TOP2 has been implicated in the removal of TOP2-DNA complexes by TDP2 upon proteasomal inhibition (Schellenberg *et al.*, 2017), although this pathway was not observed in the current study following TDP2 knockdown in K562 cells (Chapter 3, Figure 3.28). The requirement for SUMO in the processing of TOP2-DNA complexes was not investigated here, but could be tested using commercially available SUMO inhibitors such as the recently described SAE inhibitor, ML-792 (He *et al.*, 2017b).

It was not possible to conclude how levels of ubiquitinated TOP2A change following etoposide treatment, as this was affected by other variables including the efficiency of TOP2 extraction from DNA, and the gel running system used. Thus, further optimisation is required to more confidently conclude how levels of Ub-TOP2A change (if at all) after etoposide treatment. It is also possible that the perceived decrease in levels of Ub-TOP2A in etoposide-treated cells is due to the proteasomal degradation of ubiquitinated TOP2A. Indeed, proteasome-dependent degradation may be detectable in the pool of ubiquitinated TOP2A following ubiquitin pulldown or IP, but not following standard western blotting or immunofluorescence of total TOP2A protein (Chapter 3, Figure 3.10 and 3.12). While this could normally be circumvented by co-treatment of cells with a proteasome inhibitor, studies using the TARDIS assay showed that TOP2 is deubiquitinated in response to proteasome inhibition. This is itself a novel finding which is consistent with TOP2 as a highly abundant monoubiquitinated protein which is deubiquitinated upon proteotoxic stress, as previously described for histone H2A and other proteins (Dantuma *et al.*, 2006; Kim *et al.*, 2011; Udeshi *et al.*, 2012).

TOP2B ubiquitination

Less is known regarding the ubiquitination of TOP2B, although polyubiquitination of TOP2B has been demonstrated following treatment of granule cells with the TOP2 catalytic inhibitor, ICRF-193 (Isik *et al.*, 2003). In contrast, Ban et al. were unable to detect TOP2B following immunoprecipitation of ubiquitin in cells overexpressing a HA-tagged ubiquitin construct (Ban *et al.*, 2013). Consistently, ubiquitination of

TOP2B was not detected in the current study following immunoprecipitation of ubiquitinated proteins, although this could be accounted for by a number of technical issues. For example, the efficiency of ubiquitin pulldown was poor in these experiments, suggesting that a large proportion of ubiquitinated proteins were lost in the supernatant. Therefore, future experiments with TUBEs should involve optimisation of pulldown conditions. Furthermore, TOP2 levels were reduced in the whole cell lysate of etoposide-treated cells compared to untreated cells, suggesting that not all TOP2-DNA complexes were extracted for analysis by western blotting. Therefore, the extraction of TOP2 complexes should be optimised in future studies. While sonication did not appear to increase the extraction of TOP2 complexes from DNA (Appendix Table 3), other nucleases are available with superior efficiency to DNase I, such as benzonase (Turbonuclease), which should be used in future experiments. The inability to detect Ub-TOP2B could also be due to low endogenous protein levels if only a small proportion of TOP2B is ubiquitinated. Therefore, these assays could be performed in cells overexpressing a tagged TOP2B construct, which would enable both enrichment of TOP2B protein and efficient isolation by affinity purification.

Due to the complications and discrepancies described above, TOP2 ubiquitination should be investigated using another approach. For example, multiple ubiquitination sites have been identified within TOP2B by mass spectrometry (Kim *et al.*, 2011), which could be used to investigate TOP2B ubiquitination in the presence and absence of etoposide. This could be used to detect changes or the enrichment of ubiquitination at specific lysine residues following etoposide treatment, which cannot be achieved by western blotting techniques. Indeed, trapping of TOP2 on DNA may expose otherwise inaccessible ubiquitination sites, as previously shown for the PIASγ-dependent SUMOylation of TOP2A at Lys662 (Ryu *et al.*, 2010; Wendorff *et al.*, 2012).

Processing of TOP2-DNA complexes by VCP/p97

A major finding of the current study was the identification of VCP/p97 as another ubiquitin-dependent protein involved in the processing of TOP2-DNA complexes. Like inhibition of the proteasome or UAE, inhibition of VCP/p97 significantly reduced the processing of TOP2A- and TOP2B- DNA complexes and reduced the

appearance of etoposide-induced DSBs. The role of VCP/p97 was epistatic with that of the proteasomal pathway, consistent with the increasingly established role of VCP/p97 in the ubiquitin-proteasome system. It is therefore proposed that VCP/p97 facilitates the proteasomal degradation of TOP2-DNA complexes by unfolding and extracting covalently bound TOP2 from chromatin, as previously described for other chromatin-associated protein complexes like Ku80 and RNAPII. As a ubiquitin-dependent AAA ATPase, this finding further supports a ubiquitin- and proteasome-dependent pathway of TOP2-DNA complex processing.

Important evidence of this model is derived from immunoprecipitation experiments, which showed an interaction between VCP/p97 and TOP2. Interestingly, VCP/p97 interacts with TOP2 even in the absence of etoposide, which could indicate an endogenous role for VCP/p97 in the regulation of TOP2 complexes. For example, VCP/p97 could help resolve trapped TOP2-DNA complexes which arise during normal DNA metabolism. Surprisingly, this interaction was reduced in the presence of etoposide, which could be due to proteasomal degradation of TOP2 or insufficient extraction of TOP2-DNA complexes from chromatin. Extraction was improved upon preparation of lysates with benzonase, but no interaction between TOP2A and VCP/p97 was observed in the same experiment. Indeed, the interaction detected between VCP/p97 and both TOP2A and TOP2B was highly variable, and requires further confirmation with other experimental approaches. This is not necessarily surprising, as interactions between VCP/p97 and its substrates are reported to be transient and difficult to detect by IP. Instead, other studies have utilised a ‘substrate-trapping’ mutant of VCP/p97 containing a mutation in the D2 ATPase domain which increases the stability of the VCP/p97-substrate interaction (van den Boom *et al.*, 2016). Therefore, further work could involve the transfection of cells with the EQ-p97 mutant followed by IP. Future work could also include the investigation of protein interactions using mass spectrometry-coupled techniques. For example, Rapid Immunoprecipitation Mass spectrometry of Endogenous proteins (RIME) involves the isolation of chromatin-associated proteins by chromatin immunoprecipitation (ChIP), followed by the identification of interacting proteins by LC-MS/MS (Mohammed *et al.*, 2016). This would be a highly informative approach which could be used to test the interaction of etoposide-induced TOP2-DNA complexes with VCP/p97, as well as other proteins potentially involved in repair such as E3 ubiquitin ligases.

VCP/p97 binds poly- and mono- ubiquitinated proteins both directly via the N terminal domain, and indirectly through ubiquitin adaptor proteins like p47 and Ufd1-Npl4 (Park *et al.*, 2005; Pye *et al.*, 2007). Therefore, monoubiquitination of TOP2 may lead to the recruitment of VCP/p97 to TOP2-DNA complexes. However, in one study VCP/p97 was required only for the degradation of polyubiquitinated dihydrofolate reductase (DHFR) protein and not monoubiquitinated DHFR (Song *et al.*, 2015). The role of ubiquitin in the VCP/p97-dependent processing of TOP2-DNA complexes was further investigated in the current study following siRNA knockdown of Ufd1 and Npl4. Ufd1-Npl4 is involved in the degradation of other chromatin-associated protein complexes such as Ku70/80 and RNAPII (Verma *et al.*, 2011; van den Boom *et al.*, 2016; He *et al.*, 2017a). However, unlike siRNA knockdown of VCP/p97, depletion of Ufd1-Npl4 did not affect the appearance of etoposide-induced DSBs, suggesting that Ufd1-Npl4 is not required for the VCP/p97-dependent removal of TOP2-DNA complexes. Instead, VCP/p97 may be recruited directly to ubiquitinated TOP2 complexes via the VCP/p97 N terminal domain, or indirectly via other ubiquitin adaptor proteins such as FAF1. The role of other ubiquitin adaptor proteins in the processing of TOP2-DNA complexes should be investigated in future studies.

It is uncertain whether VCP/p97 can completely remove covalently bound TOP2 from DNA. Instead, VCP/p97 may facilitate TOP2 proteolysis by unfolding TOP2 as it remains covalently attached to the DNA. This would result in an unstructured protein adduct which could then be degraded by proteasomes on chromatin. Inhibition of ubiquitinating enzymes, proteasomes and VCP/p97 all prevent the processing of TOP2-DNA complexes to DSBs, as indicated by both small molecule inhibition and siRNA knockdown. While this implicates a role for ubiquitin and VCP/p97 in the proteasomal pathway of TOP2-DNA complex processing, it is important to note that perturbation of the ubiquitin-proteasome system with all of these inhibitors is reported to deplete nuclear ubiquitin (Xu *et al.*, 2004; Dantuma *et al.*, 2006; Heidelberger *et al.*, 2018). It is therefore plausible that inhibition of VCP/p97 or the proteasome simply inhibits a ubiquitin-dependent pathway of TOP2-DNA complex processing which is independent of the proteasomal pathway.

Effect of ubiquitin-proteasome system inhibitors on the response to TOP2 poisons

TOP2 poison therapy can be improved through a better understanding of how TOP2 poison-induced DNA damage is repaired. This knowledge can be exploited to increase the anticancer effects of TOP2 poisons. For example, DNA-PK is required for the repair of TOP2 poison-induced DSBs, and inhibition of DNA-PK increases the cytotoxicity of TOP2 poisons (Willmore *et al.*, 2004). Of particular interest is the development of small molecule inhibitors of the ubiquitin-proteasome system following the regulatory approval of the proteasome inhibitors bortezomib and carfilzomib. In the current study, inhibition of UAE and specific E3 ubiquitin ligases significantly increased the growth-inhibitory effects of various clinically relevant TOP2 poisons. While these effects may be attributed to multiple consequences of ubiquitin inhibition, this nonetheless demonstrates that the cytotoxicity of TOP2 poisons can be increased by targeting the ubiquitin-proteasome system. It is important to consider that ubiquitination regulates many cellular processes, through both proteasome-dependent and non-proteolytic mechanisms. Therefore, while the UAE inhibitor MLN7243 is in phase I clinical trials, UAE inhibition may be less favourable than proteasome inhibitors due to a greater potential for unwanted toxic effects. Furthermore, the development of specific E3 ubiquitin ligase inhibitors is challenging as many E3s (such as the RING or U-box E3s ligase family) lack intrinsic catalytic activity (Landre *et al.*, 2014). While the effect of VCP/p97 inhibition on the growth inhibitory effects of TOP2 poisons was not investigated in this study, VCP/p97 was identified as another druggable component of the ubiquitin-proteasome system which is involved in the repair of TOP2 poison-induced DNA damage. Notably, the VCP/p97 inhibitor CB-5083 is also in phase I clinical trials.

Micronucleus assays show that the cytotoxicity of TOP2 poisons is increased by UAE inhibition without increasing overall TOP2 poison genotoxicity, which is associated with the development of t-AML. It is hypothesised that the likelihood of leukaemogenic chromosomal translocations is reduced upon inhibition of the ubiquitin- and proteasome- dependent processing pathway by preventing the liberation of protein-free DSBs. This could be investigated further by measuring the frequency of specific etoposide-induced chromosome translocations in cells treated

with and without UAE or proteasome inhibitors, for example by DNA-FISH (Fluorescence In-Situ Hybridisation).

Proposed model

This work (summarised in Table 6) indicates a new model of TOP2-DNA complex processing by the proteasome, and is illustrated in Figure 7.1. This is a ubiquitin- and VCP/p97- dependent mechanism common to both TOP2 isoforms, whereby BMI1/RING1A-dependent monoubiquitination of TOP2 (or ubiquitination of another protein involved in repair) may lead to the recruitment of VCP/p97 to stalled TOP2-DNA complexes. VCP/p97 then facilitates the proteasomal degradation of TOP2 adducts by unfolding the covalently bound TOP2 protein, which can then be translocated into the narrow core of proteasomes present on chromatin. This liberates protein-free DSBs (attached to short phosphotyrosyl peptides), which are further processed to ligatable ends for NHEJ repair by TDP2.

In conclusion, this work clarifies a requirement for ubiquitination in the proteasomal processing of drug-stabilised TOP2A- and TOP2B- DNA complexes. A previously unreported and additional layer of complexity is the involvement of VCP/p97 in the processing of complexes to DSBs. VCP/p97 is known to facilitate the proteasomal degradation of proteins through protein unfolding and extraction from cellular components such as chromatin. It is therefore proposed that VCP/p97 is recruited to ubiquitinated TOP2-DNA complexes, leading to the unfolding of TOP2 and TOP2 proteolysis.

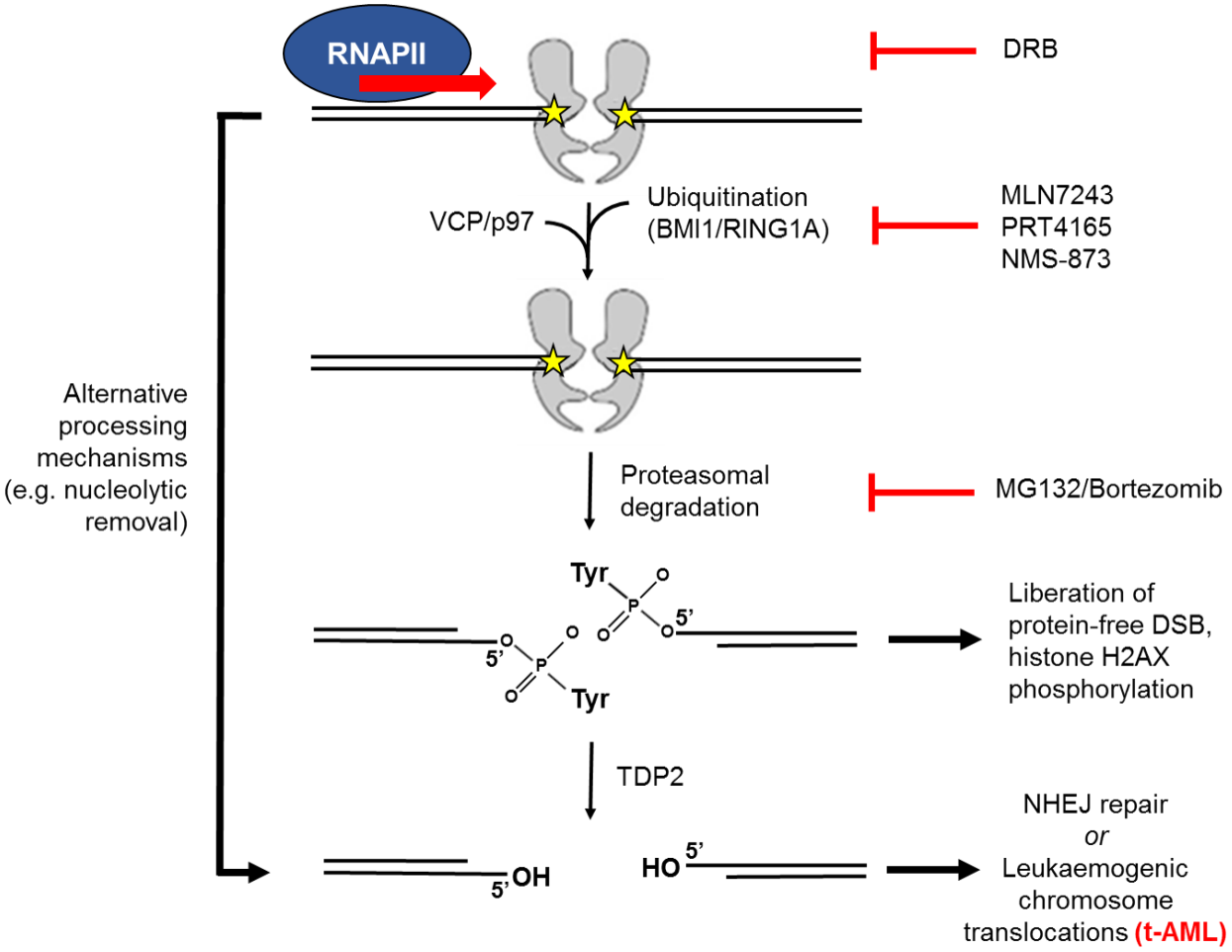

Figure 7.1. Proposed model of TOP2-DNA complex processing by VCP/p97 and the proteasome. Collision of elongating polymerases with stabilised TOP2-DNA complexes leads to the ubiquitination of TOP2 (or another protein involved in repair) by BMI1/RING1A. This leads to the recruitment of VCP/p97 to the damage site and the subsequent unfolding of TOP2 adducts on DNA. Proteasomes present on chromatin (including for example, those recruited to stalled RNA polymerases) degrade the bulk of the unfolded TOP2 protein, and liberate protein-free DSBs covalently attached to short phosphotyrosyl peptides. Final end-polishing by TDP2 produces ligatable ends for NHEJ repair. Alternatively, aberrant repair leads to the generation of leukaemogenic chromosome translocations which are associated with the development of therapy-related acute myeloid leukaemia (t-AML).

Table 6. Overview of results.

	TOP2 TARDIS	ɣH2AX assay	Ubiquitin TARDIS	XTT assay
VP-16 + Proteasome inhibitor (MG132)	Levels of remaining TOP2A- and TOP2B-DNA complexes are significantly higher after VP-16 removal. Consistent with the role of the proteasome in the degradation of TOP2-DNA covalent complexes.	Levels of VP-16-induced DSBs are significantly reduced (in K562 cells and Nalm-6 cells). Consistent with published literature and the notion that the degradation of TOP2 adducts is required for the liberation of protein-free DSBs.	Levels of ubiquitinated TOP2-DNA complexes is reduced. Combination experiments with PR-619 indicate that TOP2 complexes are actively deubiquitinated upon proteasome inhibition.	XTT data published by Lee et al. (2016) shows that proteasome inhibition significantly reduces the IC_{50} of clinically relevant TOP2 poisons (in K562 cells and Nalm-6 cells).

VP-16 + UAE inhibitor (MLN7243)	Levels of remaining TOP2A- and TOP2B-DNA complexes are significantly higher after VP-16 removal, in a manner that is epistatic with the proteasome. Indicates that the proteasomal processing of TOP2A- and TOP2B-DNA complexes is ubiquitin-dependent.	Levels of VP-16-induced DSBs are significantly reduced (in K562 cells and Nalm-6 cells). Therefore the appearance of VP-16-induced DSBs is partly ubiquitin-dependent.	Levels of ubiquitinated TOP2-DNA complexes are completely reduced to background levels. Therefore MLN7243 is a potent UAE inhibitor.	The IC_{50} of all TOP2 poisons tested were reduced in Nalm-6 cells. Potentiation was reduced in TOP2B knockout cells, indicating that potentiation by MLN7243 is partly TOP2-dependent. However, potentiation was absent or noticeably reduced in K562 cells lacking functional p53. UAE inhibition is a viable strategy for the potentiation of clinically relevant TOP2 poisons,

				but likely mediated by both TOP2-dependent and -independent mechanisms.
VP-16 + BMI1/RING1A inhibitor (PRT4165)	Levels of remaining TOP2A- and TOP2B-DNA complexes are significantly higher after VP-16 removal. Indicates that the E3 ubiquitin ligase BMI1/RING1A is involved in the processing of TOP2A- and TOP2B-DNA complexes.	Levels of VP-16-induced DSBs are significantly reduced to background levels. Indicates that BMI1/RING1A is the major E3 ligase involved in the ubiquitin-dependent processing of TOP2-DNA complexes.	Levels of ubiquitinated TOP2-DNA complexes are reduced, but not completely abolished. BMI1/RING1A is involved in the ubiquitination of TOP2. However, other E3 ligases can also ubiquitinate TOP2 (for example, Fbw7, ECV, APC/Cdh1), which may occur before or after	The IC_{50} of all TOP2 poisons (with the exception of doxorubicin) was reduced in all Nalm-6 cell lines, regardless of TOP2 levels. However, potentiation of mAMSA by PRT4165 is TOP2A-dependent. The potentiation of TOP2 poisons by PRT4165 is likely

			TOP2 is trapped on DNA.	mediated by TOP2-dependent and -independent mechanisms (e.g. inhibition of histone H2A Lys119 ubiquitination or off-target effects).
VP-16 + Transcription inhibitor (DRB)	Levels of remaining TOP2A- (but not TOP2B) DNA complexes are significantly higher after VP-16 removal. Indicates that the processing of TOP2A-DNA complexes is partly transcription-dependent, consistent with other studies.	Levels of VP-16-induced DSBs are significantly reduced following 4 hours drug exposure. Indicates a transcription-dependent mechanism of TOP2-DNA complex	Levels of ubiquitinated TOP2-DNA complexes are significantly reduced. Suggests that transcription could be involved in the ubiquitination of TOP2 (e.g. ubiquitination of TOP2 complexes after	Not investigated in the current study.

		processing to protein-free DSBs.	collision with the transcription machinery).	
VP-16 + VCP/p97 inhibitor (NMS-873)	Levels of remaining TOP2A- and TOP2B-DNA complexes are significantly increased. Suggests VCP/p97 is involved in the processing of TOP2-DNA complexes, epistatic with the proteasomal pathway.	Levels of VP-16-induced DSBs are significantly reduced in K562 cells. Consistent with the notion that VCP/p97 is required for the removal of TOP2 complexes from DNA and the subsequent appearance of protein-free DSBs.	Levels of ubiquitinated TOP2-DNA complexes are slightly but significantly increased. This could suggest that VCP/p97 targets ubiquitinated TOP2, or may simply be a consequence of increased TOP2 complex formation (independent of ubiquitination status).	Not investigated in the current study (future work).

Chapter 8 References

Acs, K., Luijsterburg, M.S., Ackermann, L., Salomons, F.A., Hoppe, T. and Dantuma, N.P. (2011) 'The AAA-ATPase VCP/p97 promotes 53BP1 recruitment by removing L3MBTL1 from DNA double-strand breaks', *Nat Struct Mol Biol*, 18(12), pp. 1345-50.

Adachi, N., So, S., Iiizumi, S., Nomura, Y., Murai, K., Yamakawa, C., Miyagawa, K. and Koyama, H. (2006) 'The human pre-B cell line Nalm-6 is highly proficient in gene targeting by homologous recombination', *DNA Cell Biol*, 25(1), pp. 19-24.

Adachi, N., Suzuki, H., Iiizumi, S. and Koyama, H. (2003) 'Hypersensitivity of nonhomologous DNA end-joining mutants to VP-16 and ICRF-193: implications for the repair of topoisomerase II-mediated DNA damage', *J Biol Chem*, 278(38), pp. 35897-902.

Adams, J. (2003) 'The proteasome: structure, function, and role in the cell', *Cancer Treat Rev*, 29 Suppl 1, pp. 3-9.

Agostinho, M., Santos, V., Ferreira, F., Costa, R., Cardoso, J., Pinheiro, I., Rino, J., Jaffray, E., Hay, R.T. and Ferreira, J. (2008) 'Conjugation of human topoisomerase 2 alpha with small ubiquitin-like modifiers 2/3 in response to topoisomerase inhibitors: cell cycle stage and chromosome domain specificity', *Cancer Res*, 68(7), pp. 2409-18.

Alchanati, I., Teicher, C., Cohen, G., Shemesh, V., Barr, H.M., Nakache, P., Ben-Avraham, D., Idelevich, A., Angel, I., Livnah, N., Tuvia, S., Reiss, Y., Taglicht, D. and Erez, O. (2009) 'The E3 ubiquitin-ligase Bmi1/Ring1A controls the proteasomal degradation of Top2alpha cleavage complex - a potentially new drug target', *PLoS One*, 4(12), p. e8104.

Allan, J.M. and Travis, L.B. (2005) 'Mechanisms of therapy-related carcinogenesis', *Nat Rev Cancer*, 5(12), pp. 943-55.

Anand, R., Ranjha, L., Cannavo, E. and Cejka, P. (2016) 'Phosphorylated CtIP Functions as a Co-factor of the MRE11-RAD50-NBS1 Endonuclease in DNA End Resection', *Mol Cell*, 64(5), pp. 940-950.

Anindya, R., Aygun, O. and Svejstrup, J.Q. (2007) 'Damage-induced ubiquitylation of human RNA polymerase II by the ubiquitin ligase Nedd4, but not Cockayne syndrome proteins or BRCA1', *Mol Cell*, 28(3), pp. 386-97.

Aparicio, T., Baer, R., Gottesman, M. and Gautier, J. (2016) 'MRN, CtIP, and BRCA1 mediate repair of topoisomerase II-DNA adducts', *J Cell Biol*, 212(4), pp. 399-408.

Austin, C.A. and Marsh, K.L. (1998) 'Eukaryotic DNA topoisomerase II beta', *Bioessays*, 20(3), pp. 215-26.

Austin, C.A., Marsh, K.L., Wasserman, R.A., Willmore, E., Sayer, P.J., Wang, J.C. and Fisher, L.M. (1995) 'Expression, domain structure, and enzymatic properties of an active recombinant human DNA topoisomerase II beta', *J Biol Chem*, 270(26), pp. 15739-46.

Austin, C.A., Sng, J.H., Patel, S. and Fisher, L.M. (1993) 'Novel HeLa topoisomerase II is the II beta isoform: complete coding sequence and homology with other type II topoisomerases', *Biochim Biophys Acta*, 1172(3), pp. 283-91.

Avemann, K., Knippers, R., Koller, T. and Sogo, J.M. (1988) 'Camptothecin, a specific inhibitor of type I DNA topoisomerase, induces DNA breakage at replication forks', *Mol Cell Biol*, 8(8), pp. 3026-34.

Ayene, I.S., Ford, L.P. and Koch, C.J. (2005) 'Ku protein targeting by Ku70 small interfering RNA enhances human cancer cell response to topoisomerase II inhibitor and gamma radiation', *Mol Cancer Ther*, 4(4), pp. 529-36.

Azarova, A.M., Lin, R.K., Tsai, Y.C., Liu, L.F., Lin, C.P. and Lyu, Y.L. (2010) 'Genistein induces topoisomerase IIbeta- and proteasome-mediated DNA sequence rearrangements: Implications in infant leukemia', *Biochem Biophys Res Commun*, 399(1), pp. 66-71.

Azarova, A.M., Lyu, Y.L., Lin, C.P., Tsai, Y.C., Lau, J.Y., Wang, J.C. and Liu, L.F. (2007) 'Roles of DNA topoisomerase II isozymes in chemotherapy and secondary malignancies', *Proc Natl Acad Sci U S A*, 104(26), pp. 11014-9.

Azuma, Y., Arnaoutov, A. and Dasso, M. (2003) 'SUMO-2/3 regulates topoisomerase II in mitosis', *J Cell Biol*, 163(3), pp. 477-87.

Bachant, J., Alcasabas, A., Blat, Y., Kleckner, N. and Elledge, S.J. (2002) 'The SUMO-1 isopeptidase Smt4 is linked to centromeric cohesion through SUMO-1 modification of DNA topoisomerase II', *Mol Cell*, 9(6), pp. 1169-82.

Balakirev, M.Y., Mullally, J.E., Favier, A., Assard, N., Sulpice, E., Lindsey, D.F., Rulina, A.V., Gidrol, X. and Wilkinson, K.D. (2015) 'Wss1 metalloprotease partners with Cdc48/Doa1 in processing genotoxic SUMO conjugates', *Elife*, 4.

Ban, Y., Ho, C.W., Lin, R.K., Lyu, Y.L. and Liu, L.F. (2013) 'Activation of a novel ubiquitin-independent proteasome pathway when RNA polymerase II encounters a protein roadblock', *Mol Cell Biol*, 33(20), pp. 4008-16.

Barthelme, D. and Sauer, R.T. (2013) 'Bipartite determinants mediate an evolutionarily conserved interaction between Cdc48 and the 20S peptidase', *Proc Natl Acad Sci U S A*, 110(9), pp. 3327-32.

Bates, A.D., Berger, J.M. and Maxwell, A. (2011) 'The ancestral role of ATP hydrolysis in type II topoisomerases: prevention of DNA double-strand breaks', *Nucleic Acids Res*, 39(15), pp. 6327-39.

Bedford, L., Layfield, R., Mayer, R.J., Peng, J. and Xu, P. (2011) 'Diverse polyubiquitin chains accumulate following 26S proteasomal dysfunction in mammalian neurones', *Neurosci Lett*, 491(1), pp. 44-7.

Bekker-Jensen, S. and Mailand, N. (2010) 'Assembly and function of DNA double-strand break repair foci in mammalian cells', *DNA Repair (Amst)*, 9(12), pp. 1219-28.

Bekker-Jensen, S. and Mailand, N. (2011) 'The ubiquitin- and SUMO-dependent signaling response to DNA double-strand breaks', *FEBS Lett*, 585(18), pp. 2914-9.

Benedik, M.J. and Strych, U. (1998) 'Serratia marcescens and its extracellular nuclease', *FEMS Microbiol Lett*, 165(1), pp. 1-13.

Bensaude, O. (2011) 'Inhibiting eukaryotic transcription: Which compound to choose? How to evaluate its activity?', *Transcription*, 2(3), pp. 103-108.

Bergink, S., Ammon, T., Kern, M., Schermelleh, L., Leonhardt, H. and Jentsch, S. (2013) 'Role of Cdc48/p97 as a SUMO-targeted segregase curbing Rad51-Rad52 interaction', *Nat Cell Biol*, 15(5), pp. 526-32.

Besche, H.C., Haas, W., Gygi, S.P. and Goldberg, A.L. (2009) 'Isolation of mammalian 26S proteasomes and p97/VCP complexes using the ubiquitin-like domain from HHR23B reveals novel proteasome-associated proteins', *Biochemistry*, 48(11), pp. 2538-49.

Beskow, A., Grimberg, K.B., Bott, L.C., Salomons, F.A., Dantuma, N.P. and Young, P. (2009) 'A Conserved Unfoldase Activity for the p97 AAA-ATPase in Proteasomal Degradation', *Journal of Molecular Biology*, 394(4), pp. 732-746.

Binaschi, M., Zagotto, G., Palumbo, M., Zunino, F., Farinosi, R. and Capranico, G. (1997) 'Irreversible and reversible topoisomerase II DNA cleavage stimulated by clerocidin: sequence specificity and structural drug determinants', *Cancer Res*, 57(9), pp. 1710-6.

Boh, B.K., Smith, P.G. and Hagen, T. (2011) 'Neddylation-induced conformational control regulates cullin RING ligase activity in vivo', *J Mol Biol*, 409(2), pp. 136-45.

Bower, J.J., Karaca, G.F., Zhou, Y., Simpson, D.A., Cordeiro-Stone, M. and Kaufmann, W.K. (2010) 'Topoisomerase IIalpha maintains genomic stability through decatenation G(2) checkpoint signaling', *Oncogene*, 29(34), pp. 4787-99.

Bromberg, K.D., Burgin, A.B. and Osheroff, N. (2003) 'A two-drug model for etoposide action against human topoisomerase IIalpha', *J Biol Chem*, 278(9), pp. 7406-12.

Brown, J.S., Lukashchuk, N., Sczaniecka-Clift, M., Britton, S., le Sage, C., Calsou, P., Beli, P., Galanty, Y. and Jackson, S.P. (2015) 'Neddylation promotes ubiquitylation and release of Ku from DNA-damage sites', *Cell Rep*, 11(5), pp. 704-14.

Budenholzer, L., Cheng, C.L., Li, Y. and Hochstrasser, M. (2017) 'Proteasome Structure and Assembly', *J Mol Biol*, 429(22), pp. 3500-3524.

Burma, S., Chen, B.P., Murphy, M., Kurimasa, A. and Chen, D.J. (2001) 'ATM phosphorylates histone H2AX in response to DNA double-strand breaks', *J Biol Chem*, 276(45), pp. 42462-7.

Canela, A., Maman, Y., Jung, S., Wong, N., Callen, E., Day, A., Kieffer-Kwon, K.R., Pekowska, A., Zhang, H., Rao, S.S.P., Huang, S.C., McKinnon, P.J., Aplan, P.D., Pommier, Y., Aiden, E.L., Casellas, R. and Nussenzweig, A. (2017) 'Genome Organization Drives Chromosome Fragility', *Cell*, 170(3), pp. 507-521.e18.

Cannavo, E. and Cejka, P. (2014) 'Sae2 promotes dsDNA endonuclease activity within Mre11-Rad50-Xrs2 to resect DNA breaks', *Nature*, 514(7520), pp. 122-5.

Cardenas, M.E., Dang, Q., Glover, C.V. and Gasser, S.M. (1992) 'Casein kinase II phosphorylates the eukaryote-specific C-terminal domain of topoisomerase II in vivo', *Embo j*, 11(5), pp. 1785-96.

Ceruti, S., Mazzola, A. and Abbracchio, M.P. (2006) 'Proteasome inhibitors potentiate etoposide-induced cell death in human astrocytoma cells bearing a mutated p53 isoform', *J Pharmacol Exp Ther*, 319(3), pp. 1424-34.

Chen, J., Odenike, O. and Rowley, J.D. (2010) 'Leukaemogenesis: more than mutant genes', *Nat Rev Cancer*, 10(1), pp. 23-36.

Chen, M.C., Chen, C.H., Chuang, H.C., Kulp, S.K., Teng, C.M. and Chen, C.S. (2011) 'Novel mechanism by which histone deacetylase inhibitors facilitate

topoisomerase IIalpha degradation in hepatocellular carcinoma cells', *Hepatology*, 53(1), pp. 148-59.

Chiang, S.Y., Azizkhan, J.C. and Beerman, T.A. (1998) 'A comparison of DNA-binding drugs as inhibitors of E2F1- and Sp1-DNA complexes and associated gene expression', *Biochemistry*, 37(9), pp. 3109-15.

Chikamori, K., Grabowski, D.R., Kinter, M., Willard, B.B., Yadav, S., Aebersold, R.H., Bukowski, R.M., Hickson, I.D., Andersen, A.H., Ganapathi, R. and Ganapathi, M.K. (2003) 'Phosphorylation of serine 1106 in the catalytic domain of topoisomerase II alpha regulates enzymatic activity and drug sensitivity', *J Biol Chem*, 278(15), pp. 12696-702.

Clarke, D.J. and Azuma, Y. (2017) 'Non-Catalytic Roles of the Topoisomerase IIalpha C-Terminal Domain', 18(11).

Clarke, D.J., Johnson, R.T. and Downes, C.S. (1993) 'Topoisomerase II inhibition prevents anaphase chromatid segregation in mammalian cells independently of the generation of DNA strand breaks', *J Cell Sci*, 105 (Pt 2), pp. 563-9.

Congdon, L.M., Pourpak, A., Escalante, A.M., Dorr, R.T. and Landowski, T.H. (2008a) 'Proteasomal inhibition stabilizes topoisomerase IIα protein and reverses resistance to the topoisomerase II poison ethonafide (AMP-53, 6-ethoxyazonafide)', *Biochemical Pharmacology*, 75(4), pp. 883-890.

Congdon, L.M., Pourpak, A., Escalante, A.M., Dorr, R.T. and Landowski, T.H. (2008b) 'Proteasomal inhibition stabilizes topoisomerase IIalpha protein and reverses resistance to the topoisomerase II poison ethonafide (AMP-53, 6-ethoxyazonafide)', *Biochem Pharmacol*, 75(4), pp. 883-90.

Connelly, J.C., de Leau, E.S. and Leach, D.R. (2003) 'Nucleolytic processing of a protein-bound DNA end by the E. coli SbcCD (MR) complex', *DNA Repair (Amst)*, 2(7), pp. 795-807.

Conradt, L., Henrich, A., Wirth, M., Reichert, M., Lesina, M., Algül, H., Schmid, R.M., Krämer, O.H., Saur, D. and Schneider, G. (2013) 'Mdm2 inhibitors synergize with topoisomerase II inhibitors to induce p53-independent pancreatic cancer cell death', *International Journal of Cancer*, 132(10), pp. 2248-2257.

Cortes Ledesma, F., El Khamisy, S.F., Zuma, M.C., Osborn, K. and Caldecott, K.W. (2009) 'A human 5'-tyrosyl DNA phosphodiesterase that repairs topoisomerase-mediated DNA damage', *Nature*, 461(7264), pp. 674-8.

Cowell, I.G. and Austin, C.A. (2012) 'Mechanism of generation of therapy related leukemia in response to anti-topoisomerase II agents', *International journal of environmental research and public health*, 9(6), pp. 2075-2091.

Cowell, I.G. and Austin, C.A. (2018) 'Visualization and Quantification of Topoisomerase-DNA Covalent Complexes Using the Trapped in Agarose Immunostaining (TARDIS) Assay', *Methods Mol Biol*, 1703, pp. 301-316.

Cowell, I.G., Sondka, Z., Smith, K., Lee, K.C., Manville, C.M., Sidorczuk-Lesthuruge, M., Rance, H.A., Padget, K., Jackson, G.H., Adachi, N. and Austin, C.A. (2012) 'Model for MLL translocations in therapy-related leukemia involving topoisomerase IIβ-mediated DNA strand breaks and gene proximity', *Proceedings of the National Academy of Sciences of the United States of America*, 109(23), pp. 8989-8994.

Cowell, I.G., Tilby, M.J. and Austin, C.A. (2011) 'An overview of the visualisation and quantitation of low and high MW DNA adducts using the trapped in agarose DNA immunostaining (TARDIS) assay', *Mutagenesis*, 26(2), pp. 253-60.

Cowell, I.G., Willmore, E., Chalton, D., Marsh, K.L., Jazrawi, E., Fisher, L.M. and Austin, C.A. (1998) 'Nuclear distribution of human DNA topoisomerase IIbeta: a nuclear targeting signal resides in the 116-residue C-terminal tail', *Exp Cell Res*, 243(2), pp. 232-40.

D'Arpa, P., Beardmore, C. and Liu, L.F. (1990) 'Involvement of nucleic acid synthesis in cell killing mechanisms of topoisomerase poisons', *Cancer Res*, 50(21), pp. 6919-24.

da Fonseca, P.C., He, J. and Morris, E.P. (2012) 'Molecular model of the human 26S proteasome', *Mol Cell*, 46(1), pp. 54-66.

Dai, R.M. and Li, C.C. (2001) 'Valosin-containing protein is a multi-ubiquitin chain-targeting factor required in ubiquitin-proteasome degradation', *Nat Cell Biol*, 3(8), pp. 740-4.

Dantuma, N.P., Acs, K. and Luijsterburg, M.S. (2014) 'Should I stay or should I go: VCP/p97-mediated chromatin extraction in the DNA damage response', *Exp Cell Res*, 329(1), pp. 9-17.

Dantuma, N.P., Groothuis, T.A.M., Salomons, F.A. and Neefjes, J. (2006) 'A dynamic ubiquitin equilibrium couples proteasomal activity to chromatin remodeling', *The Journal of Cell Biology*, 173(1), pp. 19-26.

de Campos-Nebel, M., Larripa, I. and Gonzalez-Cid, M. (2010) 'Topoisomerase II-mediated DNA damage is differently repaired during the cell cycle by non-homologous end joining and homologous recombination', *PLoS One*, 5(9).

DeLaBarre, B. and Brunger, A.T. (2005) 'Nucleotide dependent motion and mechanism of action of p97/VCP', *J Mol Biol*, 347(2), pp. 437-52.

Deweese, J.E. and Osheroff, N. (2009) 'The DNA cleavage reaction of topoisomerase II: wolf in sheep's clothing', *Nucleic Acids Res*, 37(3), pp. 738-48.

DiNardo, S., Voelkel, K. and Sternglanz, R. (1984) 'DNA topoisomerase II mutant of Saccharomyces cerevisiae: topoisomerase II is required for segregation of daughter molecules at the termination of DNA replication', *Proc Natl Acad Sci U S A*, 81(9), pp. 2616-20.

Doil, C., Mailand, N., Bekker-Jensen, S., Menard, P., Larsen, D.H., Pepperkok, R., Ellenberg, J., Panier, S., Durocher, D., Bartek, J., Lukas, J. and Lukas, C. (2009) 'RNF168 binds and amplifies ubiquitin conjugates on damaged chromosomes to allow accumulation of repair proteins', *Cell*, 136(3), pp. 435-46.

Dreveny, I., Kondo, H., Uchiyama, K., Shaw, A., Zhang, X. and Freemont, P.S. (2004) 'Structural basis of the interaction between the AAA ATPase p97/VCP and its adaptor protein p47', *Embo j*, 23(5), pp. 1030-9.

Eguren, M., Alvarez-Fernandez, M., Garcia, F., Lopez-Contreras, A.J., Fujimitsu, K., Yaguchi, H., Luque-Garcia, J.L., Fernandez-Capetillo, O., Munoz, J., Yamano, H. and Malumbres, M. (2014) 'A synthetic lethal interaction between APC/C and topoisomerase poisons uncovered by proteomic screens', *Cell Rep*, 6(4), pp. 670-83.

Emmerich, C.H. and Cohen, P. (2015) 'Optimising methods for the preservation, capture and identification of ubiquitin chains and ubiquitylated proteins by immunoblotting', *Biochem Biophys Res Commun*, 466(1), pp. 1-14.

Errington, F., Willmore, E., Leontiou, C., Tilby, M.J. and Austin, C.A. (2004) 'Differences in the longevity of topo IIα and topo IIβ drug-stabilized cleavable complexes and the relationship to drug sensitivity', *Cancer Chemotherapy and Pharmacology*, 53(2), pp. 155-162.

Errington, F., Willmore, E., Tilby, M.J., Li, L., Li, G., Li, W., Baguley, B.C. and Austin, C.A. (1999) 'Murine transgenic cells lacking DNA topoisomerase IIbeta are resistant to acridines and mitoxantrone: analysis of cytotoxicity and cleavable complex formation', *Mol Pharmacol*, 56(6), pp. 1309-16.

Facchino, S., Abdouh, M., Chatoo, W. and Bernier, G. (2010) 'BMI1 confers radioresistance to normal and cancerous neural stem cells through recruitment of the DNA damage response machinery', *J Neurosci*, 30(30), pp. 10096-111.

Fan, J.R., Peng, A.L., Chen, H.C., Lo, S.C., Huang, T.H. and Li, T.K. (2008) 'Cellular processing pathways contribute to the activation of etoposide-induced DNA damage responses', *DNA Repair (Amst)*, 7(3), pp. 452-63.

Finley, D., Ciechanover, A. and Varshavsky, A. (1984) 'Thermolability of ubiquitin-activating enzyme from the mammalian cell cycle mutant ts85', *Cell*, 37(1), pp. 43-55.

Franz, A., Pirson, P.A., Pilger, D., Halder, S., Achuthankutty, D., Kashkar, H., Ramadan, K. and Hoppe, T. (2016) 'Chromatin-associated degradation is defined by UBXN-3/FAF1 to safeguard DNA replication fork progression', *Nat Commun*, 7, p. 10612.

Galloway, S.M. (2000) 'Cytotoxicity and chromosome aberrations in vitro: experience in industry and the case for an upper limit on toxicity in the aberration assay', *Environ Mol Mutagen*, 35(3), pp. 191-201.

Gao, R., Schellenberg, M.J., Huang, S.Y., Abdelmalak, M., Marchand, C., Nitiss, K.C., Nitiss, J.L., Williams, R.S. and Pommier, Y. (2014) 'Proteolytic degradation of topoisomerase II (Top2) enables the processing of Top2.DNA and Top2.RNA covalent complexes by tyrosyl-DNA-phosphodiesterase 2 (TDP2)', *J Biol Chem*, 289(26), pp. 17960-9.

Geiss-Friedlander, R. and Melchior, F. (2007) 'Concepts in sumoylation: a decade on', *Nature Reviews Molecular Cell Biology*, 8(12), pp. 947-956.

Geoffroy, M.C. and Hay, R.T. (2009) 'An additional role for SUMO in ubiquitin-mediated proteolysis', *Nat Rev Mol Cell Biol*, 10(8), pp. 564-8.

Ghezraoui, H., Piganeau, M., Renouf, B., Renaud, J.B., Sallmyr, A., Ruis, B., Oh, S., Tomkinson, A.E., Hendrickson, E.A., Giovannangeli, C., Jasin, M. and Brunet, E. (2014) 'Chromosomal translocations in human cells are generated by canonical nonhomologous end-joining', *Mol Cell*, 55(6), pp. 829-842.

Gilbert, N. and Allan, J. (2014) 'Supercoiling in DNA and chromatin', *Curr Opin Genet Dev*, 25, pp. 15-21.

Gilroy, K.L. and Austin, C.A. (2011) 'The impact of the C-terminal domain on the interaction of human DNA topoisomerase II alpha and beta with DNA', *PLoS One*, 6(2), p. e14693.

Gilroy, K.L., Leontiou, C., Padget, K., Lakey, J.H. and Austin, C.A. (2006) 'mAMSA resistant human topoisomerase IIbeta mutation G465D has reduced ATP hydrolysis activity', *Nucleic Acids Res*, 34(5), pp. 1597-607.

Ginjala, V., Nacerddine, K., Kulkarni, A., Oza, J., Hill, S.J., Yao, M., Citterio, E., van Lohuizen, M. and Ganesan, S. (2011) 'BMI1 is recruited to DNA breaks and contributes to DNA damage-induced H2A ubiquitination and repair', *Mol Cell Biol*, 31(10), pp. 1972-82.

Gómez-Herreros, F., Romero-Granados, R., Zeng, Z., Álvarez-Quilón, A., Quintero, C., Ju, L., Umans, L., Vermeire, L., Huylebroeck, D., Caldecott, K.W. and Cortés-Ledesma, F. (2013) 'TDP2–Dependent Non-Homologous End-Joining Protects against Topoisomerase II–Induced DNA Breaks and Genome Instability in Cells and In Vivo', *PLoS Genet*, 9(3).

Groettrup, M., Pelzer, C., Schmidtke, G. and Hofmann, K. (2008) 'Activating the ubiquitin family: UBA6 challenges the field', *Trends Biochem Sci*, 33(5), pp. 230-7.

Grozav, A.G., Chikamori, K., Kozuki, T., Grabowski, D.R., Bukowski, R.M., Willard, B., Kinter, M., Andersen, A.H., Ganapathi, R. and Ganapathi, M.K. (2009) 'Casein kinase I delta/epsilon phosphorylates topoisomerase IIalpha at serine-1106 and modulates DNA cleavage activity', *Nucleic Acids Res*, 37(2), pp. 382-92.

Guzzo, C.M., Berndsen, C.E., Zhu, J., Gupta, V., Datta, A., Greenberg, R.A., Wolberger, C. and Matunis, M.J. (2012) 'RNF4-dependent hybrid SUMO-ubiquitin chains are signals for RAP80 and thereby mediate the recruitment of BRCA1 to sites of DNA damage', *Sci Signal*, 5(253), p. ra88.

Haffner, M.C., Aryee, M.J., Toubaji, A., Esopi, D.M., Albadine, R., Gurel, B., Isaacs, W.B., Bova, G.S., Liu, W., Xu, J., Meeker, A.K., Netto, G., De Marzo, A.M., Nelson, W.G. and Yegnasubramanian, S. (2010) 'Androgen-induced TOP2B-mediated double-strand breaks and prostate cancer gene rearrangements', *Nat Genet*, 42(8), pp. 668-75.

Hamilton, N.K. and Maizels, N. (2010) 'MRE11 function in response to topoisomerase poisons is independent of its function in double-strand break repair in Saccharomyces cerevisiae', *PLoS One*, 5(10), p. e15387.

Harreman, M., Taschner, M., Sigurdsson, S., Anindya, R., Reid, J., Somesh, B., Kong, S.E., Banks, C.A.S., Conaway, R.C., Conaway, J.W. and Svejstrup, J.Q. (2009) 'Distinct ubiquitin ligases act sequentially for RNA polymerase II polyubiquitylation', *Proceedings of the National Academy of Sciences of the United States of America*, 106(49), pp. 20705-20710.

Hartsuiker, E., Neale, M.J. and Carr, A.M. (2009) 'Distinct requirements for the Rad32(Mre11) nuclease and Ctp1(CtIP) in the removal of covalently bound topoisomerase I and II from DNA', *Mol Cell*, 33(1), pp. 117-23.

He, J., Zhu, Q., Wani, G., Sharma, N. and Wani, A.A. (2016) 'Valosin-containing Protein (VCP)/p97 Segregase Mediates Proteolytic Processing of Cockayne Syndrome Group B (CSB) in Damaged Chromatin', *J Biol Chem*, 291(14), pp. 7396-408.

He, J., Zhu, Q., Wani, G. and Wani, A.A. (2017a) 'UV-induced proteolysis of RNA polymerase II is mediated by VCP/p97 segregase and timely orchestration by Cockayne syndrome B protein', *Oncotarget*, 8(7), pp. 11004-11019.

He, X., Riceberg, J., Soucy, T., Koenig, E., Minissale, J., Gallery, M., Bernard, H., Yang, X., Liao, H., Rabino, C., Shah, P., Xega, K., Yan, Z.H., Sintchak, M., Bradley, J., Xu, H., Duffey, M., England, D., Mizutani, H., Hu, Z., Guo, J., Chau, R., Dick, L.R., Brownell, J.E., Newcomb, J., Langston, S., Lightcap, E.S., Bence, N. and Pulukuri, S.M. (2017b) 'Probing the roles of SUMOylation in cancer cell biology by using a selective SAE inhibitor', *Nat Chem Biol*, 13(11), pp. 1164-1171.

Heck, M.M., Hittelman, W.N. and Earnshaw, W.C. (1988) 'Differential expression of DNA topoisomerases I and II during the eukaryotic cell cycle', *Proc Natl Acad Sci U S A*, 85(4), pp. 1086-90.

Heidelberger, J.B., Voigt, A., Borisova, M.E., Petrosino, G., Ruf, S., Wagner, S.A. and Beli, P. (2018) 'Proteomic profiling of VCP substrates links VCP to K6-linked ubiquitylation and c-Myc function', *EMBO Rep*, 19(4).

Higgins, N.P. (2012) 'A human TOP2A core DNA binding X-ray structure reveals topoisomerase subunit dynamics and a potential mechanism for SUMO modulation of decatenation', *J Mol Biol*, 424(3-4), pp. 105-8.

Hjerpe, R., Aillet, F., Lopitz-Otsoa, F., Lang, V., England, P. and Rodriguez, M.S. (2009) 'Efficient protection and isolation of ubiquitylated proteins using tandem ubiquitin-binding entities', *EMBO Rep*, 10(11), pp. 1250-8.

Ho, C.K., Law, S.L., Chiang, H., Hsu, M.L., Wang, C.C. and Wang, S.Y. (1991) 'Inhibition of microtubule assembly is a possible mechanism of action of mitoxantrone', *Biochem Biophys Res Commun*, 180(1), pp. 118-23.

Hoa, N.N., Shimizu, T., Zhou, Z.W., Wang, Z.Q., Deshpande, R.A., Paull, T.T., Akter, S., Tsuda, M., Furuta, R., Tsutsui, K., Takeda, S. and Sasanuma, H. (2016) 'Mre11 Is Essential for the Removal of Lethal Topoisomerase 2 Covalent Cleavage Complexes', *Mol Cell*, 64(3), pp. 580-592.

Hoeijmakers, J.H. (2001) 'Genome maintenance mechanisms for preventing cancer', *Nature*, 411(6835), pp. 366-74.

Huen, M.S., Grant, R., Manke, I., Minn, K., Yu, X., Yaffe, M.B. and Chen, J. (2007) 'RNF8 transduces the DNA-damage signal via histone ubiquitylation and checkpoint protein assembly', *Cell*, 131(5), pp. 901-14.

Hyer, M.L., Milhollen, M.A., Ciavarri, J., Fleming, P., Traore, T., Sappal, D., Huck, J., Shi, J., Gavin, J., Brownell, J., Yang, Y., Stringer, B., Griffin, R., Bruzzese, F., Soucy, T., Duffy, J., Rabino, C., Riceberg, J., Hoar, K., Lublinsky, A., Menon, S., Sintchak, M., Bump, N., Pulukuri, S.M., Langston, S., Tirrell, S., Kuranda, M., Veiby, P., Newcomb, J., Li, P., Wu, J.T., Powe, J., Dick, L.R., Greenspan, P., Galvin, K., Manfredi, M., Claiborne, C., Amidon, B.S. and Bence, N.F. (2018) 'A small-molecule inhibitor of the ubiquitin activating enzyme for cancer treatment', *Nature Medicine*.

Inobe, T. and Matouschek, A. (2014) 'Paradigms of protein degradation by the proteasome', *Curr Opin Struct Biol*, 24, pp. 156-64.

Isakov, E. and Stanhill, A. (2011) 'Stalled proteasomes are directly relieved by P97 recruitment', *J Biol Chem*, 286(35), pp. 30274-83.

Ishida, R., Iwai, M., Marsh, K.L., Austin, C.A., Yano, T., Shibata, M., Nozaki, N. and Hara, A. (1996) 'Threonine 1342 in human topoisomerase IIalpha is phosphorylated throughout the cell cycle', *J Biol Chem*, 271(47), pp. 30077-82.

Isik, S., Sano, K., Tsutsui, K., Seki, M., Enomoto, T., Saitoh, H. and Tsutsui, K. (2003) 'The SUMO pathway is required for selective degradation of DNA topoisomerase IIbeta induced by a catalytic inhibitor ICRF-193(1)', *FEBS Lett*, 546(2-3), pp. 374-8.

Ismail, I.H., Andrin, C., McDonald, D. and Hendzel, M.J. (2010) 'BMI1-mediated histone ubiquitylation promotes DNA double-strand break repair', *J Cell Biol*, 191(1), pp. 45-60.

Ismail, I.H., McDonald, D., Strickfaden, H., Xu, Z. and Hendzel, M.J. (2013) 'A small molecule inhibitor of polycomb repressive complex 1 inhibits ubiquitin signaling at DNA double-strand breaks', *J Biol Chem*, 288(37), pp. 26944-54.

Jacquemont, C. and Taniguchi, T. (2007) 'Proteasome function is required for DNA damage response and fanconi anemia pathway activation', *Cancer Res*, 67(15), pp. 7395-405.

Jiang, N., Shen, Y., Fei, X., Sheng, K., Sun, P., Qiu, Y., Larner, J., Cao, L., Kong, X. and Mi, J. (2013) 'Valosin-containing protein regulates the proteasome-mediated degradation of DNA-PKcs in glioma cells', *Cell Death Dis*, 4, p. e647.

Jin, J., Li, X., Gygi, S.P. and Harper, J.W. (2007) 'Dual E1 activation systems for ubiquitin differentially regulate E2 enzyme charging', *Nature*, 447(7148), pp. 1135-8.

Jin, S., Inoue, S. and Weaver, D.T. (1998) 'Differential etoposide sensitivity of cells deficient in the Ku and DNA-PKcs components of the DNA-dependent protein kinase', *Carcinogenesis*, 19(6), pp. 965-71.

Jobson, A. (2004) 'Mechanism of action of putative dual Topoisomerase I and II poisons XR5944 and XR11576'.

Ju, B.G., Lunyak, V.V., Perissi, V., Garcia-Bassets, I., Rose, D.W., Glass, C.K. and Rosenfeld, M.G. (2006) 'A topoisomerase IIbeta-mediated dsDNA break required for regulated transcription', *Science*, 312(5781), pp. 1798-802.

Kantidze, O.L., Iarovaia, O.V. and Razin, S.V. (2006) 'Assembly of nuclear matrix-bound protein complexes involved in non-homologous end joining is induced by inhibition of DNA topoisomerase II', *J Cell Physiol*, 207(3), pp. 660-7.

Kantidze, O.L. and Razin, S.V. (2007) 'Chemotherapy-related secondary leukemias: A role for DNA repair by error-prone non-homologous end joining in topoisomerase II - Induced chromosomal rearrangements', *Gene*, 391(1-2), pp. 76-9.

Kapuscinski, J. and Darzynkiewicz, Z. (1986) 'Relationship between the pharmacological activity of antitumor drugs Ametantrone and mitoxantrone (Novatrone) and their ability to condense nucleic acids', *Proc Natl Acad Sci U S A*, 83(17), pp. 6302-6.

Kim, S.Y., Kim, S.J., Kim, B.J., Rah, S.Y., Chung, S.M., Im, M.J. and Kim, U.H. (2006) 'Doxorubicin-induced reactive oxygen species generation and intracellular Ca2+ increase are reciprocally modulated in rat cardiomyocytes', *Exp Mol Med*, 38(5), pp. 535-45.

Kim, W., Bennett, E.J., Huttlin, E.L., Guo, A., Li, J., Possemato, A., Sowa, M.E., Rad, R., Rush, J., Comb, M.J., Harper, J.W. and Gygi, S.P. (2011) 'Systematic and quantitative assessment of the ubiquitin modified proteome', *Molecular cell*, 44(2), pp. 325-340.

Kitagaki, J., Agama, K.K., Pommier, Y., Yang, Y. and Weissman, A.M. (2008) 'Targeting Tumor Cells Expressing p53 with a Water Soluble Inhibitor of Hdm2', *Molecular cancer therapeutics*, 7(8), pp. 2445-2454.

Komander, D. (2009) 'The emerging complexity of protein ubiquitination', *Biochemical Society Transactions*, 37(5).

Komander, D. and Rape, M. (2012) 'The Ubiquitin Code', *Annual Review of Biochemistry*, 81(1), pp. 203-229.

Lafon, A., Taranum, S., Pietrocola, F., Dingli, F., Loew, D., Brahma, S., Bartholomew, B. and Papamichos-Chronakis, M. (2015) 'INO80 Chromatin Remodeler Facilitates Release of RNA Polymerase II from Chromatin for Ubiquitin-Mediated Proteasomal Degradation', *Molecular Cell*, 60(5), pp. 784-796.

Landre, V., Rotblat, B., Melino, S., Bernassola, F. and Melino, G. (2014) 'Screening for E3-ubiquitin ligase inhibitors: challenges and opportunities', *Oncotarget*, 5(18), pp. 7988-8013.

Lang, A.J., Mirski, S.E., Cummings, H.J., Yu, Q., Gerlach, J.H. and Cole, S.P. (1998) 'Structural organization of the human TOP2A and TOP2B genes', *Gene*, 221(2), pp. 255-66.

Law, J.C., Ritke, M.K., Yalowich, J.C., Leder, G.H. and Ferrell, R.E. (1993) 'Mutational inactivation of the p53 gene in the human erythroid leukemic K562 cell line', *Leuk Res*, 17(12), pp. 1045-50.

Le, L.T., Kang, W., Kim, J.Y., Le, O.T., Lee, S.Y. and Yang, J.K. (2016) 'Structural Details of Ufd1 Binding to p97 and Their Functional Implications in ER-Associated Degradation', *PLoS One*, 11(9), p. e0163394.

Lee, K.C. (2016) 'Molecular Pharmacology of DNA Topoisomerase II drugs'.

Lee, K.C., Bramley, R.L., Cowell, I.G., Jackson, G.H. and Austin, C.A. (2016) 'Proteasomal inhibition potentiates drugs targeting DNA topoisomerase II', *Biochem Pharmacol*, 103, pp. 29-39.

Lee, K.C., Padget, K., Curtis, H., Cowell, I.G., Moiani, D., Sondka, Z., Morris, N.J., Jackson, G.H., Cockell, S.J., Tainer, J.A. and Austin, C.A. (2012) 'MRE11 facilitates the removal of human topoisomerase II complexes from genomic DNA', *Biol Open*, 1(9), pp. 863-73.

Leontiou, C., Lakey, J.H. and Austin, C.A. (2004) 'Mutation E522K in human DNA topoisomerase IIbeta confers resistance to methyl N-(4'-(9-acridinylamino)-phenyl)carbamate hydrochloride and methyl N-(4'-(9-acridinylamino)-3-methoxy-phenyl) methane sulfonamide but hypersensitivity to etoposide', *Mol Pharmacol*, 66(3), pp. 430-9.

Leontiou, C., Lakey, J.H., Lightowlers, R., Turnbull, R.M. and Austin, C.A. (2006) 'Mutation P732L in human DNA topoisomerase IIbeta abolishes DNA cleavage in the presence of calcium and confers drug resistance', *Mol Pharmacol*, 69(1), pp. 130-9.

Leontiou, C., Watters, G.P., Gilroy, K.L., Heslop, P., Cowell, I.G., Craig, K., Lightowlers, R.N., Lakey, J.H. and Austin, C.A. (2007) 'Differential selection of acridine resistance mutations in human DNA topoisomerase IIbeta is dependent on the acridine structure', *Mol Pharmacol*, 71(4), pp. 1006-14.

Liao, S., Tammaro, M. and Yan, H. (2016) 'The structure of ends determines the pathway choice and Mre11 nuclease dependency of DNA double-strand break repair', *Nucleic Acids Res*, 44(12), pp. 5689-701.

Lim, N.C. and Jackson, S.E. (2015) 'Molecular knots in biology and chemistry', *J Phys Condens Matter*, 27(35), p. 354101.

Lin, C.P., Ban, Y., Lyu, Y.L. and Liu, L.F. (2009) 'Proteasome-dependent processing of topoisomerase I-DNA adducts into DNA double strand breaks at arrested replication forks', *J Biol Chem*, 284(41), pp. 28084-92.

Lindsey, R.H., Jr., Pendleton, M., Ashley, R.E., Mercer, S.L., Deweese, J.E. and Osheroff, N. (2014) 'Catalytic core of human topoisomerase IIalpha: insights into enzyme-DNA interactions and drug mechanism', *Biochemistry*, 53(41), pp. 6595-602.

Liu, T. and Huang, J. (2016) 'DNA End Resection: Facts and Mechanisms', *Genomics Proteomics Bioinformatics*, 14(3), pp. 126-130.

Liu, X., Zhao, B., Sun, L., Bhuripanyo, K., Wang, Y., Bi, Y., Davuluri, R.V., Duong, D.M., Nanavati, D., Yin, J. and Kiyokawa, H. (2017) 'Orthogonal ubiquitin transfer identifies ubiquitination substrates under differential control by the two ubiquitin activating enzymes', *Nat Commun*, 8, p. 14286.

Lou, Z., Minter-Dykhouse, K. and Chen, J. (2005) 'BRCA1 participates in DNA decatenation', *Nat Struct Mol Biol*, 12(7), pp. 589-93.

Lyu, Y.L., Lin, C.P., Azarova, A.M., Cai, L., Wang, J.C. and Liu, L.F. (2006) 'Role of topoisomerase IIbeta in the expression of developmentally regulated genes', *Mol Cell Biol*, 26(21), pp. 7929-41.

Madabhushi, R., Gao, F., Pfenning, A.R., Pan, L., Yamakawa, S., Seo, J., Rueda, R., Phan, T.X., Yamakawa, H., Pao, P.C., Stott, R.T., Gjoneska, E., Nott, A., Cho, S., Kellis, M. and Tsai, L.H. (2015) 'Activity-Induced DNA Breaks Govern the Expression of Neuronal Early-Response Genes', *Cell*, 161(7), pp. 1592-605.

Maede, Y., Shimizu, H., Fukushima, T., Kogame, T., Nakamura, T., Miki, T., Takeda, S., Pommier, Y. and Murai, J. (2014) 'Differential and common DNA repair pathways for topoisomerase I- and II-targeted drugs in a genetic DT40 repair cell screen panel', *Mol Cancer Ther*, 13(1), pp. 214-20.

Magnaghi, P., D'Alessio, R., Valsasina, B., Avanzi, N., Rizzi, S., Asa, D., Gasparri, F., Cozzi, L., Cucchi, U., Orrenius, C., Polucci, P., Ballinari, D., Perrera, C., Leone, A., Cervi, G., Casale, E., Xiao, Y., Wong, C., Anderson, D.J., Galvani, A., Donati, D., O'Brien, T., Jackson, P.K. and Isacchi, A. (2013) 'Covalent and allosteric inhibitors of the ATPase VCP/p97 induce cancer cell death', *Nat Chem Biol*, 9(9), pp. 548-556.

Mailand, N., Bekker-Jensen, S., Faustrup, H., Melander, F., Bartek, J., Lukas, C. and Lukas, J. (2007) 'RNF8 ubiquitylates histones at DNA double-strand breaks and promotes assembly of repair proteins', *Cell*, 131(5), pp. 887-900.

Malik, M., Nitiss, K.C., Enriquez-Rios, V. and Nitiss, J.L. (2006) 'Roles of nonhomologous end-joining pathways in surviving topoisomerase II-mediated DNA damage', *Mol Cancer Ther*, 5(6), pp. 1405-14.

Manville, C.M., Smith, K., Sondka, Z., Rance, H., Cockell, S., Cowell, I.G., Lee, K.C., Morris, N.J., Padget, K., Jackson, G.H. and Austin, C.A. (2015) 'Genome-wide ChIP-seq analysis of human TOP2B occupancy in MCF7 breast cancer epithelial cells', *Biol Open*, 4(11), pp. 1436-47.

Mao, Y., Desai, S.D. and Liu, L.F. (2000) 'SUMO-1 conjugation to human DNA topoisomerase II isozymes', *J Biol Chem*, 275(34), pp. 26066-73.

Mao, Y., Desai, S.D., Ting, C.Y., Hwang, J. and Liu, L.F. (2001) '26 S proteasome-mediated degradation of topoisomerase II cleavable complexes', *J Biol Chem*, 276(44), pp. 40652-8.

Martensson, S., Nygren, J., Osheroff, N. and Hammarsten, O. (2003) 'Activation of the DNA-dependent protein kinase by drug-induced and radiation-induced DNA strand breaks', *Radiat Res*, 160(3), pp. 291-301.

Mattiroli, F., Vissers, J.H., van Dijk, W.J., Ikpa, P., Citterio, E., Vermeulen, W., Marteijn, J.A. and Sixma, T.K. (2012) 'RNF168 ubiquitinates K13-15 on H2A/H2AX to drive DNA damage signaling', *Cell*, 150(6), pp. 1182-95.

McNamara, S., Wang, H., Hanna, N. and Miller, W.H., Jr. (2008) 'Topoisomerase IIbeta negatively modulates retinoic acid receptor alpha function: a novel mechanism of retinoic acid resistance', *Mol Cell Biol*, 28(6), pp. 2066-77.

Meczes, E.L., Gilroy, K.L., West, K.L. and Austin, C.A. (2008) 'The impact of the human DNA topoisomerase II C-terminal domain on activity', *PLoS One*, 3(3), p. e1754.

Meerang, M., Ritz, D., Paliwal, S., Garajova, Z., Bosshard, M., Mailand, N., Janscak, P., Hubscher, U., Meyer, H. and Ramadan, K. (2011) 'The ubiquitin-selective segregase VCP/p97 orchestrates the response to DNA double-strand breaks', *Nat Cell Biol*, 13(11), pp. 1376-1382.

Merin, N.M. and Kelly, K.R. (2014) 'Clinical use of proteasome inhibitors in the treatment of multiple myeloma', *Pharmaceuticals (Basel)*, 8(1), pp. 1-20.

Meyer, H., Bug, M. and Bremer, S. (2012) 'Emerging functions of the VCP/p97 AAA-ATPase in the ubiquitin system', *Nat Cell Biol*, 14(2), pp. 117-23.

Meyer, H.H., Shorter, J.G., Seemann, J., Pappin, D. and Warren, G. (2000) 'A complex of mammalian Ufd1 and Npl4 links the AAA-ATPase, p97, to ubiquitin and nuclear transport pathways', *The EMBO Journal*, 19(10), pp. 2181-2192.

Mimnaugh, E.G., Chen, H.Y., Davie, J.R., Celis, J.E. and Neckers, L. (1997) 'Rapid deubiquitination of nucleosomal histones in human tumor cells caused by proteasome inhibitors and stress response inducers: effects on replication, transcription, translation, and the cellular stress response', *Biochemistry*, 36(47), pp. 14418-29.

Misra, M., Kuhn, M., Lobel, M., An, H., Statsyuk, A.V., Sotriffer, C. and Schindelin, H. (2017) 'Dissecting the Specificity of Adenosyl Sulfamate Inhibitors Targeting the Ubiquitin-Activating Enzyme', *Structure*, 25(7), pp. 1120-1129.e3.

Miwa, S., Uchida, C., Kitagawa, K., Hattori, T., Oda, T., Sugimura, H., Yasuda, H., Nakamura, H., Chida, K. and Kitagawa, M. (2006) 'Mdm2-mediated pRB downregulation is involved in carcinogenesis in a p53-independent manner', *Biochem Biophys Res Commun*, 340(1), pp. 54-61.

Mohammed, H., Taylor, C. and Brown, G.D. (2016) 'Rapid immunoprecipitation mass spectrometry of endogenous proteins (RIME) for analysis of chromatin complexes', 11(2), pp. 316-26.

Mondal, N. and Parvin, J.D. (2001) 'DNA topoisomerase IIalpha is required for RNA polymerase II transcription on chromatin templates', *Nature*, 413(6854), pp. 435-8.

Moreau, S., Ferguson, J.R. and Symington, L.S. (1999) 'The nuclease activity of Mre11 is required for meiosis but not for mating type switching, end joining, or telomere maintenance', *Mol Cell Biol*, 19(1), pp. 556-66.

Moudry, P., Lukas, C., Macurek, L., Hanzlikova, H., Hodny, Z., Lukas, J. and Bartek, J. (2012) 'Ubiquitin-activating enzyme UBA1 is required for cellular response to DNA damage', *Cell Cycle*, 11(8), pp. 1573-82.

Murakawa, Y., Sonoda, E., Barber, L.J., Zeng, W., Yokomori, K., Kimura, H., Niimi, A., Lehmann, A., Zhao, G.Y., Hochegger, H., Boulton, S.J. and Takeda, S. (2007) 'Inhibitors of the proteasome suppress homologous DNA recombination in mammalian cells', *Cancer Res*, 67(18), pp. 8536-43.

Murata, S., Yashiroda, H. and Tanaka, K. (2009) 'Molecular mechanisms of proteasome assembly', *Nat Rev Mol Cell Biol*, 10(2), pp. 104-15.

Muslimovic, A., Nystrom, S., Gao, Y. and Hammarsten, O. (2009) 'Numerical analysis of etoposide induced DNA breaks', *PLoS One*, 4(6), p. e5859.

Nakamura, K., Kogame, T., Oshiumi, H., Shinohara, A., Sumitomo, Y., Agama, K., Pommier, Y., Tsutsui, K.M., Tsutsui, K., Hartsuiker, E., Ogi, T., Takeda, S. and Taniguchi, Y. (2010) 'Collaborative action of Brca1 and CtIP in elimination of covalent modifications from double-strand breaks to facilitate subsequent break repair', *PLoS Genet*, 6(1), p. e1000828.

Navon, A. and Ciechanover, A. (2009) 'The 26 S proteasome: from basic mechanisms to drug targeting', *J Biol Chem*, 284(49), pp. 33713-8.

Nayak, M.S., Yang, J.M. and Hait, W.N. (2007) 'Effect of a single nucleotide polymorphism in the murine double minute 2 promoter (SNP309) on the sensitivity to topoisomerase II-targeting drugs', *Cancer Res*, 67(12), pp. 5831-9.

Neale, M.J., Pan, J. and Keeney, S. (2005) 'Endonucleolytic processing of covalent protein-linked DNA double-strand breaks', *Nature*, 436(7053), pp. 1053-7.

Nie, M., Aslanian, A., Prudden, J., Heideker, J., Vashisht, A.A., Wohlschlegel, J.A., Yates, J.R., 3rd and Boddy, M.N. (2012) 'Dual recruitment of Cdc48 (p97)-Ufd1-Npl4 ubiquitin-selective segregase by small ubiquitin-like modifier protein (SUMO) and ubiquitin in SUMO-targeted ubiquitin ligase-mediated genome stability functions', *J Biol Chem*, 287(35), pp. 29610-9.

Nie, M. and Boddy, M.N. (2016) 'Cooperativity of the SUMO and Ubiquitin Pathways in Genome Stability', *Biomolecules*, 6(1), p. 14.

Nitiss, J.L. (2009) 'Targeting DNA topoisomerase II in cancer chemotherapy', *Nat Rev Cancer*, 9(5), pp. 338-50.

Nur, E.K.A., Meiners, S., Ahmed, I., Azarova, A., Lin, C.P., Lyu, Y.L. and Liu, L.F. (2007) 'Role of DNA topoisomerase IIbeta in neurite outgrowth', *Brain Res*, 1154, pp. 50-60.

Ogiso, Y., Tomida, A., Lei, S., Omura, S. and Tsuruo, T. (2000) 'Proteasome inhibition circumvents solid tumor resistance to topoisomerase II-directed drugs', *Cancer Res*, 60(9), pp. 2429-34.

Padget, K., Pearson, A.D. and Austin, C.A. (2000) 'Quantitation of DNA topoisomerase IIalpha and beta in human leukaemia cells by immunoblotting', *Leukemia*, 14(11), pp. 1997-2005.

Pan, M.R., Peng, G., Hung, W.C. and Lin, S.Y. (2011) 'Monoubiquitination of H2AX protein regulates DNA damage response signaling', *J Biol Chem*, 286(32), pp. 28599-607.

Panier, S. and Durocher, D. (2009) 'Regulatory ubiquitylation in response to DNA double-strand breaks', *DNA Repair (Amst)*, 8(4), pp. 436-43.

Papadopoulos, C., Kirchner, P., Bug, M., Grum, D., Koerver, L., Schulze, N., Poehler, R., Dressler, A., Fengler, S., Arhzaouy, K., Lux, V., Ehrmann, M., Weihl, C.C. and Meyer, H. (2017) 'VCP/p97 cooperates with YOD1, UBXD1 and PLAA to drive clearance of ruptured lysosomes by autophagy', *Embo j*, 36(2), pp. 135-150.

Park, S., Isaacson, R., Kim, H.T., Silver, P.A. and Wagner, G. (2005) 'Ufd1 exhibits the AAA-ATPase fold with two distinct ubiquitin interaction sites', *Structure*, 13(7), pp. 995-1005.

Patel, S., Keller, B.A. and Fisher, L.M. (2000) 'Mutations at arg486 and glu571 in human topoisomerase IIalpha confer resistance to amsacrine: relevance for antitumor drug resistance in human cells', *Mol Pharmacol*, 57(4), pp. 784-91.

Paull, T.T., Rogakou, E.P., Yamazaki, V., Kirchgessner, C.U., Gellert, M. and Bonner, W.M. (2000) 'A critical role for histone H2AX in recruitment of repair factors to nuclear foci after DNA damage', *Curr Biol*, 10(15), pp. 886-95.

Pendleton, M., Lindsey, R.H., Jr., Felix, C.A., Grimwade, D. and Osheroff, N. (2014) 'Topoisomerase II and leukemia', *Ann N Y Acad Sci*, 1310, pp. 98-110.

Perillo, B., Ombra, M.N., Bertoni, A., Cuozzo, C., Sacchetti, S., Sasso, A., Chiariotti, L., Malorni, A., Abbondanza, C. and Avvedimento, E.V. (2008) 'DNA oxidation as triggered by H3K9me2 demethylation drives estrogen-induced gene expression', *Science*, 319(5860), pp. 202-6.

Pommier, Y. (2013) 'Drugging topoisomerases: lessons and challenges', *ACS Chem Biol*, 8(1), pp. 82-95.

Pommier, Y., Kiselev, E. and Marchand, C. (2015) 'Interfacial inhibitors', *Bioorg Med Chem Lett*, 25(18), pp. 3961-5.

Pommier, Y., Leo, E., Zhang, H. and Marchand, C. (2010) 'DNA topoisomerases and their poisoning by anticancer and antibacterial drugs', *Chem Biol*, 17(5), pp. 421-33.

Porter, A.C. and Farr, C.J. (2004) 'Topoisomerase II: untangling its contribution at the centromere', *Chromosome Res*, 12(6), pp. 569-83.

Postow, L. (2011) 'Destroying the ring: Freeing DNA from Ku with ubiquitin', *FEBS Letters*, 585(18), pp. 2876-2882.

Puumalainen, M.R., Lessel, D., Ruthemann, P., Kaczmarek, N., Bachmann, K., Ramadan, K. and Naegeli, H. (2014) 'Chromatin retention of DNA damage sensors DDB2 and XPC through loss of p97 segregase causes genotoxicity', *Nat Commun*, 5, p. 3695.

Pye, V.E., Beuron, F., Keetch, C.A., McKeown, C., Robinson, C.V., Meyer, H.H., Zhang, X. and Freemont, P.S. (2007) 'Structural insights into the p97-Ufd1-Npl4 complex', *Proc Natl Acad Sci U S A*, 104(2), pp. 467-72.

Pye, V.E., Dreveny, I., Briggs, L.C., Sands, C., Beuron, F., Zhang, X. and Freemont, P.S. (2006) 'Going through the motions: the ATPase cycle of p97', *J Struct Biol*, 156(1), pp. 12-28.

Quennet, V., Beucher, A., Barton, O., Takeda, S. and Lobrich, M. (2011) 'CtIP and MRN promote non-homologous end-joining of etoposide-induced DNA double-strand breaks in G1', *Nucleic Acids Res*, 39(6), pp. 2144-52.

Ramadan, K., Bruderer, R., Spiga, F.M., Popp, O., Baur, T., Gotta, M. and Meyer, H.H. (2007) 'Cdc48/p97 promotes reformation of the nucleus by extracting the kinase Aurora B from chromatin', *Nature*, 450(7173), pp. 1258-62.

Rao, T., Gao, R., Takada, S., Al Abo, M., Chen, X., Walters, K.J., Pommier, Y. and Aihara, H. (2016) 'Novel TDP2-ubiquitin interactions and their importance for the repair of topoisomerase II-mediated DNA damage', *Nucleic Acids Res*, 44(21), pp. 10201-10215.

Rape, M., Hoppe, T., Gorr, I., Kalocay, M., Richly, H. and Jentsch, S. (2001) 'Mobilization of processed, membrane-tethered SPT23 transcription factor by CDC48(UFD1/NPL4), a ubiquitin-selective chaperone', *Cell*, 107(5), pp. 667-77.

Rastogi, N. and Mishra, D.P. (2012) 'Therapeutic targeting of cancer cell cycle using proteasome inhibitors', *Cell Div*, 7(1), p. 26.

Ray, S., Panova, T., Miller, G., Volkov, A., Porter, A.C.G., Russell, J., Panov, K.I. and Zomerdijk, J.C.B.M. (2013) 'Topoisomerase IIα promotes activation of RNA polymerase I transcription by facilitating pre-initiation complex formation', *Nat Commun*, 4, p. 1598.

Roberts, S.A., Strande, N., Burkhalter, M.D., Strom, C., Havener, J.M., Hasty, P. and Ramsden, D.A. (2010) 'Ku is a 5'-dRP/AP lyase that excises nucleotide damage near broken ends', *Nature*, 464(7292), pp. 1214-7.

Rocha, J.C., Busatto, F.F., de Souza, L.K. and Saffi, J. (2016) 'Influence of nucleotide excision repair on mitoxantrone cytotoxicity', *DNA Repair (Amst)*, 42, pp. 33-43.

Rogakou, E.P., Pilch, D.R., Orr, A.H., Ivanova, V.S. and Bonner, W.M. (1998) 'DNA double-stranded breaks induce histone H2AX phosphorylation on serine 139', *J Biol Chem*, 273(10), pp. 5858-68.

Rogojina, A.T. and Nitiss, J.L. (2008) 'Isolation and characterization of mAMSA-hypersensitive mutants. Cytotoxicity of Top2 covalent complexes containing DNA single strand breaks', *J Biol Chem*, 283(43), pp. 29239-50.

Rothenberg, M., Kohli, J. and Ludin, K. (2009) 'Ctp1 and the MRN-complex are required for endonucleolytic Rec12 removal with release of a single class of oligonucleotides in fission yeast', *PLoS Genet*, 5(11), p. e1000722.

Rouiller, I., Butel, V.M., Latterich, M., Milligan, R.A. and Wilson-Kubalek, E.M. (2000) 'A Major Conformational Change in p97 AAA ATPase upon ATP Binding', *Molecular Cell*, 6(6), pp. 1485-1490.

Ryu, H., Furuta, M., Kirkpatrick, D., Gygi, S.P. and Azuma, Y. (2010) 'PIASy-dependent SUMOylation regulates DNA topoisomerase IIalpha activity', *J Cell Biol*, 191(4), pp. 783-94.

Ryu, H., Yoshida, M.M., Sridharan, V., Kumagai, A., Dunphy, W.G., Dasso, M. and Azuma, Y. (2015) 'SUMOylation of the C-terminal domain of DNA topoisomerase IIalpha regulates the centromeric localization of Claspin', *Cell Cycle*, 14(17), pp. 2777-84.

Saito, M., Fujimitsu, Y., Sasano, T., Yoshikai, Y., Ban-Ishihara, R., Nariai, Y., Urano, T. and Saitoh, H. (2014) 'The SUMO-targeted ubiquitin ligase RNF4 localizes to etoposide-exposed mitotic chromosomes: implication for a novel DNA damage response during mitosis', *Biochem Biophys Res Commun*, 447(1), pp. 83-8.

Salmena, L., Lam, V., McPherson, J.P. and Goldenberg, G.J. (2001) 'Role of proteasomal degradation in the cell cycle-dependent regulation of DNA topoisomerase IIalpha expression', *Biochem Pharmacol*, 61(7), pp. 795-802.

Schellenberg, M.J., Appel, C.D., Adhikari, S., Robertson, P.D., Ramsden, D.A. and Williams, R.S. (2012) 'Mechanism of repair of 5'-topoisomerase II-DNA adducts by mammalian tyrosyl-DNA phosphodiesterase 2', *Nat Struct Mol Biol*, 19(12), pp. 1363-71.

Schellenberg, M.J., Lieberman, J.A., Herrero-Ruiz, A., Butler, L.R., Williams, J.G., Munoz-Cabello, A.M., Mueller, G.A., London, R.E., Cortes-Ledesma, F. and Williams, R.S. (2017) 'ZATT (ZNF451)-mediated resolution of topoisomerase 2 DNA-protein cross-links', 357(6358), pp. 1412-1416.

Schoeffler, A.J. and Berger, J.M. (2008) 'DNA topoisomerases: harnessing and constraining energy to govern chromosome topology', *Q Rev Biophys*, 41(1), pp. 41-101.

Sdek, P., Ying, H., Chang, D.L., Qiu, W., Zheng, H., Touitou, R., Allday, M.J. and Xiao, Z.X. (2005) 'MDM2 promotes proteasome-dependent ubiquitin-independent degradation of retinoblastoma protein', *Mol Cell*, 20(5), pp. 699-708.

Seiberlich, V., Goldbaum, O., Zhukareva, V. and Richter-Landsberg, C. (2012) 'The small molecule inhibitor PR-619 of deubiquitinating enzymes affects the microtubule network and causes protein aggregate formation in neural cells: implications for neurodegenerative diseases', *Biochim Biophys Acta*, 1823(11), pp. 2057-68.

Senturk, J.C., Bohlman, S. and Manfredi, J.J. (2017) 'Mdm2 selectively suppresses DNA damage arising from inhibition of topoisomerase II independent of p53', *Oncogene*, 36(44), pp. 6085-6096.

Smith, K.A., Cowell, I.G., Zhang, Y., Sondka, Z. and Austin, C.A. (2013) 'The role of topoisomerase II beta on breakage and proximity of RUNX1 to partner alleles RUNX1T1 and EVI1', *Genes, Chromosomes and Cancer*, 53, pp. 117-128.

Snider, J., Thibault, G. and Houry, W.A. (2008) 'The AAA+ superfamily of functionally diverse proteins', *Genome Biol*, 9(4), p. 216.

Song, C., Wang, Q., Song, C. and Rogers, T.J. (2015) 'Valosin-containing protein (VCP/p97) is capable of unfolding polyubiquitinated proteins through its ATPase domains', *Biochem Biophys Res Commun*, 463(3), pp. 453-7.

Soucy, T.A., Smith, P.G., Milhollen, M.A., Berger, A.J., Gavin, J.M., Adhikari, S., Brownell, J.E., Burke, K.E., Cardin, D.P., Critchley, S., Cullis, C.A., Doucette, A., Garnsey, J.J., Gaulin, J.L., Gershman, R.E., Lublinsky, A.R., McDonald, A., Mizutani, H., Narayanan, U., Olhava, E.J., Peluso, S., Rezaei, M., Sintchak, M.D., Talreja, T., Thomas, M.P., Traore, T., Vyskocil, S., Weatherhead, G.S., Yu, J., Zhang, J., Dick, L.R., Claiborne, C.F., Rolfe, M., Bolen, J.B. and Langston, S.P. (2009) 'An inhibitor of NEDD8-activating enzyme as a new approach to treat cancer', *Nature*, 458(7239), pp. 732-6.

Stach, L. and Freemont, P.S. (2017) 'The AAA+ ATPase p97, a cellular multitool', *Biochem J*, 474(17), pp. 2953-2976.

Stingele, J. and Jentsch, S. (2015) 'DNA-protein crosslink repair', *Nat Rev Mol Cell Biol*, 16(8), pp. 455-60.

Stingele, J., Schwarz, M.S., Bloemeke, N., Wolf, P.G. and Jentsch, S. (2014) 'A DNA-dependent protease involved in DNA-protein crosslink repair', *Cell*, 158(2), pp. 327-338.

Stohr, B.A. and Kreuzer, K.N. (2001) 'Repair of topoisomerase-mediated DNA damage in bacteriophage T4', *Genetics*, 158(1), pp. 19-28.

Sumner, A.T. (1995) 'Inhibitors of topoisomerase II delay progress through mitosis and induce a doubling of the DNA content in CHO cells', *Exp Cell Res*, 217(2), pp. 440-7.

Sunter, N.J. (2008) 'DNA damage responses'.

Sunter, N.J., Cowell, I.G., Willmore, E., Watters, G.P. and Austin, C.A. (2010) 'Role of Topoisomerase IIbeta in DNA Damage Response following IR and Etoposide', *J Nucleic Acids*, 2010.

Takahashi, Y., Yong-Gonzalez, V., Kikuchi, Y. and Strunnikov, A. (2006) 'SIZ1/SIZ2 control of chromosome transmission fidelity is mediated by the sumoylation of topoisomerase II', *Genetics*, 172(2), pp. 783-94.

Takeshita, T., Wu, W., Koike, A., Fukuda, M. and Ohta, T. (2009) 'Perturbation of DNA repair pathways by proteasome inhibitors corresponds to enhanced chemosensitivity of cells to DNA damage-inducing agents', *Cancer Chemother Pharmacol*, 64(5), pp. 1039-46.

Tammaro, M., Barr, P., Ricci, B. and Yan, H. (2013) 'Replication-dependent and transcription-dependent mechanisms of DNA double-strand break induction by the topoisomerase 2-targeting drug etoposide', *PLoS One*, 8(11), p. e79202.

Tammaro, M., Liao, S., Beeharry, N. and Yan, H. (2016) 'DNA double-strand breaks with 5' adducts are efficiently channeled to the DNA2-mediated resection pathway', *Nucleic Acids Res*, 44(1), pp. 221-31.

Thakurela, S., Garding, A., Jung, J., Schubeler, D., Burger, L. and Tiwari, V.K. (2013) 'Gene regulation and priming by topoisomerase IIalpha in embryonic stem cells', *Nat Commun*, 4, p. 2478.

Tian, X., Isamiddinova, N.S., Peroutka, R.J., Goldenberg, S.J., Mattern, M.R., Nicholson, B. and Leach, C. (2011) 'Characterization of selective ubiquitin and ubiquitin-like protease inhibitors using a fluorescence-based multiplex assay format', *Assay Drug Dev Technol*, 9(2), pp. 165-73.

Tiwari, V.K., Burger, L., Nikoletopoulou, V., Deogracias, R., Thakurela, S., Wirbelauer, C., Kaut, J., Terranova, R., Hoerner, L., Mielke, C., Boege, F., Murr, R., Peters, A.H., Barde, Y.A. and Schubeler, D. (2012) 'Target genes of Topoisomerase IIbeta regulate neuronal survival and are defined by their chromatin state', *Proc Natl Acad Sci U S A*, 109(16), pp. E934-43.

Tomko, R.J., Jr. and Hochstrasser, M. (2013) 'Molecular architecture and assembly of the eukaryotic proteasome', *Annu Rev Biochem*, 82, pp. 415-45.

Toyoda, E., Kagaya, S., Cowell, I.G., Kurosawa, A., Kamoshita, K., Nishikawa, K., Iiizumi, S., Koyama, H., Austin, C.A. and Adachi, N. (2008) 'NK314, a topoisomerase II inhibitor that specifically targets the alpha isoform', *J Biol Chem*, 283(35), pp. 23711-20.

Tsang, W.P., Chau, S.P., Kong, S.K., Fung, K.P. and Kwok, T.T. (2003) 'Reactive oxygen species mediate doxorubicin induced p53-independent apoptosis', *Life Sci*, 73(16), pp. 2047-58.

Uchida, C., Miwa, S., Kitagawa, K., Hattori, T., Isobe, T., Otani, S., Oda, T., Sugimura, H., Kamijo, T., Ookawa, K., Yasuda, H. and Kitagawa, M. (2005) 'Enhanced Mdm2 activity inhibits pRB function via ubiquitin-dependent degradation', *Embo j*, 24(1), pp. 160-9.

Udeshi, N.D., Mani, D.R., Eisenhaure, T., Mertins, P., Jaffe, J.D., Clauser, K.R., Hacohen, N. and Carr, S.A. (2012) 'Methods for quantification of in vivo changes in protein ubiquitination following proteasome and deubiquitinase inhibition', *Mol Cell Proteomics*, 11(5), pp. 148-59.

Uemura, T., Ohkura, H., Adachi, Y., Morino, K., Shiozaki, K. and Yanagida, M. (1987) 'DNA topoisomerase II is required for condensation and separation of mitotic chromosomes in S. pombe', *Cell*, 50(6), pp. 917-25.

Uuskula-Reimand, L., Hou, H., Samavarchi-Tehrani, P., Rudan, M.V., Liang, M., Medina-Rivera, A., Mohammed, H., Schmidt, D., Schwalie, P., Young, E.J., Reimand, J., Hadjur, S., Gingras, A.C. and Wilson, M.D. (2016) 'Topoisomerase II beta interacts with cohesin and CTCF at topological domain borders', *Genome Biol*, 17(1), p. 182.

van den Boom, J. and Meyer, H. (2018) 'VCP/p97-Mediated Unfolding as a Principle in Protein Homeostasis and Signaling', *Mol Cell*, 69(2), pp. 182-194.

van den Boom, J., Wolf, M., Weimann, L., Schulze, N., Li, F., Kaschani, F., Riemer, A., Zierhut, C., Kaiser, M., Iliakis, G., Funabiki, H. and Meyer, H. (2016) 'VCP/p97 Extracts Sterically Trapped Ku70/80 Rings from DNA in Double-Strand Break Repair', *Mol Cell*, 64(1), pp. 189-198.

Vaz, B., Halder, S. and Ramadan, K. (2013) 'Role of p97/VCP (Cdc48) in genome stability', *Front Genet*, 4, p. 60.

Verma, R., Oania, R., Fang, R., Smith, G.T. and Deshaies, R.J. (2011) 'Cdc48/p97 mediates UV-dependent turnover of RNA Pol II', *Mol Cell*, 41(1), pp. 82-92.

von Metzler, I., Heider, U., Mieth, M., Lamottke, B., Kaiser, M., Jakob, C. and Sezer, O. (2009) 'Synergistic interaction of proteasome and topoisomerase II inhibition in multiple myeloma', *Exp Cell Res*, 315(14), pp. 2471-8.

Wang, W., Daley, J.M., Kwon, Y., Krasner, D.S. and Sung, P. (2017) 'Plasticity of the Mre11-Rad50-Xrs2-Sae2 nuclease ensemble in the processing of DNA-bound obstacles', *Genes Dev*, 31(23-24), pp. 2331-2336.

Wei, Y., Diao, L.X., Lu, S., Wang, H.T., Suo, F., Dong, M.Q. and Du, L.L. (2017) 'SUMO-Targeted DNA Translocase Rrp2 Protects the Genome from Top2-Induced DNA Damage', *Mol Cell*, 66(5), pp. 581-596.e6.

Wells, N.J., Addison, C.M., Fry, A.M., Ganapathi, R. and Hickson, I.D. (1994) 'Serine 1524 is a major site of phosphorylation on human topoisomerase II alpha protein in vivo and is a substrate for casein kinase II in vitro', *J Biol Chem*, 269(47), pp. 29746-51.

Wendorff, T.J., Schmidt, B.H., Heslop, P., Austin, C.A. and Berger, J.M. (2012) 'The structure of DNA-bound human topoisomerase II alpha: conformational mechanisms for coordinating inter-subunit interactions with DNA cleavage', *J Mol Biol*, 424(3-4), pp. 109-24.

Willmore, E., Caux, S.d., Sunter, N.J., Tilby, M.J., Jackson, G.H., Austin, C.A. and Durkacz, B.W. (2004) 'A novel DNA-dependent protein kinase inhibitor, NU7026, potentiates the cytotoxicity of topoisomerase II poisons used in the treatment of leukemia', *Blood*, 103(12), pp. 4659-4665.

Willmore, E., Errington, F., Tilby, M.J. and Austin, C.A. (2002) 'Formation and longevity of idarubicin-induced DNA topoisomerase II cleavable complexes in K562 human leukaemia cells', *Biochem Pharmacol*, 63(10), pp. 1807-15.

Willmore, E., Frank, A.J., Padget, K., Tilby, M.J. and Austin, C.A. (1998) 'Etoposide targets topoisomerase IIalpha and IIbeta in leukemic cells: isoform-specific cleavable complexes visualized and quantified in situ by a novel immunofluorescence technique', *Molecular pharmacology*, 54(1), pp. 78-85.

Wilson, M.D., Harreman, M. and Svejstrup, J.Q. (2013) 'Ubiquitylation and degradation of elongating RNA polymerase II: the last resort', *Biochim Biophys Acta*, 1829(1), pp. 151-7.

Wilson, M.D., Saponaro, M., Leidl, M.A. and Svejstrup, J.Q. (2012) 'MultiDsk: a ubiquitin-specific affinity resin', *PLoS One*, 7(10), p. e46398.

Wilstermann, A.M. and Osheroff, N. (2001) 'Base excision repair intermediates as topoisomerase II poisons', *J Biol Chem*, 276(49), pp. 46290-6.

Woessner, R.D., Mattern, M.R., Mirabelli, C.K., Johnson, R.K. and Drake, F.H. (1991) 'Proliferation- and cell cycle-dependent differences in expression of the 170 kilodalton and 180 kilodalton forms of topoisomerase II in NIH-3T3 cells', *Cell Growth Differ*, 2(4), pp. 209-14.

Wu, C.C., Li, T.K., Farh, L., Lin, L.Y., Lin, T.S., Yu, Y.J., Yen, T.J., Chiang, C.W. and Chan, N.L. (2011) 'Structural basis of type II topoisomerase inhibition by the anticancer drug etoposide', *Science*, 333(6041), pp. 459-62.

Wu, C.C., Li, Y.C., Wang, Y.R., Li, T.K. and Chan, N.L. (2013) 'On the structural basis and design guidelines for type II topoisomerase-targeting anticancer drugs', *Nucleic Acids Res*, 41(22), pp. 10630-40.

Xiao, H. and Goodrich, D.W. (2005) 'The retinoblastoma tumor suppressor protein is required for efficient processing and repair of trapped topoisomerase II-DNA-cleavable complexes', *Oncogene*, 24(55), pp. 8105-13.

Xiao, H., Mao, Y., Desai, S.D., Zhou, N., Ting, C.Y., Hwang, J. and Liu, L.F. (2003) 'The topoisomerase IIbeta circular clamp arrests transcription and signals a 26S proteasome pathway', *Proc Natl Acad Sci U S A*, 100(6), pp. 3239-44.

Xu, P., Duong, D.M., Seyfried, N.T., Cheng, D., Xie, Y., Robert, J., Rush, J., Hochstrasser, M., Finley, D. and Peng, J. (2009) 'Quantitative proteomics reveals the function of unconventional ubiquitin chains in proteasomal degradation', *Cell*, 137(1), pp. 133-45.

Xu, Q., Farah, M., Webster, J.M. and Wojcikiewicz, R.J. (2004) 'Bortezomib rapidly suppresses ubiquitin thiolesterification to ubiquitin-conjugating enzymes and inhibits ubiquitination of histones and type I inositol 1,4,5-trisphosphate receptor', *Mol Cancer Ther*, 3(10), pp. 1263-9.

Yang, X., Li, W., Prescott, E.D., Burden, S.J. and Wang, J.C. (2000) 'DNA topoisomerase IIbeta and neural development', *Science*, 287(5450), pp. 131-4.

Yang, Y., Ludwig, R.L., Jensen, J.P., Pierre, S.A., Medaglia, M.V., Davydov, I.V., Safiran, Y.J., Oberoi, P., Kenten, J.H., Phillips, A.C., Weissman, A.M. and Vousden, K.H. (2005) 'Small molecule inhibitors of HDM2 ubiquitin ligase activity stabilize and activate p53 in cells', *Cancer Cell*, 7(6), pp. 547-59.

Ye, Y., Meyer, H.H. and Rapoport, T.A. (2003) 'Function of the p97-Ufd1-Npl4 complex in retrotranslocation from the ER to the cytosol: dual recognition of nonubiquitinated polypeptide segments and polyubiquitin chains', *J Cell Biol*, 162(1), pp. 71-84.

Yu, X., Davenport, J.W., Urtishak, K.A., Carillo, M.L., Gosai, S.J., Kolaris, C.P., Byl, J.A.W., Rappaport, E.F., Osheroff, N., Gregory, B.D. and Felix, C.A. (2017) 'Genome-wide TOP2A DNA cleavage is biased toward translocated and highly transcribed loci', *Genome Res*, 27(7), pp. 1238-1249.

Yun, J., Kim, Y.I., Tomida, A. and Choi, C.H. (2009) 'Regulation of DNA topoisomerase IIalpha stability by the ECV ubiquitin ligase complex', *Biochem Biophys Res Commun*, 389(1), pp. 5-9.

Yun, J., Tomida, A., Andoh, T. and Tsuruo, T. (2004) 'Interaction between glucose-regulated destruction domain of DNA topoisomerase IIalpha and MPN domain of Jab1/CSN5', *J Biol Chem*, 279(30), pp. 31296-303.

Zagnoli-Vieira, G. and Caldecott, K.W. (2017) 'TDP2, TOP2, and SUMO: what is ZATT about?', *Cell Res*, 27(12), pp. 1405-1406.

Zdraljevic, S., Strand, C., Seidel, H.S., Cook, D.E., Doench, J.G. and Andersen, E.C. (2017) 'Natural variation in a single amino acid substitution underlies physiological responses to topoisomerase II poisons', *PLoS Genet*, 13(7), p. e1006891.

Zeng, Z., Cortés-Ledesma, F., El Khamisy, S.F. and Caldecott, K.W. (2011) 'TDP2/TTRAP Is the Major 5′-Tyrosyl DNA Phosphodiesterase Activity in Vertebrate

Cells and Is Critical for Cellular Resistance to Topoisomerase II-induced DNA Damage*', *J Biol Chem*, 286(1), pp. 403-9.

Zhang, A., Lyu, Y.L., Lin, C.P., Zhou, N., Azarova, A.M., Wood, L.M. and Liu, L.F. (2006) 'A protease pathway for the repair of topoisomerase II-DNA covalent complexes', *J Biol Chem*, 281(47), pp. 35997-6003.

Zhao, Y., Brickner, J.R., Majid, M.C. and Mosammaparast, N. (2014) 'Crosstalk between ubiquitin and other post-translational modifications on chromatin during double-strand break repair', *Trends in Cell Biology*.

Appendices

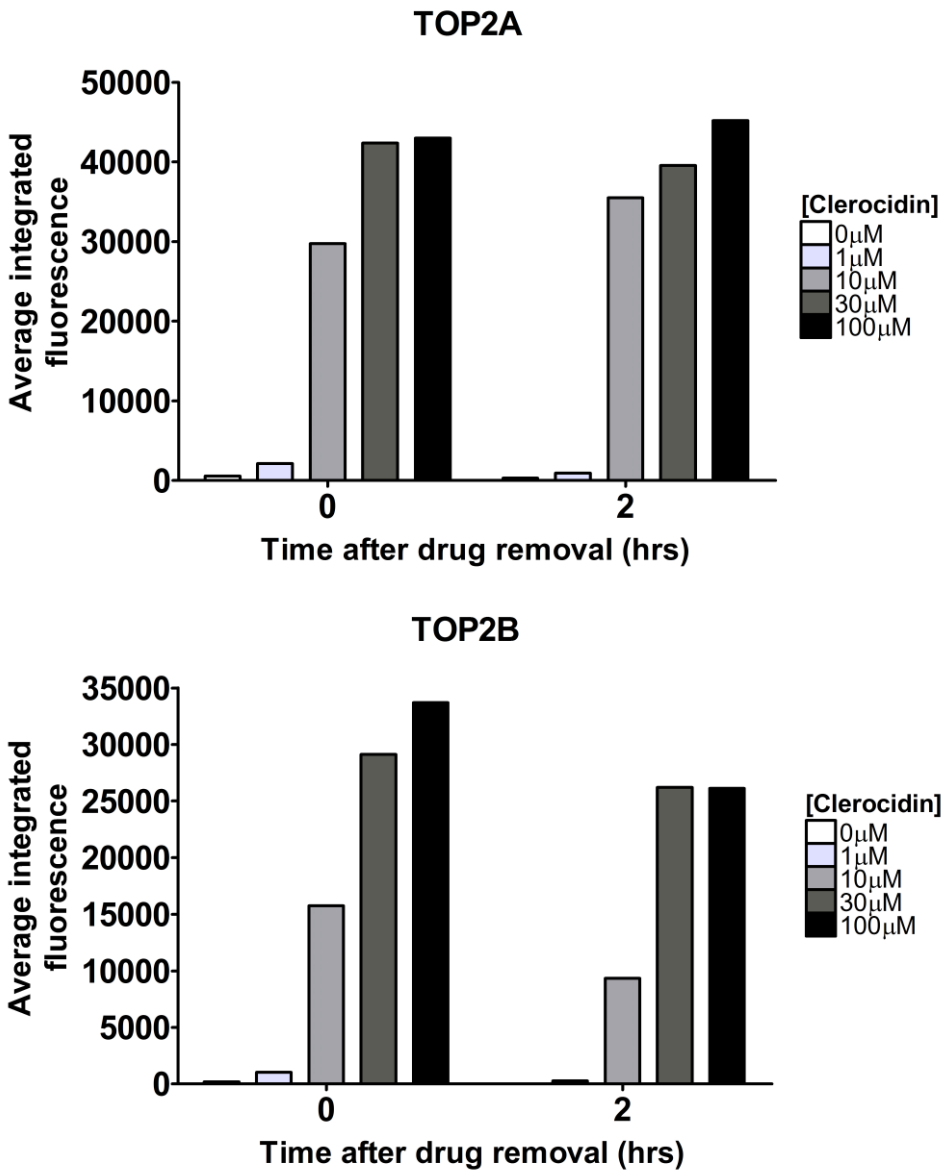

Figure 1. Using the TARDIS assay to measure levels of TOP2A- and TOP2B- DNA complexes in response to the irreversible TOP2 poison clerocidin.K562 cells were treated with the indicated concentration of clerocidin for 2 hours, followed by 2 hours incubation in drug-free medium. Levels of TOP2A- and TOP2B- DNA complexes were measured immediately following 2 hours continuous exposure to clerocidin (0 hours after drug removal) and 2 hours after clerocidin removal. Histograms show raw median values from a single experiment.

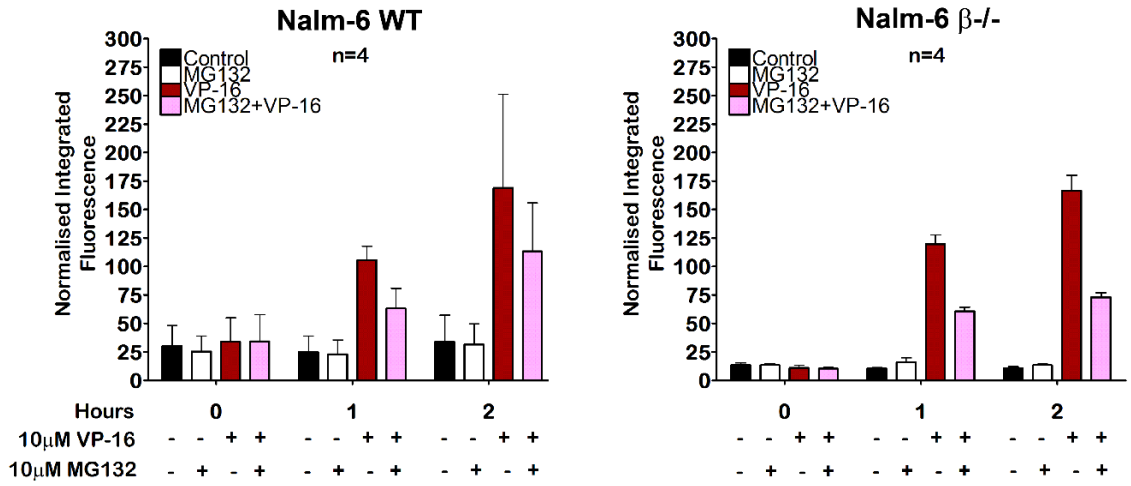

Figure 2. The appearance of etoposide-induced γH2AX foci is reduced in Nalm-6 cell lines following co-treatment with the proteasome inhibitor, MG132. Nalm-6 wild type (WT, left panel) or Nalm-6$^{TOP2B-/-}$ cells (right panel) were treated with 10 μM etoposide (VP-16) alone or in combination with 10 μM MG132 for 0, 1 or 2 hours. Levels of histone H2AX phosphorylation were measured by γH2AX assay. Values represent the mean of median integrated fluorescence ± SEM from at least three replicate experiments, and are normalised to an additional 1 hour 10 μM VP-16 positive control. Drug treatments were performed by RS, and immunofluorescence/microscopy/data analysis by Charlotte Sanders.

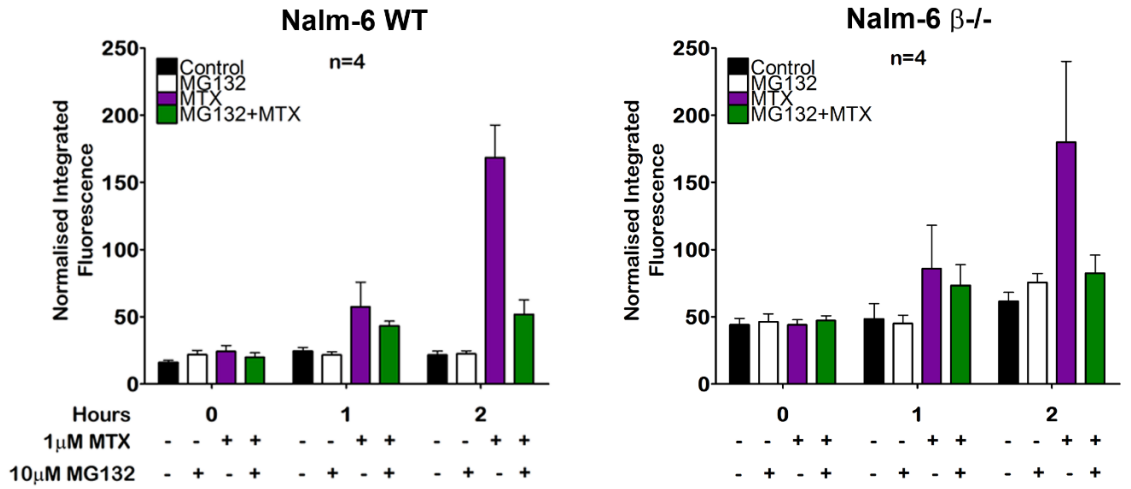

Figure 3. The appearance of mitoxantrone-induced γH2AX foci is reduced in Nalm-6 cell lines following co-treatment with the proteasome inhibitor, MG132. Nalm-6 wild type (WT, left panel) or Nalm-6$^{TOP2B-/-}$ cells (right panel) were treated with 1 μM mitoxantrone (MTX) alone or in combination with 10 μM MG132 for 0, 1 or 2 hours. Levels of histone H2AX phosphorylation were measured by γH2AX assay. Values represent the mean of median integrated fluorescence ± SEM from at least three replicate experiments, and are normalised to an additional 1 hour 1 μM MTX positive control. Drug treatments were performed by RS, and immunofluorescence/microscopy/data analysis by Charlotte Sanders.

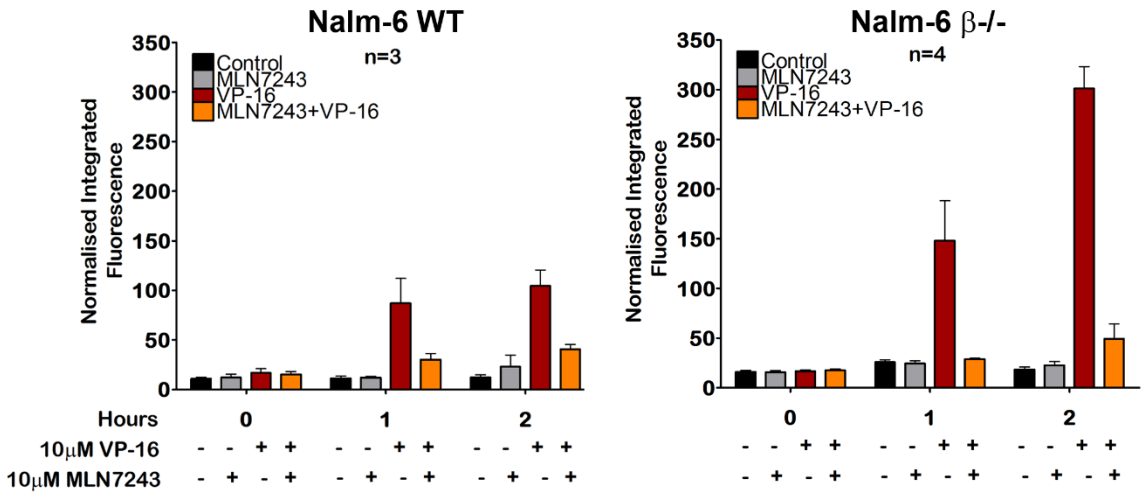

Figure 4. The appearance of etoposide-induced ɣH2AX foci is reduced in Nalm-6 cell lines following co-treatment with the UAE inhibitor, MLN7243. Nalm-6 wild type (WT, left panel) or Nalm-6$^{TOP2B-/-}$ cells (right panel) were treated with 10 μM etoposide (VP-16) alone or in combination with 10 μM MLN7243 for 0, 1 or 2 hours. Levels of histone H2AX phosphorylation were measured by ɣH2AX assay. Values represent the mean of median integrated fluorescence ± SEM from at least three replicate experiments, and are normalised to an additional 1 hour 10 μM VP-16 positive control. Drug treatments were performed by RS, and immunofluorescence/microscopy/data analysis by Charlotte Sanders.

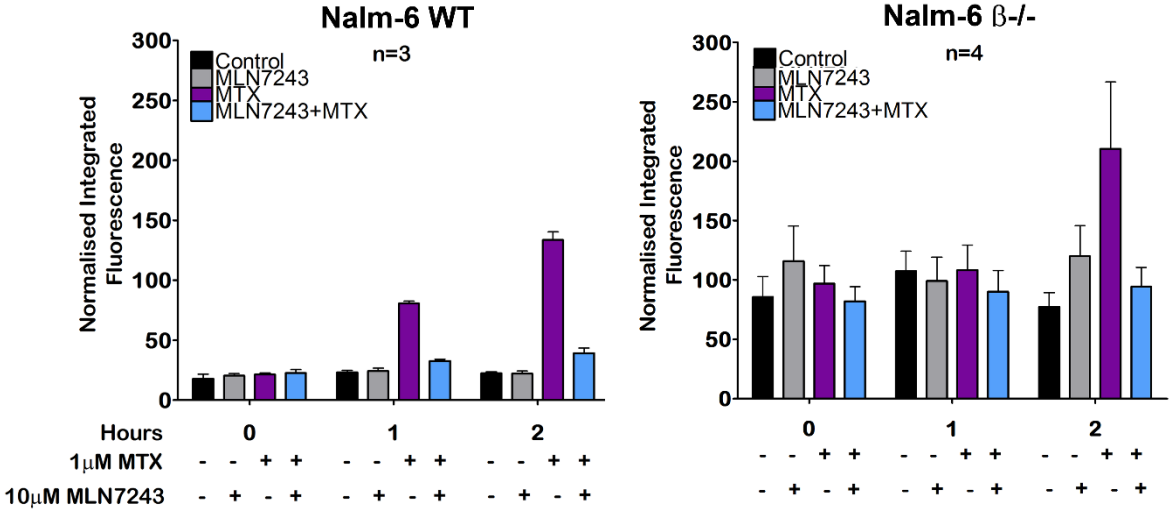

Figure 5. The appearance of mitoxantrone-induced ɣH2AX foci is reduced in Nalm-6 cell lines following co-treatment with the UAE inhibitor, MLN7243. Nalm-6 wild type (WT, left panel) or Nalm-6$^{TOP2B-/-}$ cells (right panel) were treated with 1 μM mitoxantrone (MTX) alone or in combination with 10 μM MLN7243 for 0, 1 or 2 hours. Levels of histone H2AX phosphorylation were measured by ɣH2AX assay. Values represent the mean of median integrated fluorescence ± SEM from at least three replicate experiments, and are normalised to an additional 1 hour 1 μM MTX positive control. Drug treatments were performed by RS, and immunofluorescence/microscopy/data analysis by Charlotte Sanders.

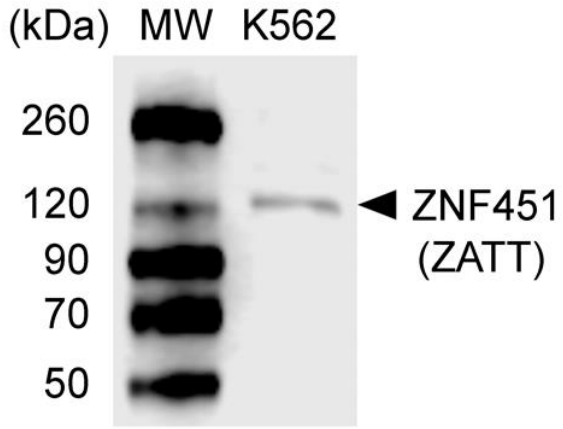

Figure 6. Expression of ZATT (ZNF451) in K562 cells, shown by western blot. K562 cell lysate was prepared as described in Chapter 2, section 2.6.1. Levels of ZATT protein was analysed by SDS-PAGE followed by western blotting.

Table 1. Investigating the TOP2 poison-induced proteasomal degradation of TOP2 by western blotting

Experiment	Biological replicates (*n* drug treatments)	Technical replicates (*n* western blots)	Result	
			TOP2A	TOP2B
100 µM VP-16 +/- 50 µM MG132 (Figure 3.10)	1 of 1 (treated 14/05/2015)	1 of 5 (22/05/2015)	N/A, actin failed	N/A, actin failed
		2 of 5 (28/05/2015) Protein quantification by Bradford assay repeated to improve loading	TOP2A levels decreased in VP-16 treated cells compared to DMSO control. Decrease is proteasome dependent.	No TOP2B signal – antibody issue?
		3 of 5 (04/06/2015)	TOP2A levels decreased in VP-16 treated cells compared to DMSO control. Decrease is proteasome dependent.	Poor TOP2B signal after stripping blot – has stripping removed protein?
		4 of 5 (10/05/2015) 2 identical gels for TOP2A and TOP2B to avoid stripping)	TOP2A levels decreased in VP-16 treated cells compared to DMSO	TOP2B detected in some lanes and not others (even DMSO control) despite even

			control. Decrease is proteasome dependent.	loading. Antibody issue?
		5 of 5 (10/05/2015)	TOP2A levels are not affected by etoposide treatment. TOP2B appears reduced in etoposide-treated cells compared to untreated control	TOP2B levels are slightly decreased compared to untreated control.
100 µM VM-26 +/- 50 µM MG132 (data not shown)	1 of 2 (treated 27/05/2015)	1 of 1 (08/06/2015)	TOP2A levels decreased in VP-16 treated cells compared to DMSO control. Decrease is proteasome dependent.	TOP2B antibody failed
	2 of 2 (treated 14/05/2015)	1 of 1 (10/06/2015)	TOP2A levels decreased in VP-16 treated cells compared to DMSO control. Decrease is proteasome dependent.	No TOP2B signal

100 µM VM-26 +/- 50 µM PRT4165 (drug treatment and WCE by R. Swan, blots by Alessandro Mozzarelli, data not shown)	1 of 1 (treated 10/07/2015)	22/07/2015	N/A (Not probed)	Uneven loading, bands missing TOP2B levels unaffected by VM-26 treatment
		23/07/2015	TOP2A levels unaffected by VM-26 treatment	No TOP2B signal
250 µM VP-16 +/- 50 µM MG132 (data not shown)	1 of 1 (treated 28/07/2015)	31/07/2015	TOP2A levels unaffected by VP-16 treatment	N/A (not probed)

Table 2. Investigating the ubiquitination of TOP2 using GST-TUBEs

Experiment	Conditions	Result	Problems	Optimisation for future experiments
#1 (16/04/2016)	1 x 10^6 cells per condition, RIPA buffer + DNase I, incubation with 1.8 µM GST-TUBE2 for 1 hour at 4°C	Successful ubiquitin pulldown	No TOP2A or TOP2B detected in input, though some detected on beads. Protein concentration too low?	• Could include GST-TUBE1 in lysis buffer to protect proteins from non-specific proteolysis and DUBs
#2 (19/04/2016)	1 x 10^6 cells per condition, RIPA buffer + DNase I, incubation with 1.8 µM GST-TUBE2 for 1 hour at 4°C. GST-TUBE1 included in lysis buffer.	Ub-TOP2A detected after GST-TUBE1 pulldown	TOP2A not detected in input	
#3 (3/08/16) (Figure 4.15)	1 x 10^6 cells per condition, RIPA buffer + DNase I, incubation with 1.8 µM GST-TUBE1 for 1 hour at	Ub-TOP2A detected in input and after GST-TUBE pulldown	Ubiquitin conjugates detected in input but not on beads	• DNase I is not sufficient for complete extraction of covalently-linked

	4°C. GST-TUBE1 included in lysis buffer.	Poor pulldown efficiency – ubiquitin conjugates lost in supernatant	Less TOP2A in lysate of etoposide-treated cells compared to untreated control, suggesting incomplete extraction of TOP2 complexes from DNA	TOP2-DNA complexes. Future studies should include an alternative nuclease such as benzonase

Table 3. Investigating the ubiquitination of TOP2 using MultiDsk2

Experiment	Conditions	Result	Problems	Optimisation for future experiments
#1 (23/02/2016)	2 x 10^6 cells per condition, RIPA buffer + DNase I, incubation with 0.2 µM MultiDsk2 for 4 hours at 4°C	Ubiquitin conjugates depleted in supernatant (pulldown successful)	Too much protein loaded, film overexposed and unable to strip blot ~55-60 kDa bands corresponding to GST when probing with TOP2 antibodies, as 4566 and 4555 are raised to GST fusion proteins	• Repeat with serial dilutions of sample, less cells • Blots ran in duplicate to avoid stripping • Develop blots using the LiCor C-DiGit blot scanner to avoid saturation • Other TOP2 antibodies to be used where possible
#2 (1/03/2016)	1 x 10^6 cells per condition, RIPA buffer + DNase I, incubation with 0.2 µM	Highly efficient pulldown of K48-linked ubiquitin conjugates (none detected in supernatant,	Multiple bands present when probing for TOP2A (4566), including a ~50	• Higher concentration of protease inhibitors to avoid

	MultiDsk2 for 4 hours at 4°C	even with prolonged exposure on film). An efficient pulldown may be achieved with lower concentration of MultiDsk2.	kDa GST band and an unknown band ~90 kDa	degradation of sample • All wash steps performed in cooled centrifuge and samples handled in cold room or on ice at all times • Test lower concentration of MultiDsk2 to preserve reagent
#3 (10/03/2016)	1 x 10^6 cells per condition, RIPA buffer + DNase I, incubation with 0.1 µM MultiDsk2 for 4 hours at 4°C		Ubiquitin pulldown less efficient (a significant amount of ubiquitin conjugates remains in supernatant) No TOP2 protein detected (even in input) suggesting antibody failure (including 4566 and 30400)	• 0.2 µM MultiDsk2 required for efficient ubiquitin pulldown

#4 (31/03/2016)	1 x 10^6 cells per condition, RIPA buffer + DNase I, incubation with 0.2 µM MultiDsk2 for 4 hours at 4°C		Ubiquitin pulldown unsuccessful even with 0.2 µM MultiDsk2 No TOP2 protein detected	• RIPA buffer may not be appropriate to study protein-protein interactions. Repeat with TENT buffer as per Anindya et al 2007 (mild lysis buffer requires sonication to disrupt the nucleus)
#5 (8/06/2017) Figure 4.16	1 x 10^6 cells per condition, TENT buffer + sonication [2 rounds (15 seconds, 5 cycles, 20% power)], followed by incubation with 0.2 µM MultiDsk2 at 4°C overnight (as per Anindya et al 2007)	Full length TOP2 protein detect in input and enriched by MultiDsk2	Insufficient ubiquitin pulldown Gloopy sample difficult to load, suggests sonication is insufficient to adequately break up DNA	• More rounds of sonication required to break up DNA
#6 (15/06/2017)	1 x 10^6 cells per condition, TENT buffer + sonication		No ubiquitin conjugates detected on beads	• Use new batch of GSH beads – old

	[5 rounds (15 seconds, 5 cycles, 20% power)],, followed by incubation with 0.2 µM MultiDsk2 at 4°C overnight		(though some Ub-TOP2A present) Poor ubiquitin pulldown	beads are expired and may not bind GST if oxidised
#7 (23/06/2017)	1 x 10^6 cells per condition, TENT buffer + sonication [5 rounds (15 seconds, 5 cycles, 20% power)],, followed by incubation with 0.2 µM MultiDsk2 at 4°C overnight	Pulldown efficiency improved	Gloopy samples difficult to load	• Extraction conditions to be optimised in future experiments (include nuclease like DNase I or benzonase)